SEDIMENTARY AND NEOTECTONIC HISTORY OF LAKE OHRID (ALBANIA/MACEDONIA): ACQUISITION AND INTERPRETATION OF NEW HYDRO-ACOUSTIC AND SEISMIC DATA

DISSERTATION

zur Erlangung des Doktorgrades

an der Mathematisch-Naturwissenschaftlichen Fakultät

der Christian-Albrechts-Universität zu Kiel

vorgelegt von

Katja Lindhorst

Kiel, 2012

Referent	Prof. Dr. Sebastian Krastel-Gudegast
Koreferent	Prof. Dr. Kerstin Schrottke
Tag der mündlichen Prüfung	25. Oktober 2012

Zum Druck genehmigt:

……

Der Dekan

Hiermit erkläre ich eidesstattlich, dass ich die vorliegende Dissertation selbständig und ohne zuhilfenahme unerlaubter Hilfsmittel angefertigt habe. Bisher ist die Arbeit noch nicht an anderer Stelle im Rahmen eines Prüfungsverfahrens vorgelegt worden. Die Arbeit ist unter Einhaltung der Regeln guter wissenschaftlicher Praxis der Deutschen Forschungsgemeinschaft entstanden.

Kiel, den

Katja Lindhorst

Abstract

Ancient Lake Ohrid an oligotrophic lake is probably the oldest existing lake in Europe. It is located on the Balkan Peninsula within the Dinaride-Albanide-Hellenide mountain belt, and is often referred to as a hotspot of endemic biodiversity.

This study sheds light on the tectonic and sedimentary evolution of Lake Ohrid based on newly-acquired hydro-acoustic and seismic data sets. It testifies the importance of Lake Ohrid as a valuable archive susceptible to provide a continuous sediment record within the scope of the International Continental Drilling Program (ICDP) campaign scheduled for September/October 2012.

Interpretation of multichannel seismic cross sections and bathymetric data reveals that Lake Ohrid formed in two main deformation phases: (1) a transtensional phase resulted in an opening of a pull-apart basin probably in Late Miocene; and (2) an extensional phase since the Pliocene to recent that led to the present geometry of Lake Ohrid. After initial opening during phase 1 a symmetrical graben formed, bounded by the Central Basin faults that acted as master faults

The early stage geometry of the basin has a typical rhomboidal shape restricted by two sets of major normal faults, namely Lini and Kaneo (NE-SW), Piskupat and Pescani (NW-SE) Faults. The location of the basin initiation coincides with the greatest depth of the acoustic basement; nowadays a thick succession yof undisturbed sediments is found in this area. Neotectonic activity since the Pliocene takes place along the roughly N-S directed Eastern and Western Major Boundary Normal faults that are partly exposed at the floor of the lake. Numerous faults are present in the northern area offsetting syn-tectonic sediments, thus confirming the hypothesis that Lake Ohrid Basin is still experiencing extension. Furthermore, the active Gorenci sinistral strike slip Fault is most likely responsible for the opening of the Struga Graben detectable at the lake floor as a NE-SW directed elongated graben structure.

Seismic stratigraphic interpretation revealed a regular depositional pattern of fluvial deposits overlying the pre-rift basement, the uppermost unit shows deep lacustrine sediments, which form the majority of the entire sedimentary infill; such a sedimentary succession is comparable to a tripartite sediment succession described for rift lakes indicating the different stages of basin evolution.

A major outcome of this study is the establishment of a chrono-stratigraphic scheme developed for undisturbed lacustrine sediments back to an age of 430 kyr indicating that these sediments document glacial and interglacial cycles back to Marine Isotope Stage (MIS) 12. A refined calculation on the basis of our new geological data set revealed a limnological age of at least 2 Myr for Lake Ohrid.

Stacked clinoforms indentified on seismic lines in the southern area indicate significantly lower lake levels prior to MIS 6. This period is also characterized by a progressive rise of water level with intermittent stillstands since its existence as water-filled body, which might have favored expansion of endemic species within Lake Ohrid. Significant lake level fluctuations with prominent lowstands of ca. 60 and 35 m below the present water level occurred during MIS 6 and 5, respectively. The effect of these lowstands on the biodiversity along most of the coasts of the lake is probably negligible, due to only small changes in lake surface area, coastline, and habitat. In contrast, the biodiversity in shallow-lacustrine areas was more severely affected due to disconnection of sublacustrine springs from the main water body.

Other interesting features in Lake Ohrid are mass movement deposits that are widespread within the basin and have been mapped at different stratigraphic levels of the basin. A cluster of slide deposits around Magic Mountain (a prominent basement high in the central basin) indicates a relationship between mass movement events and the activation of faults that bound the intrabasinal high. In general slides are present adjacent to major fault structures such as the Lini fault, the Eastern and Western Major Boundary faults, and the Udenisht fault in the south suggesting that they are seismically triggered.

The Udenisht slide complex in the southwestern part of the lake is by far the largest mass failure event within the basin. The slide deposits cover an area of ~27 km², are up to 50 m thick, and sum up to a volume of ~0.11 km³. First age estimations suggest that the Udenisht Slide is less than 1,500 years old. Although the volume of the Udenisht slide is well within the range of landslide volumes capable to trigger tsunamis, detailed analysis of our data suggests that no major tsunami was triggered. In contrast, subsurface and morphological indications for lake floor instabilities along the western margin outline potential rotational slumping with a high risk of tsunami generation in the future.

Kurzfassung

Der oligotrophe Ohridsee ist wahrscheinlich der älteste existierende See in Europa. Er befindet sich in der Dinariden-Albaniden-Helleniden Bergkette auf der Balkanhalbinsel und wird häufig als Hotspot für endemische Biodiversität genannt.

Diese Arbeit untersucht die tektonische und sedimentologische Entwicklung des Ohridsees auf der Basis neu aufgezeichneter hydroakustischer und seismischer Datensätze. Sie verdeutlichen die Bedeutung des Ohridsees als wertvolles Archiv für die Erbohrung eines langen, koninuierlichen Sedimentkernes im Rahmen eines Bohrprojektes des International Continental Drilling Program (ICDP), das im September/Oktober 2012 stattfindet.

Die Auswertung und Interpretation von seismischen Profilen und bathymetrischen Daten ergab, dass der Ohridsee in zwei Hauptdeformationsphasen entstand. Im späten Miozän öffenete sich ein Pull-Apart Becken aufgrund einer transtensionalen Phase (1). Die heutige vorherrschende Geometrie des Ohridbecken ist eine Folge einer O-W Ausdehnung, die das Gebiet seit dem Pliozän beeinflusst (2). Das ursprünglich geöffnete Becken entwickelte sich zu einem symmetrischen Graben der von zwei Hauptabschiebungen, den Central Basin Störungen, eingegrenzt ist.

Desweiteren entwickelte sich während des frühen Entwicklungsstadiums des Beckens eine typische rhombische Form, die jeweils von zwei Störungssystemen an jeder Seite begrenzt ist: die Lini und Kaneo Störungen (NO-SW) sowie die Piskupat und Pescani Störungen (NW-SO). An der Stelle, an der die Beckenentwicklung wahrscheinlich begann, befindet sich heute die größte Tiefe des Grundgebirges, die von mächtigen, ungestörten Sedimenten (>700m) überdeckt ist. Neotektonische Aktivitäten seit dem Pliozän wurden entlang der N-S streichenden östlichen und westlichen Hauptverwerfungen beobachtet. Die Hauptstörungen streichen teilweise am Seeboden aus. Zahlreiche Abschiebungen wurden im nördlichen Bereich des Ohridsees beobachtet und bestätigen damit die Hypothese, dass sich der Ohridsee auch rezent noch weiter dehnt. Diese Störungen versetzen die jüngsten Sedimente und werden daher als aktive Störungen interpretiert. Die Gorenci Störung, eine sinistrale Blattverschiebung, wird als Auslöser für die Entwicklung des Struga Graben, einem NO-SW gerichteten längliche Vertiefung im nördlichen Bereich des Sees, interpretiert.

Im Becken wurde regelmässig wiederkehrende Ablagerungsstrukturen beobachtet. Das Grundgebirge wird von fluviatilen Ablagerungen bedeckt. Der Hauptteil der Sedimente, die

sich im Becken befinden, bestehen aus lakustriinen Sedimenten die darauf hinweisen, dass der See über einen langen Zeitraum Wasser enthielt und nicht austrocknete. Die Abfolge an Ablagerungen (fluviatile, gefolgt von lakustrine) wird auch in den meisten Riftseen beobachtet, wo sie Aufschluss über die einzelnen Stadien der Seenentwicklung geben.

Ein Hauptergebnis der Arbeit ist die Entwicklung eines chrono-stratigraphischen Modells für ungestörte Sedimente mit einem maximalen Alter von 430 kyrs im zentralen Teil des Sees. Mit Hilfe dieses Modells konnte gezeigt werden, dass die sedimentären Ablagerungen im Ohridsee wertvolle Informationen über die glazialen und interglazialen Stadien enthalten, mindestens bis zum MIS 12. Desweiteren konnte die Altersabschätzung des Sees verbessert werden. Das limnologische Alter wird nun auf mindestens 2 Millionen Jahre geschätzt.

Seismische Profile, die den südlichen Teil des Sees abbilden zeigen Klinoformen, die in verschiedenen Untergrundtiefen auftreten. Diese Strukturen weisen daraufhin, dass der Seespiegel des Ohrids vor dem MIS 6 signifikant geringer war als heute. Ein stetiger Anstieg des Seespiegels ist charakteristisch für diese Zeitperiode und begünstigte möglicherweise die Ausbreitung vieler endemischer Arten im See. Bedeutende Seespiegelschwankungen im MIS 5 und 6 konnten anhand von Terrassenstrukturen im Bereich der Ohridbucht in 35 und 60 m Tiefe belegt werden. Allerdings wirkten sich diese Seespiegelschwankungen eher gering auf die Ausbreitung der Arten aus, da sich die Seeoberfläche, die Küstenlinie sowie die Lebensräume nur wenig änderten. In sehr flachen Bereichen, an denen Unterwasserquellen austreten und sich Lebensräume für ganz spezielle Lebensformen entwickelten, ist dagegen bereits der Einfluss einer geringen Änderung des Seespiegels entscheidend.

Eine weitere Besonderheit des Ohridsees sind Massenumlagerungen, die sich in verschiedenen stratigraphischen Tiefen wiederfinden. Eine Häufung dieser Rutschungsablagerungen findet man um den Magic Mountain herum (eine dominante Erhöhung im See), was darauf schließen lässt, dass diese Rutschungsablagerungen mit der seismischen Aktiviät entlang der Störung en in Zusammenhang stehen. Weiterhin findet man in der Nähe von Störungen wie zum Beispiel der Lini oder der Ost- und West-Hauptverwerfungen sowie der Udenisht Störung häufig solche Massenumlagerungen; ein Hinweis darauf, dass diese Rutschungen durch einen seismischen Trigger ausgelöst wurden.

Im südwestlichen Teil des Ohridsees befindet sich der Udenisht Rutschungskomplex, eine der größten Flächen, die auf eine Rutschung zurückzuführen ist. Die Ablagerungen bedecken eine Fläche von ~27 km², sind bis zu 50 m mächtig und haben ein Volumen von ~0,11 km ³. Erste

Altersabschätzungen ergeben ein Alter von weniger als 1500 Jahr für die Udenisht Rutschung. Das Volumen der Rutschung ist groß genug um einen Tsunami auszulösen allerdings weist eine detaillierte Analyse unserer Daten nicht daraufhin, dass es einen größen Tsunami im Ohridsee gegeben haben könnte. Hingegen nördlich der Udenisht Rutschung entlang des westlichen Hanges gibt es weitere Hinweise auf Instabilitäten. Eine Interpretation der morphologischen Strukturen deutet darauf hin, dass es sich um rotationale Deformationen handelt, welche ein höheres Risiko haben zukünftig einen Tsunami auszulösen.

Table of Figures

Fig. 1: Overview map of the surrounding area of Lake Ohrid and its sister Lake Prespa on the Balkan Peninsula. M: Mokra Mountain Chain, G: Galicica Mountain chain. The globe in the upper left corner shows the overall location of the area. 27

Fig. 2: Map showing the Balkan Peninsula and the location of Lake Ohrid and its sister Lake Prespa. Grey shaded area marks the South Balkan Extensional Regime (SBER). Location of the Mesta and Strymon detachment faults are shown (modified after Burchfiel et al. 2003, 2008b. Location of the Hellenic subduction zone and the North Anatolian Fault (NAF) is given. ESZ: Earthquake source zone (Aliaj et al. 2004) 28

Fig. 3: Lake Ohrid and its adjacent mountain chains Mokra Mountain in the west and Galicica Mountains in the east. The main populated areas are marked with red dots. Pink areas show the subsurface springs: (1) Sum, (2) Dobra Voda, (3) Bej Bunar, (4) Bijana, (5) Tushemisht, and (6) Zagorican (Albrecht and Wilke, 2008). The subaquatic springs are shown in blue: (7) Kalishta, (8) Kaneo, (9) Elesec, (10) Veli Dab, (11) Sveti Naum (Matter et al. 2010). White dots are proposed drill sites: (1) Struga, (2) Lini, (3) DEEP, (4) Gradiste, and (5) Cerava (see chapter 4.3 for details).Green dots are sediment cores retrieved within Lake Ohrid: (6) CO 1200, 1201, (7) CO1202, (8) Lz1120, and (9) JR2004 (see chapter 2.4 for details). Red lines are multichannel seismic tracks. 31

Fig. 4: Sketches illustrating the tectonic evolution (A) until the Late Paleozoic time within a Paleotethys environment, (B) during Mesoic time when microcontinents drifted northward away from Gondwana and the Pindos Ocean opened, (C) evolution through time of the Lake Ohrid Area, and finally (D) since the Miocene to present with interpretation of the subdug slab. Modified after: (A) Robertson 2012, (B) Robertson et al. 1991, (B) Nieuwland et al. 2001, (D) Hoffmann et al. 2010. 32

Fig. 5: (A) Geological units and their ages within the broader area of Lake Ohrid (modified after Dilek et al., 2006). (B) Geological map of Lake Ohrid area (modified after Wagner et al., 2008b). 33

Fig. 6: Map showing location of significant major earthquakes (M>5) including the most recent ones from June 2012 around Lake Ohrid (downloaded from

http://earthquake.usgs.gov/earthquakes/eqarchives/epic/ accessed on June 19th, 2012) _____ 35

Fig. 7: Map showing the Italian Volcanoes that are potential sources for ash layers identified in Lake Ohrid (modified after Giaccio et al.,. 2008). _____ 37

Fig. 8: Photographs of the Macedonian research vessel. (A) Seismic equipment loaded on deck. (B) ELAC 1180 multibeam system mounted at the bow of the vessel. (C) in the hangar for constructing the holder for multibeam device. _____ 41

Fig. 9: Seismic cross section (W-E) illustrating seismic facies defined within Lake Ohrid. _ 43

Fig. 10: Example of seismic cross section running from south to north imaging the internal sedimentary and tectonic structure of Lake Ohrid (Top.) Uninterpreted section, line drawing and interpretation (Bottom). _____ 46

Fig. 11: Bathymetric map of Lake Ohrid viewed from Ohrid Bay toward the SW illustrating the most striking morphological features: (1) Gradiste subbasin, (2) intrabasinal high, so called Magic Mountain, (3) deepest area within the lake with water depths up to 293 m, (4) smooth topography within the central part of Lake Ohrid, (5) area of slide deposits of the Udenisht slide (Lindhorst et al., 2012), (6) sediments covering the western margin, (7) surface of an active Normal Fault outcropping at the lake floor, (8) elongated graben structure indicating active faulting, (9) pockmark-like structures, (10) rough topography indicating sliding, (11) fold structures, and (12) terraces within Ohrid Bay (Lindhorst et al., 2010). A, B mark areas of special interest of this study. LP: Lini Peninsula, O: Ohrid city, P: Progradec. _____ 48

Fig. 12: Seismic cross section showing the location of the proposed drill site DEEP._____ 49

Fig. M3 1: Map of the Balkan Peninsula showing the location of Lake Ohrid (1) and its sister Lake Prespa (2). Geological units surrounding the lakes are illustrated (Pindos - greenish, Pelagonian – blueish adapted from Ghikas et al. 2010). ESZ: Earthquake Source Zone of the Korca-Ohrid area described by Aliaj et al. 2004. Grey area with dashed line marks the South Balkan Extensional Regime (SBER, Burchfiel et al. 2008). A cross section highlights the basin and range situation with Lake Ohrid being the westernmost and subsequently youngest graben. The Ioannina Basin (3) is marked.

Black line with squares indicates the active subduction zone with a strike slip segment. _____ 133

Fig. M3 2: Lake Floor morphology illustrating the most striking features within Lake Ohrid (blue line marks the shore line). The lake is divided in four main areas **(I)** northern area with a) folds, b) graben with distinct morphological step, c) pockmark structures, d) rough topography, and e) terrace structures in Ohrid Bay, **(II)** Major Eastern Boundary Fault Zone with f) NE-SW trending lineations, g) Gradiste Sub-basin, and h) Cerava terrace structure. **(III)** Major Western Boundary Fault Zone with i) smooth topography zone, j)-1-2-3 slump areas, k) rounded pockmark-like shape, and l) NW-SE trending lineament. **(IV)** Central Basin with m) zone of smooth topography, o) exposure of Lini Fault, p) Magic Mountain, q) deepest sub-basin, and r) channel incisions. Grey points mark locations of sediment cores obtained in lake Ohrid. __ 134

Fig. M3 3: Seismic facies defined in the multichannel seismic data in Lake Ohrid_____ 135

Fig. M3 4: Seismic cross section showing the horst and graben structure in the northern area of Lake Ohrid. Top: uninterpreted, bottom: line drawing and interpretation. Note the 500 m wide fault zone in the center of the profile that has been interpreted as active strike-slip fault most likely connected with a pull-apart basin that is currently opening. _____ 136

Fig. M3 5: Seismic cross section imaging the prominent Lini Fault and the associated half-graben. Top: uninterpreted, bottom: line drawing and interpretation. _____ 137

Fig. M3 6: Seismic cross section imaging the central part of Lake Ohrid characterized by thick sediment successions. Top: uninterpreted; bottom: line drawing and interpretation. The fault architecture points to symmetrical graben structure. A 2 km segment (black square) was used to develop seismic chrono-stratigraphical model which allowed us to interpret the basin in terms of glacial and interglacial cycles (see text for details). _____ 138

Fig. M3 7: Seismic cross section imaging the South central basin, Magic Mountain, and the active Gradiste Basin. Top: uninterpreted, bottom: line drawing and interpretation. The area is affected by extensive active faulting indicated by numerous mass wasting

events especially adjacent to Magic Mountain but also by a roll over structure next to the Memelisht Normal Fault. 139

Fig. M3 8: Seismic cross section showing the complex basin structure within the southern area. Top: uninterpreted, bottom: line drawing and interpretation. (See text for further details). 140

Fig. M3 9: Fault interpretation based on the acoustic basement as calculated from the picks within multichannel seismic lines. Black lines highlighting faults that are characterized by scarps forming the flank of the basement along with thick sediment cover of lacustrine deposits suggesting that those faults have been inactive for some time. Dashed line indicates an inferred dextral strike-slip fault related to the initial opening of the basin (see text for explanation). Blue line marks present shore. 141

Fig. M3 10: Compilation of the bathymetric map and topography of the surrounding area. See also Fig. M3 9. Thick dashed red lines mark minor faults identified within the multichannel seismic data. Thin dashed red lines are inferred faults. Yellow lines mark faults mapped onshore (Hoffmann et al. 2010, Reicherter et al. 2010). Dashed yellow lines are inferred fault continuation of onshore and offshore data set. 142

Fig. M3 11: Correlation of a 2 km transect of the seismic data central part within Lake Ohrid (see Fig. M3 6 for location) with pollen analysis and respective Marine Isotope stages (colored lines from 1 to12) adapting a model proposed by Tzedakis, (1994). Pollen concentration and $\delta^{18}O$ curves are extracted from a 160 m long sediment sequence of the Ioannina basin in northwest Greece (Tzedakis, 1994) Glacial stages (bluish) are characterized by low vegetation cover and a high precipitation with subsequently high sediment input of clastic material caused by enhanced erosion within the catchment area (high amplitude reflectors). In contrast, the interglacial (orange) are characterized by a dense vegetation cover leading to a stabilization of the soil within the catchment area and mostly biogenic sedimentation within the basin (low amplitude reflectors). See text for further details. 143

Fig. M3 12: Synoptic 3D models for the two major deformational phases of basin development: (A) Basin initiation as a pull-apart basin in a short transtensional phase

during the Late Miocene and (B) Basin widening caused by E-W extension since Pliocene to recent. _____ 144

Fig. B 1: Seismic cross sections of proposed ICDP drill sites within the SCOPSCO project. _____ 161

Fig. B 2: Seismic cross section showing sedimentary structures in the northern area. The active Gorenci strike-slip fault is imaged on the profile. _____ 162

Fig. B 3: Seismic cross section showing sedimentary structures in the northern area. The active Gorenci strike-slip fault is imaged on the profile. _____ 163

Fig. B 4: Seismic cross section showing sedimentary structures in the northern area. The active Gorenci strike-slip fault is imaged on the profile. _____ 165

Fig. B 5: Seismic cross section showing sedimentary structures in the northern area. The active Gorenci strike-slip fault adjacent to the Struga graben illustrated by distinct sidewalls is imaged on the profile. _____ 166

Fig. B 6: Seismic cross section imaging the half graben with Lini a major bounding fault. Colored lines and respective numbers from 1-12 indicate the chronological interpretation related to the Marine Isotope Stages. _____ 169

Fig. B 7: Seismic cross section imaging the half graben with Lini a major bounding fault. Colored lines and respective numbers from 1-12 indicate the chronological interpretation related to the Marine Isotope Stages. Dark grey area indicates bright spot. The inferred strike slip fault in between the Central Basin faults is marked that is most likely responsible for the initial basin opening. _____ 171

Fig. B 8: Seismic cross section imaging the central part of Lake Ohrid. Colored lines and respective numbers from 1-12 indicate the chronological interpretation related to the Marine Isotope Stages. Dark grey area indicates bright spot. The inferred strike slip fault in between the Central Basin faults is marked that is most likely responsible for the initial basin opening. _____ 173

Fig. B 9: Seismic cross section imaging the central part of Lake Ohrid. Colored lines and respective numbers from 1-12 indicate the chronological interpretation related to the

Marine Isotope Stages. Dark grey area indicates bright spot. The inferred strike slip fault in between the Central Basin faults is marked that is most likely responsible for the initial basin opening. _____ 175

Fig. B 10: Seismic cross section imaging the southern area of Lake Ohrid. Colored lines and respective numbers from 1-12 indicate the chronological interpretation related to the Marine Isotope Stages. Slide deposits of the prominent Udenisht slide can be found in the western part of the profile _____ 177

Fig. B 11: Seismic cross section imaging the internal sedimentary structure of the western margin. Colored lines and respective numbers from 1-12 indicate the chronological interpretation related to the Marine Isotope Stages. Slide deposits of the prominent Udenisht slide can be found in the southern part of the profile. _____ 179

Fig. B 12: Seismic cross section imaging the internal sedimentary structure starting in the south toward the Lini fault. Several slide deposits can be found in the southern area. Colored lines and respective numbers from 1-12 indicate the chronological interpretation related to the Marine Isotope Stages. Toward the north an increase in faulting can be observed._____ 181

Fig. B 13: Seismic cross section crossing Lake Ohrid from south to north imaging the overall sedimentary structure of the basin. Several slide deposits can be found in the south. The central basin is characterized by thick undisturbed sediments. Colored lines and respective numbers from 1-12 indicate the chronological interpretation related to the Marine Isotope Stages. The inferred strike slip fault in between the Central Basin faults is marked that is most likely responsible for the initial basin opening. In the northern area the active Gorenci fault is detectable on the profile. Extensive faulting evidenced can be observed by numerous normal faults offsetting the syn-tectonic infill. _____ 183

Fig. B 14: Seismic cross section crossing Lake Ohrid from south to north imaging the overall sedimentary structure of the basin. Colored lines and respective numbers from 1-12 indicate the chronological interpretation related to the Marine Isotope Stages. The active Gorenci fault is present in the north._____ 185

Contents

Abstract ..... **vii**

Kurzfassung ..... **ix**

Table of Figures ..... **xiii**

1 Introduction **21**

1.1 Objectives 21

1.2 Thesis outline 23

2 Lake Ohrid **27**

2.1 Hydrology and Climate 27

2.2 Geological evolution and tectonic framework 29

2.3 Active tectonics 34

2.4 Research at Lake Ohrid 35

2.5 SCOPSCO – ICDP Campaign 38

3 Data and Methology **41**

3.1 Acquisition of sediment echosounder and multichannel seismic 41

3.2 Processing of multichannel seismic data 42

3.3 Interpretation strategy and seismic facies analysis 43

3.4 Acquisition and processing of multibeam data 44

4 Results **45**

4.1 Internal sedimentary structure – an overview 45

4.2 Lake Floor morphology 47

4.3 Proposed drill sites on the basis of the seismic data set 48

5 Peer-reviewed publications **51**

5.1 Manuscript #1 53

5.2 Manuscript #2 73

5.3 Manuscript #3 93

5.4 Manuscript #4 103

Abstract *105*

Introduction *107*

General Setting *108*

Hydrology and Climate *108*

Geological and Tectonic Framework *110*

Active tectonics and seismicity *111*
Hydro-acoustic Dataset *111*
Results *112*
Seismic facies analysis and stratigraphy *112*
Lake Floor morphology *113*
Basement morphology *115*
Syn-sedimentary faulting *116*
Discussion *117*
Seismic chronology of the central basin *117*
Accumulation rates and ages of the basin infill *119*
Tectono-sedimentary evolution *119*
Active tectonics and comparison with onshore data sets *120*
Tectonic development of the Lake Ohrid basin *121*
Geodynamic context of basin development *123*
Conclusion *124*
Acknowledgement *126*
References *126*
Figures *131*
6 Summary and Outlook 145
Acknowledgement 151
References 153
Appendix 159
Curriculum Vitae 187

1 Introduction

1.1 Objectives

Within the terrestrial realm lakes are excellent sedimentary archives of earth and ecosystem history that are highly resolved in time. Ancient lakes, due to their long existence, further provide important constraints on timing of past climate change, rates of evolutionary change in species, and investigate the timing of pollutant introduction into watersheds (Cohen, 2003). Large scale depositional pattern in rift lakes represent an interplay between tectonic and climatic forces, factors that operate on somewhat different time scales (Carroll and Bohacs, 1999).

Lake Ohrid, probably the oldest lake in Europe, is situated on the Balkan Peninsula (Fig. 1) and could be grouped with rift systems because it is a product of extension and thinning of the crust (Cohen, 2003). Lake Ohrid is a favorable site for a variety of scientific disciplines. For example, analysis of sediment cores suggests that long-term environmental changes and short term events are recorded in Lake Ohrid (Wagner et al. 2010). Tephra layers identified in sediment cores of Lake Ohrid were assigned to distinct explosive eruption of Italian volcanoes suggesting that it is a promising site for tephrochronolgy studies (Wagner et al., 2008c; Caron et al., 2010; Sulpizio et al., 2010; Vogel et al., 2010). Biological studies have shown that Lake Ohrid is a unique water body because it hosts more than 200 endemic species and considering its size it has one of the largest densities of endemism (Albrecht and Wilke, 2008). Several active faults were identified by hydro-acoustic measurements of the upper 50 m of sediments (Wagner et al. 2008b). Subaerial linear step-like fault scarps indicate that the basin is still tectonically active (Reicherter et al. 2011).

Although Lake Ohrid has been investigated intensively a profound knowledge about its origin, age, internal structure and tectono-sedimentological evolution is missing. Therefore, this study will focus on the reconstruction of the tectonic and sedimentary development of Lake Ohrid by using hydro-acoustic methods imaging the internal structure of Lake Ohrid and hence get a better understanding of the following aspects:

- **Initial opening of the basin**

  It has been suggested that Lake Ohrid was tectonically formed during extension that affected the entire interior of Albania since Pliocene times (Wagner et al., 2008b). In a

recent paper it has been proposed that Lake Ohrid opened as a pull-apart basin in a short transtensional phase already during the Late Miocene (Reicherter et al., 2011). However, these hypotheses lack evidences from the area where the opening probably started because it is located offshore. Hydro-acoustic and seismic data sets allow to investigate the morphological structure of the acoustic basement containing useful information of the early stage geometry, related normal faults, and hence reflects the different deformational phases that affected Lake Ohrid since its formation.

- **Age and origin**
  The age of Lake Ohrid is highly debated and age estimations range from 1 – 10 Ma (Albrecht and Wilke, 2008). What does the interpretation of seismic lines of areas where the sediment thickness is as maximum tells us about the limnological age of Lake Ohrid?

- **Tectonic evolution**
  After formation of the basin how did Lake Ohrid evolve to the present shape? Are the faults present in the basin still active and hence the extension still ongoing? What does the hydro-acoustic dataset tells us about the subsidence history of Lake Ohrid Basin? What role does Lake Ohrid play within the South Balkan Extensional Regime at present?

- **Sediment thickness**
  Sediment echosounder profiles of the upper 50 m suggest that Lake Ohrid is filled by thick undisturbed sediments within the central part (Wagner et al., 2008b). However, it is still uncertain what are the maximum sediment thickness and where it is located. Are those sediment successions suitable as a site for a deep drilling campaign?

- **Sedimentary evolution**
  What kind of sedimentary features are present in the basin that give insights in the sedimentary evolution of Lake Ohrid? Did Lake Ohrid experience lake level fluctuations and what are the evidences for those changes on multichannel seismic profiles? Are those changes in the hydrological regime tectonically or climatically induced or even both? Did the lake exist continuously or can we find evidences for major nondepositional/erosional phases?

- **Mass movement events and natural hazards**
  Indications for mass wasting were found onshore and offshore of Lake Ohrid (Wagner et al., 2008b, Reicherter et al., 2011). This thesis will put constraints on the location, sizes, and volumes of such slide bodies. What are possible trigger mechanisms of such sliding events? Do they have the potential to trigger tsunamis within Lake Ohrid?

- **Potential of Lake Ohrid for a deep drilling**
  Where would be, according to our data, the best suitable sites for obtaining a long continuous sediment record are? What are additional sites suitable to refine interpretation of the tectonic activity, hydrological regime, and lake level fluctuations?

1.2 Thesis outline

Chapter 2 provides an introduction to the regional setting of Lake Ohrid. It describes the hydrology and climate (chapter 2.1), the geological evolution and tectonic framework (chapter 2.2), active tectonics (chapter 2.3), summarizes research activities prior to this study (chapter 2.4), and presents the main goals of the SCOPSCO ICDP project (chapter 2.5).

Chapter 3 gives an overview about the acquisition and processing of the hydro-acoustic data set as well as the interpretation strategy. The main results of the thesis are presented in **chapter 4.** The internal structure of Lake Ohrid revealed by interpretation of the sediment echosounder profiles and multichannel seismic lines are highlighted in chapter 4.1. Chapter 4.2 presents the main morphological features identified on the bathymetry map. Chapter 4.3 briefly discusses drill sites, which have been proposed to ICDP based on the seismic data presented in this thesis.

Chapter 5 contains three peer-reviewed publications and one submitted manuscript. Chapter 5.1 presents a publication examining the impact of lake level fluctuations on the biodiversity in Lake Ohrid in detail. Terrace structures within Ohrid Bay indicate a change in the base level during Quaternary. Interpretation of sedimentological data extracted from a core taken within this area reveals that the lake level was not constant since the penultimate glacial period but it changed less significant than described for other lakes, e.g. within tropical regions (e.g. Scholz et al., 1995). The fact that Lake Ohrid is bounded by steep margins on each side makes it very unlikely that broader areas were exposed during lake level lowstands and lake level fluctuations had probably only a minor effect on the habitat of the endemic

species. However, it will be further investigated that Lake Ohrid experienced major lake level changes since its formation as evidenced by clinoform structures mapped in the southern area.

A neotectonic study integrating onshore and offshore data sets of the broader area of the Lake Ohrid basin is presented in chapter 5.2. It examines fault structures that are observable in the landscape via the naked eye as well as faults measured by paleostress analysis. K. Lindhorst is co-author and distributed two multichannel seismic profiles and their interpretation of two important sites where active faulting can be studied within the lake. The first example shows a half-graben structure where an alternation of slides and hemipelagic sediments and a tilting of strata indicate several phases of subsidence and quiescence of the adjacent fault. The second example images slides in close vicinity of the major active Lini fault along the western margin suggesting that it is a favorable site to study paleoseismicity within Lake Ohrid basin.

Mass movement events are common in Lake Ohrid, especially in the southern area where numerous events have been detected at different stratigraphic levels. A detailed description of the morphological structure of a major sliding event covering almost 10 % of the entire lake floor is given in chapter 5.3. The origin and possible trigger mechanisms of this major sliding event will be examined. Furthermore, the tsunami potential of subaquatic slides within Lake Ohrid Basin will be discussed.

While chapters 5.1 to 5.3 are very specific in terms of the aspects they are presenting, chapter 5.4 summarizes the tectonic and sedimentary history of Lake Ohrid. The manuscript displays and interprets new geophysical data that was collected during several surveys at Lake Ohrid. Seismic cross sections image the complex internal structure of the basin. Thick undisturbed sediments are present within the central part of the basin. The northern area is characterized by extensive faulting and has been found to be a very active region with horst and grabens forming during the Quaternary. The same is true for the margins bounding Lake Ohrid on the western and eastern side. The southern area is delineated by several mass movement events in combination with active faulting especially along the eastern major boundary fault zone. A newly formed active sub-basin, the Gradiste basin, is an important area within Lake Ohrid as it was probably disconnected from the main basin during its formation. Therefore, it may be of major importance for the biodiversity evolution within Lake Ohrid.
One major outcome is a map showing major active and inactive faults and their continuations onshore. A model highlighting the initial opening of Lake Ohrid as a pull-apart basin during a transtensional phase is presented and evaluated based on tectonic interpretation. Furthermore,

a seismic chronological scheme for the central part of the basin is developed interpreting the alternating high and low amplitude reflectors in terms of a climatically induced signal that can finally be linked back to MIS 12. Subsequently, an improved calculation of sedimentation rates for Lake Ohrid results in a better estimation of the maximum age of the basin and suggests that the limnological age is not much greater than 3 Myr. The overall outcomes of the study will be summarized in **chapter 6** followed by an outlook to future work at Lake Ohrid.

2 Lake Ohrid

2.1 Hydrology and Climate

Lake Ohrid (41°01´N, 20°43´E) is a transboundary lake located on the Balkan Peninsula with two thirds of its area belonging to the Former Yugoslavian Republic of Macedonia (only named Macedonia in the following) and one third to Albania (Fig. 1). The lake is situated in a tectonically active graben system of South Balkan Extensional Regime (SBER; Fig. 2;

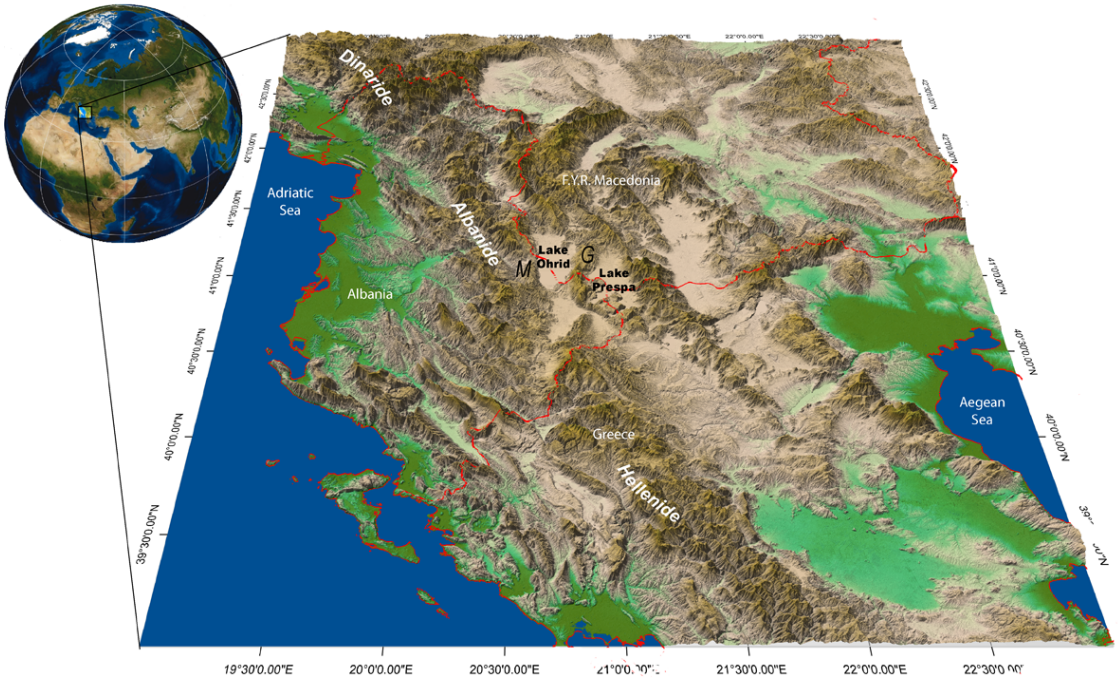

Fig. 1: Overview map of the surrounding area of Lake Ohrid and its sister Lake Prespa on the Balkan Peninsula. M: Mokra Mountain Chain, G: Galicica Mountain chain. The globe in the upper left corner shows the overall location of the area.

Burchfiel et al., 2008); current lake level is at 693 m above sea level (a.s.l.).

Lake Ohrid has a length of about 30 km and a width of 15 km with an area of 360 km² (Fig. 3, Stankovic, 1960). It has a very simple bathtub shape morphology with average water depths of 150 m and a total volume of 50.7 km³ (Popovska and Bonacci, 2007). The lake is surrounded by high mountain chains on each side: Mokra Mountain in the west and Galicica Mounatin in the east reaching heights of 2300 m a.s.l. Although an increase of phosphorus leads to progressing eutrophication, Lake Ohrid is still classified as oligotrophic (Matzinger et al., 2007). Water enters Lake Ohrid by some rivers (Fig. 3, Sateska in the north and Cerava in

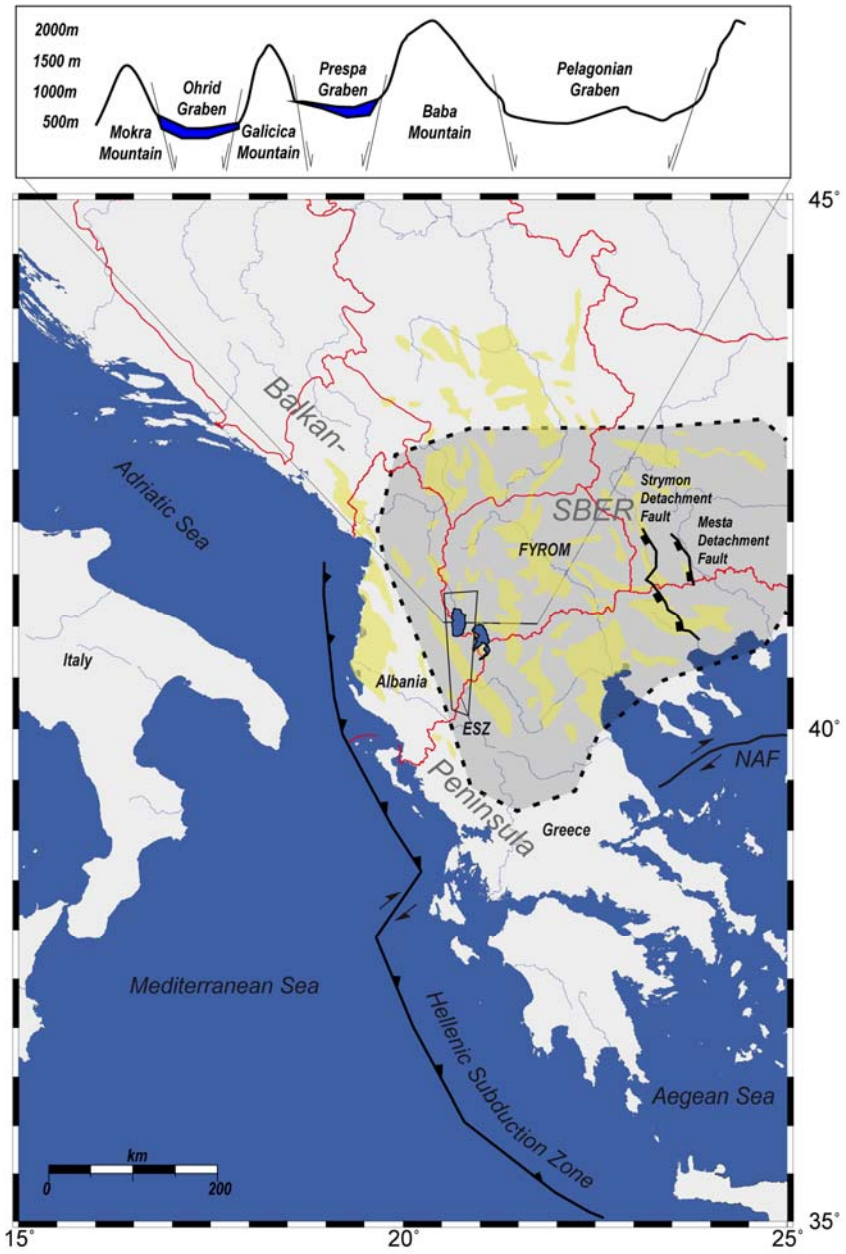

Fig. 2: Map showing the Balkan Peninsula and the location of Lake Ohrid and its sister Lake Prespa. Grey shaded area marks the South Balkan Extensional Regime (SBER). Location of the Mesta and Strymon detachment faults are shown (modified after Burchfiel et al. 2003, 2008b. Location of the Hellenic subduction zone and the North Anatolian Fault (NAF) is given. ESZ: Earthquake source zone (Aliaj et al. 2004)

the south), karstic springs both sublacustrine (49%) and surface springs (51%), and direct precipitation (Matzinger et al., 2006b). Five main areas of such sub-aquatic springs have been described so far: Kalista, Kaneo, Elesec, Veli Dab, and Sveti Naum (Fig. 3, Albrecht and Wilke, 2008; Matter et al., 2010). Surface springs can be found within the spring lake at Sveti Naum Monastry and sister spring complex Zagorican/Tushemist; some minor springs can be

found in the northern area of Lake Ohrid (Fig. 3; Popovska and Bonacci, 2007; Albrecht and Wilke, 2008). The river River Sateska was artificially diverted in 1962 resulting in a reduction of the river discharge (Matzinger et al., 2006b). Karst aquifers charged from precipitation on the surrounding mountain ranges and from Lake Prespa, form up to 50% of the net inflow today (Matzinger et al., 2006b).

Lake Ohrid has a relatively small catchment area (2600 km²) or even smaller if one excludes the sister Lake Prespa (1002 km², Popovska and Bonacci, 2007). Water leaves Lake Ohrid through the River Crn Drim (~60%) and by evaporation (~40%; Watzin et al., 2002; Matzinger et al., 2006b). The climate today is influenced by both Mediterranean and continental conditions due to its location in a high mountain range adjacent to the Adriatic Sea (Fig. 1; Watzin et al., 2002). The lake never freezes (Popovska and Bonacci, 2007). Average annual water temperatures are around 11°C and summer air temperatures reliably less than 23°C (Popovska and Bonacci, 2007). Belonging to the Mediterranean pluviometric regime, the Lake Ohrid region shows a precipitation pattern that is highest during winter and lowest during summer (Watzin et al., 2002). Prevailing northerly wind directions drive a counter clockwise surface current, which is the main driver of particle transport in Lake Ohrid (Matzinger et al., 2006b; Vogel et al., 2010b).

2.2 Geological evolution and tectonic framework

The area of Lake Ohrid is part of the Dinaride-Albanide-Hellenide mountain system of the Balkan Peninsula (Fig. 1) that formed during a later phase of the alpine orogeny as a result of the final closure of the Tethyan Ocean. The detailed tectonic development of the area is still strongly debated due to difficulties in interpreting complicated geological assemblages (Robertson and Dixon, 1984; Robertson et al., 1996; Robertson, 2012). Reconstructing tectonic development of the area is further complicated by the nomenclature of geological units as they differ depending on the nationality of the author or the study area, mainly between Albania and Greece. There is nonetheless general agreement that main geological units reflect: (i) opening and closure of the Paleotethys, a large ocean separating Laurasia and Gondwana during the Paleozoic, (ii) rifting, drifting of microcontinents from Gondwana with subsequent subduction and final closure of the Tethys during the Mesozoic, and (iii) the development of sedimentary basins within the South Balkan Extensional Regime (SBER; Fig. 2). Paleozoic metamorphic and magmatic rocks forming the basement rocks around Lake

Ohrid are related to the existence of a now-disappeared large ocean called the Paleotethys (Fig. 4A; Fig. 5; Reicherter et al., 2011; Robertson, 2012). The basin hosting Lake Ohrid was formed at the boundary of two major geological units: Pelagonian Zone and Pindos Zone (Fig. 5A). The exact origin and mode of emplacement is still highly debated (Robertson et al., 1996; Robertson, 2012). Mesozoic metamorphic and magmatic rocks also occur around Lake Ohrid (Fig. 5B). Mesozoic granites are most likely related to an ancient subduction zone (Robertson, 2012). The Pelagonian Zone is seen as a remnant of continental crust that rifted from Gondwana and then drifted away northwards until it got accreted either northward beneath Eurasia or southward beneath Gondwana depending on the geodynamic model (Fig. 4; Fig. 5; Robertson et al., 1996; Robertson, 2012). An alternative interpretation relates the drifting to the northward subduction beneath Eurasia whereas the Paleotethys, which is located southward, got consumed by northward and/or southward subduction (Robertson, 2012). A different model describes Pelagonia as a promontory of Gondwana which got exhumed during the post-collisional phase after the Paleotethys already had closed (Robertson, 2012).

Ophiolites of Jurassic age belonging to the Pindos Zone were mapped along the western side of Lake Ohrid (Fig. 5). The Pindos Zone is located between the conjugate passive margin sequences evidenced by karstified Triassic carbonates and clastics of the microcontinents Apulia and Pelagonia on the west and east, respectively (Fig. 4; Fig. 5; Robertson et al., 1991; Dilek et al., 2006; Ghikas et al., 2010; Reicherter et al., 2011). Therefore, a restricted ocean basin, the Pindos Ocean, is assumed to have existed between the Apulian and the Pelagonian continent (Robertson et al., 1991). The Vardar Ocean existed simultaneously farther to the east of the Pelagonian microcontinent (Fig. 4). Ophiolites were first emplaced eastward onto the western margin of the Pelagonian Zone in Late Jurassic as a result of a trench-continent collision, then westward caused by final collision of Africa and Eurasia in Middle Paleogene (Fig. 4; Robertson et al., 1991; Ghikas et al., 2010).

Macedonia and Albania are part of the SBER which experienced three phases of extension leading to the formation of numerous sedimentary basins with progressively younger ages toward the west (Fig. 2; Dumurdzanov et al., 2005; Burchfiel et al., 2008b). These three extensional phases took place during (1) Paleogene, most likely connected to the final closure of the Vardar Ocean, (2) Early to Late Miocene, related to roll back at the Hellenic subduction

slab, and (3) Late Miocene to Recent, connected to processes at the Hellenic trench but additionally influenced by the onset of the North Anatolian Fault zone.

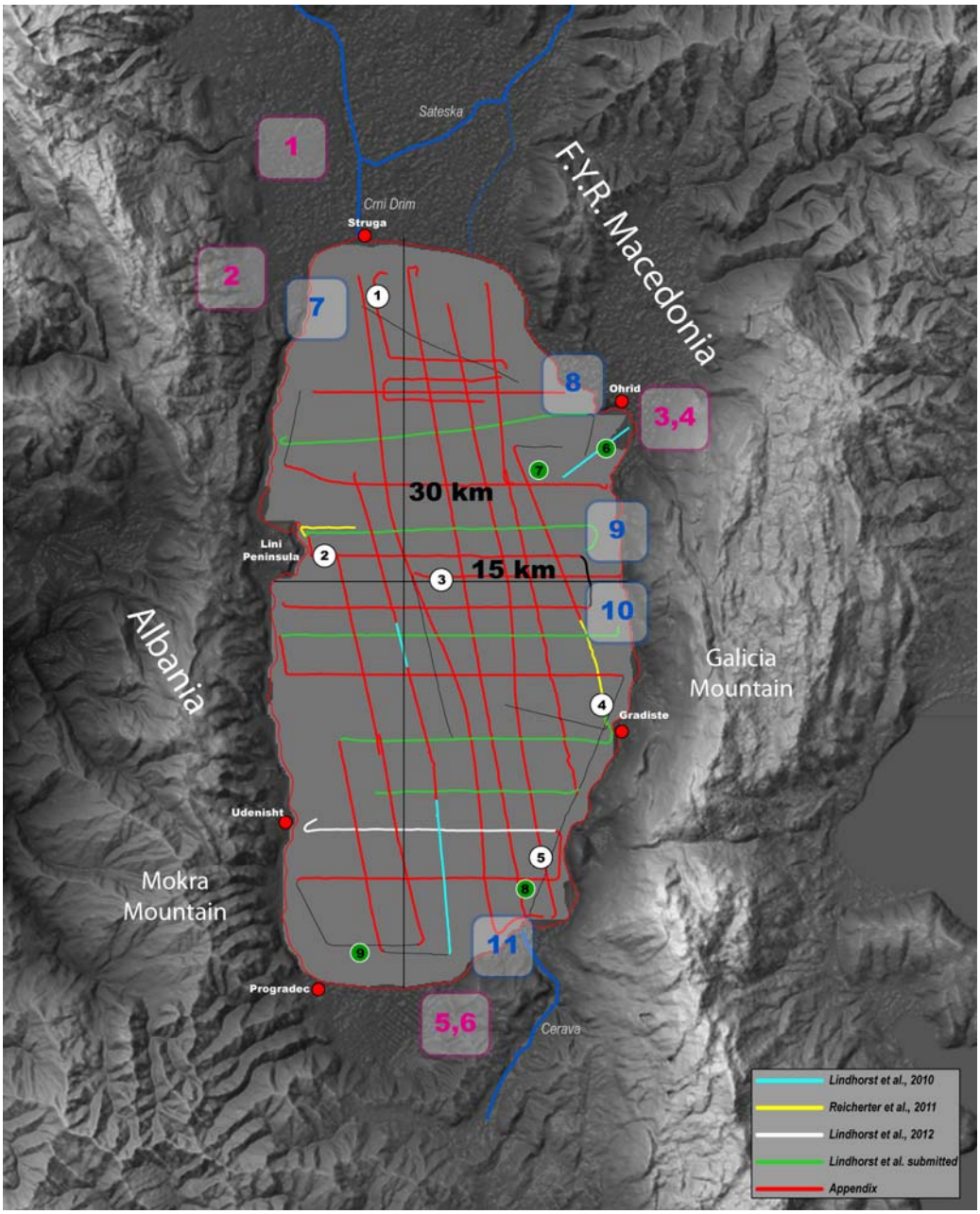

Fig. 3: Lake Ohrid and its adjacent mountain chains Mokra Mountain in the west and Galicica Mountains in the east. The main populated areas are marked with red dots. Pink areas show the subsurface springs: (1) Sum, (2) Dobra Voda, (3) Bej Bunar, (4) Bijana, (5) Tushemisht, and (6) Zagorican (Albrecht and Wilke, 2008). The subaquatic springs are shown in blue: (7) Kalishta, (8) Kaneo, (9) Elesec, (10) Veli Dab, (11) Sveti Naum (Matter et al. 2010). White dots are proposed drill sites: (1) Struga, (2) Lini, (3) DEEP, (4) Gradiste, and (5) Cerava (see chapter 4.3 for details).Green dots are sediment cores retrieved within Lake Ohrid: (6) CO 1200, 1201, (7) CO1202, (8) Lz1120, and (9) JR2004 (see chapter 2.4 for details). Red lines are multichannel seismic tracks.

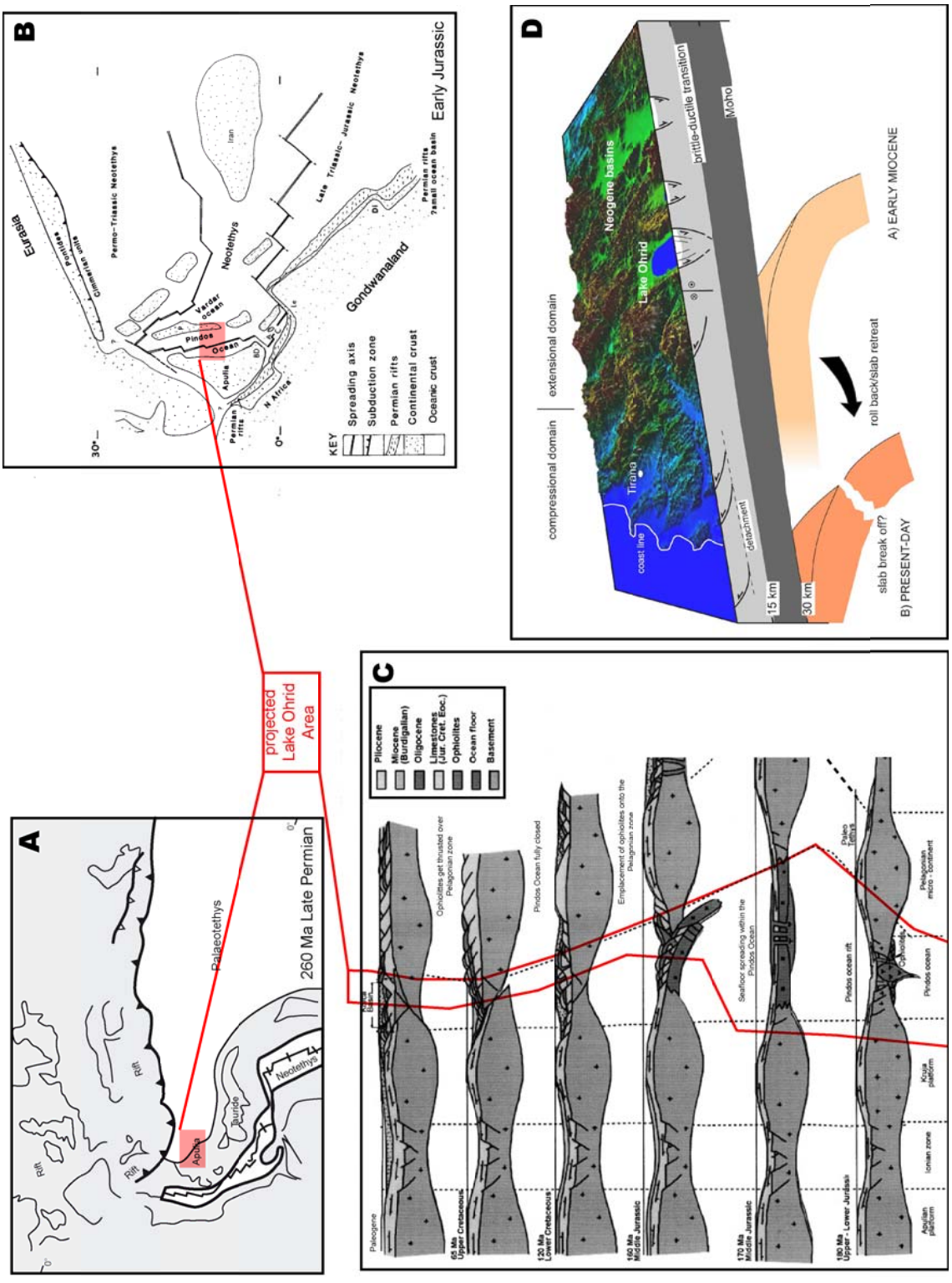

Fig. 4: Sketches illustrating the tectonic evolution (A) until the Late Paleozoic time within a Paleotethys environment, (B) during Mesoic time when microcontinents drifted northward away from Gondwana and the Pindos Ocean opened, (C) evolution through time of the Lake Ohrid Area, and finally (D) since the Miocene to present with interpretation of the subdug slab. Modified after: (A) Robertson 2012, (B) Robertson et al. 1991, (B) Nieuwland et al. 2001, (D) Hoffmann et al. 2010.

(NAF, Fig. 2, Burchfiel et al., 2008b). Since late Pleistocene time two extensional systems act more or less independently with an overlap zone in eastern Macedonia and NW Greece: (1) an E-W extension in western Macedonia and shortening in western Albania caused by convergence of the north Hellenic trough, and (2) a westward migrating N-S extension related to geodynamic processes at the south Hellenic trough (Burchfiel et al., 2008b).

As Lake Ohrid is located in the western part of the SBER it is one of the younger sedimentary basins (Aliaj et al., 2001; Burchfiel et al., 2008a). It was probably formed during the third phase of extension but mostly related to the continued rollback of the Hellenic subduction slab (Reicherter et al., 2011). It is likely that the Ohrid Basin was only slightly influenced by the development of the North Anatolian Fault (Fig. 2, Hoffmann et al., 2010; Reicherter et al., 2011).

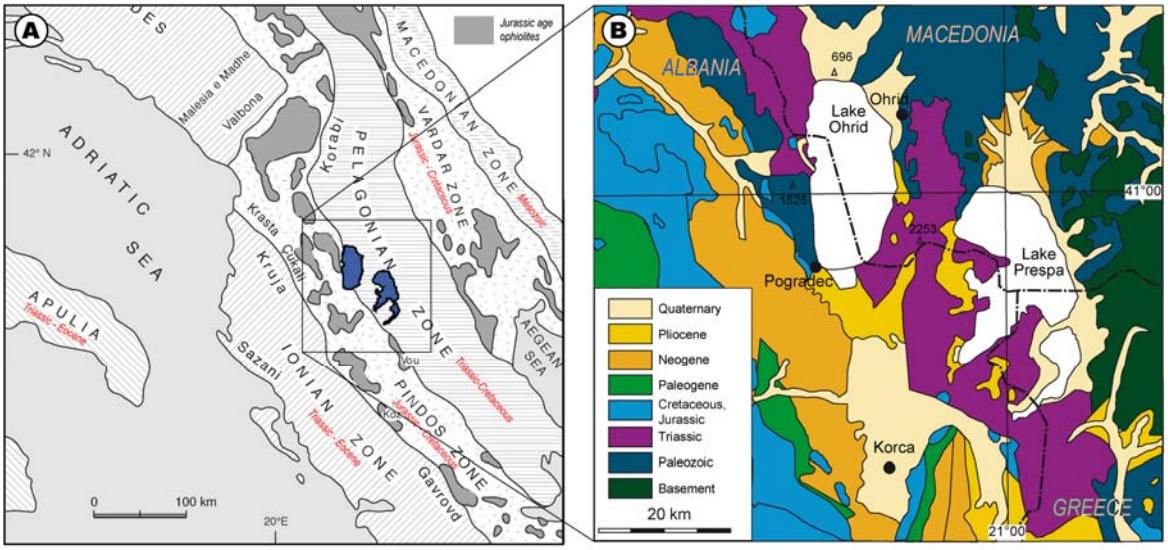

Fig. 5: (A) Geological units and their ages within the broader area of Lake Ohrid (modified after Dilek et al., 2006). (B) Geological map of Lake Ohrid area (modified after Wagner et al., 2008b).

Burchfiel et al. (2008b) proposed the existence of major westward dipping detachment faults in the eastern region of the SBER, referred to as Mesta and Strymon detachment faults (Fig. 2). The Strymon fault is a branch of the Mesta fault. It developed subsequently to deactivation of the eastern part of the Mesta fault. This pattern of fault migration within the SBER is similar to the Basin and Range province in western United States (Lister and Davis, 1989). According to this model, the sedimentary basins farther west, including the Ohrid

Basin, could have formed within the hanging wall of the Strymon detachment fault, but such geometry has not been identified in the field yet (Burchfiel et al., 2008b).

Extensional tectonic movements since the Pliocene led to subsidence and the formation of graben-shaped Quaternary lakes like Lake Ohrid and its sister lake Prespa (Aliaj et al., 2001). Lake Ohrid is situated in a NE-SW oriented graben structure extending from the Korca plain to north of Lake Ohrid (Fig. 1, Aliaj et al., 2001; Burchfiel et al., 2008b). Dumurdzanov et al. (2004) described four main alternating periods of rapid and slow subsidence associated with distinct sedimentation patterns within the sedimentary basins. They suggested that the formation of the Ohrid and Prespa basin occurred during late Miocene – Pliocene times. Uplift of the surrounding areas and subsidence of the Korca and Pogradeci plains caused the formation of a deep graben bounded by normal faults in the east and west (Fig. 2 and 5). This graben structure eventually became the origin for Lake Ohrid. According to Dumurdzanov et al. (2004) Lake Ohrid and Lake Prespa are remnants of an extensive Pleistocene lake system. The actual age and onset of the limnological phase of Lake Ohrid is unknown today. This thesis addresses this issue, providing important constraints relevant for a better understanding of the biogeographical history of the lake and the evolution of its inhabitants (Stankovic, 1960, Albrecht and Wilke, 2008).

2.3 Active tectonics

Lake Ohrid and the surrounding area belong to the Western Macedonian seismic zone (Aliaj et al., 2004). The Ohrid and Korca depressions are located within a N-S directed Earthquake Source Zone (ESZ, Fig. 2) as defined by Aliaj et al. (2004).

The terrains of western Macedonia and the Pelagonian horst are the most lifted ones with the main active faults zones striking NE-SW to ENE – WSW with length of 40-60 km and segments of 10-30 km in length (Fig. 2; Arsovsky and Hadzievsky, 1970; Mountrakis et al., 2006). Several medium to large earthquakes have occurred within the last 2000 years such as the 518 AD event that nearly destroyed the entire cities of Ohrid and Skopje (Arsovsky and Hadzievsky, 1970; Hoffmann et al., 2010), the 1896 and 1912 events at Lake Ohrid had Magnitudes of 6.4 and 5.0, respectively (Arsovsky and Hadzievsky, 1970; Ambraseys and Jackson, 1990; Muço et al., 2002). According to the catalog of Significant Worldwide Earthquakes (NOAA) was the 1911 event (M=6.7), located at a fault in the southeastern area in close vicinity to Lake Ohrid (Fig. 6). The most destructive earthquake in the younger

history of Macedonia in 1963, close to the capital city Skopje (M=6.1, Suhadolc et al., 2004). Major events in direct proximity to Lake Ohrid were recorded for example on April 7th, 2004 (M_w=5.0), November, 23th 2004 (M_w=5.5), and September, 6th 2009 (M_w=5.6, Fig. 6). Three moderate events from June 2012 are added to the map in Figure 6. They demonstrate that the area around Lake Ohrid is one of the most active areas on the Balkan Peninsula (Wagner et al., 2008b; Hoffmann et al., 2010; Reicherter et al., 2011).

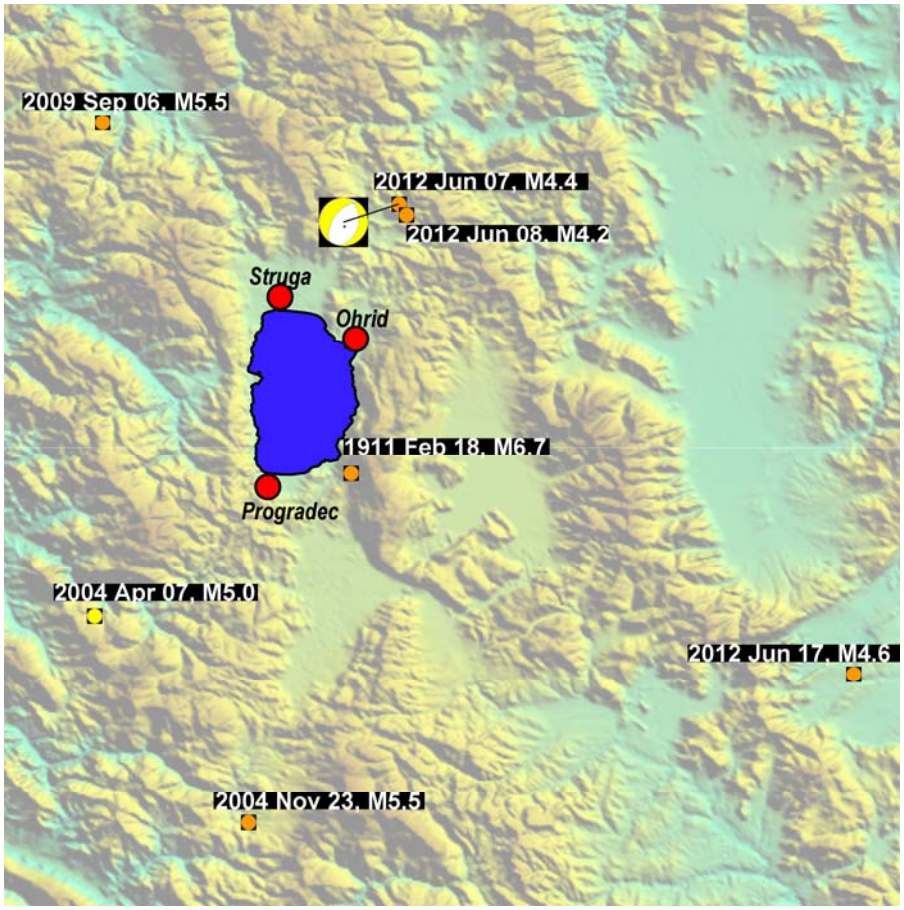

Fig. 6: Map showing location of significant major earthquakes (M>5) including the most recent ones from June 2012 around Lake Ohrid (downloaded from http://earthquake.usgs.gov/earthquakes/eqarchives/epic/ accessed on June 19th, 2012)

Seismicity is mainly concentrated along N-S trending Pliocene – Quaternary normal faults on the eastern and western side of the Ohrid basin, usually in depths of about 10 km (Aliaj et al., 2004; Hoffmann et al., 2010). Paleostress analysis revealed a synthetic fault plane solution for the Lake Ohrid region fitting in the E-W extensional domains associated with Neogene basins and normal faults of the SBER (Dumurdzanov et al., 2005; Reicherter et al., 2011).

2.4 Research at Lake Ohrid

Research at Lake Ohrid is going on for more than 100 years. In this chapter I want to give a short overview about studies conducted at and around Lake Ohrid and their contributions for a better understanding of this unique water body.

A detailed description of the historical evolution of research activity at Lake Ohrid is provided by Albrecht and Wilke (2008). Lake Ohrid has been recognized as a peculiar lake by two zoologists from Vienna at the end of the 19th century (Albrecht and Wilke, 2008). The geology, geomorphology, and limnology of Lake Ohrid were intensively studied by Cvijic (1865-1927). He stated that Lake Ohrid is of tectonic origin and formed in the Pliocene (2-5 Ma; Cvijic, 1911). Unfortunately, Cvijic only published his results in Serbian language. Another outstanding publication that has to be mentioned is Stankovic (1960), who founded the Hydrological Institute in Ohrid in 1935 (Albrecht and Wilke, 2008). Beside an overall description of Lake Ohrid and its surrounding area he also summarized findings from previous studies. During the last decade research at Lake Ohrid in multiple disciplines made significant progress that subsequently led to a better understanding of the hydrology and limnology (Spirkovski et al., 2001; Matzinger et al., 2006a; 2006b; 2007; Popovska and Bonacci, 2007), geological and tectonic processes (Dumurdzanov et al., 2004; 2005, Burchfiel et al., 2008a; 2008b), and the biodiversity, endemism, and evolution of the inhabitants of Lake Ohrid as summarized in Albrecht and Wilke (2008 and references therein).

Recent sedimentological studies have shown that Lake Ohrid is a valuable archive not only for investigating its biodiversity but also for reconstructing the paleoenvironment on a long-term basis (Wagner et al., 2008a; 2008b; 2008c; Vogel et al., 2010a; 2010c). First hydro-acoustic data by means of sediment echosounder revealed that the central basin host undisturbed sediments. On the basis of these seismic profiles three sites (northeastern central basin CO1202, southeast Lz1120, and southwestern part located in Albania JO2004, see Fig. 3 for location of cores) were picked to drill short sediment cores dating back to the penultimate glacial stage. The karstic system was most likely completely interrupted and inactive during the last glacial period due to the formation of permafrost in large parts of the calcareous mountains (Belmecheri et al., 2009; Lézine et al., 2010). Analysis of the lithological, sedimentological, geochemical, physical properties, and stable isotopes of cores revealed enhanced productivity during interglacials and a cold climate with relatively stable low productivity during glacial (Vogel et al., 2010a; Leng et al., 2010). Furthermore, vegetation in the last 40 kyr around Lake Ohrid changed from forest dominated during warm (Interglacials) to steppe-like in cold (glacial) periods (Wagner et al., 2008c). Holtvoeth et al. (2010) analyzed biomarkers in CO1202 and Lz1120 and concluded that this method would be suitable to reconstruct the vegetation cover in Lake Ohrid which will then be applied to deep cores after the ICDP campaign took place. Tephras layers related to explosive eruptions of the

Italian Volcanoes have been identified within the sedimentological record (Fig. 7; Wagner et al., 2008c; Caron et al., 2010; Sulpizio et al., 2010; Vogel et al., 2010c). Tephrochronology is an important method applied to sediment cores retrieved in Lake Ohrid because the lake is located eastwards of the Italian Volcanoes (Fig. 7) and hence acting as a valuable terrestrial archive for ash dispersals of prominent Quaternary explosive eruptions (Paterne et al., 1988; Sulpizio et al., 2003; Wulf et al., 2004).

To better understand the nomenclature of the tephras layers a short excursion is included here. Tephra layers found in a specific horizon are labeled according to the foraminiferal zone of the horizon they occurred in (from U to Z – from oldest to the most recent) and a number where as for example Y-1 would be younger than Y-2 (Keller et al., 1978). Vogel et al. (2010c) identified 10 tephra horizons within the 15 m long core CO1202 (see Fig. 3 for core location). Core JO2004 within the southern region of Lake Ohrid analyzed by Caron et al. (2010) contained five tephras layers that could successfully correlated with terrestrial proximal counterparts and with both marine and lacustrine tephras already known in the central Mediterranean area (see Fig. 3 for core location). In Lake Ohrid the most prominent ash layers are the Y-3, Y-5, X-6 originating from Campi Flegrei with ages of 32 kyrs, 40 kyrs, 107 kyrs, respectively, and P-11 (131 kyrs) representing deposits of an eruption on the island Pantelleria (see Fig. 7 for location).

Fig. 7: Map showing the Italian Volcanoes that are potential sources for ash layers identified in Lake Ohrid (modified after Giaccio et al.,. 2008).

In addition two ash layers could be correlated associated to deposits of the Green Tuff from the Pantelleria Island (Y-6) with an estimated age of 51 kyrs, as well as another eruption from the Campi Flegrei Caldera (X-5, 105 kyrs, Vogel et al., 2010c). The P-11 tephra layer is the

oldest so far identified in Lake Ohrid; it testifies that extensive ashes can disperse over a distance of 900 km and are still thick enough to be found in lacustrine deposits (Sulpizio et al., 2010). Furthermore, some of the tephra layers are recognized for the first time on the Balkan Peninsula (Caron et al., 2010). They are of great importance for analyzing the explosive history and subsequent ash dispersal patterns of Italian volcanoes.

Although the location of Lake Ohrid east of the Adriatic Sea is somehow favorable for the deposition of ash layers, they only occur as very thin (<5 cm) sediment layers or even cryptotephras (fine dispersed tephras layers) due to the fact that the lake is located at some distance from the source volcanoes. Nevertheless, it has been proven that they are suitable to exactly date certain sediment layers as those tephras are very specific for a distinct eruption (Giaccio et al., 2008). Therefore, tephrostratigraphy and tephrochronology are promising methods for constructing a chronological model for Lake Ohrid in deep sedimentary cores.

Sedimentation during glacials is dominated by detrital clastic material and frequent occurrences of dropstones; warm periods on the other hand that are characterized by deposition of high amounts of carbonates and low amounts of clastic detritus (Vogel et al., 2010c). Sedimentation rates increase during glacial periods due to a high input of terrestrial material from the catchment area in contrast to deposition that is biogenic induced and hence slower (Vogel et al., 2010c).

The high density of endemism within Lake Ohrid attracts biologist in order to understand the evolution of the inhabitants of the lake and the impact of geological and environmental factors on these species. A conference on speciation in ancient lakes was held in Ohrid in September 2009. A special issue on the evolutionary and geological history of Balkan lakes Ohrid and Prespa published in Geobiosciences in 2010 shows the close connection of all research fields (Wagner and Wilke, 2010).

2.5 SCOPSCO – ICDP Campaign

In this section I will shortly introduce the project Scientific Collaboration On Past Speciation Condition in Lake Ohrid (SCOPSCO) because major outcomes of this thesis were of great importance for the preparation for a deep drilling campaign within the International Continental Drilling Program (ICDP) which is supposed to start in September 2012.

The major objectives of the SCOPSCO project are (i) to shed light on the actual age and origin of Lake Ohrid, (ii) obtain essential information on major geological, environmental, and climatic changes during the entire Quaternary, and (iii) as Lake Ohrid has been proven to be a unique site with respect to its high endemism density, to unravel the driving forces for biotic evolution.

From geological point of view the sedimentary succession of Lake Ohrid preserves essential information on seismic activity, changes in the vegetation of the surrounding area related to climate changes, as well as tephras and cryptotephra layers of Italian volcanoes. Previous sedimentological investigations of short cores (<20 m) covering the last glacial/interglacial cycle already provide information on large scale environmental changes and short term events, such as the Heinrich events or changes in the North Atlantic Oscillation.

The science team expects to conduct tephrochronology analysis on the deep cores that allow giving exact dates for distinct sediment layers. This information are essential for the development of an age model for the drilling cores. Although we do not expect to find thick tephra layers with high impedance contrast within the cores it is still possible after identification of tephras to correlate them with our seismic data as has been shown for the Y-5 tephra by Lindhorst et al. (2010, see chapter 5.1).

High resolution seismic and paleostress analysis at several sites along the coast provide evidences for active faulting . Beside the long continuous record proposed within the central part of the basin a site closer to shore penetrating sediments that got affected by neotectonic movement will provide crucial information:

- On the temporal basin evolution of Lake Ohrid that allow a better understanding of processes within the overall extensional regime of the South Balkan region,
- To investigate whether seismic shaking is a possible trigger for mass movements identified within the multichannel seismic data,
- For the reconstruction of slip rates of faults, subsidence phases and rates.

In order to pick the best possible drill site within the lake to fulfill the objectives of the SCOPSCO project, acoustic data were collected at different resolution and penetration. The acquisition, processing, and interpretation of the acoustic data were done in the frame of this thesis.

3 Data and Methology

3.1 Acquisition of sediment echosounder and multichannel seismic

The first sediment echosounder profiles were collected in 2004. Inspired by outcomes of the sedimentary interpretation of these seismic cross sections a first multichannel seismic pre-site survey of the Macedonian part of Lake Ohrid was carried out in 2007. A second multichannel seismic survey was carried out in June 2008. This survey was complemented by acquisition of sediment echosounder and sidescan sonar data. For the first time it was possible to cross the Macedonian-Albanian border using the Macedonian research vessel that is owned by the Hydrobiological Institute in Ohrid (Fig. 8).

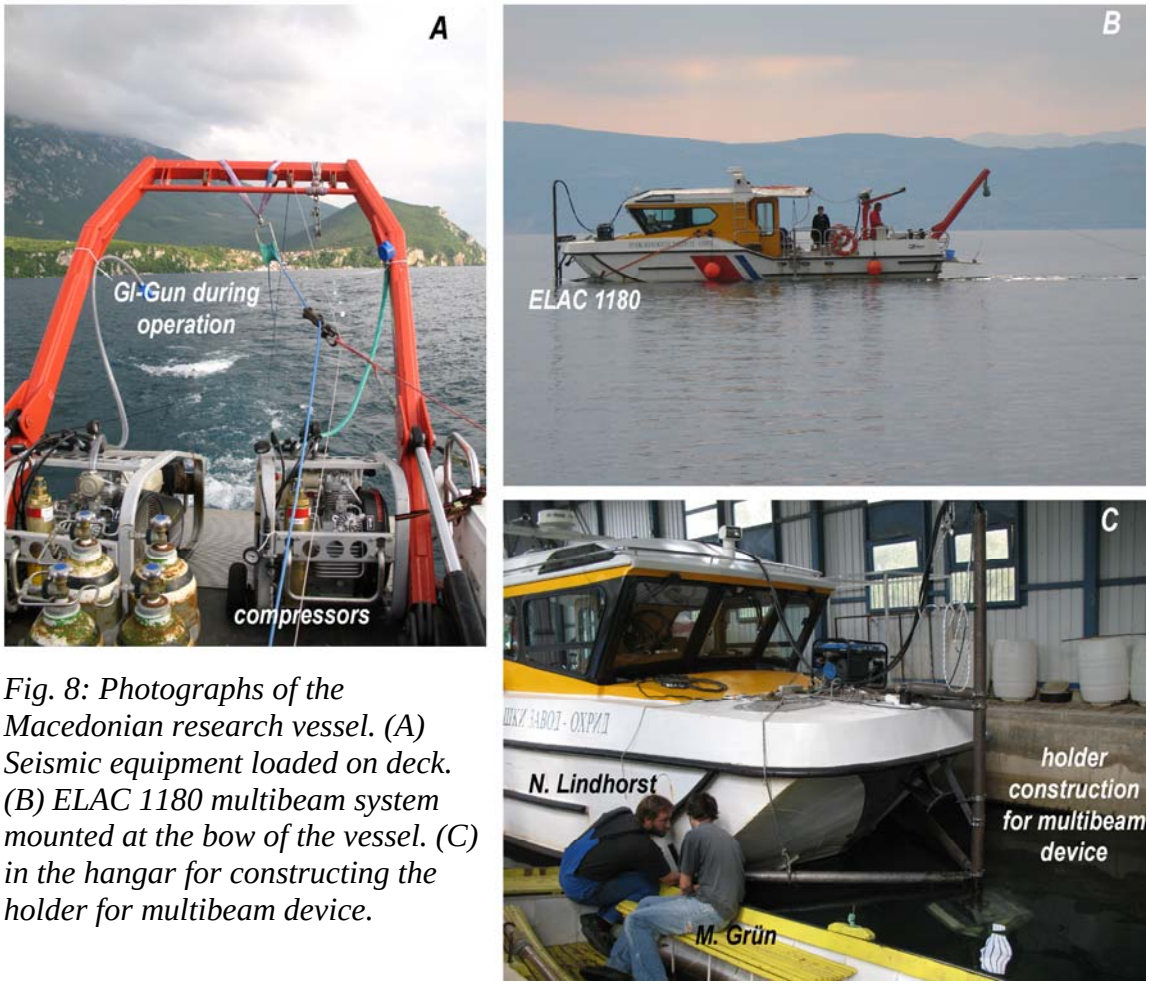

Fig. 8: Photographs of the Macedonian research vessel. (A) Seismic equipment loaded on deck. (B) ELAC 1180 multibeam system mounted at the bow of the vessel. (C) in the hangar for constructing the holder for multibeam device.

A Mini GI-Gun was used as a source with two different volumes (in 2007 0.25 l and in 2008 0.1 l), resulting in a higher resolution of the 2008 data set in contrast to deeper penetration in

2007. Air for the sources was provided by small diving compressors (Fig. 8). The energy was recorded with a 100 m-long, 16 channel streamer from the University of Bremen. In total, 47 seismic lines were collected.

An echosounder system of the Innomar GmbH with a main frequency of 10 kHz was used to collect sediment echosounder data. It was operated simultaneously to the multichannel seismic survey allowing a direct comparison of multichannel seismic data with high resolution images of the uppermost sediment layers. Two adjacent pings were stacked to improve the signal-to-noise ratio. Water depth and sediment penetration were calculated assuming a constant velocity of 1470 m/s. A dense grid of sediment echosounder lines with a spacing of less than 500 m is now available for Lake Ohrid.

Sidescan sonar data were acquired using a Klein 3000 dual frequency sonar with 100 kHz and 500 kHz in 2008. The Ohrid Bay area was mapped between 3 and about 100 m water depth. The sonar was usually adjusted to cover 75–100 m on either side with individual profiles spaced 75–100 m apart. In this way, complete coverage of the working area was achieved. Processing of the data was mainly done by M. Wessels of the Institute for Lake Research in Langenargen.

3.2 Processing of multichannel seismic data

The seismic data was processed using GEDCO VISTA Seismic Data Processing. Geometry was set using special software implemented by Hanno Keil (University Bremen). First processing steps included elimination of erroneous channel and individual traces, static corrections, and band pass filtering (frequent content: 35/60 – 600/900 Hz). We used a constant velocity of 1500 m/s for the normal move-out correction due to the fact that the streamer is quite short considering a maximum water depth of about 300 m. In a final step the data was stacked and a FD time migration was applied in order to increase the spatial resolution by moving dipping reflectors to their true subsurface position and collapse diffractions. One seismic feature we had to struggle with was the high energy of multiple reflectors overlying the actual structures and anticipating interpretation of the subsurface. This was especially disturbing for the purpose of finding the site with the maximum sediment thickness and subsequently deepest acoustic basement favorable for the deep drilling within the scope of the SCOPSCO ICDP campaign. A predictive deconvolution was applied

resulting in the reduction of energy of the uppermost multiple reflectors, but multiples are still clearly visible in the fully processed data.

3.3 Interpretation strategy and seismic facies analysis

For interpretation purposes all seismic data was loaded into IHS KINGDOM Suite software. It allows marking and tracing of prominent horizons over several profiles. By defining arbitrary lines it is further possible to follow sedimentary features identified on a N-S directed profile towards the east or west, respectively. In a first step the acoustic basement was mapped in order to calculate a grid that subsequently allows interpreting major normal faults offsetting the basement. Although IHS KINGDOM software provides a special tool for fault mapping, major normal faults in Lake Ohrid were interpreted by mapping distinct morphological steps within the acoustic basement grid and then cross-checked within individual seismic lines. The software further allows loading in images as overlays as for example a geological, bathymetric, or topographic map on the basemap in order to evaluate interpreted structures.

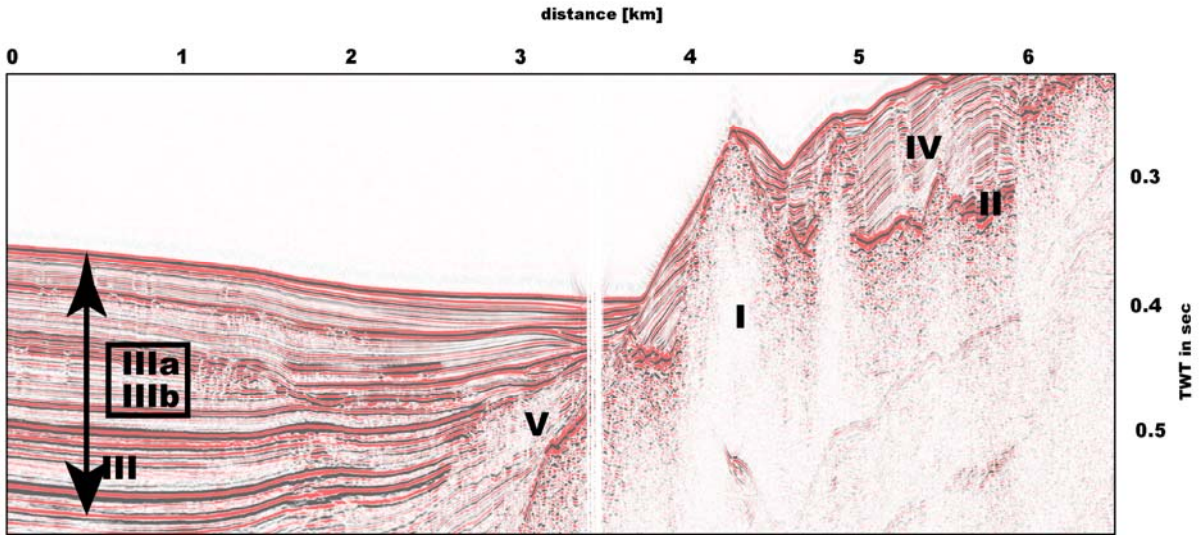

Fig. 9: Seismic cross section (W-E) illustrating seismic facies defined within Lake Ohrid.

In a second step, seismic facies within multichannel seismic lines were defined on the basis of reflection character such as the presence or absence of reflectors, relative amplitude, and their geometrical configuration. Five major seismic facies are present: (I) diffuse incoherent, locally hyperbolic reflections, (II) Sub-parallel, discontinuous high amplitude reflections (III) successive parallel, continuous, and basin-wide reflectors that can further be subdivided in

sub facies of very high amplitudes (IIIa) and medium to low amplitude reflections (IIIb), (IV) rather continuous, parallel to sub-parallel reflections showing a variety of amplitude densities, and (V) transparent bodies with or without internal incoherent reflectors (Fig. 9).

3.4 Acquisition and processing of multibeam data

An additional survey by means of an ELAC Seabeam 1180 multibeam system was carried out in 2009. The system uses 126 beams with a total opening angle of 153° and operates at a frequency of 180 kHz. A special frame for the holder construction had to be built in order to vertically attach the two transducers at the bow of the Macedonian research vessel in approximately 1 m water depth (Fig. 8). An OCTANS IV motion sensor measured roll, pitch, and heave in order to correct the ship movement. Sound velocity profiles (VSP) are critical for ray tracing and where therefore taken at different locations in Lake Ohrid. After calibrating the system, the bathymetry of Lake Ohrid was successfully measured in water depth greater than 50 m. The Ohrid Bay area was intensively surveyed due to the fact that we had to pass this twice a day, when leaving/approaching the berth. Hence, a high resolution grid of the morphological structure as shallow as 20 m is available for Ohrid Bay. A dense grid of sediment echosounder lines covering the Ohrid Bay is another side effect allowing an integration of seismic data with sediment cores taken within Ohrid Bay area in order to explain the existence of terrace structures. Processing of the data was needed because the VSP collected within the lake had to be adapted in order to improve the quality of the data. Outer beams were eliminated as well as individual erroneous pings. Finally, a high resolution bathymetric grid was calculated imaging the complex morphological structure of the lake floor.

4 Results

4.1 Internal sedimentary structure – an overview

In this section I will describe the internal sedimentary structure of Lake Ohrid on the basis of a long N-S trending seismic cross section shown in Figure 10. A more detailed seismic stratigraphic analysis of Lake Ohrid basin is given in chapter 5.4. With the help of seismic facies (I-IV) identified within the multichannel seismic data, four main seismic units were defined (A - oldest to C, D – youngest deposits). Table 1 summarizes the relationship between seismic facies and seismic units and their tectono-sedimentary interpretation.

Seismic unit	**Seismic facies**	**Geological Interpretation**	**Tectonic interpretation**
A	I	Acoustic basement most likely associated with the host rock	Pre-rift stage
B	II	Fluvial and or alluvial deposits	Initiation and slow basin subsidence in a number of linked, small sub-basin within the marginal areas in respective lake development stages
C	Alternation of IIIa and IIIb, V	Deep-water lacustrine and mass movement deposits	Syn-rift stage where subsidence is larger than sedimentation, reflects a deepening of the basin as a result of increased subsidence a flattening of reflectors toward younger strata indicates an decrease in subsidence assuming a constant sediment supply
D	IV, V	Deep water lacustrine deposits, mass movement deposits	Syn-rift stage within sub-basins and the northern area

Tab. 1: Relationship of seismic facies and seismic units defined within the multichannel seismic data and their geological and tectonic interpretation after Schlische and Olsen (1990) and Prosser (1993).

Seismic Unit A has been identified on all seismic lines as the acoustic basement that limits the penetration of the seismic energy. Unit A is interpreted at the host rock that can also be mapped onshore.

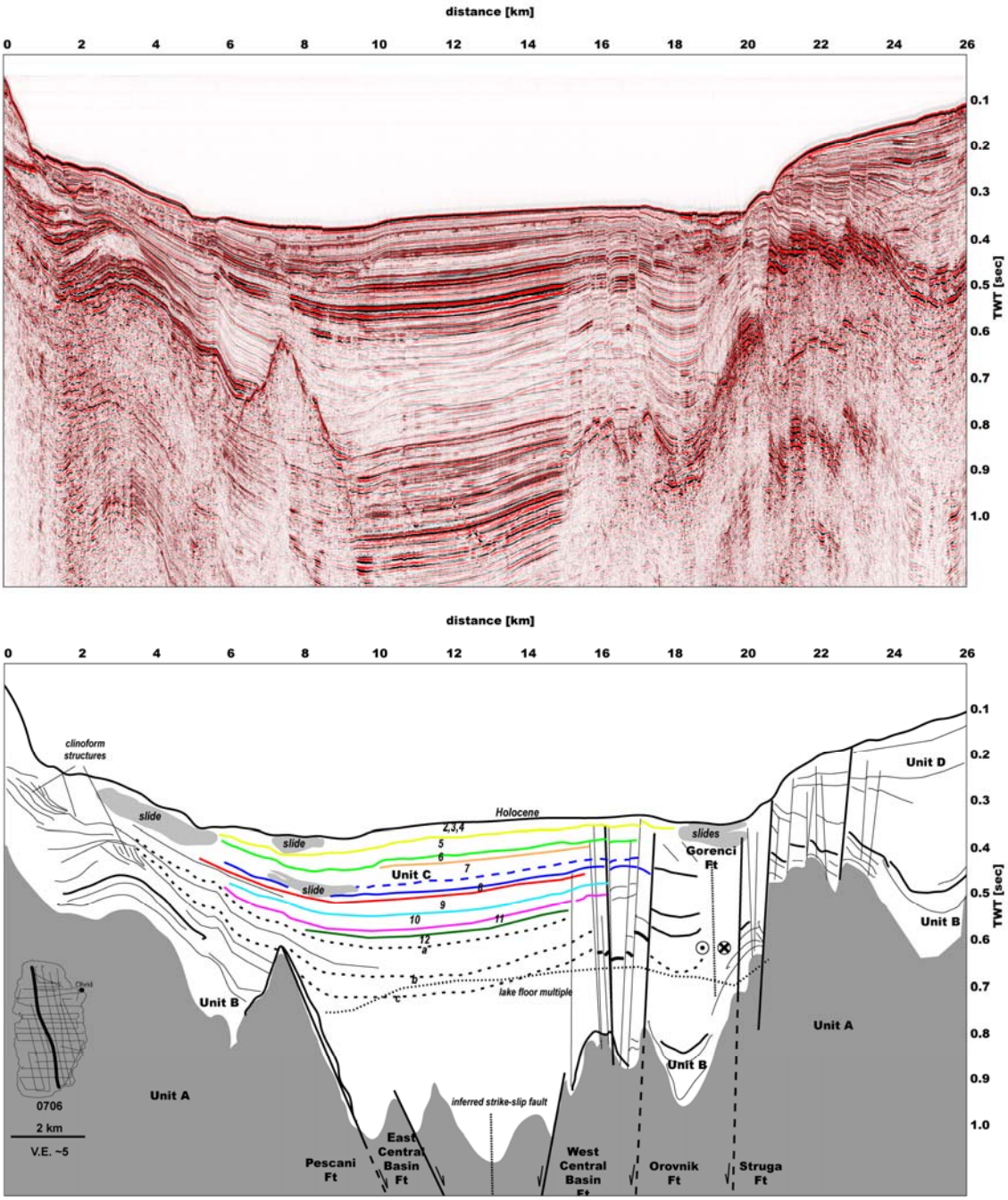

Fig. 10: Example of seismic cross section running from south to north imaging the internal sedimentary and tectonic structure of Lake Ohrid (Top.) Uninterpreted section, line drawing and interpretation (Bottom).

The sedimentary fill overlying the basement starts with deposits of Unit B, interpreted as fluvial and/or alluvial deposits in an early extensional stage after initiation of the basin or after a new fault got active and formed a sub-basin in shallower water depth (Fig. 10). Unit C makes up the majority of the sedimentary infill within the basin and is deciphered as deep water lacustrine deposits representing the syn-rift stage of Lake Ohrid after the basin was deep enough to be filled with water. Although reflectors towards younger strata flatten, indicating a decrease in subsidence, the basin is still in an underfilled stage (Carroll and Bohacs, 1999), meaning that extension is still an ongoing process with the consequence of a deepening and widening of the basin. The area in the north shows evidences for extensive faulting. Two major active normal faults, namely the Orovnik and the Struga Fault, are present (Fig. 10). In between the Orovnik and Struga fault a sinistral strike-slip fault entitled Gorenci fault is imaged. The tectonic significance of those faults for the overall basin evolution and within the neotectonic situation of Lake Ohrid area will be discussed in chapter 5.4. The presence of the Struga fault anticipates a direct tracing of reflectors from the central basin toward the north, therefore an addition Unit D had to be introduced characterized by seismic facies IV (Fig. 9).

Several mass movements and clinoform structures have been identified within the south testifying that the lake experienced lake-level changes since its existence as water filled body; lake level fluctuations will be examined in chapter 5 in detail. Mass movements are a common depositional process within the lake. The Udenisht slide is the most prominent one affecting the southwestern part of the lake. Its slide deposits cover 10 % of the entire lake floor; a detailed investigation of the slide is presented in chapter 5.3.

4.2 Lake Floor morphology

A detailed description and interpretation of morphological features identified within Lake Ohrid will be given in chapter 5.4. Therefore within this section I will only shortly introduce the bathymetric map and describe the most striking features as major outcomes from this study. It is noteworthy that prior to this study bathymetric maps already existed which were calculated by using numerous point depth measurements and already impressively show the overall shape of Lake Ohrid (Stankovic, 1960). After the first sediment echosounder survey was carried out in 2004 this map was further refined imaging for the first time the intrabasinal high within the southeastern part of Lake Ohrid. This high was named Magic Mountain

(Denner, 2006; Wagner et al., 2008b). The high resolution bathymetric map available now allows us to describe morphological features that were unknown before. The most striking ones are depicted in Figure 11. It demonstrates that the central part of Lake Ohrid is characterized by an overall smooth topography whereas the surrounding areas are either affected by seismic activity or sliding events that are most likely also related to neotectonic movements along active faults.

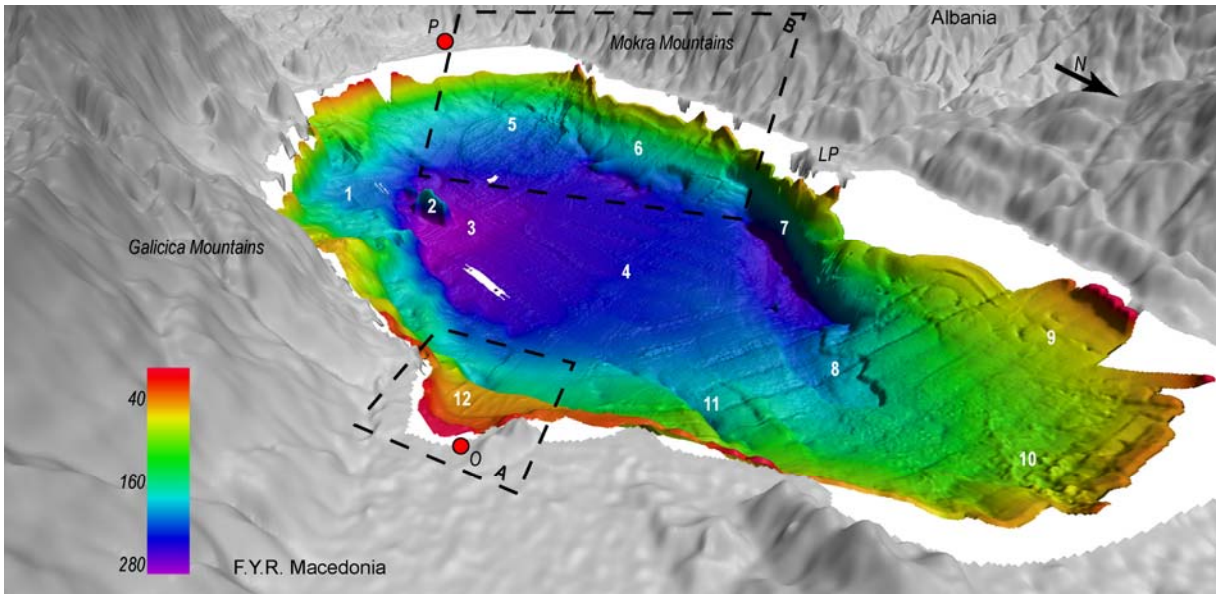

Fig. 11: Bathymetric map of Lake Ohrid viewed from Ohrid Bay toward the SW illustrating the most striking morphological features: (1) Gradiste subbasin, (2) intrabasinal high, so called Magic Mountain, (3) deepest area within the lake with water depths up to 293 m, (4) smooth topography within the central part of Lake Ohrid, (5) area of slide deposits of the Udenisht slide (Lindhorst et al., 2012), (6) sediments covering the western margin, (7) surface of an active Normal Fault outcropping at the lake floor, (8) elongated graben structure indicating active faulting, (9) pockmark-like structures, (10) rough topography indicating sliding, (11) fold structures, and (12) terraces within Ohrid Bay (Lindhorst et al., 2010). A, B mark areas of special interest of this study. LP: Lini Peninsula, O: Ohrid city, P: Progradec.

4.3 Proposed drill sites on the basis of the seismic data set

Based on the newly acquired hydro-acoustic data set presented here, five primary drill sites were selected (see Fig. 3 for location). The most important site (DEEP, labeled 3 on Fig. 3) is located in the central part in a water depth of about 250 m where we expect a thick and undisturbed sediment succession in order to obtain a long continuous record. It was chosen on the basis of the calculated acoustic basement grid as mapped from seismic lines because it

limits the penetration depth of the drilling. We picked the best possible drill site on profile 0711 because a deep basement reflector has been identified here in a depth of 1.2 s Two Way Travel Time (TWTT). The basement is overlain by a package of parallel reflectors with a thickness of 0.9 s TWTT (~800 m calculated with 1700 m/s sound velocity, Fig. 12). Four additional sites were chosen namely Struga, Lini, Gradiste, and Cerava (Fig. 3, Fig. B 1).

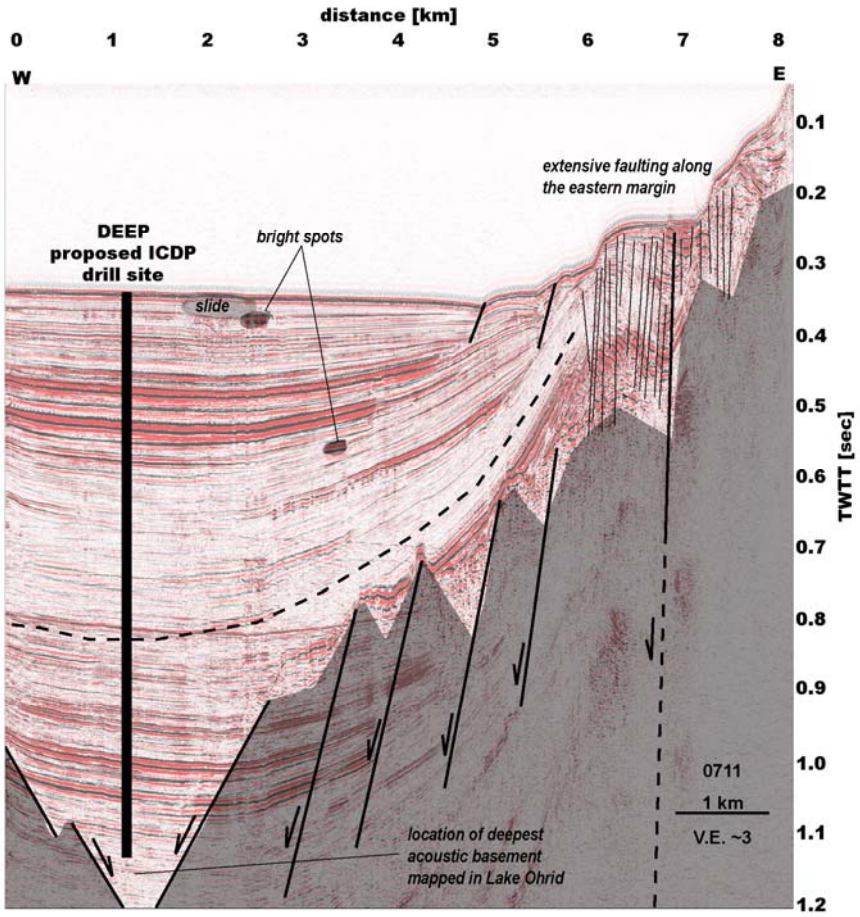

Fig. 12: Seismic cross section showing the location of the proposed drill site DEEP.

The Struga site in the north shows a clinoform structure in about 0.1 s (~85 m) subsurface depth. Such a clinoform indicates significant lateral sediment input from the north in the past, which is surprising because at present the site is located close to the main modern outflow of the lake (Fig. B 1). Therefore, the site will provide essential information on major changes of the hydrological regime. Additionally, horst and graben structures in the northern part partly continue onshore and are probably younger than the remaining basin. Extensive faulting in the transition from the northern part towards the central basin hampers a correlation of reflections between these two areas.

The site Cerava is located on a terrace in 125 m water depth close to the feeder springs of Sveti Naum (Fig. 3). This site was chosen to shed light on lake level fluctuations and terrace

formation within Lake Ohrid because at this site it is possible to obtain ages of clinoform structures by dating sediment deposits overlying them (Fig. B 1).

The sites Lini and Gradiste, located in close vicinity to major normal faults on the western and eastern margins, respectively, were chosen in order to provide crucial information on the tectonic activity within Lake Ohrid basin and their relation to mass movement deposits that are found on the hanging walls of the faults. The Gradiste sub-basin is a very active newly formed graben, containing sediments that cannot directly be linked with reflectors in the central part of Lake Ohrid. Consequently, it would be favorable to drill a deep core and derive information on fault structures of the Eastern Major Boundary Fault zone. It is very likely that the Gradiste Graben contains significant information on the evolution of endemic species that differ from those within the central part because it was most likely isolated as a shallow basin during its evolution as indicated by fluvial deposition within the Gradiste Basin (see chapter 5.4 and Fig. B 1). The basin is bounded by distinct morphological steps as well as the Magic Mountain forming a barrier for water exchange after formation and hence it is likely that species experienced different living conditions compared to the main Lake Ohrid Basin.

5 Peer-reviewed publications

Manuscript #1

Lindhorst, K., Vogel, H., Krastel, S., Wagner, B., Hilgers, A., Zander, A., Schwenk, T., Wessels, M. and Daut, G. (2010) Stratigraphic analysis of lake level fluctuations in Lake Ohrid: an integration of high resolution hydro-acoustic data and sediment cores. *Biogeosciences*, **7,** 3531-48, *doi:10.5194/bgd-7-3651-2010*

Manuscript #2

Reicherter, K., Hoffmann, N., Lindhorst, K., Krastel, S., Fernandez-Steeger, T., Gruetzner, C. and Wiatr, T. (2011) Active basins and neotectonics: morphotectonics of the Lake Ohrid Basin (FYROM and Albania). *Zeitschrift der Deutschen Gesellschaft für Geowissenschaften*, **162,** 217-34,

Manuscript #3

Lindhorst, K., Gruen, M., Krastel, S. and Schwenk, T. (2012) Hydroacoustic Analysis of Mass Wasting Deposits in Lake Ohrid (FYR Macedonia/Albania). *Submarine Mass Movements and Their Consequences***,** 245-53,

Manuscript #4

Lindhorst, K., Krastel, S., Reicherter, K., Stipp, M., Wagner, B. and Schwenk, T. (submitted July 2012), Tectonic and Sedimentary Evolution of Lake Ohrid (Albania/Macedonia). *Basin Research* (in review)

5.1 Manuscript #1

STRATIGRAPHIC ANALYSIS OF LAKE LEVEL FLUCTUATIONS IN LAKE OHRID: AN INTEGRATION OF HIGH RESOLUTION HYDRO-ACOUSTIC DATA AND SEDIMENT CORES

K. Lindhorst[1], H. Vogel[2], S. Krastel[1], B. Wagner[2], A. Hilgers[3], A. Zander[3], T. Schwenk[4], M. Wessels[5], G. Daut[6]

1 Leibniz-Institute for Marine Sciences, IFM-GEOMAR, Cluster of Excellence: The Future Ocean, Christian-Albrecht-University, Kiel, Germany

2 Institute for Geology and Mineralogy, University of Cologne, Cologne, Germany

3 Institute of Geography, University of Cologne, Cologne, Germany

4 Department of Geoscience at University of Bremen, Bremen, Germany

5 Institute for Lake Research, LUBW, Langenargen, Germany

6 Institute for Geography, Friedrich Schiller University, Jena, Germany

Published by Copernicus Publications on behalf of the European Geosciences Union in 2010 in a special issue: Wagner, B. Wilke, T., and Brovkin (eds) - Evolutionary and geological history of Balkan lakes Ohrid and Prespa:Lindhorst, K., Vogel, H., Krastel, S., Wagner, B., Hilgers, A., Zander, A., Schwenk, T., Wessels, M. and Daut, G. (2010) Stratigraphic analysis of lake level fluctuations in Lake Ohrid: an integration of high resolution hydro-acoustic data and sediment cores. Biogeosciences, 7, 3531-48, doi:10.5194/bgd-7-3651-2010

Biogeosciences, 7, 3531–3548, 2010
www.biogeosciences.net/7/3531/2010/
doi:10.5194/bg-7-3531-2010

Biogeosciences

Stratigraphic analysis of lake level fluctuations in Lake Ohrid: an integration of high resolution hydro-acoustic data and sediment cores

K. Lindhorst[1], H. Vogel[2], S. Krastel[1], B. Wagner[2], A. Hilgers[3], A. Zander[3], T. Schwenk[4], M. Wessels[5], and G. Daut[6]

[1]Leibniz-Institute for Marine Sciences, IFM-GEOMAR, Cluster of Excellence: The Future Ocean, Christian-Albrecht-University, Kiel, Germany
[2]Institute for Geology and Mineralogy, University of Cologne, Cologne, Germany
[3]Institute of Geography, University of Cologne, Cologne, Germany
[4]Department of Geosciences at University of Bremen, Bremen, Germany
[5]Institute for Lake Research, LUBW, Langenargen, Germany
[6]Institute for Geography, Friedrich Schiller University, Jena, Germany

Received: 3 May 2010 – Published in Biogeosciences Discuss.: 20 May 2010
Revised: 21 October 2010 – Accepted: 3 November 2010 – Published: 10 November 2010

Abstract. Ancient Lake Ohrid is a steep-sided, oligotrophic, karst lake that was tectonically formed most likely within the Pliocene and often referred to as a hotspot of endemic biodiversity. This study aims on tracing significant lake level fluctuations at Lake Ohrid using high-resolution acoustic data in combination with lithological, geochemical, and chronological information from two sediment cores recovered from sub-aquatic terrace levels at ca. 32 and 60 m water depth. According to our data, significant lake level fluctuations with prominent lowstands of ca. 60 and 35 m below the present water level occurred during Marine Isotope Stage (MIS) 6 and MIS 5, respectively. The effect of these lowstands on biodiversity in most coastal parts of the lake is negligible, due to only small changes in lake surface area, coastline, and habitat. In contrast, biodiversity in shallower areas was more severely affected due to disconnection of today sublacustrine springs from the main water body. Multichannel seismic data from deeper parts of the lake clearly image several clinoform structures stacked on top of each other. These stacked clinoforms indicate significantly lower lake levels prior to MIS 6 and a stepwise rise of water level with intermittent stillstands since its existence as water-filled body, which might have caused enhanced expansion of endemic species within Lake Ohrid.

Correspondence to: K. Lindhorst
(klindhorst@ifm-geomar.de)

1 Introduction

Within the terrestrial realm, ancient lakes are valuable archives providing crucial information on past climate, environmental conditions, and speciation among endemic taxa. With its inferred existence since the Pliocene, its location in the northern Mediterranean borderland and its high degree of endemic diversity (Stankovic, 1960; Albrecht and Wilke, 2008), Lake Ohrid (Fig. 1) provides a unique site to study climatic and environmental changes over long time scales and their possible links to evolutionary patterns.

As documented by numerous paleoclimate studies, the Mediterranean region has experienced large scale climate fluctuations over the last glacial-interglacial cycle (Allen et al., 1999, 2002; Bar-Matthews et al., 1999, 2000; Tzedakis et al., 2003; Martrat et al., 2004; Drysdale et al., 2005; Zanchetta et al., 2008; Vogel et al., 2010a). While information on past temperature variability at relatively high spatial resolution has become available during the past decade (Peyron et al., 1998; Allen et al., 1999; Martrat et al., 2004; Hayes et al., 2005; Marino et al., 2009), information on hydrological changes in the northern Mediterranean borderland is relatively sparse over long time scales (Tzedakis et al., 2003; Bordon et al., 2009). In order to gain a better understanding of the variability of hydrologic changes in this climate-sensitive region, additional spatially distributed paleoclimate records must be investigated. Ancient Lake Ohrid can provide such a record in the northern Mediterranean borderland with its sensitivity to recent and past climatic and environmental changes (Matzinger et al., 2006, 2007;

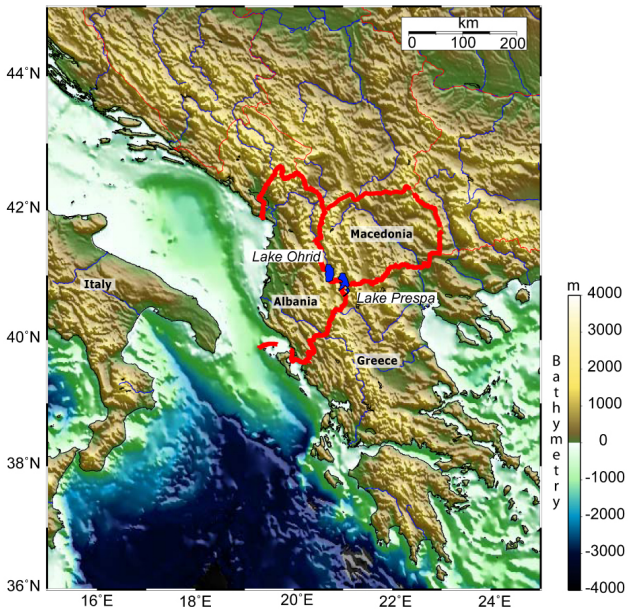

Fig. 1. Map of southern Europe with Lake Ohrid and its sister Lake Prespa located on the Balkan Peninsula.

Wagner et al., 2009; Vogel et al., 2010a). This promising location, however, has never been the subject of a quantitative study reconstructing past changes in hydrology. The detection and dating of subaquatic and subaerial terraces is a robust approach to infer past variations in the hydrological budget of an individual lake (Magny et al., 2009; Moernaut et al., 2010).

Among different possible climate-related factors affecting lacustrine ecosystems, changes of the water budget and associated lake level fluctuations have been identified as one important mechanism influencing biodiversity (Johnson et al., 1996; Sturmbauer et al., 2001; Genner et al., 2010). This is because lake level fluctuations are commonly accompanied with changes of the lake chemistry, surface area, coastline, and habitat distribution and thus directly affect species living in the lake (Martens, 1997). Many studies have investigated lake level fluctuations with special focus on climate change (Scholz and Rosendahl, 1988; D'Agostino et al., 2002; Anselmetti et al., 2006, 2009; Daut et al., 2010; Moernaut et al., 2010). In this study we try to minimize uncertainties in magnitude and timing of lake level changes by combining acoustic and sedimentological data in order to link it to biodiversity and speciation in Lake Ohrid.

Seismo-acoustic data provide images of continuous subsurfaces illustrating stacking trends, strata terminations, and geomorphology (Catuneanu et al., 2009). Depositional sequences can be subdivided into smaller stratigraphic units, termed system tracts, indicating their depositional regime during specific intervals of relative lake level changes (Posamentier et al., 1992; Hunt and Tucker, 1992; Allen and Allen, 2005). Shoreline trajectory describes the cross-sectional path of the shoreline as it migrates due to a change in lake level (Helland-Hansen and Martinsen, 1996). Three main factors determine the direction of the migration of the shoreline. These are the rate of relative lake level change, sediment supply, and basin physiography (Helland-Hansen and Martinsen, 1996). On a flat shelf area sediment is bypassed and falling relative lake level may cause the deposition of a set of down stepping prograding wedges in a forced regression system tract (FRST, Hunt and Tucker, 1992; Allen and Allen, 2005). Following a rise in lake level a Highstand System Tract (HST) with clinoform geometries evolves that onlaps onto the underlying sequence boundary in a landward direction (Allen and Allen, 2005). Clinoforms composed of topset, foreset and bottomset reflections are the fundamental building blocks of sedimentary basins (Gilbert, 1890; Pirmez et al., 1998).

While the magnitude of lake level change can be inferred relatively easily from the shoreline trajectory, dating of one particular stillstand is a rather difficult task. Radiocarbon dating of organic macrofossils is one tool, which can provide age control for the past ∼40 kyrs. Beyond that time, dating of lacustrine sediments requires other techniques with generally higher uncertainties. Positioned downwind of most of the Italian volcanoes active during the Quaternary, Lake Ohrid contains a sediment record that is an excellent archive of volcanic ash (Wagner et al., 2008a, b; Vogel et al., 2010b; Sulpizio et al., 2010). Since these tephra layers can be identified and, most importantly, correlated based on their chemical and morphological characteristics to eruptions with known ages, they serve as important stratigraphic and chronological markers. Other techniques such as luminescence and electron spin resonance (ESR) dating extend the datable range of the lake terrace levels.

The main objectives of this study are to describe and quantify lake level changes within ancient Lake Ohrid that have been identified in seismic data up to a penetration depth of 0.7 s Two Way Travel Time (TWT). We investigated patterns of lake level fluctuations by combining hydro-acoustic data with sedimentological and chronological data from lake sediment records. Specific objectives are: (i) to analyze whether lake level changes have occurred quickly, (ii) to date periods with constant lake levels in the past, (iii) to reconstruct ancient coastlines, (iv) to investigate the paleoenvironmental evolution of Ohrid Bay since the penultimate glacial period (MIS 6), and (v) to evaluate whether changes of the lake surface area and volume can be linked to changes in biodiversity within ancient Lake Ohrid.

2 Setting

Lake Ohrid (41°01′ N, 20°43′ E; Fig. 1) is located in a tectonically active graben system of the Western Macedonian geotectonic zone (Aliaj et al., 2001) at an altitude of 693 m

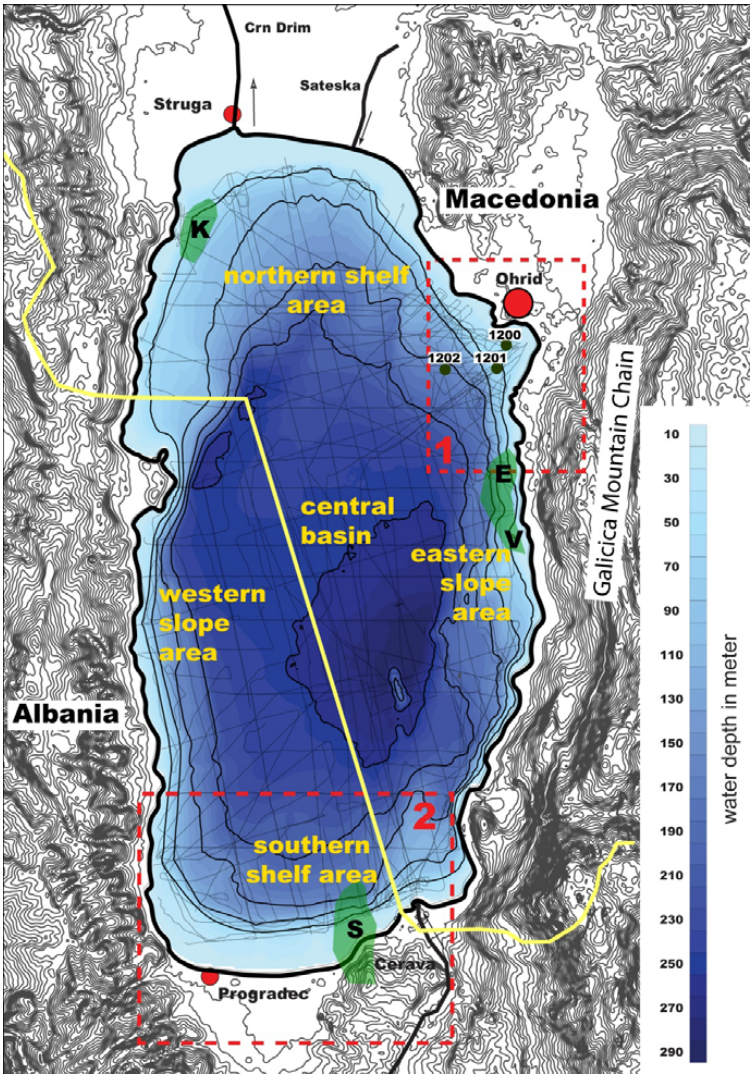

Fig. 2. Map showing bathymetry and topography of ancient Lake Ohrid and its surrounding area. The lake can be divided into six morphological sections: Ohrid Bay, southern and northern shelf area, western and eastern slope area, and central basin. Three rivers: Crn Drim, Sateska, and Cerava are marked with an arrow indicating the direction of flow. Red dashed line indicates two major study areas: 1: Ohrid Bay with core locations of Co1200 – 1202 as green spots, 2: southern Area. Yellow line is the boundary between Macedonia and Albania. Spring areas are marked in light green (K = Kalista, E = Elesec, V = Veli Dab, and S = subaquatic and subsurface springs near the monastery Sveti Naum). Light gray lines mark seismic surveys since 2004.

above sea level (Fig. 1). The lake has a maximum length of ca. 30 km, a maximum width of ca. 15 km, and covers an area of ca. 360 km^2 (Stankovic, 1960, Fig. 2). The morphology of the Lake Ohrid basin is relatively simple with a deep flat central basin, steep margins along major boundary faults at its eastern and western terminations, and shallow shelf areas in the northern and southern region (Wagner et al., 2008a, Fig. 2). The average water depth of the lake is ca. 150 m with a maximum water depth of 290 m and a total volume of 50.7 km^3 (Popovska and Bonacci, 2007, Fig. 2).

Karst aquifers, charged from precipitation in the surrounding mountain ranges and from its sister Lake Prespa, enter Lake Ohrid as sub-aquatic springs (∼49%) in water depth up to 150 m (Matzinger et al., 2006; Albrecht and Wilke, 2008; Matter et al., 2010,) and as surface springs (51%, Fig. 2, Albrecht and Wilke, 2008). Four main areas of sub-aquatic springs have been described so far: Kalista, Elesec, Veli Dab, and Sveti Naum (Albrecht and Wilke, 2008; Matter et al., 2010, Fig. 2). Surface springs can be found within the spring lake at Sveti Naum Monastry and sister spring complex Zagorican/Tushemist as well as some minor springs in the northern area of Lake Ohrid (Popovska and Bonacchi, 2007; Albrecht and Wilke, 2008, Fig. 2). In addition to karstic inflows, water enters Lake Ohrid by rivers and

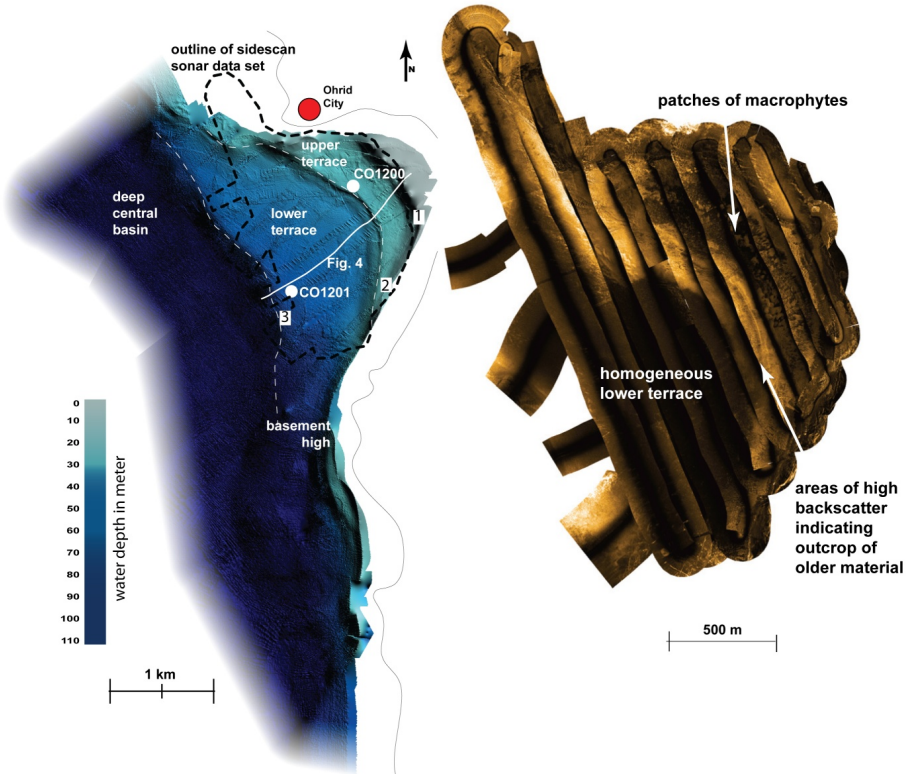

Fig. 3. Bathymetric map of Ohrid Bay (left) with major morphological features such as upper and lower terrace, deep central basin, three morphological steps (1, 2, 3 at water depth 15 m, 35 m, and 60 m, respectively). Locations of sediment cores (Co1200, Co1201) are marked as white dots. Sidescan sonar mosaic (right) images the upper portion of Ohrid Bay. Bright colors are areas of high backscatter. The outline of the sidescan sonar mosaic is shown as dashed line on the bathymetry. Note the different scales for each map. See Fig. 2 for location.

direct precipitation (Matzinger et al., 2006). At present, the Sateska and Cerava Rivers are the main riverine inflows to Lake Ohrid. Water leaves Lake Ohrid through the River Crn Drim (∼60%) and by evaporation (∼40%, Matzinger et al., 2006, Fig. 2). No significant riverine inlets are found in close proximity to Ohrid Bay.

3 Methods

3.1 Hydro-acoustics

The first hydro-acoustic data were acquired in spring 2004 by means of a parametric sediment echosounder (Wagner et al., 2008a). In September 2007 and June 2008 we carried out two multichannel seismic surveys using a small airgun (0.25 l and 0.1 l) and a 100 m-long 16-channel streamer. The processing procedure included trace editing, set-up geometry, static corrections, velocity analysis, normal move-out corrections, band-pass frequency filtering (frequency content: 35/60–600/900 Hz), stack, and time migration. We applied a common midpoint spacing of 5 m throughout. During both multichannel surveys a parametric sediment echosounder with a main frequency of 10 kHz was operated simultaneously. Stacking of two adjacent pings improved the signal-to-noise ratio. We calculated water depth and penetration from the echosounder using a constant velocity of 1470 ms^{-1}. A dense net of sediment echosounder lines with a spacing of less than 500 m (in Ohrid Bay even less than 100 m) is now available for Lake Ohrid (Fig. 2).

Sidescan sonar data were acquired in 2008 using a Klein 3000 dual frequency sonar with 100 kHz and 500 kHz. The Ohrid Bay area was mapped between 3 and about 100 m water depth. The sonar was usually adjusted to cover 75–100 m on either side with individual profiles spaced 75–100 m apart. In this way, complete coverage of the working area was achieved.

In September/October 2009, we collected high-resolution bathymetric data by means of ELAC Seabeam 1180 system. The system uses 126 beams with a total opening angle of 153° and operates with a frequency of 180 kHz. The transducers were mounted at the bow of the vessel. Vessel motion was measured using an OCTANS IV motion sensor that provides roll, pitch, and heave correction. We collected sound velocity profiles at different locations across Lake Ohrid. Processing of the data was mainly done by means of the software package MBSystem (Caress and Chayes, 2005) and

Table 1. Radiocarbon ages and calendar ages inferred using CalPal-2007online (Danzeglocke et al., 2008) of plant macrofossils from cores Co1200 and Co1201.

Sample ID	Core ID	Depth(cm)	^{14}C age (yrs BP)	Calendar age (cal yrs BP)
KIA37138	Co1200	6	1954 AD	1954 AD
KIA37139	Co1200	13	21 610 ± 185	25 815 ± 522
KIA37140	Co1201	15	5010 ± 35	5773 ± 82
KIA37141	Co1201	18	15 810 ± 155	19 030 ± 244

Table 2. Dating results and radioactivity data. Ages from core Co1201 were derived by IRSL dating, sample K-5764 from core Co1200 was ESR[1] dated.

Lab. Code	Sample ID	Water content (weight-%)[2]	Burial depth (m)	U (ppm)[3]	Th (ppm)	K (%)	De (Gy)	D_0 (Gy ka^{-1})	Age (ka)	IRSL-Age Fading corrected (ka)
C-L2573	Co1201-5 I (340-377 cm)	30.3 ± 4.5	17.75	4.11 ± 0.14	15.75 ± 0.72	2.45 ± 0.05	479.6 ± 33.0	4.0 ± 0.2	119 ± 10	157 ± 21
C-L2574	Co1201-5 I (377-408 cm)	29.9 ± 4.5	17.95	4.19 ± 0.14	16.00 ± 0.74	2.47 ± 0.05	558.0 ± 31.8	4.1 ± 0.3	137 ± 127	181 ± 24
C-L2575	Co1201-5 III (503-550 cm)	29.2 ± 4.4	19.50	3.76 ± 0.13	14.86 ± 0.68	2.45 ± 0.05	372.3 ± 24.6	4.0 ± 0.2	93.4 ± 8.1	123 ± 16
C-L2576	Co1201-5 III (550-597 cm)	30.9 ± 4.6	20.00	4.04 ± 0.14	15.67 ± 0.72	2.50 ± 0.05	438.1 ± 40.2	4.0 ± 0.3	109 ± 12	143 ± 21
K-5764	Co1200-6 III (230-262 cm)	35–50		0.41 ± 0.04	0.33 ± 0.03	0.06 ± 0.01	16.40 ± 1.23		130 ± 28	

[1] The dose rates and ESR-ages were calculated for different water contents and different thicknesses of an overlying sediment unit and water column, as the depositional history was complex. The age estimate is the average from the maximum and minimum ages resulting from dose rate modelling.
[2] Water content is the in-situ water content with 15 % uncertainty.
[3] Internal U-content: 0.07 ± 0.01 ppm

GMT (Wessel and Smith, 1991). The area of Ohrid Bay is covered from 20 m water depth into the deep basin.

3.2 Sediment cores

Cores Co1200 and Co1201 were recovered in fall 2007 from the northeastern part of Lake Ohrid where hydro-acoustic surveys indicated two sub-aquatic terrace levels at 32 and 60 m water depth (Fig. 3). The surface sediments and deeper sediments were collected using a 0.6-m gravity corer and a 3-m-long percussion piston corer, respectively (both UWITEC Co.). The overlapping 3-m long core segments were subdivided into 1-m-long segments in the field.

Prior to sub-sampling one core halve was used for high-resolution X-ray fluorescence (XRF) scanning by means of an ITRAX core scanner (COX Ltd.), equipped with a Mo-tube set to 30 kV and 30 mA and a Si-drift chamber detector. Scanning was performed at 2.5 mm resolution and an analysis time of 20 s per measurement. The obtained count rates for Ti, K, and Ca can be used as estimates of the relative concentrations for these elements (Croudace et al., 2006).

Sub-sampling was performed at 2 cm intervals. The water content (WC) for each sample was determined from the weight difference between wet and freeze-dried samples. Aliquots of the freeze-dried subsamples were ground to a particle size below 63 µm using a planetary mill for subsequent biogeochemical analyses, which was done at 6 cm resolution. Total carbon (TC) concentrations, were measured with a Vario Micro Cube combustion CNS elemental analyzer (VARIO Co.). Samples for total organic carbon (TOC) analysis were pre-treated with HCl (10%) at a temperature of 80 °C to remove carbonates and then analyzed using a Leco CS-225 carbon-sulfur detector (LECO Corp.). The amount of total inorganic carbon (TIC) was determined from the difference between TC and TOC. The calcite ($CaCO_3$) content was calculated from TIC under the assumption that TIC solely originates from $CaCO_3$.

In order to develop a chronological framework for cores Co1200 and Co1201 radiocarbon, infrared stimulated luminescence (IRSL), electron spin resonance (ESR) dating, and tephrostratigraphy was applied. For radiocarbon dating plant macrofossils from 6 and 13 cm depth in core Co1200 and from 15 and 18 cm depth in core Co1201 were used (Table 1). Radiocarbon dating was performed by accelerator mass spectrometry (AMS) at the Leibniz Laboratory for Radiometric Dating and Isotope Research in Kiel, Germany. The obtained ages were calibrated into calendar years before

Table 3. Relationship between morphological, seismic (multichannel and sediment echosounder) and lithological data of Ohrid Bay. LGM = Last Glacial Maximum, MIS = Marine Isostage.

Morphology	stratigraphy		cores	system tracts	age	lake level	base level	shoreline trajectory
step 1	seismic units	Litho-facies						
upper terrace	H	I	Co1200	HST 9	Holocene	modern		transgression
	G	II	Co1200	HST 9	LGM	modern		transgression
	F	III	Co1200	FRST 8	MIS 5	stage 3	~35 m	minor regression
step 2	outcrop F	III	Co1200	FRST 8	MIS 5	stage 3	~35 m	minor regression
lower terrace	H	I	Co1201	HST 9	Holocene	modern		transgression
	G	II	Co1201	HST 9	LGM	modern		transgression
	E_2	–	–	HST 7	late MIS 6/ MIS 5	stage 2	~25 m	transgression
	E_1	IV	Co1201	FRST 6	MIS 6	stage 1	~60 m	continuous regression
step 3	outcrop E	IV	Co1201	FRST 6	MIS 6	stage 1	~60 m	continuous regression
deep central basin								

present (cal yrs BP) using CalPal-2007online and the CalPal2007_HULU calibration curve (Danzeglocke et al., 2008).

IRSL dating was solely performed on four samples from core Co1201. In the laboratory under subdued illumination about 20 cm^3 material was taken from four different depths (340–377, 377–408, 503–550, and 550–597 cm, Table 2) using the core half, which was not XRF scanned. Additionally samples at each of the four depths were taken for dose rate measurements. The concentrations of U, Th and K were determined by gamma-ray spectrometry using approximately 400 g of sediment per sample. Several dating attempts applied to quartz extracts like a standard optically stimulated luminescence single aliquot regeneration protocol or an isothermal TL approach failed due to saturation effects. Hence, IRSL measurements were carried out on potassium-rich feldspar extracts in the blue detection range (410 nm interference filter) using a single aliquot regeneration protocol. Fading tests and fading corrections were applied to the IRSL ages as described by Auclair et al. (2003), Lamothe et al. (2003), and Preusser et al. (2008) for further details on luminescence dating and the problem of fading.

We performed ESR dating only on one horizon in core Co1200. For this purpose we collected large mollusk shell fragments from a horizon at 230–262 cm depth (Table 2). In order to determine the radionuclide contents of the surrounding sediment and of the mollusks themselves we applied inductively coupled plasma (ICP)-mass spectrometry. We carried out ESR measurements using an additive dose protocol for multiple aliquots (Schellmann et al., 2008). Results of IRSL and ESR dating are summarized in Table 2.

Both cores Co1200 and Co1201 contained peculiar horizons consisting almost entirely of volcanic glass shards (tephra). Tephra horizons in core Co1200 occur at 38–40 and 85.5–120.5 cm. Tephra horizons in core Co1201 occur at 110–126, 184–186, and 190–192. From these horizons we washed and sieved about 1 cm^3. The >40 µm fraction was embedded in epoxy resin and screened for glass shards and micro-pumice fragments using scanning electron microscopy (SEM). We performed energy-dispersive-spectrometry (EDS) analyses of glass shards and micro-pumice fragments using an EDAX-DX micro-analyzer mounted on a Philips SEM 515 (operating conditions: 20 kV acceleration voltage, 100 s live time counting, 200–500 nm beam diameter, 2100–2400 shots per second, ZAF correction is a common matrix correction used in electron microprobe analysis. Z = atomic number, A = absorption, F = flourescence).

3.3 Seismic stratigraphy and correlation with cores

In total we defined 8 seismic units named from A (oldest unit overlying the basement) to H (most recent deposition only found in Ohrid Bay). Seismic sequences identified within the sediment echosounder profiles in Ohrid Bay could be directly assigned to lithofacies described in cores Co1200 and Co1201. A major fault at the southwestern end of Ohrid Bay

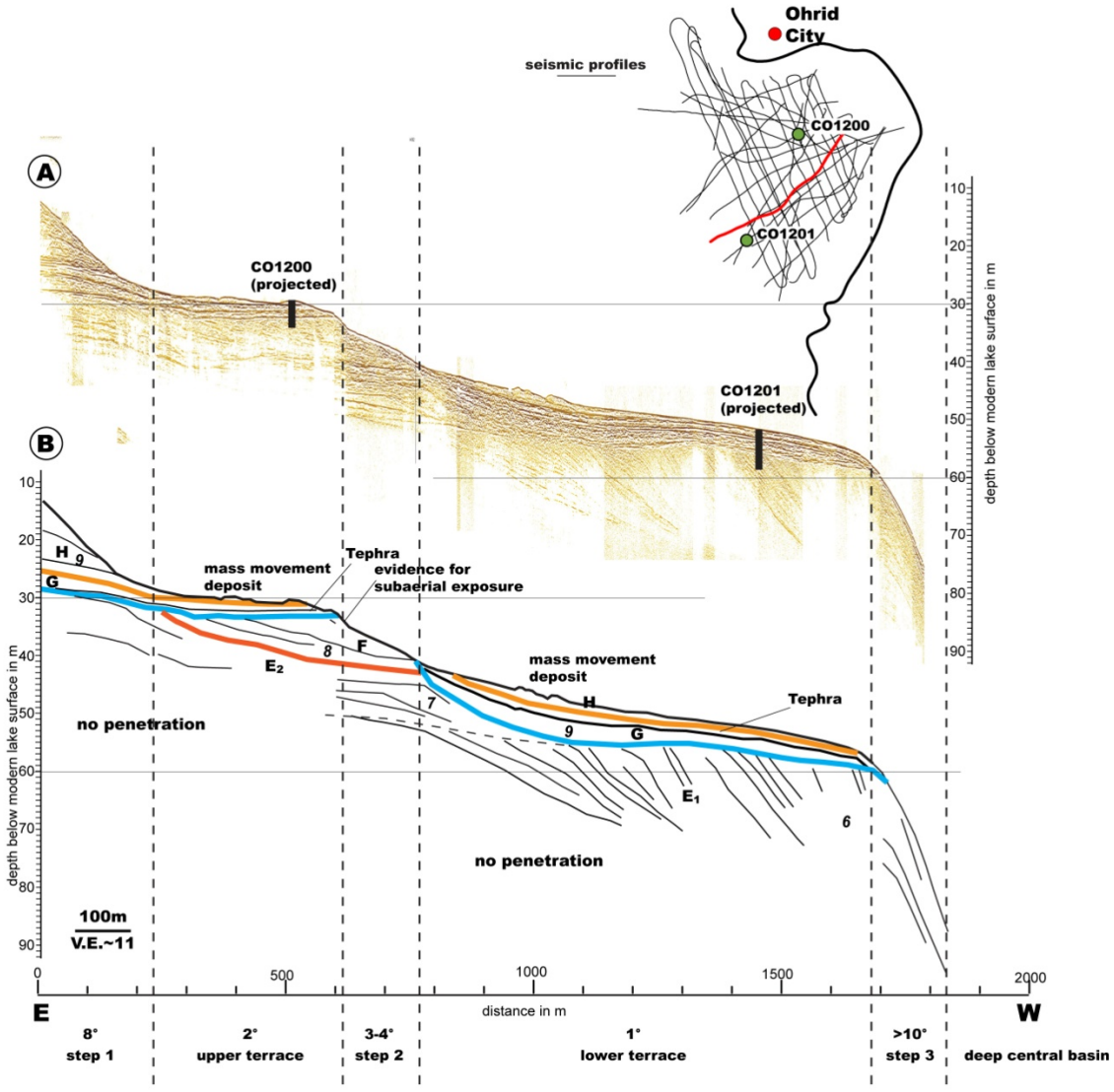

Fig. 4. East-west directed sediment echosounder line across Ohrid Bay over a distance of 2 km (see map inlet for location). **(A)** Uninterpreted section with projection of sediment cores **(B)** line drawing and interpretation of the section (colors indicating the base of each seismic unit are the same as colors used for Lithofacies in Figs. 5, 6). The profile shows the internal structure of the upper and lower terraces. Seismic units E_1, E_2 F, G, H and System tracts 6, 7, 8, 9, a tephra layer most likely assigned to (CI)/Y5 and areas with mass wasting deposits as evidenced by a hummocky topography are labeled. Slope angles are indicated at the bottom of the line drawing.

anticipated a direct tracing of prominent reflections within the sediment echosounder data in Ohrid Bay through the central basin into the southern area. For that reason we used additional lithological data available from Co1202 (Vogel et al., 2010a) below this fault in a water depth of 145 m comprising the same lithofacies as found in Co1200 and Co1201 of this study. This approach allowed correlating seismic signals observed in Ohrid Bay into the deeper part of the lake.

4 Results

4.1 Ohrid Bay

4.1.1 Bathymetry and lake floor morphology

High-resolution bathymetric data gathered offshore from the City of Ohrid show two gently dipping (<1°) plateaus (upper and lower terraces in Fig. 3) as well as three distinct morphological steps. The first morphological step drops down to a water depth of 30 m. The upper terrace in ∼30 m water

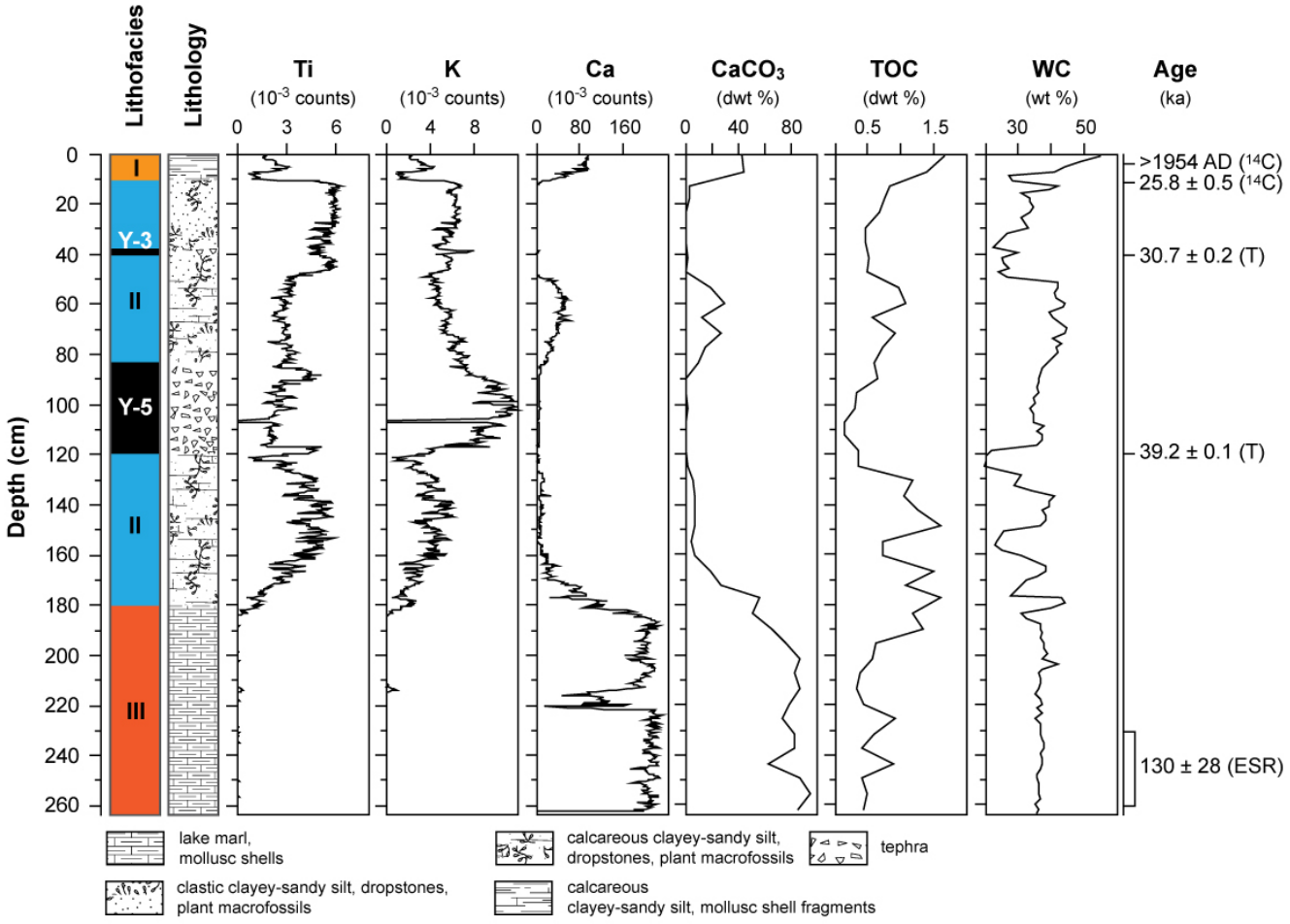

Fig. 5. Lithofacies, lithology, Ti-, K- , Ca- intensities, $CaCO_3$, total organic carbon (TOC) dry weight percentages, water content (WC), and age control points of core Co1200. ^{14}C = calibrated radiocarbon age, T = tephra age, ESR = electron spin resonance age. Location of core is shown on Figs. 3 and 4.

depth has an average width of 400 m (Figs. 3, 4). The outer edge of this upper terrace is characterized by a clear break in the slope gradient from ∼2° to ∼4° (step 2 on Fig. 4), which can be traced in a half circle parallel to the present-day northern coastline. At this break in slope the lake floor drops down to the up to 800 m-wide lower terrace in ∼60 m water depth. Another prominent step in morphology (labeled 3 on Fig. 4) defines the outer edge of the lower terrace. At this step the lake floor drops to more than 200 m water depth with a slope angle of up to 10° down into the central basin. A sub-lacustrine basement high that crops out in the southern part of the Ohrid Bay area is clearly visible in the bathymetric data (Fig. 3). The terminology used for each data set within Ohrid Bay is summarized in Table 3.

A side scan sonar mosaic images the surface texture of each individual terrace. High backscatter values along morphological steps mark exposures of terrace-building sediment sequences (Fig. 3). Small-scale patches of strong backscatter values on top of the upper terrace in a water depth of 30 m are indications of ancient eroded surfaces partly overlain by younger sediments. The distribution of macrophytes in littoral areas of Ohrid Bay is traceable by side scan sonar data.

4.1.2 Stratigraphy

The sediment echosounder dataset covers the entire Ohrid Bay showing the internal structure of the sediments up to a sub-surface depth of 50 m below the lake bottom. The grid of seismic lines is very dense (Fig. 4, map inlet). A set of parallel lines is running from north to south with a line spacing of less than 100 m. In addition, numerous profiles were collected from the central lake basin perpendicular to the coastline across both terraces. The density of high-resolution seismic profiles allows us to correlate between the profiles.

Stratigraphic Unit E is divided into sub-units E1 and E2 (Fig. 4). Sub-unit E1 is characterized by oblique, parallel to sub-parallel reflections with increasing dip angles to the

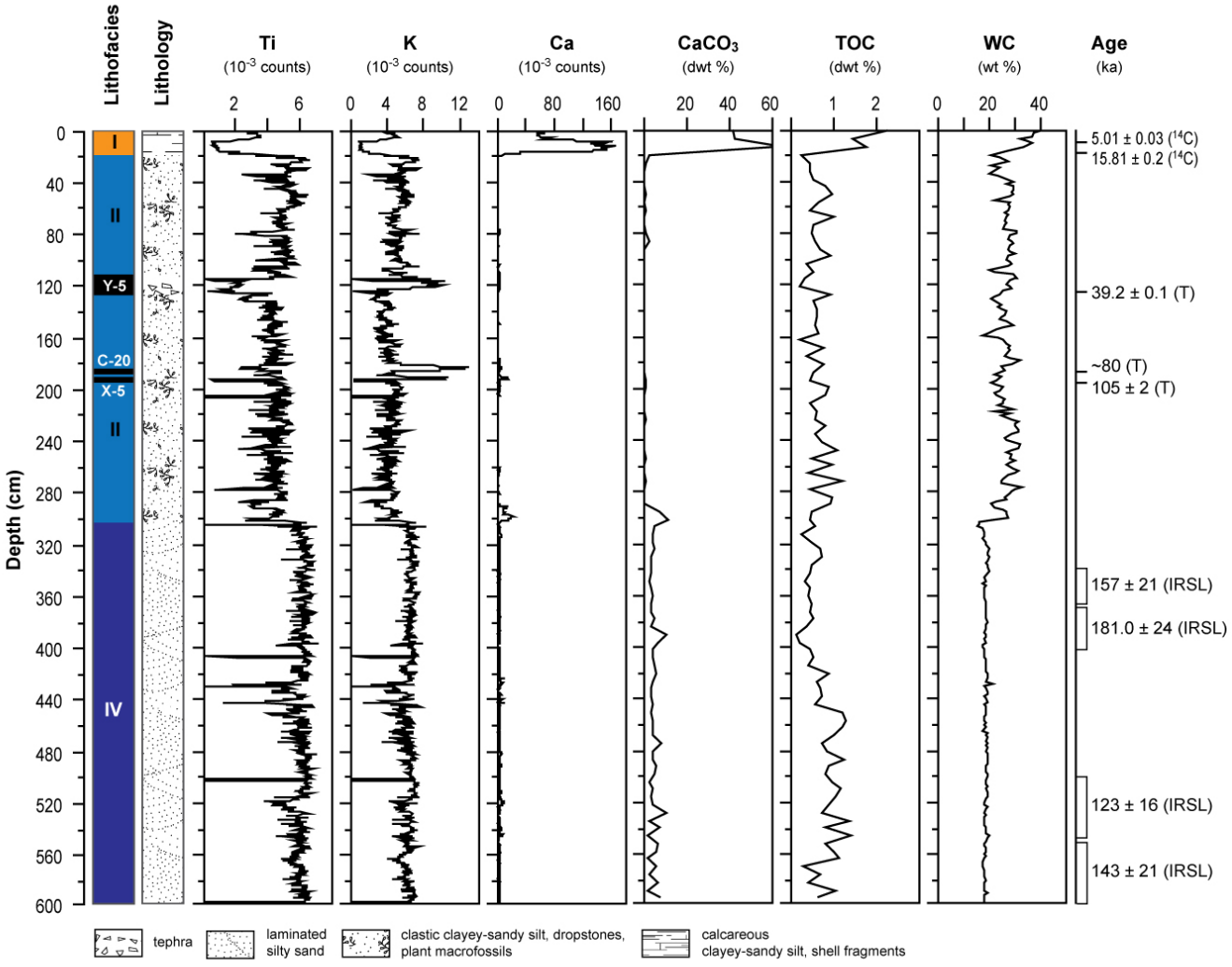

Fig. 6. Lithofacies, lithology, Ti-, K- , Ca- intensities, $CaCO_3$, total organic carbon (TOC) dry weight percentages, water content (WC), and age control points of core Co1201. ^{14}C = calibrated radiocarbon age, T = tephra age, IRSL = infrared stimulated luminescence age. Location of core is shown on Figs. 3 and 4.

west, and a toplap surface as upper boundary. Due to the limited penetration of the acoustic waves, the lower boundary of Sub-unit E1 cannot be detected. A steep slope with an angle of 15° forms the transition to the profundal part of the lake. Sub-unit E2 forming a prograding clinoform with medium amplitude reflections (Fig. 4) is stacked on top of sub-unit E1.

Unit F appears in the seismic data as a low-amplitude wedge truncated by erosional surfaces on top and to the west. Penetration into Unit F is limited, therefore only a few internal reflections are visible that indicate slightly basinward dipping strata (Fig. 4). Towards the west, Unit F crops out and causes high backscatter visible in the sidescan data.

Sediment depositions assigned to units G and H are found on both terraces. In a water depth of about 50 m (lower terrace) Unit G onlaps onto Unit F suggesting a transgressive sequence boundary (Fig. 4). A thinning of strata towards the west is observed. In close proximity to the lakeshore at water depths of about 30 m (upper terrace), sediments of units G and H discordantly cover Unit F. A high amplitude horizon within Unit G can be assigned to Y-5 tephra (see below). The youngest seismic Unit H is recognized by slightly lower-amplitude reflections. A hummocky topography on both terraces indicates deposits of mass wasting processes (Fig. 4).

The cores recovered from the terraces in Ohrid Bay measure 2.63 m (Co1200) and 5.97 m (Co1201) after correlation by lithological core descriptions and XRF data of individual core segments. Lithological characteristics, geochemical indicators, and chronological constrains imply a subdivision of the sedimentary successions of cores Co1200 and Co1201 into four distinctly different lithological facies (Figs. 5, 6).

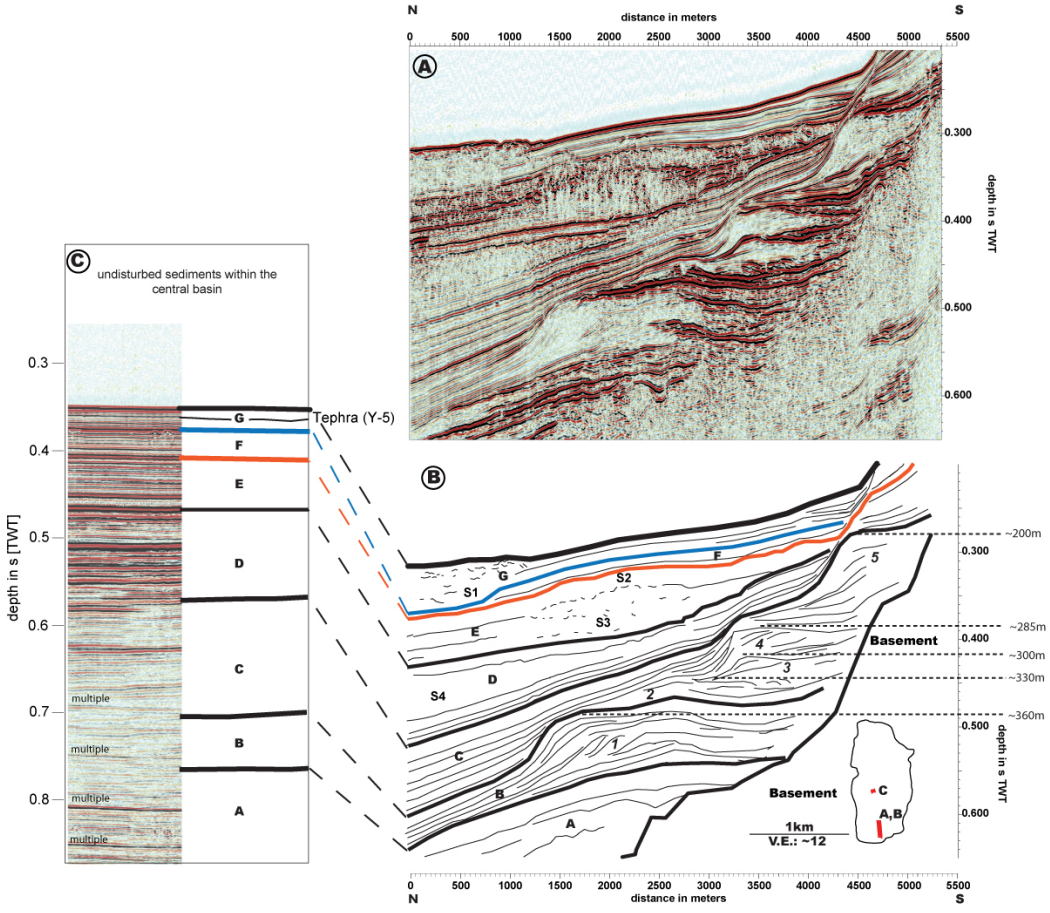

Fig. 7. Multichannel seismic cross section of sedimentary structures within the southern area running in a north-south direction over a distance of 5.5 km. **(A)** uninterpreted and **(B)** interpreted section (colors indicating the base of each seismic unit are the same as colors used for Lithofacies in Fig. 5, 6). Interpretation of the seismic section shows that Lake Ohrid has a complex sedimentary evolution with a stepwise lake-level rise since its existence as water filled body as suggested by five major clinoform structures (1–5). Within younger sequences several mass wasting deposits were found indicating that sliding events are common in the southern area. A correlation of prominent reflections that bound major seismic units (A–G) with well stratified sediments in the central basin of Lake Ohrid is shown in **(C)**.

Lithofacies IV corresponding to seismic Unit E (see Table 3) forms the basal succession of core Co1201 between 305 and 597 cm depth and is limited at its top by a 0.5 cm thick sand layer with clear erosional base (Fig. 6). The sediments appear laminated with laminae width of 0.2–1 cm, dark to light grey, and are mainly composed of clastic sandy silt. The dominance of clastic material in Lithofacies IV is well correlated to high Ti and K intensities. Terrestrial plant macrofossils and reworked mollusk shells are abundant in variable quantities explaining relatively high TOC concentrations and detectable amounts of $CaCO_3$. Chronological control for Lithofacies IV sediments is given by IRSL dating of feldspar specimens sieved from the sand fraction of four horizons. IRSL dating on feldspars from the horizons at 340–377, 377–408, 503–550, and 550–597 cm yielded ages of 157 ± 21, 181 ± 24, 123 ± 16, and 143 ± 21 ka, respectively (Fig. 6, Table 2). These results can be regarded as minimum ages, since underestimation of the burial age for feldspar samples from deposits beyond 100 ka notwithstanding correction procedures can be assumed (Wallinga et al., 2007). Dose rate measurements yielded very consistent nuclide concentrations (Table 2) for the four samples, suggesting a uniform sediment deposition. By contrast, the IRSL ages show no age increase with depth but an inconsistent array. This indicates partly insufficient bleaching before deposition or post-sedimentary influences and changes in the stratigraphic sequence after sedimentation. Variations in density, thickness of the overlying sediments or the water column do affect the dose rate calculations and might also contribute to the scatter of the ages. Taking all uncertainties into account, the

IRSL dating results support a correlation of this stratigraphic unit with MIS 6.

Lithofacies III (corresponding to seismic Unit F, see Table 3) comprises the basal succession of core Co1200 between 181.5 and 263 cm (Fig. 5). A similar lithofacies is absent in core Co1201 (Fig. 6). Sediments assigned to Lithofacies III appear grayish-white and consist almost entirely of silt-sized endogenicic calcite (CaCO3 >70%), intact mollusk shells, and mollusk shell fragments. As indicated by extremely low Ti and K intensities clastic matter is almost absent. Low TOC (<1.2%) concentrations originate from finely dispersed organic matter (OM) and few leave and shaft fragments of chara algae. ESR dating of mollusk shells collected in between 230 and 262 cm yielded a modeled age of 130 ± 28 ka (Table 2). This age, however, has a high uncertainty, because the post-depositional history regarding the thickness of the overlying sediment and water column has a high impact on the dose rate calculation for these deposits with very low radioactivity. A larger data set would be preferable to support this first age estimation. The transition from sediments of lithofacies III to II in core Co1200 is abrupt and occurs within a few centimeters. These transitional centimeters contain gravel, sand, and reworked mollusk shells without any grading.

Sediments deposited between 120.5–181.5 and 16–85.5 cm in core Co1200 (Fig. 5) and between 126–305 and 18.5–110 cm in core Co1201 (Fig. 6) are assigned to Lithofacies II (corresponding to seismic Unit G, see Table 3). Its sediments appear dark-gray and consist of clastic clayey-sandy silts with frequent occurrences of gravel grains. Small reworked shell fragments occur in low abundance at both sites. $CaCO_3$ concentrations are <40% and TOC concentrations are <2%. Despite the general similarities for Lithofacies II sediments at both sites, some differences were also observed. For example, larger intact chara fragments are abundant in sediments of core Co1200, but only small leave and shaft pieces were found in core Co1201. Another difference is the amount of finely dispersed OM and $CaCO_3$, which is higher in Lithofacies II of core Co1200 compared to Co1201.

A prominent and extensive tephra horizon can be seen by visual core inspection between 85.5–120.5 cm in core Co1200 and 110–126 cm in core Co1201. Geochemical and morphological correlation of glass shards from both tephra deposits point to the Campanian Ignimbrite (CI)/Y-5 eruption of the Campi Flegrei Caldera (Figs. 5, 6; Sulpizio et al., 2010), which is Ar/Ar dated to 39.2 ± 0.1 ka (De Vivo et al., 2001). Apart from this extensive tephra deposit additional tephra layers are found in both cores (Figs. 5, 6). A slightly younger tephra layer only identified in core Co1200 at 38–40 cm can be correlated to the Y-3 tephra layer (Campi Flegrei, Sulpizio et al., 2010), which is dated at 30.67 ± 0.2 ka (Sulpizio et al., 2003). Two additional tephra layers were recovered only in Co1201: One layer recognized at 184–186 cm that can be correlated to the C20 marine tephra (dated at 79–80 ka, Paterne et al., 1988). A second layer at 190–192 cm corresponds to the marine tephra X-5 (Sulpizio et al., 2010), which has an age of 105 ± 2 ka (Keller et al., 1978; Kraml, 1997).

The transition from Lithofacies II to Lithofacies I (corresponding to seismic Unit F, see Table 3) is characterized by a 2–3 cm thick sand layer between 13–16 cm (Co1200, Fig. 5) and 16.5–18.5 cm (Co1201, Fig. 6) with apparent erosive base in both cores. The sand layers show no upward fining in grain size, which would be typical for deposition from turbidity current, but is probably best explained as originating from some sort of mass movement process rather than lake level low stand. Radiocarbon dating of plant macrofossils just below the sand layer at 13 cm in core Co1200 and at 18 cm in core Co1201 yielded ages of $25\,815 \pm 522$ and $19\,030 \pm 244$ cal kyrs BP (Table 1), respectively, implying a hiatus in the cores after the Last Glacial Maximum (LGM).

Lithofacies I occurring in both cores (0–13 cm in Co1200 and 0–16.5 cm in Co1201; Figs. 5, 6) as light-brown layer is composed of calcareous ($CaCO_3$ > 40 %) clayey silt and contains complete bivalve shell and their fragments. TOC concentrations of up to 2% can be explained by finely dispersed OM as well as small leave and shaft parts from chara algae. Radiocarbon dating of plant macrofossils from Lithofacies I at 15 cm in core Co1201 yielded an age of 5773 ± 82 cal yrs BP (Table 1). The modern age of plant macrofossils from 6 cm in core Co1200 is probably a result of contamination with recent plant material.

4.2 Southern area

We observed several well-preserved prograding delta deposits within multichannel seismic data in the southern part of Lake Ohrid reflecting significant lake level changes in the past (Fig. 7). Stacked sigmoidally shaped clinoforms are recognized in the seismic cross section (Fig. 7). These clinoforms are characterized by low-amplitude bodies composed of topset, foreset, and bottomset reflections. Reflections within individual clinoform packages are marked in the interpreted seismic section (Fig. 7). Several high-amplitude reflections overly each wedge numbered as 1 to 5 from oldest to youngest.

Basinward of the clinoforms seven depositional sequences (A to G) were defined by tracing unconformities or their correlative conformities of reflections-bounding clinoform structures. The acoustic basement that limits penetration is recognized in the southern part of the profile rising up from the deeper central basin towards shallower shore areas. Unit A, the oldest sequence overlying the basement is characterized by several high amplitude reflections. Units B and C have very similar seismic characteristics showing well-stratified, continuous reflections with medium amplitudes that onlap on foresets of clinoforms. Within each unit one or more prominent reflections are observed and marked in the interpreted section (Fig. 7). The next younger units, D and E, display the most complex seismic architecture within

this cross-section. Three major mass movements deposits (S2 to S4, Fig. 7), imaged as transparent units, are identified in units D and E. Prominent and continuous horizons occasionally mark the base of mass movement deposits and divide the unit in sub-units. Additional high-amplitude reflections within Unit E are well imaged. We speculate that the top of Unit E most likely marks the transition of the penultimate glacial period (MIS 6) to the last interglacial period (MIS 5) as the bounding reflection is of the same age as its counterpart in Ohrid Bay. Furthermore, units F and G correspond to the last interglacial period (MIS 5), and the last glacial period (MIS 4, 3, and 2), respectively. Although a direct correlation to cores in Ohrid Bay is not possible, prominent reflections of each individual unit (F and G) can be traced to core Co1202 located within the bottomset of the lower terrace assigned to Lithofacies IV (Fig. 2, Vogel et al., 2010b) and therefore are reliably dated to the same age as their corresponding units identified in Ohrid Bay. Within well-stratified sediments of Unit G, a prominent reflection most likely correlates to tephra layer Y-5 found in both cores described in this study (Figs. 4–7) as well as in Co1202 (Vogel et al., 2010a, b). Towards the north, one thick slide deposit characterized by a chaotic seismic facies is onlapping on well-stratified sediments of Unit G. Seismic stratigraphic units described above can be traced into the central basin characterized by thick undisturbed sediments (Fig. 7c).

5 Discussion

5.1 Paleoenvironmental reconstructions

Based on the data available, we reconstructed four main phases of lake level dynamics back to MIS 6 in Ohrid Bay. In a temporal context these phases can be described as follows: (1) the buildup of a lower terrace, 60 m below the present water table (Unit E1, Lithofacies IV) during the penultimate glacial period (MIS 6), (2) the development of the upper terrace (Unit F, Lithofacies III) during the last interglacial period (MIS 5), (3) sedimentation of Lithofacies II assigned to seismic Unit G during the last glacial period, and (4) mid-Holocene to modern sedimentation as evident by Lithofacies I referring to seismic Unit H.

High amounts of coarse silt to sand-sized clastic material in Lithofacies IV in combination with the width of the lower terrace, implies sedimentation close to a river mouth over a significant time span. The seismic and sedimentological data suggest that the water-level of Lake Ohrid was up to 60 m lower than today, which could be due to significantly drier conditions. A drier climate at Lake Ohrid during MIS 6 correlates well with other reconstructions from northeastern Greece (Tzedakis et al., 2003) and the Levant region (Bar Matthews et al., 2003) and infers that most of the eastern Mediterranean was affected by these conditions. Since there is no significant inlet close to Ohrid Bay today, we assume that dewatering of the watershed during MIS 6 differed significantly in the past.

The only significant valley, which enters the Ohrid Bay, is a valley expanding from the northwestern slope of Galicica Mountains (Fig. 2). Today, this valley not drained by a significant river. However, higher discharge in the past, with a significant supply of clastic material forming the lower terrace, could have been due to abundance and advance of local glaciers, which are known to have reached mid-valley positions during MIS 6 in the region (Hughes et al., 2006). These glaciers might have supplied enough water and eroded material during spring-summer melt water pulses even though climate conditions were probably significantly drier than today.

The observed sediment characteristics of Lithofacies III deposited on the upper terrace (Table 3), in combination with chronological and stratigraphical constrains, point to deposition of the corresponding sediments in a shallow-water, low-energy regime during the last interglacial period. The identification of gently dipping foresets supports a deposition of sediments in a low-energy regime. However, at the same time the area was affected by wave-action resulting in a transport of material towards the edge of the subaquatic terrace. Input of coarse-grained clastic material by riverine inflows was negligible, thus implying the river draining the valley on the northeastern slope of Lake Ohrid was active during the last interglacial period (MIS 5). The high amount of bio-induced carbonate and the absence of clastic material within Lithofacies III indicate a warm climate and also support humid conditions favoring Mediterranean tree cover and related soil stability in the surrounding mountains as suggested by Lézine et al. (2010). Warm climate conditions during the last interglacial period are reported from other paleoclimate records within the Mediterranean region (Tzedakis et al., 2003; Martrat et al., 2004; Allen and Huntley, 2009; Vogel et al., 2010a).

Lithofacies II has been identified in both cores but with slight differences in composition indicating that time and depth of deposition slightly changed. In core Co1201 on the lower terrace the chara fragments were less abundant and less intact compared to the upper terrace pointing to a higher energy regime during deposition. Furthermore the finely dispersed OM and $CaCO_3$ was less than in Lithofacies II of core Co1200. Our interpretation is that the water level at the beginning of the last glacial period (MIS 4, 3, and 2) was about 30 m or less so that sediment got deposited mostly on the lower terrace. Broken fragments within Lithofacies II of core Co1201 indicate a transport of material from the upper terrace before final deposition. At the end of the last glacial period the water level must have rose and finally covered also the upper terrace. Another indication for a lake level rise within the last glacial period is the difference in thickness and age between the cores within the same Lithofacies. In core Co1201 (lower terrace) Lithofacies II is 120 cm thicker

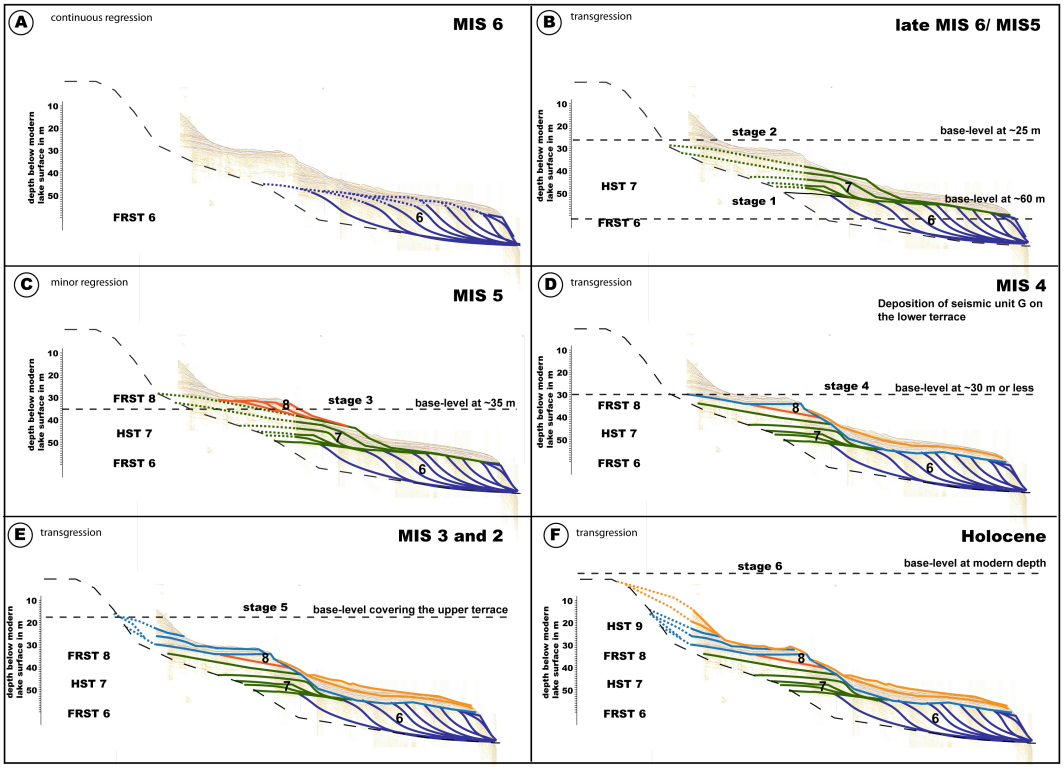

Fig. 8. The conceptual model illustrates the sedimentary evolution of terraces in Ohrid Bay since MIS 6 (penultimate glacial period). (FRST = Forced Regression System Tract, HST = Highstand System Tract, MIS = Marine Isotope Stage). As the significantly older clinoforms within the southern area are labeled 1–5, the numbering in this model for Ohrid bay starts with FRST 6. After a continuous regression during MIS 6 with subsequent formation of FRST 6 **(A)** the lake level rose to about 35 m as indicated by HST 7 **(B)**. This period is followed by a falling lake level evidenced by FRST 8 **(C)**. After a lowstand with an exposure of the upper terrace and subsequent erosion of HST 7 and FRST 8 the lake level rose in two steps during MIS 4, 3, and 2. After the first rise, only the lower terrace was covered by lake water **(D)** following the second lake level rise, also the upper terrace was then covered by water and sediments were deposited on both terraces **(E)**. Finally, deposition of sediments assigned to lithofacies II and I took place **(F)** at modern water depth.

compared to core Co1200 and comprises two additional ash layers (C-20, X-5) that could be dated to 80 ka and 105 ka. Only the CI/Y-5-tephra dated to 39 ka was identified in both cores.

The most recent sediments comprising Lithofacies I in cores Co1200 and Co1201 represent a deposition of mid-Holocene to modern-day sediments at both sites. Since larger intact chara fragments and coarser clasts are absent throughout Lithofacies I we conclude that both sites remained well below the chara belt (>30 m) throughout the period of deposition. The hemipelagic characteristics of units G and H suggest environmental conditions comparable to those of today.

By now we have shown that our data can be used to reconstruct paleoenvironmental conditions in Lake Ohrid since the penultimate glacial period though the effect of subsidence was neglected. Lake Ohrid is a tectonic active basin that experienced subsidence since its formation although exact subsidence rates are unknown. Ohrid Bay is one area within the lake that only subsided slightly at least during the time span we investigated in this study because it is comparable to a hinged margin setting or a relay ramp (linkage between two segments between overlapping faults, Gawthorpe and Leeder, 2000) within the eastern major boundary fault complex. These settings are well known to experience the lowest subsidence rates within a fault complex. Hence subsidence is assumed to be small. In addition we do not observe active faults on our sediment echosounder profiles of Ohrid Bay and therefore no indication for active local tectonics. Subsidence caused by sediment load due to the load itself and compaction processes is also expected to be low because significant effects are only reported for larger time spans and higher dimensional margins (Sclater et al., 1980; Reynolds et al., 1991; Moore et al., 1997).

Our detailed survey by means of echosounder profiling and bathymetric mapping of almost the entire lake floor revealed that Ohrid Bay is the only area suitable for investigating lake level fluctuations. One would assume that such deltaic structure as observed offshore the City of Ohrid could also be found in the northern shore area and/or offshore Sveti

Naum where the river Cerava enters the lake. The latter area shows a huge delta structure but unfortunately it is altered by tectonic forces anticipating an interpretation in terms of lake level fluctuations. In addition, no core information is available for this part of the lake, which is essential to date prominent reflectors in sediment echosounder data. The northern area on the other hand is not suitable for two reasons. No river enters Lake Ohrid in that area hence there is a lack of depositional material. More importantly, this area has experienced several events of mass movement resulting in a downward transport of reworked material and hence the loss of stratigraphic information.

5.2 Lake level fluctuations and biodiversity

We interpreted four major shoreline trajectories inferred from system tracts since the penultimate glacial period as inferred from sediment echosounder data from Ohrid Bay, which were combined with lithological information (Fig. 8). These system tracts include: (i) a forced regression system tract (FRST 6), (ii) a Highstand system tract (HST 7), (iii) a minor FRST 8, and (iv) a transgressive system tract or HST 9. All numbers referring to lake levels are given in meters below the modern water table.

A base level for the formation of FRST 6 (Fig. 8a) cannot clearly be identified. However, ostracods found within cores taken on land in vicinity to Ohrid Bay suggest that the shoreline of the lake was further landwards than at present (Hoffmann et al., personal. commun.). Hence we conclude that the base level must have been higher than today. A maximum of regression at a base level of 60 m is evident by truncation of topsets of FRST 6 (stage 1, Fig. 8b). A relative wide lower terrace still evident within the modern morphology, further suggests that the process of sediment bypassing took place over a long period (Figs. 3, 4, 8).

HST 7, which is only detectable by sediment echosounder data (Figs. 4, 8) and stacked on top of FRST 6, probably formed after a subsequent transgression to a base level of about 25 m (stage 2, Fig. 8b). Since the sediment cores did not recover material from sub-unit E_2, exact dating of this period was not possible. Based on the superposition of HST 7 on top of the truncated surface of FRST 6, we suggest that HST 7 occurred during late MIS 6 or early MIS 5 (Fig. 8b).

A minor drop within MIS 5 (stage 3, Fig. 8c) following the previous HST 7 period is evidenced by FRST 8 (Unit F and Lithofacies III). Since Unit F shows evidences for calm conditions during deposition and subsequent sub-aerial exposure we conclude that the base level fell below the upper terrace level to a depth of about 35 m (Fig. 8c).

At the beginning of the last glacial period MIS 4 (stage 4, Fig. 8d) accumulation of sediments only took place on the lower terrace as evident by a difference in thickness of Lithofacies II of core Co1201 (seismic unit G) on the lower terrace and core Co1200 on the upper terrace. We speculate that deposition of seismic unit G on the upper terrace started

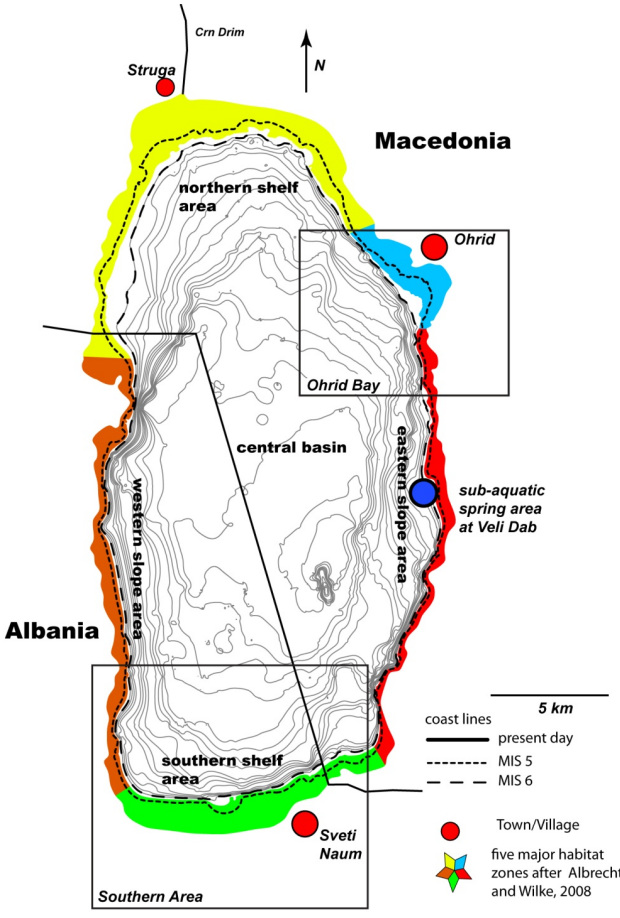

Fig. 9. Map of Lake Ohrid with major habitat zones (Albrecht and Wilke, 2008). Ancient coastlines as reconstructed in the study are shown as dashed lines. For details see text.

only 60 kyr ago indicated by the absence of tephras C-20 and X-5 (stage 5, Fig. 8e).

Finally, seismic units G and H as well as lithofacies II and I point to a rapid lake level rise and subsequent stillstand after FRST 8, which led to depositional conditions of hemipelagic sediments that is still ongoing today (Fig. 8f).

The effect on the coastlines for the significant lake level fluctuations since the penultimate glacial period is illustrated in Fig. 9. Reconstruction of these ancient coastlines shows that only relatively small areas are affected by a 60 m drop in lake level. However, these areas are important for the endemism in Lake Ohrid (Albrecht and Wilke, 2008). For example, species have been identified as being endemic to the area around the sub-aquatic spring of Veli Dab (Fig. 9, Albrecht and Wilke, 2008). A minor drop in lake level probably results in a desiccation of this area and destruction of the habitat. On the other hand the initial drowning of that area can possibly be linked to the time where the punctuated endemism evolved. Although it is highly speculative it shows that lake level fluctuations can have an influence on

the biodiversity within Lake Ohrid. Furthermore, Hauffe et al. (2010) observed that almost all gastropods live within a depth zone of 5–50 m. A minor drop in lake level may lead to a disconnection and/or isolation of certain areas from the proper lake resulting in allopatric speciation. Therefore we suggest that the evolution of endemic species is tentatively correlated with significant lake level fluctuations. Nevertheless this correlation remains speculative due to high uncertainties in speciation rate (Martens, 1997) and the timings of lake level stages or changes (Genner et al., 2010 and this study). Allopatric speciation involves a strict geographical barrier that prevents or reduces gene flow among subpopulations (for details see Albrecht and Wilke, 2008), and such a barrier apparently did not exist in ancient Lake Ohrid. The bathymetry of Lake Ohrid indicates that no subbasins or sub-aerial islands existed during MIS 6, when the lake level was 60 m lower than present day (Fig. 8). In comparison to the African Lake Malawi, where a magnitude of lake level changes greater than 550 m and subsequent expansion and establishment of rock fish populations was reconstructed (Genner et al., 2010), the magnitude of lake level change for Lake Ohrid since MIS 6 was probably too small for a major effect on speciation. One explanation is that the inferred lake level changes at Lake Ohrid had only a minor impact on the environment, particularly at the eastern shore, where rocky cliffs continue into deeper waters and an adaptation of species to a new living environment was not necessary. A change from calm conditions during lake level highstands to more dynamic conditions within the littoral zone after a drop in lake level may have an effect on species, which have been evolved during calm conditions as explained by Martens (1997). Within Lake Ohrid this is valid for small areas bounded by cliffs along the eastern shore line and more importantly within Ohrid Bay. These areas, although they were not completely desiccated, experienced a significant change in water depth with subsequent change in dynamic conditions.

Significant changes could have also affected the northern shore area where the bathymetry indicates a gently dipping sandy lake floor (Fig. 9). Here, even a minor transgression/regression of the shoreline would lead to drastic changes of subsurface properties and, subsequently, may have a major impact on the living environment.

In a longer term perspective, the endemism in the lake could have been affected by gradual lake level rise, since Lake Ohrid became established as water filled body. This lake level rise can be deduced from the five clinoform structures seen in the multichannel seismic data (Fig. 7) at the southern part of Lake Ohrid. Ancient depths of lake levels can be estimated by picking topset reflections. Using an average sound velocity of 1600 ms^{-1} for sediments, distinct reflections occur at 200, 285, 300, 330, and 360 m depth below the modern lake level. We cannot assume that these numbers directly correspond to ancient lake levels because the subsidence history of the basin is not well known and current depths of the clinoforms are a combined effect of tectonic movements and lake level fluctuations. Nevertheless, pronounced clinoforms indicate significantly lower lake levels in the past with subsequent sudden changes in lake level.

A first attempt of dating individual clinoforms in the southern part of lake Ohrid was done by tracing reflections directly above or below the clinoforms to areas of undisturbed sediments within the central lake basin and assuming constant sedimentation rates. For example, the reflection interpreted to mark the transition of MIS 6 to MIS 5 can be traced all over Lake Ohrid. By using this reflection as a marker horizon an average sedimentation rate of 0.28 mm/yr for the period younger than 130 ka. can be calculated for the deep basin. This sedimentation rate would provide an age of ∼41 kyr for the Y-5 tephra, which is close to its real age. Extrapolation of this sedimentation rate leads to age estimations of ∼510 kyr, ∼600 kyr, ∼800 kyr, ∼940 kyr, and ∼1.1 Myr for the base of Unit E, D, C, B, and the basement (or base of Unit A), respectively. However, these numbers are only first estimates and inhibit great uncertainties due to a lack of lithological information of sediments older than 130 ka. For example, our age estimate for the basement is much lower than ages suggested by other authors (Aliaj et al., 2001; Spirkovski et al., 2001; Dumurdzanov et al., 2005; Susnik et al., 2006) though the actual age of Lake Ohrid is still highly debated. The calculated ages can probably regarded as minimum values as velocities for sediments increase with depth and our model does not include possible hiatuses that would lead to older ages for the basement of Lake Ohrid. Seismic stratigraphy, however, shows that clinoforms offshore Sveti Naum are significantly older than MIS 6 (Fig. 7). Final interpretation can only be achieved by combining seismic data with the information from a deep drilling campaign, which will provide crucial information for reconstructing the subsidence history of the basin and a profound age model for the older sediments.

6 Conclusions

Our study illustrates that a combined geophysical and sedimentological approach is a powerful tool to investigate lake level fluctuations and link them to biodiversity in ancient lakes. Hydro-acoustic data show that Lake Ohrid has undergone significant lake level fluctuations. Multichannel seismic data penetrating into deeper parts of the sediments suggest that, in general, lake level rose stepwise since its establishment as water filled body. The topset reflections up to depths of 360 m below modern lake level as evident by pronounced clinoforms offshore Sveti Naum suggest that lake surface of Lake Ohrid was significantly reduced in former time periods. Further lithological data is needed to reduce uncertainties with respect to age estimates of prominent reflections as well as the subsidence history of the entire basin. An analysis of sediment echosounder profiles and core data

within Ohrid Bay allows a more detailed reconstruction back to the penultimate glacial period. Two terraces are well preserved as morphological pattern within Ohrid Bay. The lower terrace (Unit E1, Lithofacies IV, FRST 6) is most likely a relic of a fan delta that formed in a high energy shallow water environment close to a river mouth during MIS 6. In contrast, the upper terrace (Unit F, Lithofacies III, FRST 8) formed in a low energy regime potentially under warm climate conditions with only minor rivers draining into Ohrid Bay during MIS 5. Four major shoreline trajectories can be deduced since the penultimate glacial period. A formation of sub-basins or sub-aerial parts since penultimate glacial is unlikely, since the lake level lowering by 30 or 60 m did not significantly affect the overall surface area of Lake Ohrid. However, the lake level changes may have had a significant impact on the speciation, since a great proportion of endemic species are found above 50 m water depth in modern Lake Ohrid.

Acknowledgements. We would like to thank our Macedonian colleagues G. Kostski, S. Trajanovski, and Z. Brdarovski from the Hydrobiological Institute Ohrid for their administrative and logistic support during numerous field campaigns to Lake Ohrid. Our undergraduate and graduate students are greatly acknowledged for their enthusiasm and help in the field and laboratory. We would like to thank workgroup of H. Villinger for providing a Streamer system in 2008. Thanks to W. Weinrebe and N. Lindhorst for their technical support during the field campaign in 2009. We are grateful to S. Hall for valuable comments on earlier version of the manuscript. We received helpful reviews and short comments from M. Strasser of the MARUM in Bremen, Germany, C. Beck from Université de Savoie in France, and Jens Holtvoeth from University of Liverpool. This research was supported by DFG grants Kr2222/7, WA2109/1, We2210/3, and Da563/2.

Edited by: V. Brovkin

References

Albrecht, C. and Wilke, T.: Ancient Lake Ohrid: biodiversity and evolution, Hydrobiologia, 615, 103–140, 2008.

Aliaj, S., Baldassarre, G., and Shkupi, D.: Quaternary subsidence zones in Albania: some case studies, B. Eng. Geol. Environ., 59, 313–318, 2001.

Allen, J., Brandt, U., Brauer, A., Hubberten, H., Huntley, B., Keller, J., Kraml, M., Mackensen, A., Mingram, J., and Negendank, J.: Rapid environmental changes in southern Europe during the last glacial period, Nature, 400, 740–743, 1999.

Allen, J., Watts, W., McGee, E., and Huntley, B.: Holocene environmental variability – the record from Lago Grande di Monticchio, Italy, Quatern. Int., 88, 69–80, 2002.

Allen, J. and Huntley, B.: Last Interglacial palaeovegetation, palaeoenvironments and chronology: a new record from Lago Grande di Monticchio, southern Italy, Quaternary Sci. Rev., 28, 1521–1538, 2009.

Allen, P. A. and Allen, J. R.: Basin Analysis Principles and Applications, 2nd ed., Blackwell Publishing, 549 pp., 2005.

Anselmetti, F., Ariztegui, D., Hodell, D., Hillesheim, M., Brenner, M., Gilli, A., McKenzie, J., and Mueller, A.: Late Quaternary climate-induced lake level variations in Lake Petén Itzá, Guatemala, inferred from seismic stratigraphic analysis, Palaeogeogr. Palaeocl., 230, 52–69, 2006.

Anselmetti, F., Ariztegui, D., Batist, M., Gebhardt, A., Haberzettl, T., Niessen, F., Ohlendorf, C., and Zolitschka, B.: Environmental history of southern Patagonia unraveled by the seismic stratigraphy of Laguna Potrok Aike, Sedimentology, 873–892, doi:10.1111/j.1365-3091.2008.01002.x, 2009.

Auclair, M., Lamothe, M., and Huot, S.: Measurement of anomalous fading for feldspar IRSL using SAR, Radiat. Meas., 37, 487–492, 2003.

Bar-Matthews, M., Ayalon, A., Kaufman, A., and Wasserburg, G.: The Eastern Mediterranean paleoclimate as a reflection of regional events: Soreq cave, Israel, Earth Planet Sc. Lett., 166, 85–95, 1999.

Bar-Matthews, M., Ayalon, A., and Kaufman, A.: Timing and hydrological conditions of Sapropel events in the Eastern Mediterranean, as evident from speleothems, Soreq cave, Israel, Chem. Geol., 169, 145–156, 2000.

Bar-Matthews, M., Ayalon, A., Gilmour, M., Matthews, A., and Hawkesworth, C.: Sea-land oxygen isotopic relationships from planktonic foraminifera and speleothems in the Eastern Mediterranean region and their implication for paleorainfall during interglacial intervals, Geochimica et Cosmochimica Acta, 67, 3181–3199, 2003.

Bordon, A., Peyron, O., Lézine, A., Brewer, S., and Fouache, E.: Pollen-inferred Late-Glacial and Holocene climate in southern Balkans (Lake Maliq), Quatern. Int., 200, 19–30, 2009.

Caress, D. and Chayes, D.: MB-SYSTEM Release 5, www.ldgo.columbia.edu/MB-System, 2005.

Catuneanu, O., Abreu, V., Bhattacharya, J., Blum, M., Dalrymple, R., Eriksson, P., Fielding, C., Fisher, W., Galloway, W., and Gibling, M.: Towards the standardization of sequence stratigraphy, Earth Science Reviews, 92, 1–33, 2009.

Croudace, I., Rindby, A., and Rothwell, G.: ITRAX: description and evaluation of a new multi-function X-ray core scanner, New techniques in sediment core analysis, 267, 51–63, 2006.

D'Agostino, K., Seltzer, G., Baker, P., Fritz, S., and Dunbar, R.: Late-Quaternary lowstands of Lake Titicaca: evidence from high-resolution seismic data, Palaeogeogr. Palaeocl., 179, 97–111, 2002.

Danzeglocke, U., Jöris, O., and Weninger, B.: CalPal-2007online, http://calpal_online.de/, 2008.

Daut, G., Mäusbacher, R., Baade, J., Gleixner, G., Kroemer, E., Mügler, I., Wallner, J., Wang, J., and Zhu, L.: Late Quaternary hydrological changes inferred from lake level fluctuations of Nam Co (Tibetan Plateau, China), Quatern. Int., 218, 86–93, doi:10.1016/j.quaint.2010.01.001, 2010.

De Vivo, B., Rolandi, G., Gans, P., Calvert, A., Bohrson, W., Spera, F., and Belkin, H.: New constraints on the pyroclastic eruptive history of the Campanian volcanic Plain (Italy), Miner. Petrol., 73, 47–65, 2001.

Drysdale, R., Zanchetta, G., Hellstrom, J., Fallick, A., and Zhao, J.: Stalagmite evidence for the onset of the Last Interglacial in southern Europe at 129 ± 1 ka, Geophys. Res. Lett., 32, doi:10.1029/2005GL024658, 2005.

Dumurdzanov, N., Serafimovski, T., and Burchfiel, B.: Cenozoic

tectonics of Macedonia and its relation to the South Balkan extensional regime, Geosphere, 1, 1–22, 2005.

Gawthorpe, R., and Leeder, M.: Tectono-sedimentary evolution of active extensional basins, Basin Res., 12, 195–218, 2000.

Genner, M., Knight, M., Haesler, M., and Turner, G.: Establishment and expansion of Lake Malawi rock fish populations after a dramatic Late Pleistocene lake level rise, Mol. Ecol., 19, 170–182, doi: 10.1111/j.1365-294X.2009.04434.x, 2010.

Gilbert, G.: Lake Bonneville, United States Geological Survey, 438 pp., 1890.

Hauffe, T., Albrecht, C., Schreiber, K., Birkhofer, K., Trajanovski, S., and Wilke, T.: Spatially explicit analyses of gastropod biodiversity in ancient Lake Ohrid, Biogeosciences Discuss., 7, 4953–4985, doi:10.5194/bgd-7-4953-2010, 2010.

Hayes, A., Kucera, M., Kallel, N., Sbaffi, L., and Rohling, E.: Glacial Mediterranean sea surface temperatures based on planktonic foraminiferal assemblages, Quaternary Sci. Rev., 24, 999–1016, 2005.

Helland-Hansen, W. and Martinsen, O.: Shoreline trajectories and sequences: description of variable depositional-dip scenarios, J. Sediment. Res. B., 66, 670–688, 1996.

Hughes, P., Woodward, J., and Gibbard, P.: Quaternary glacial history of the Mediterranean mountains, Prog. Phys. Geog., 30, 334–364, doi: 10.1191/0309133306pp481ra, 2006.

Hunt, D. and Tucker, M.: Stranded parasequences and the forced regressive wedge systems tract: deposition during base-level fall, Sediment. Geol., 81, 1–9, 1992.

Johnson, T., Scholz, C., Talbot, M., Kelts, K., Ricketts, R., Ngobi, G., Beuning, K., Ssemmanda, I., and McGill, J.: Late Pleistocene desiccation of Lake Victoria and rapid evolution of cichlid fishes, Science, 273, 1091–1093, doi:10.1126/science.273.5278.1091, 1996.

Keller, J., Ryan, W., Ninkovich, D., and Altherr, R.: Explosive volcanic activity in the Mediterranean over the past 200,000 yr as recorded in deep-sea sediments, Bull. Geol. Soc. Am., 89, 591–604, 1978.

Kraml, M.: Laser-Ar/Ar-Datierungen and distalen marinen Tephren des jung-quartären mediterranen Vulkanismus (Ionisches Meer, M25/4), Ph. D., Albert-Ludwings-Universität Freiburg, Freiburg, 216 pp., 1997.

Lamothe, M., Auclair, M., Hamzaoui, C., and Huot, S.: Towards a prediction of long-term anomalous fading of feldspar IRSL, Radiat. Meas., 37, 493–498, 2003.

Lézine, A., Von Grafenstein, U., Andersen, N., Belmecheri, S., Bordon, A., Caron, B., Cazet, J., Erlenkeuser, H., Fouache, E., and Grenier, C.: Lake Ohrid, Albania, provides an exceptional multiproxy record of environmental changes during the last glacial-interglacial cycle, Palaeogeogr. Palaeocl., 287, 116–127, 2010.

Magny, M., Peyron, O., Gauthier, E., Rouèche, Y., Bordon, A., Billaud, Y., Chapron, E., Marguet, A., Pétrequin, P., and Vannière, B.: Quantitative reconstruction of climatic variations during the Bronze and early Iron ages based on pollen and lake-level data in the NW Alps, France, Quatern. Int., 200, 102–110, 2009.

Marino, G., Rohling, E., Sangiorgi, F., Hayes, A., Casford, J., Lotter, A., Kucera, M., and Brinkhuis, H.: Early and middle Holocene in the Aegean Sea: interplay between high and low latitude climate variability, Quaternary Sci. Rev., 28, 3246–3262, 2009.

Martens, K.: Speciation in ancient lakes, Trends in Ecology & Evolution, 12, 177–182, 1997.

Martrat, B., Grimalt, J., Lopez-Martinez, C., Cacho, I., Sierro, F., Flores, J., Zahn, R., Canals, M., Curtis, J., and Hodell, D.: Abrupt temperature changes in the Western Mediterranean over the past 250 000 years, Science, 306, 1762, 2004.

Matter, M., Anselmetti, F. S., Jordanoska, B., Wagner, B., Wessels, M., and Wüest, A.: Carbonate sedimentation and effects of eutrophication observed at the Kališta subaquatic springs in Lake Ohrid (Macedonia), Biogeosciences Discuss., 7, 4715–4747, doi:10.5194/bgd-7-4715-2010, 2010.

Matzinger, A., Spirkovski, Z., Patceva, S., and Wuest, A.: Sensitivity of ancient Lake Ohrid to local anthropogenic impacts and global warming, J. Great Lakes Res., 32, 158–179, 2006.

Matzinger, A., Schmid, M., Veljanoska-Sarafiloska, E., Patceva, S., Guseska, D., Wagner, B., Müller, B., Sturm, M., and Wüest, A.: Eutrophication of ancient Lake Ohrid: Global warming amplifies detrimental effects of increased nutrient inputs, Limnol. Oceanogr., 52, 338–353, 2007.

Moernaut, J., Verschuren, D., Charlet, F., Kristen, I., Fagot, M., and Batist, M. D.: The seismic-stratigraphic record of lake-level fluctuations in Lake Challa: Hydrological stability and change in equatorial East Africa over the last 140 kyr, Earth Planet Sc. Lett., 290, 214–223, doi:10.1016/j.epsl.2009.12.023, 2010.

Paterne, M., Guichard, F., and Labeyrie, J.: Explosive activity of the South Italian volcanoes during the past 80,000 years as determined by marine tephrochronology, J. Volcanol. Geoth. Res., 34, 153–172, 1988.

Peyron, O., Guiot, J., Cheddadi, R., Tarasov, P., Reille, M., de Beaulieu, J., Bottema, S., and Andrieu, V.: Climatic reconstruction in Europe for 18 000 yr BP from pollen data, Quaternary Res., 49, 183–196, 1998.

Pirmez, C., Pratson, L., and Steckler, M.: Clinoform development by advection-diffusion of suspended sediment: Modeling and comparison to natural systems, J. Geophys. Res.-Sol. Ea., 103, 24141–24157, 1998.

Popovska, C. and Bonacci, O.: Basic data on the hydrology of Lakes Ohrid and Prespa, Hydrol. Process., 21, 658–664, 2007.

Posamentier, H., Allen, G., James, D., and Tesson, M.: Forced regressions in a sequence stratigraphic framework: concepts, examples, and exploration significance, AAPG Bull., 76, 1687–1687, 1992.

Preusser, F., Degering, D., Fuchs, M., Hilgers, A., Kadereit, A., Klasen, N., Krbetschek, M., Richter, D., and Spencer, J.: Luminescence dating: Basics, methods and applications, Quaternary Science Journal (Eiszeitalter und Gegenwart), 57, 95–149, 2008.

Schellmann, G., Beerten, K., and Radtke, U.: Electron spin resonance (ESR) dating of Quaternary materials, Eiszeitalter und Gegenwart, 57, 150–178, 2008.

Scholz, C. and Rosendahl, B.: Low lake stands in Lakes Malawi and Tanganyika, East Africa, delineated with multifold seismic data, Science, 240, 1645–1648, 1988.

Sclater, J. and Christie, P.: Continental stretching: an explanation of the post-mid-Cretaceous subsidence of the central North Sea basin, J. Geophys. Re., 85, 3711–3739, 1980.

Spirkovski, Z., Avramovski, O., and Kodzoman, A.: Watershed management in the Lake Ohrid region of Albania and Macedonia, Lakes & reservoirs: research and management, 6, 237–242, 2001.

Stankovic, S.: The Balkan Lake Ohrid and Its Living World, W.

Junk, 357 pp., 1960.

Sturmbauer, C., Baric, S., Salzburger, W., Ruber, L., and Verheyen, E.: Lake level fluctuations synchronize genetic divergences of cichlid fishes in African lakes, Mol. Biol. Evol., 18, 144–154, 2001.

Sulpizio, R., Zanchetta, G., Paterne, M., and Siani, G.: A review of tephrostratigraphy in central and southern Italy during the last 65 ka, Il Quaternario, 16, 91–108, 2003.

Sulpizio, R., Zanchetta, G., D'Orazio, M., Vogel, H., and Wagner, B.: Tephrostratigraphy and tephrochronology of lakes Ohrid and Prespa, Balkans, Biogeosciences, 7, 3273–3288, doi:10.5194/bg-7-3273-2010, 2010.

Susnik, S., Knizhin, I., Snoj, A., and Weiss, S.: Genetic and morphological characterization of a Lake, J. Fish Biol., 68, 2–23, 2006.

Tzedakis, P., Frogley, M., and Heaton, T.: Last Interglacial conditions in southern Europe: evidence from Ioannina, northwest Greece, Global Planet. Change, 36, 157–170, 2003.

Vogel, H., Wagner, B., Zanchetta, G., Sulpizio, R., and Rosén, P.: A paleoclimate record with tephrochronological age control for the last glacial-interglacial cylce from Lake Ohrid, Albania and Macedonia, J. Paleolimnol., doi:10.1007/s10933-009-9404-x, 2010a.

Vogel, H., Zanchetta, G., Sulpizio, R., Wagner, B., and Nowaczyk, N.: A tephrostratigraphic record for the last glacial–interglacial cycle from Lake Ohrid, Albania and Macedonia., J. Quaternary Sci., 25, 320–338, 2010b.

Wagner, B., Reicherter, K., Daut, G., Wessels, M., Matzinger, A., Schwalb, A., Spirkovski, Z., and Sanxhaku, M.: The potential of Lake Ohrid for long-term palaeoenvironmental reconstructions, Palaeogeogr. Palaeocl., 259, 341–356, 2008a.

Wagner, B., Sulpizio, R., Zanchetta, G., Wulf, S., Wessels, M., Daut, G., and Nowaczyk, N.: The last 40 ka tephrostratigraphic record of Lake Ohrid, Albania and Macedonia: a very distal archive for ash dispersal from Italian volcanoes, J. Volcanol. Geoth. Res., 177, 71–80, 2008b.

Wagner, B., Lotter, A., Nowaczyk, N., Reed, J., Schwalb, A., Sulpizio, R., Valsecchi, V., Wessels, M., and Zanchetta, G.: A 40,000-year record of environmental change from ancient Lake Ohrid (Albania and Macedonia), J. Paleolimnol., 41, 407–430, 2009.

Wallinga, J., Bos, A., Dorenbos, P., Murray, A., and Schokker, J.: A test case for anomalous fading correction in IRSL dating, Quat. Geochronol., 2, 216–221, 2007.

Wessel, P. and Smith, W.: Free software helps map and display data, Eos Trans. AGU, 72, 445–446, 1991.

Zanchetta, G., Sulpizio, R., Giaccio, B., Siani, G., Paterne, M., Wulf, S., and D'Orazio, M.: The Y-3 tephra: A Last Glacial stratigraphic marker for the central Mediterranean basin, J. Volcanol. Geoth. Res., 177, 145–154, 2008.

5.2 Manuscript #2

ACTIVE BASINS AND NEOTECTONICS: MORPHOTECTONICS OF LAKE OHRID BASIN (FYROM AND ALBANIA)

Klaus Reicherter[1], Nadine Hoffmann[1], Katja Lindhorst[2], Sebastian Krastel[2], Tomás Fernández-Steeger[3], Christoph Grützner[1], and Thomas Wiatr[1]

1 Institute of Neotectonics and Natural Hazards, RWTH Aachen University, Lochnerstr. 420, 52056 Aachen, Germany

2 Leibniz-Institute for Marine Sciences, IFM-GEOMAR, Cluster of Excellence: The Future Ocean, Christian-Albrecht-University, Kiel, Germany

3 Chair of Engineering Geology and Hydrogeology, RWTH Aachen University, Germany

Published by E. Schweizerbart'sche Verlagsbuchhandlung, Stuttgart, Germany in 2011 as Reicherter, K., Hoffmann, N., Lindhorst, K., Krastel, S., Fernandez-Steeger, T., Grutzner, C. and Wiatr, T. (2011) Active basins and neotectonics: morphotectonics of the Lake Ohrid Basin (FYROM and Albania). Zeitschrift der Deutschen Gesellschaft für Geowissenschaften, 162, 217-34

5.3 Manuscript #3

HYDROACOUSTIC ANALYSIS OF MASS WASTING DEPOSITS IN LAKE OHRID (FYR MACEDONIA/ALBANIA)

Katja Lindhorst[1], Matthias Grün[1], Sebastian Krastel[1], and Tilmann Schwenk[2]

1 Leibniz-Institute for Marine Sciences, IFM-GEOMAR, Cluster of Excellence: The Future Ocean, Christian-Albrecht-University, Kiel, Germany

3 Department of Geoscience at University of Bremen, Bremen, Germany

Published by Springer Science+Business Media B.V. in 2012: Y. Yamada et al. (eds.), Submarine Mass Movements and Their Consequences, Advances in Natural and Technological Hazards Research, Vol. 31 as Lindhorst, K., Gruen, M., Krastel, S. and Schwenk, T. (2012) Hydroacoustic Analysis of Mass Wasting Deposits in Lake Ohrid (FYR Macedonia/Albania). Submarine Mass Movements and Their Consequences, 245-53

Chapter 22
Hydroacoustic Analysis of Mass Wasting Deposits in Lake Ohrid (FYR Macedonia/Albania)

Katja Lindhorst, Matthias Gruen, Sebastian Krastel, and Tilmann Schwenk

Abstract Lake Ohrid is a tectonically formed basin on the Balkan Peninsula. The Udenisht slide complex (USC), in the southwestern part of the lake, is by far the largest mass failure event within the basin. The slide deposits cover an area of ~27 km², are up to 50 m thick, and sum up to a volume of ~0.11 km³. The USC extends for up to 10 km into the central basin. First age estimations suggest that the USC is less than 1,500 years old. The volume of the USC is well within the range of landslide volumes capable to trigger tsunamis. However, since the slide event was retrogressive with at least two sub-events and sudden failures of major blocks are not supported by available data, no major tsunami was triggered by the USC. In contrast, subsurface and morphological indications for lake floor instabilities north of the USC suggest rotational slumping processes occurring in this area with higher possibility for tsunami generation in the future.

Keywords Lake Ohrid • Sublacustrine landslides • Lake floor morphology • Hydro-acoustic methods • Tsunamigenic potential

22.1 Introduction

Studies of mass movements in lakes are important especially in seismically active regions as their temporal record can be used for unraveling the paleoseismicity of a certain area (Chapron et al. 2004; Strasser et al. 2006; Moernaut et al. 2007).

K. Lindhorst (✉) • M. Gruen • S. Krastel
Leibniz Institute of Marine Sciences (IFM-GEOMAR), Wischhofstr. 1-3,
24148 Kiel, Germany
e-mail: klindhorst@ifm-geomar.de

T. Schwenk
Department of Geosciences, University of Bremen, Bremen, Germany

Y. Yamada et al. (eds.), *Submarine Mass Movements and Their Consequences*,
Advances in Natural and Technological Hazards Research 31,
DOI 10.1007/978-94-007-2162-3_22, © Springer Science+Business Media B.V. 2012

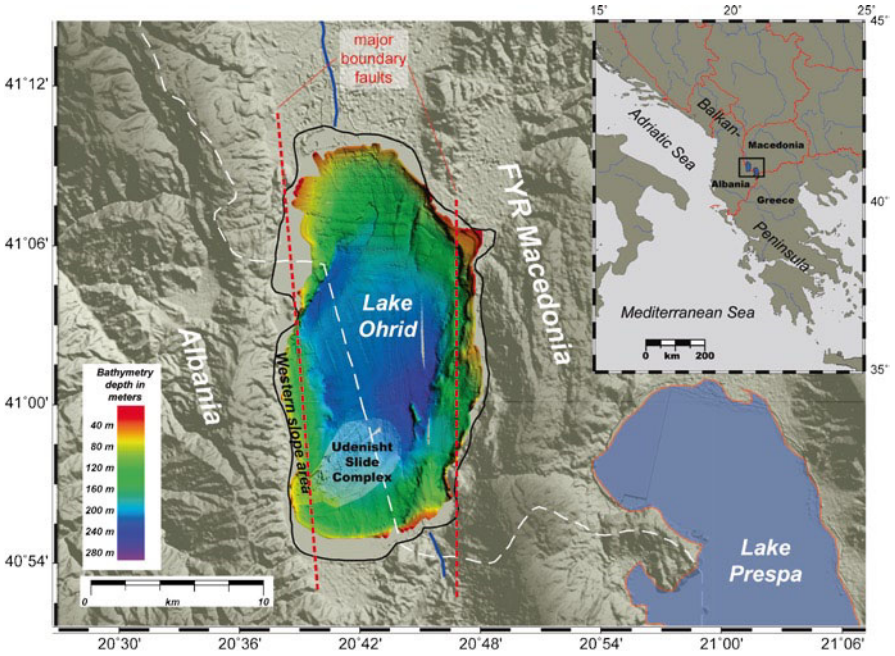

Fig. 22.1 Overview map of the topography (*grey*) and bathymetry (*colored*) of Lake Ohrid and the surrounding area. *White dashed line* marks the boundary between Albania and FYR Macedonia. Main boundary faults are shown as *red dashed lines*. The USC is found in the southwestern part of the lake. Inlet shows the general location of Lake Ohrid on the Balkan Peninsula

Furthermore, lakes offer the opportunity to investigate slope failure events in great detail due to the restricted area (Strasser et al. 2007).

Lake Ohrid is most likely one of the oldest lakes in Europe (3–5 Ma) located on the border between FYR of Macedonia and Albania (Albrecht and Wilke 2008). The lake is surrounded by high mountain chains on the eastern and western sides; the lake level is at an altitude of 693 m above sea level (Fig. 22.1). Lake Ohrid extends 30 km (N-S) by 15 km (E-W) covering an area of ~360 km². Maximum water depth is 293 m.

The region around Lake Ohrid is seismically active with several medium to large earthquakes that have occurred within the last 2,000 years (Wagner et al. 2008). One prominent example is the 518 AD event that nearly entirely destroyed the city of Ohrid (Hoffmann et al. 2010).

Landslide deposits are widespread in Lake Ohrid. In this article we present a detailed morphological description of the Udenisht Slide Complex (USC) area through the analysis of bathymetric data. In addition, we use high resolution seismic profiles to delineate the internal structure of the slide itself and the sediments deposited before the failure. We further provide a first age estimation and discuss possible causes and trigger mechanisms of the USC. Moreover, we examine the tsunamigenic potential of the western slope area of Lake Ohrid.

22.2 Seismic Stratigraphy and Slide Bodies

Interpretation of seismic lines (sediment echo-sounder and multichannel seismic data collected during several surveys between 2004 and 2009) provide new insights into the internal structure of the southwestern part of Lake Ohrid. The seismic stratigraphic analysis of the southwestern part of the lake is based on variations in seismic facies; the seismic sections have been divided into three units (A–C; oldest to youngest, respectively) overlying the acoustic basement (Fig. 22.2). In general,

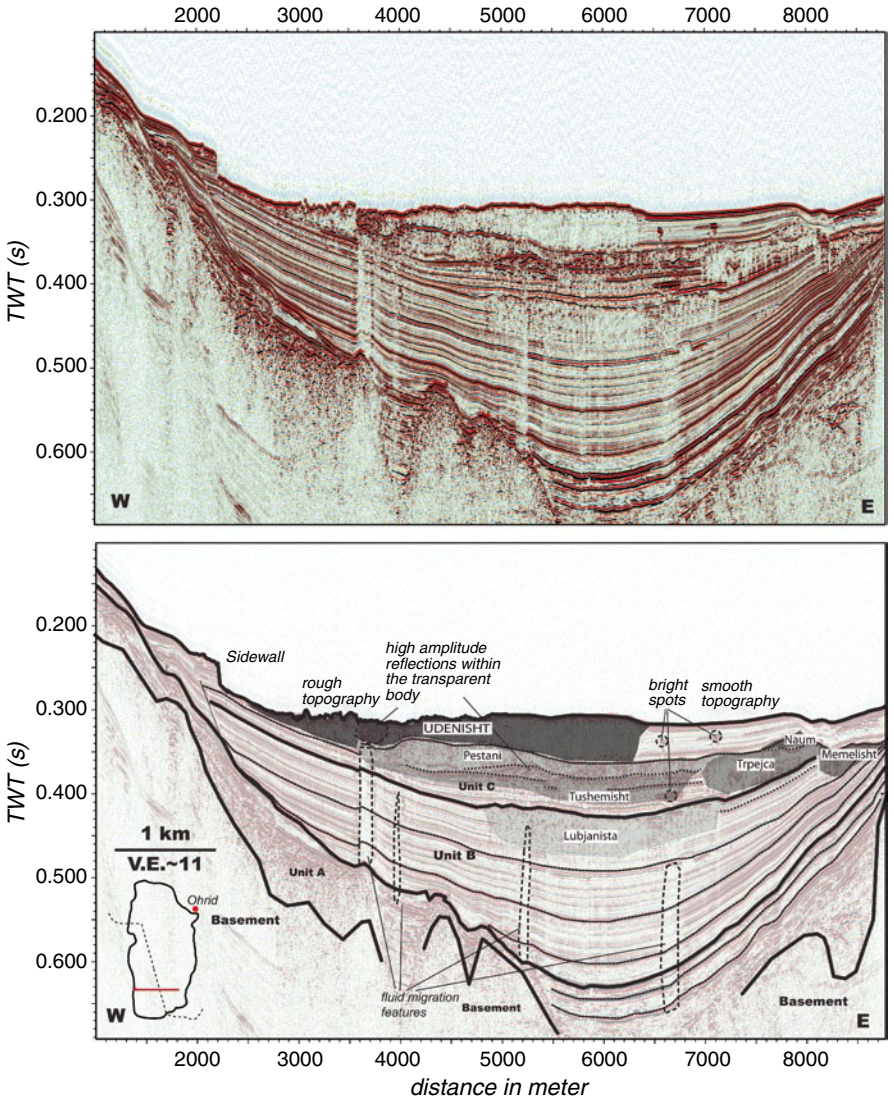

Fig. 22.2 W-E seismic section crossing the USC (*top*) and interpretation (*bottom*)

all units thicken toward the central part of the basin. Seismic reflections onlap the western margin but are sub-parallel and tilted on the eastern side (Fig. 22.2).

Unit A consists of high amplitude reflections of partially deformed sediments filling sub-basins of the basement. Alternating high and low amplitude reflections, including several prominent horizons, can be observed within the overlying Unit B. The unit is characterized by thick (~150 m) undisturbed sediments without clear evidence of reworking processes aside from a transparent body, the Lubjanista slide, recognized within the central part of the profile (Fig. 22.2). The youngest Unit C hosts several additional transparent bodies interpreted as slide deposits (Pestani, Tushemisht, Naum, Trpejca, and Memelisht). The most recent slide, the USC is imaged over a length of 4 km. In addition, several fluid migration features and bright spots are imaged mainly in the deepest part of the basin (Fig. 22.2).

22.3 Udenisht Slide Complex

22.3.1 Morphological Pattern

Bathymetric data were collected in 2009 using an ELAC Seabeam 1180 system operating at a frequency of 180 kHz allowing a detailed morphological description of the USC (Fig. 22.3). We divided the area affected by the mass movement event into a failure surface and a displaced mass deposit area (Fig. 22.3).

Although the Udenisht head scarp was not detected in the bathymetry, the uppermost part is clearly defined by steep slope angles of up to 10° confined by sidewalls up to 25 m height and several isolated blocks (~40–60 m × 10 m; Fig. 22.3). The sliding area widens further downslope and the northern sidewall changes its direction northwards at water depths of ~150–220 m (Fig. 22.3). The slide deposit area starts at water depths of ~150 m and is accompanied by a decrease in slope angle to <4° (Fig. 22.3). The largest part of the slide deposits with a run-out distance of 10 km is hardly distinguishable from the overall smooth morphology in this area (Fig. 22.3). Slope angles decrease to values less than 1.5°. Two distinct morphological steps occur at ~100 m and ~180 m water depth (Fig. 22.3) indicating the presence of fault lineaments cross cutting the slide area in N-S direction. A continuation of the lower fault structure is imaged on the northern side of the slide area as a morphological step in the bathymetric data.

Channel structures were recognized further north and may also be related to faulting (Fig. 22.2). Two additional slides are imaged north of the USC in water depths around 180 m (Fig. 22.2). They have short run out lengths and resemble typical slump features.

22.3.2 Internal Structure

Sediment echo-sounder penetration depth within the upslope area of the USC is limited due to the steep slope and a strong lake floor reflector prevents deeper penetration.

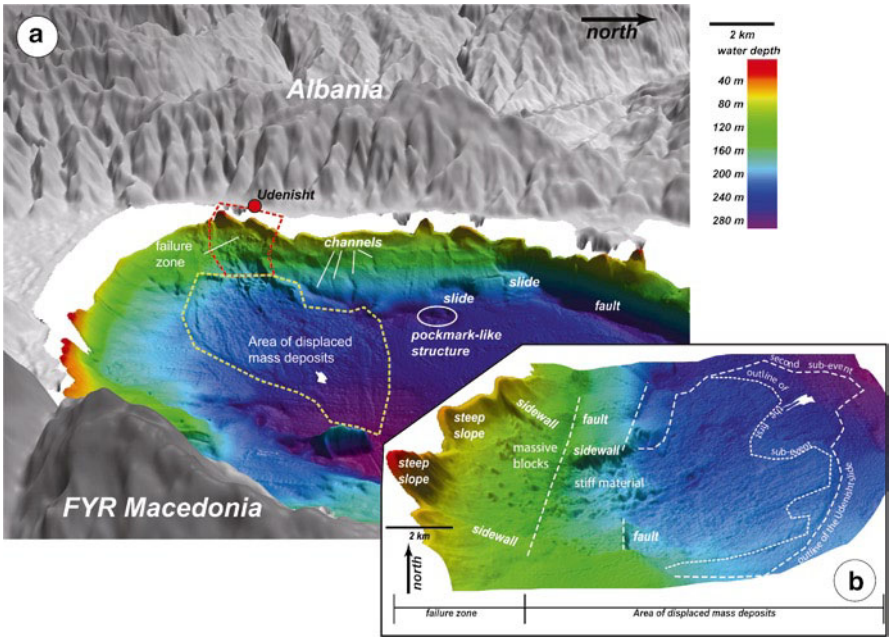

Fig. 22.3 (**a**) Westward 3D perspective view of the southern area of Lake Ohrid. *Dashed red line* indicates the failure zone of the USC, while the main slide deposits are surrounded by the *orange dashed line*. Two additional smaller-scale slides, sediment evacuation channels, pockmark-like structures and one prominent normal fault are marked north of the USC. (**b**) Detailed 3D image of the USC area with the most prominent morphological features described in the text

The lake floor reflector shows a sudden increase in water depth across the failure surface (Fig. 22.4). Further downslope, areas of massive blocks occur with a subsequent increase in slope angle. The lower series of blocks have trapped some slide deposits upslope, while undisturbed sedimentary successions inclined towards the central basin are imaged further downslope (Fig. 22.4). An up to 50 thick transparent body representing the main slide deposits is visible from 250 m water depth on (corresponding to 300 ms Two-Way Travel Time, TWT).

The main transparent body can be divided laterally into three sections differentiated by their internal structures, thicknesses, and surface morphology (Fig. 22.4). The first section (I) is defined by overall higher amplitudes, with some sub-parallel layered reflections and one prominent horizon representing the base of the slide. The second section (II) is thickest (up to 50 m) and shows a chaotic to transparent seismic facies. Due to the high reflectivity of the lake floor reflector, the base of the slide is not well imaged. A sudden decrease in thickness of the transparent body in combination with a morphological step marks the transition to the third section (III), which is characterized by patchy, discontinuous lake floor reflectors indicating a high roughness. Downslope of section III, undisturbed parallel to sub-parallel horizons are imaged in the central basin.

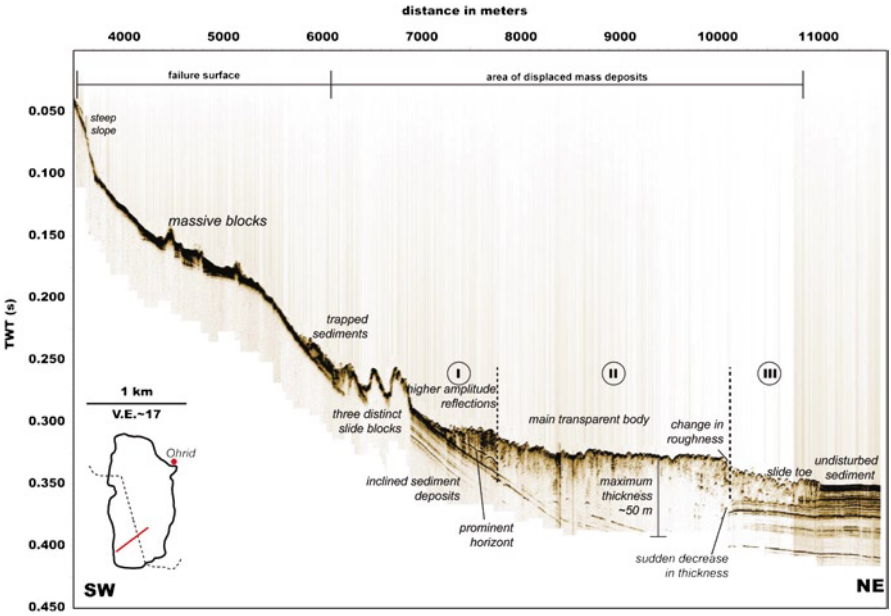

Fig. 22.4 Sediment echo-sounder profile crossing the slide area from SW to NE

The sediment echo-sounder and multichannel seismic data allowed estimating the extent and the volume of the USC. The failure surface covers an area of about 8 km² in contrast to the much larger area of deposition of 24 km². The total volume of the slide material is estimated to 0.11 km³. A change in thickness can be observed within the depositional area suggesting that the USC was probably not a single event but a sequence of at least two events with sufficient energy to transport material far into the central basin (Fig. 22.4).

22.4 Discussion

22.4.1 Age Estimations of Landslides

Age determination of the USC is difficult because no cores are currently available within the slide area. We can only estimate the age of the USC by analyzing the thickness of post slide sediments covering the acoustically transparent slide body. No undisturbed drape is detectable on the sediment echo-sounder profiles (Fig. 22.4). We operated the sediment echo-sounder at a frequency of 10 kHz, resulting in a theoretical vertical resolution of ~10 cm. Rough surface morphologies reduce the theoretical vertical resolution by lateral smearing effects, but a drape exceeding

30 cm would be detectable on the sediment echo-sounder data; hence we consider 30 cm as the maximal thickness of post-slide sediments. A drape less than 30 cm implies that the slide is a relatively recent event. Cores taken from the northeastern part of the lake show a sedimentation rate of 0.2 mm/a for the Holocene (Wagner et al. 2009). Holocene sedimentation rates should be relative homogenous across the lake. Taking 0.2 mm/a as sedimentation rate for the USC area results in a maximum age of 1,500 years for the youngest event of the USC. This number is obviously quite ambiguous due to the uncertainties of thickness of the drape and variations in accumulation rate. However, the slide must have occurred in the late Holocene.

The other six transparent units older than the USC indicate that the southwestern part of Lake Ohrid has a long history of mass wasting. No measured age data are available for the deeper reflectors but Lindhorst et al. (2010) developed a preliminarily age model based on sedimentation rates and seismic data. According to this age model, the slides within Unit C must be older than 130 kyr and the deepest slide in Unit B (Lubjanista) has an age greater than 510 kyr. No major mass movements older than 600 kyr are imaged on the seismic data.

22.4.2 Pre-conditioning Factors and Triggering Mechanisms

As Lake Ohrid is located in a seismically active region it is most likely that the USC was triggered by an earthquake. Nevertheless, some pre-conditioning factors must prevail before an earthquake triggers a sediment failure. The slopes in the USC area are very steep (up to 10°), which is one important pre-conditioning factor. Pockmarks and bright spots point to the importance of fluids in the USC area (Fig. 22.2); as a result high pore pressure may develop in distinct layers, which are sandwiched between fine-grained impermeable layers. Such over pressured layers are another important pre-conditioning factor for slope failure (Masson et al. 2010). Numerous fluid migration features at the western margin of Lake Ohrid imply that overpressured layers maybe widespread, which would make the western margin prone for future slope failures.

Our data suggest that the USC behaved as a retrogressive slide with at least two separated mass transport events. Within the slide area, two faults are clearly associated with activity along the western major boundary fault complex (Fig. 22.2). Even minor activity along these faults can induce slope failures in an area characterized by thick sedimentary successions deposited on high slope angles. Material removal at a water depth of ~180 m (location of the lower fault, Fig. 22.3) would result in loss of support for sediments further upslope. In connection with small earthquakes along local active faults, a second slope failure (~100 m water depth, location of the second fault, Fig. 22.3) may have occurred. It is not possible to infer the time interval between the two failures based on the acoustic data.

22.4.3 Tsunamigenic Potential of Slides in Lake Ohrid

The high resolution seismic stratigraphic analysis of Lake Ohrid shows that the western margin of Lake Ohrid has a long history of mass wasting. The current setting with indications for over pressured horizons and steep slope angles suggest that western margin of Lake Ohrid is prone to future slope failures. It is therefore pertinent to discuss whether the USC could have triggered a tsunami and further to evaluate the geohazard potential of the entire western margin. Studies of submarine landslides that caused tsunamis with local run-up heights of more than 15 m reveal that the most important factor is a high vertical displacement of an intact block in shallow water close to the coast at high initial accelerations (Okal and Synolakis 2003; Watts et al. 2003; Grilli and Watts 2005).

There is absence of onshore evidence or historical reports of waves that may have hit the coast within the last 1,500 years. According to Murty (2003) the volume of the USC is sufficient to trigger a tsunami. Yet, the largest uncertainties are related to the submergence depth and the initial acceleration of the USC. If we assume that an intact block with the volume of the USC failed in water depths of about 100 m, tsunami generation is likely. Our bathymetric data, however, shows that the USC has a long run-out distance, which points to quick disintegration and massive internal deformation. Therefore we exclude the movement of a rigid block with a high vertical displacement. In addition, slope failure occurred in two phases, thereby reducing the volume of individual events of the USC. Due to these observations, it is very unlikely that the USC triggered a major tsunami. In contrast, the two slump-features observed further to the north show less internal deformation indicating a smaller degree of disintegration. If similar events would occur at shallow water depth in the future, they have a higher tsunami potential though their initial acceleration is unknown.

In light of the results presented in this study, the western margin of Lake Ohrid is potentially unstable. The region is susceptible to seismic activity along active faults; hence it is most likely that mass failures will occur in the future, which might be tsunamigenic.

22.5 Conclusions

The USC is a young (<1,500 years) event that occurred in the southwestern part of Lake Ohrid. Older slides suggest a long history of sliding in this part of the lake. Ruptures along active faults crossing the USC area most likely acted as final trigger. The long run-out distance points to quick disintegration with intense sediment deformation. It is unlikely that such a flow triggered a significant tsunami, especially as it occurred in at least two phases in a retrogressive pattern. Slumps north of the USC show less disintegration and might have triggered tsunamis. Migrating fluids resulting in over pressured layers in combination with steep slope angles and ongoing seismicity make future slope failures likely. As such failures might occur

in a similar pattern as the slumps north of the USC, we cannot fully exclude that tsunamis will be initiated in the future.

Acknowledgments We would like to thank our Macedonian colleagues from the Hydrobiological Institute Ohrid for their logistic support. Thanks to W. Weinrebe and N. Lindhorst for their technical support. We are grateful to S. Hall and C. Berndt for valuable comments on earlier versions of the manuscript. We are grateful to comments of the reviewers P. Mazzanti and N. Waldmann that further improved the paper. This research was supported by DFG grant Kr2222/7.

References

Albrecht C, Wilke T (2008) Ancient Lake Ohrid: biodiversity and evolution. Hydrobiologia 615:103–140

Chapron E, Van Rensbergen P, De Batist M et al (2004) Fluid-escape features as a precursor of a large sublacustrine sediment slide in Lake Le Bourget, NW Alps, France. Terra Nova 16:305–311

Grilli S, Watts P (2005) Tsunami generation by submarine mass failure. I: modeling, experimental validation, and sensitivity analyses. J Waterw Port Coast Ocean Eng 131:283–297

Hoffmann N, Reicherter K, Fernández-Steeger T, Grützner C (2010) Evolution of ancient Lake Ohrid: a tectonic perspective. Biogeosciences 7:4641–4664

Lindhorst K, Vogel H, Krastel S et al (2010) Stratigraphic analysis of lake level fluctuations in Lake Ohrid: an integration of high resolution hydro-acoustic data and sediment cores. Biogeosciences 7:3531–3548

Masson DG, Wynn RB, Talling PJ (2010) Large landslides on passive continental margins: processes, hypotheses and outstanding questions. In: Mosher DC et al (eds) Submarine mass movements and their consequences, vol 28, Advances in natural and technological hazards research. Springer, Dordrecht, pp 153–165

Moernaut J, De Batist M, Charlet F et al (2007) Giant earthquakes in South-Central Chile revealed by Holocene mass-wasting events in Lake Puyehue. Sediment Geol 195:239–256

Murty T (2003) Tsunami wave height dependence on landslide volume. Pure Appl Geophys 160:2147–2153

Okal E, Synolakis C (2003) A theoretical comparison of tsunamis from dislocations and landslides. Pure Appl Geophys 160:2177–2188

Strasser M, Anselmetti F, Fah D et al (2006) Magnitudes and source areas of large prehistoric northern Alpine earthquakes revealed by slope failures in lakes. Geology 34:1005–1008

Strasser M, Stegmann S, Bussmann F et al (2007) Quantifying subaqueous slope stability during seismic shaking: Lake Lucerne as model for ocean margins. Mar Geol 240:77–97

Wagner B, Reicherter K, Daut G et al (2008) The potential of Lake Ohrid for long-term palaeoenvironmental reconstructions. Palaeogeogr Palaeoclim Palaeoecol 259:341–356

Wagner B, Lotter A, Nowaczyk N et al (2009) A 40,000-year record of environmental change from ancient Lake Ohrid (Albania and Macedonia). J Paleolimnol 41:407–430

Watts P, Grilli S, Kirby J et al (2003) Landslide tsunami case studies using a Boussinesq model and a fully nonlinear tsunami generation model. Nat Hazards Earth Sys Sci 3:391–402

5.4 Manuscript #4

SEDIMENTARY AND TECTONIC EVOLUTION OF ANCIENT LAKE OHRID

Katja Lindhorst[1], Sebastian Krastel[1], Klaus Reicherter[2], Tilmann Schwenk[3], Michael Stipp[1], Bernd Wagner[4]

1 Leibniz-Institute for Marine Sciences, IFM-GEOMAR, Cluster of Excellence: The Future Ocean, Christian-Albrecht-University, Kiel, Germany

2 Institute of Neotectonics and Natural Hazards, RWTH Aachen University, Lochnerstr. 420, 52056 Aachen, Germany

3 Department of Geoscience at University of Bremen, Bremen, Germany

4 Institute for Geology and Mineralogy, University of Cologne, Cologne, Germany

Submitted to Basin Research in July 2012 as Lindhorst, K., Krastel, S., Reicherter, K., Stipp, M., Wagner, B. and Schwenk, T. (in review) Tectonic and Sedimentary Evolution of Lake Ohrid (Albania/Macedonia). Basin Research

Sedimentary and tectonic evolution of Lake Ohrid (Macedonia/Albania)

Katja Lindhorst[1], Sebastian Krastel[1], Klaus Reicherter[2], Michael Stipp[1], Bernd Wagner[3], and Tilmann Schwenk[4]

[1] Leibniz-Institute for Marine Sciences, IFM-GEOMAR, Cluster of Excellence: The Future Ocean, Christian-Albrecht-University, Kiel, Germany

[2] Institute of Neotectonics and Natural Hazards, RWTH Aachen University, Lochnerstr. 4-20, 52056 Aachen, Germany

[3] Institute for Geology and Mineralogy, University of Cologne, Zülpicher Str. 49a, 50674 Cologne, Germany

[4] Department of Geosciences at University of Bremen, Bremen, Germany

Abstract

Lake Ohrid located on the Balkan Peninsula within the Dinaride-Albanide-Hellenide mountain belt is a tectonically active graben within the South Balkan Extensional Regime (SBER). Interpretation of multichannel seismic cross sections and bathymetric data reveals that Lake Ohrid formed in two main deformation phases: (1) a transtensional phase initially opened a pull-apart basin, (2) an extensional phase led to the present geometry of Lake Ohrid. After the initial opening, a symmetrical graben formed bounded by the Central Basin faults acting as master faults in a pull-apart like basin during a short transtensional phase in Late Miocene. The early-stage geometry of the basin has a typical rhomboidal shape restricted by two sets of major normal faults, namely Lini, Piskupat, Pescani, and Kaneo Faults. The location of the basin initiation coincides with the location of the greatest basement depth where today thick undisturbed sediments are present. Neotectonic activity since the Pliocene takes place along the roughly N-S directed Eastern and Western Major Boundary Normal faults that are partly exposed at the present lake floor. The tectono-sedimentary structure of the basin is divided in four main seismic units starting with the acoustic pre-rift basement (Unit A), overlain by fluvial deposits (Unit B), and lacustrine sediments (units C and D). Unit

C forms the majority of the entire infill comparable to a three-part depositional history described for rift lakes indicating the different stages of basin evolution. A detailed seismic fracies analysis reveals a prominent cyclic pattern of high- and low amplitude reflectors, which can be correlated with vegetational changes within the surrounding area caused by glacial/interglacial cycles. This type of chrono-stratigraphic interpretation results in age estimation of ~2 Myrs for Lake Ohrid.

.

Introduction

This paper documents the sedimentary and tectonic evolution of Lake Ohrid as revealed by hydro- and seismo-acoustic data collected during several surveys in between 2004 and 2008. Lake Ohrid is a transboundary lake located on the Balkan Peninsula with two thirds of its area belonging to the Former Yugoslav Republic of Macedonia (FYROM, in the following referred to as Macedonia) and one third to Albania (Fig. 1). The lake is situated in a tectonically active graben system within the Southern Balkan Extensional Regime (SBER, Burchfiel et al., 2008). Although its actual age is highly debated, Lake Ohrid is one of the oldest lakes in Europe (2-5 Ma). With more than 200 endemic species described it is a valuable archive not only for reconstructing the paleoclimatic environment within the Mediterranean region but also to study biodiversity and speciation patterns and their relation to geological changes over a long time period. Recent sedimentological and lithological studies covering the last 130 ka have shown that Lake Ohrid is a complex system that evolved within a highly variable environment depending on a range of interacting processes as for example spring activity, decomposition, and preservation of organic matter (Wagner et al., 2008a; Vogel et al., 2010). Interpretation of a sediment echosounder line revealed thick undisturbed sediment successions within the central basin (Wagner et al., 2008b). Slide bodies and fault structures have been detected making the lake is a prominent site for paleoseismic investigations (Reicherter et al., 2011). Lindhorst et al. (2010) suggested that Lake Ohrid experienced major lake level fluctuations that are most likely climatically induced, however they do not take into account the possibility of basin subsidence.

Here we present new geophysical data on the morphological structure and tectono-sedimentary evolution of Lake Ohrid, which enables us to make a spatial and temporal description and interpretation of depositional patterns within the basin. Through seismic stratigraphic interpretation of a thick sediment succession within the central basin, we try to analyze the nature of the sedimentary infill associated with glacial/interglacial cycles of the Quaternary and develop a first chronological framework in order to refine the age estimation of previous studies. The onset of subsidence as well as the spatial and temporal evolution of the overall basin architecture will be discussed in terms of its tectono-sedimentary development. Within the basin we examined areas that are recently very active with fault scarps exposed at the lake floor and those that are related to the initial opening of the basin but are not experiencing subsidence today. We also suggest evidence for fault continuation on

land. A model will be presented suggesting that the Lake Ohrid Graben opened as a pull-apart basin associated with a short period of transtensional stress and subsequent widening of the basin related to E-W extension caused by roll back of the Hellenic subduction slab. This paper is a case study for the structure and evolution of pull-apart basins within an extensional regime similar to the Basin and Range style (Lister and Davis, 1989) and is therefore applicable to other extensional basins developed in a similar geodynamic environment.

General Setting

Hydrology and Climate

Lake Ohrid has a length of about 30 km and a width of 15 km with an area of 360 km² (Stankovic, 1960). It has a simple bathtub shape morphology with average water depth of 150 m and a total volume of 50.7 km³ (Popovska and Bonacci, 2007). The current lake level is at 693 m above sea level (a.s.l.). The lake is surrounded by high mountain chains reaching heights of up to 2300 m a.s.l. on each side: the Mokra Mountains to the west and the Galicica Mountains on the eastern side (Fig. 1).

Water enters Lake Ohrid by two main rivers (the Sateska in the north and the Cerava in the south, Fig. 2), karstic springs fed by waters from its sister Lake Prespa located 150 m higher east of Lake Ohrid (both sublacustrine and surface springs), and direct precipitation (Fig. 2, Matzinger et al., 2006). Karst aquifers recharged from precipitation on the surrounding mountain ranges and from Lake Prespa, form approximately half of the net inflow today (Matzinger et al., 2006). Lake Ohrid has a relatively small catchment area (2600 km²) or even smaller if one exclude the sister Lake Prespa (1002 km², Popovska & Bonacci, 2007). Water leaves Lake Ohrid through the River Crn Drim (Fig. 2, ~60%) and by evaporation (~40%, Matzinger et al., 2006; Watzin et al., 2002).

The climate today is influenced by both Mediterranean and continental conditions due to its location in a high mountain range adjacent to the Adriatic Sea (Watzin et al., 2002). Average annual water temperatures are around 11°C. The lake does not freeze and summer air temperatures are reliably less than 23°C (Popovska and Bonacci, 2007). Belonging to the Mediterranean pluviometric regime, the Lake Ohrid region receives highest precipitation during winter and lowest during summer. Prevailing northerly wind directions drive a counter clockwise surface current, which is the main driver for particle transport in Lake Ohrid (Vogel et al., 2010b; Matzinger et al., 2006).

Paleoclimate, paleoenvironment and paleovegetation patterns within Lake Ohrid region have been studied through the analysis of sediment cores with a maximum age of 130 kyrs. Rapid climate and environmental changes have been recorded for the last 1000 yrs which could be an expression of the increasing human impact on Lake Ohrid (Wagner et al., 2008c; 2010; Vogel et al., 2010a) The productivity of Lake Ohrid was relatively high during the Holocene, when warm and humid conditions prevailed and were only interrupted by short-term cooling events (Wagner et al., 2008a). Inactivity of the karst springs during the glacial periods due to permafrost in large parts of the calcareous mountains has been suggested by a multi-proxy analysis of ostracods, pollen, sedimentology, and tephrochronology (Belmecheri et al., 2009; Lézine et al., 2010), but this was not confirmed by other studies (e.g. Vogel et al., 2010) and does not agree with recent geomorphological studies focusing on glaciation (G. Zanchetta, pers. comm.). Biological studies analyzing biomarkers and molluscs reveal major changes within the faunal and vegetation cover since the last Interglacial (Albrecht et al., 2010; Holtvoeth et al., 2010). According to Wagner et al. (2008c) the Late Pleistocene was cold and stable with steppe vegetation in the catchment and partially ice covered in winter whereas the Holocene was warmer and forest-dominated. During interglacial periods climatically induced changes in hydrology and productivity of the lake occur. In contrast, during glacial periods the basin experiences changes in the catchment dynamics and wind activity (Sulpizio et al., 2010; Vogel et al., 2010a).

Interpreting results between different terrestrial sites is rather difficult because the paleoclimate is highly dependent on factors such as the distance to an ocean, the latitude, and/or the elevation or geomorphology in the surrounding. However, paleoclimate studies of lake sediments Lago Grande di Monticchio of southern Italy (Allen et al. 1999; Wulf et al. 2004; Allen and Huntley 2009) and pollen analysis of a terrestrial sediment sequence in the Pindos of northwestern Greece (Tzedakis 1993; 1994; Tzedakis et al., 2003) show similar patterns as described for Lake Ohrid Basin. Both regions lie at approximately the same latitude as Lake Ohrid. A striking general feature of the Monticchio pollen record is the very short period of time over which forest or wooded steppe biomes replace steppe biomes and vice versa (Allen et al., 1999; Allen and Huntley, 2009). Forest biomes ensure a more stable catchment, with less erosion and runoff of mineral materials, and thus a biogenic dominated deposition was observed within sediments of Lago Grande di Monticchio at these intervals. As Lake Ohrid is in a very comparable setting, it is reasonable to assume a similar situation as for Lake Monticchio (Wulf et al., 2004).

Based on paleoclimate reconstructions of the Mediterranean region, Leeder et al. (1998) proposed enhanced precipitation in winter during glacial periods. With increased winter runoff and erosion as well as overall high annual erosion, the Mediterranean winter wet steppes were highly erodible. Evidence from sediment cores of Lake Ohrid (Wagner et al. 2008c; 2010; Lézine et al., 2010) seems to support this theory. Furthermore Leeder et al. (1998) stated that within Mediterranean environments, catchments are postulated to feed more sediment and water to lake environments during glacial periods. Increased winter runoff during glacial times leads to high lake levels at the same time as enhanced sediment supply (Lindhorst et al., 2010).

Another factor influencing the productivity, hydrology and vegetation cover within Lake Ohrid region is the growth or retreat of glaciers. Hughes et al. (2006) suggest that glaciers reached mid-valley positions during Marine Isotope Stage (MIS) 6 on the Pindos Mountains southeast of Lake Ohrid region, which would have an important influence on the sediment input into Lake Ohrid. During MIS 12 multiple glacier advances reaching maximum down-valley elevations of ~1000 m a.s.l. are suggested by a diamicton sequence found in the mountains of Greece (Hughes et al., 2006). Old moraine structures within the Galicica Mountains around 1400-1500 m a.s.l. further indicate that Lake Ohrid area was glaciated prior to Pleistocene times.

Geological and Tectonic Framework

The sedimentary basin that hosts modern Lake Ohrid developed above the contact between the Pelagonian and the Pindos Zone (Fig. 1). The Pelagonian Zone constitutes a continental remnant of the Vardar closure that was accreted to the Balkan area during the Mesozoic; it is composed of Paleozoic metamorphic and magmatic rocks as well as Triassic to Lower Jurassic carbonates and clastics that are widely exposed to the east, southeast and northwest of the lake (Burchfiel et al., 2008; Reicherter et al., 2011). Within the Pindos, Upper Cretaceous shallow-water limestones, sandstones, and claystones overlay obducted ophiolites of mainly Jurassic age (Channell and Kozur, 1997; Robertson 2004). Three main deformation phases are evident within the present geological structure of the Lake Ohrid region (Burchfiel et al., 2008): (1) NW-SE striking folds and thrust faults formed during the Late Cretaceous to Miocene compressional regime, (2) NW-SE trending dextral strike-slip faults are most likely related to a short transtensional phase in the Late Miocene due to a diminishing uplift and the beginning of the Dinarides-Albanides-Hellenides collapse with subsequent formation of

sedimentary basins in the hinterland from east to west, and (3) E-W extension within the SBER starting in late Miocene. Extension and normal faulting were most likely related to changes in the geometry of the subducting slab as well as slab roll back along the Hellenic subduction zone (Burchfiel et al., 2008). Located in western Macedonia and eastern Albania, Lake Ohrid is the youngest basin within the SBER (Fig. 1). The setting of the SBER is similar to the Basin and Range region in western USA (Lister and Davis, 1989) is illustrated in Fig. 1 with the Mokra, Galicica, and Baba Mountain as horsts and the Ohrid, Prespa and Pelagonian depressions as grabens (Aliaj et al., 2006). Shortening is still ongoing in western Albania associated with late orogenic strike-slip faulting and escape tectonics (Picha, 2002). However, it seems that only the Ohrid graben was suitable to develop a lake that completely desiccated and is therefore a valuable sedimentary archive within the continental Mediterranean realm (Wagner et al., 2008b).

Active tectonics and seismicity

Lake Ohrid is located within the Korca-Ohrid Earthquake Source Zone (ESZ, Fig. 1) where several medium to large earthquakes have occurred within the last 2000 years such as the 518 AD event that nearly destroyed the entire cities of Ohrid and Skopje (Aliaj et al., 2004), the 1911 event at Lake Ohrid with a Magnitude of M=6.7 (Ambraseys and Jackson, 1990; Muco et al., 2002) and the most destructive earthquake in the recent history of Macedonia that occurred in 1963 close to capital city of Macedonia, Skopje (M=6.1, Suhadolc et al., 2004). More recent smaller events occurred on November, 23rd, 2004 (Mw=5.4) and September, 6th 2009 (Mw=5.6) indicating that the area around Lake Ohrid is tectonically active (Wagner et al., 2008b; Hoffmann et al. 2010; Reicherter et al., 2011). Seismicity is mainly concentrated along roughly N-S trending normal faults on the eastern and western side of the Ohrid basin with earthquake epicenters at depths of about 10 km (Hoffmann et al., 2010; Aliaj et al., 2004). Paleostress analysis revealed a synthetic fault plane solution for Lake Ohrid region fitting in the E-W extensional domains associated with Neogene basins and normal faults of the SBER (Dumurdzanov et al., 2005; Reicherter et al., 2011).

Hydro-acoustic Dataset

Using a Mini GI Gun as a source and a 16-channel 100 m-long streamer as receiver, we completed two multichannel seismic surveys. Two different volumes of the source (namely 0.25l in 2007 and 0.1l in 2008) resulted in higher penetration of the seismic signal during the

survey in 2007 and higher resolution during the survey in 2008. We installed the equipment on an 11.5 m long Macedonian research vessel owned by the Hydrobiological Institute in Ohrid. The cruising speed was held constant at approximately 3 kn. We obtained positioning data using a Garmin GPS. Two diving compressors provided the air supply. A shot interval between 5 and 7 s was obtained. A grid of 47 seismic lines is now available (Fig. 2).

After geometry parameters were set, a despiking algorithm muted most of the spikes in the data. Velocity was assumed to be 1460 m/s at the seafloor with a constant increase to 1500m/s at 500 ms Two Way Travel Time (TWTT). A Normal Moveout (NMO) correction and stacking of the data proved that this assumption was reasonable. No reliable velocity information could be obtained due to the relative short streamer. At least the first multiple reflectors within the high resolution dataset of 2008 could be attenuated by applying a deconvolution algorithm. All data has undergone 2D Finite Differences (FD) Migration using the same velocity file as for NMO correction and stacking. A Band Pass Filter was applied before exporting the data to The IHS Kingdom Suite for display and interpretation.

In 2009 an additional campaign was carried out in order to acquire a detailed morphological map of the lake floor of Lake Ohrid by means of an ELAC 1180 Seabeam system. The system operates at water depths up to 600 m by transmitting 126 beams with frequencies of 180 kHz, and an opening angle of about 153°. The transducers were mounted at the bow of the vessel in about 1 m water depth. An OCTANS IV motion sensor provides the correction for roll, pitch, and heave. Additionally several sound profiles were collected at different locations across Lake Ohrid. Processing and mapping was accomplished using MBSystem (Caress and Chayes, 2005), GMT (Wessel and Smith, 1991), and Global Mapper.

Results

Seismic facies analysis and stratigraphy

We defined five seismic facies in the multichannel seismic lines as illustrated in Figure 3: (I) diffuse incoherent, locally hyperbolic reflections, (II) sub-parallel, discontinuous high amplitude reflections filling up sub-basins or forming a drape on top of the basement, (III) parallel, continuous, and basin-wide reflections that can further be subdivided in a subfacies showing very high (IIIa) and another one with medium to low amplitude reflections (IIIb), (IV) rather continuous, parallel to sub-parallel reflections showing a variety of amplitude variations, and (V) chaotic deposits sometimes imaged as transparent bodies with or without

incoherent reflections within these units interpreted as a mass wasting deposit. Seismic Unit A (acoustic basement) expressed by seismic facies I outcrops on the lake floor associated with steep slopes, as at the locations offshore Lini Peninsula, Magic Mountain, and along the eastern margin (Figs. 4-8). The basement (Seismic Unit A) is overlain by three seismic units (B to D) imaging the syn-sedimentary infill. Unit B represents the oldest deposits on top of the acoustic basement. A clear onlap relation of Unit B on the Basement is obvious (Figs. 4-8). Reflectors of Unit B are observed as fillings of sub-basins within Unit A, mainly along the margins and within the deepest part of the basin. Because seismic penetration is limited and multiple reflections overprint the primary reflectors and become more dominant with depth, Unit B is difficult to identify in the deep basin. However, there are indications of tilted reflectors inhibiting steeper slope angles than the multiple reflectors; these tilted reflectors are assigned to seismic facies II (Unit B), best imaged in the center of Fig. 6.

A change from seismic facies II to III forms the boundary between Unit B and C (Figs. 4-8). Within the older sediments, Unit C is mainly built out of deposits assigned with seismic facies IIIb characterized by continuous reflectors with low to medium amplitudes (Fig. 6). Toward the younger strata of C an alternation between seismic facies IIIa and IIIb is detectable. Furthermore, Unit C is characterized by concave reflectors with decreasing curvature toward the lake floor (Fig. 6).

On the seismic profile illustrated in Fig. 8 we identified transparent bodies assigned to seismic facies V up to a depth of 0.5 sec TTWT. These facies are evidences that mass movement events have occurred in Lake Ohrid Basin especially within the southern area and adjacent to major faults such as the Lini Fault and around Magic Mountain (Figs. 4-8). A direct tracing of reflectors from the basin into areas around the lake that are cut off by major faults is anticipated; hence an additional Unit D is introduced; it is characterized by seismic facies IV and can be found in northern area, along the margin, and in the Gradiste Sub-basin (Figs. 4-8).

Lake Floor morphology

The bathtub shape of Lake Ohrid is bounded by two major normal fault zones on the eastern and western margin. We divided Lake Ohrid in four major morphological areas: (I) the northern part, (II, III) the areas related to the major boundary faults along each side of the basin, and (IV) a deep central basin including the Magic Mountain area (Fig. 2).

In the north is an area with water depths shallower than 200 m. Tectonic features such as two elongated fold structures, a graben structure with distinctive sidewalls, and pockmark structures in the west are clearly visible on the bathymetric map (labeled a,b,c on Fig. 2). An area characterized by a rough topography with sidewalls has been detected offshore the city of Struga (labeled d on Fig. 2). Distinct terraces are visible within the Ohrid Bay area (labeled e on Fig. 2).

The Eastern Major Boundary Fault Zone (EMBFZ, Area II) is characterized by numerous lineaments and distinct morphological steps that are more or less aligned in NE-SW direction (labeled f on Fig. 2). The area has an overall rough topography and steep flanks along the margin with slope angles reaching up to 5°. Within this area the Gradiste sub-basin (labeled g on Fig. 2) shows water depths similar to those of the central basin. At the southern edge of the basin a remarkable terrace structure cut by active faults is recognized offshore the location where the river Cerava enters the lake (labeled h on Fig. 2).

The Western Major Boundary Fault Zone (WMBFZ, Area III) is characterized by shallow water depths (< 100 m) and a general smooth topography suggesting a thicker sediment cover compared to its eastern counterpart (labeled j on Fig. 2). Several minor slumps are visible in different water depths (labeled j-1 and j-2 on Fig. 2) indicating an unstable western margin. A circular depression resembling a pockmark structure is situated at the transition toward the central basin (labeled k on Fig. 2). In the southern part of this margin an area characterized by distinctive sidewalls and blocks has been interpreted as the Udenisht Slide (labeled j-3 on Fig. 2; Lindhorst et al., 2012).

The northern part of the central basin (Area IV) shows water depths greater than 200 m and an overall smooth topography (labeled m on Fig. 2). In contrast, the southwestern part is characterized by a hummocky topography representing the distal deposits of the Udenisht Slide (labeled j-3 on Fig. 2), which covers almost 10% of the lake floor (Lindhorst et al. 2012). An outstanding morphological step with flanks as steep as 25° and a lake floor rise from 280 m to 160 m water depth at the north-western edge of the central basin marks the exposure of the active Lini Fault (labeled o on Fig. 2). A prominent NW-SE elongated morphological high, the so called Magic Mountain, crops out more than 100 m in the southeastern part of the basin surrounded by an area that is slightly deeper than the remaining central basin (labeled p and q on Fig. 2). Here the maximum water depth of 293 m has been

measured. The Progradec shelf area marks the southern boundary of the central basin where channel incisions are evident in several locations (labeled r on Fig. 2).

Basement morphology

We calculated a grid showing the depth of the acoustic basement as interpreted from all seismic lines (Fig. 9). In general the basement structure resembles the lake floor morphology with a deep central basin and steep margins along the western and eastern side (Fig. 9). The Struga Graben, a deep elongated basin, forms the continuation of the Central Basin toward the north whereas on the southern end the central basin narrows significantly (Fig. 9). The deepest part of the acoustic basement is found in the center of the Lake Ohrid Basin (Fig. 9). On the basis of distinct morphological steps within the basement topography we interpreted 16 major normal faults as shown in Fig. 9. The N-S trending Eastern and Western Central Basin Faults bound the deepest depression found within the seismic data (Figs. 6, and 9). Especially in the data set of 2007 where we used a slightly larger GI-Gun, the enhanced seismic penetration and less dominant multiple reflections allow an identification of the acoustic basement and faults even in great subsurface depth. Four normal faults arranged in a rhombus shape in map view are bounding the main part of the central basin (Fig. 9): A set of two NE-SW trending faults such as the Lini Fault in the northwest and the Pescani Fault in the southeast, and another set of two NW-SE trending faults such as the Kaneo Fault in the northeast, and the Piskupat Fault in the southwest (Fig. 9). Each pair of faults has opposing dips. The Pescani, Kaneo, and Piscupat faults have offsets greater than 200 m and are completely covered by sediment, an indication that they are most likely inactive today (Figs. 6 and 10). In contrast, the Lini Fault scarp is exposed on the present lake floor by a sudden water depth increase of more than 100 m forming the steepest margin with angles of up to 25° (Figs. 5, 9, and 10); hence it is assumed to be an active fault. In the north of Lake Ohrid Basin a complex system of NE-SW trending en-echelon sidewall faults have been identified bounding the Struga Graben (Figs. 4, 9, and 10). These faults include the east dipping Struga Fault as well as the Orovnik and Podmolje faults with opposing dips toward the west (Figs. 4, 9, 10). All these faults have been recently active as evidenced by offsets within the overlying lacustrine sediment cover (Fig. 4). In the south a set of similar trending en-echelon faults (namely the Memelisht, Progradec, and Tushemisht faults) can be found bounding the southern continuation of the central basin with decreasing offsets toward the south (Figs. 7-10). The northernmost Memelisht Fault is partly exposed at the lake floor and has a minimum

offset of 530 m (Fig. 7). A roll-over structure adjacent to the fault further indicates recent activity (Fig. 7). In contrast the Progradec Fault has an offset of 100 m and is completely covered by sediment without evidences of recent activity (Fig. 8). The ~N-S trending, westward dipping Cerava Fault forms the eastern boundary of the South Central Basin and has been classified as a major fault as it shows an offset of more than 250 m (Figs. 8-10). In the southeastern part of Lake Ohrid two additional faults can be easily seen on the basement grid bounding the intrabasinal high (East and West Magic Mountain Faults, Figs.7, 9, and 10). These two sub-parallel NW-SE trending faults dip away from each other with great offsets of up to 500 m (Figs.7, 9, 10). Fault scarps of the Magic Mountain faults are even outcropping on the lake floor with a down-dip exposure of 100 m (Figs.7, 9, 10).

Syn-sedimentary faulting

Faults described in the previous section have been detected mainly by means of distinct morphological steps on the basement grid map shown in Fig. 9. As Lake Ohrid is located in an active Graben major faults are also present within the syn-sedimentary fill of the basin. Fig. 10 shows an overview map of all major faults that have been identified within Lake Ohrid. This section concentrates on the description of faults that offset seismic reflectors of Units B - D within the multichannel seismic data and/or within the bathymetric map (Figs. 4-10). Along the eastern margin those faults trend in a NE-SW direction and dip toward the west (Figs. 7-10). One exception forms the West Gradiste Fault as it bounds the Gradiste Graben, and has an opposite dip (Figs. 7-10). Some minor faults within the EMBFZ are clearly visible on the bathymetric map supporting the observation that the eastern side is highly segmented (Fig. 10). In contrast, the displacement on the western margin south of the Lini Peninsula seems to concentrate mainly on the N(W)-S(E) striking West Major Boundary Fault (Figs.6, 9, and 10). In general this part of the western margin has a smoother topography compared to its eastern counterpart indicating that it is less active (Fig. 10). On the other hand, the western margin seems to be less stable as evidenced by several mass wasting events which may be related to fluid flow along active faults as indicated by pockmark-like structure at the transition toward the central basin (Fig. 10). A prominent sliding event (the Udenisht slide) has affected the southernmost part of the western margin (Fig. 10).

Discussion

Seismic chronology of the central basin

In order to describe the temporal sedimentary evolution develop a seismic chronostratigraphic scheme that is applicable to seismic lines crossing the central basin of Lake Ohrid. For our model we combined several datasets from sediment cores available from Lake Ohrid as well as sedimentological studies from areas, which we consider to be comparable to the Lake Ohrid setting.

First of all, we used all information available from tephrostratigraphic, sedimentological, geochemical, and biostratigraphical investigations on sediment cores retrieved within Lake Ohrid (see Fig. 2 for location) in order to estimate sedimentation rates and to get a better understanding of the general sedimentation pattern of deposits (Wagner et al., 2008c; Belmecheri et al., 2009; Albrecht et al., 2010; Caron et al., 2010; Leng et al., 2010; Lézine et al., 2010; Reed et al., 2010; Sulpizio et al., 2010; Vogel et al., 2010a). Unfortunately, these cores only cover the sedimentary history up to an age of 130 ka correlating with the seismic reflector representing the transition from the penultimate glacial to the last interglacial and subsequently traced into the central basin by Lindhorst et al (2010). Tephras, which were partly used to establish age-depth models on the recovered sediment cores (Caron et al., 2010; Sulpizio et al., 2010; Vogel et al. 2010b), apparently do not lead to a significant change of seismic impedance, as they are probably too thin (< 5 cm). Hence, they cannot be responsible for high amplitude reflectors observed in our data.

We observe a regular pattern of alternating sequences of high amplitude reflectors with those of medium to low amplitude ones (Fig. 6). This led us to the hypothesis that the seismic image reflects a climatic induced signal that can be interpreted using the marine oxygen isotope record to evolve a depth-age curve for the late Quaternary. A 2 km long transect within the seismic line of Fig. 6 crossing the deep central basin was chosen for this approach. Subsidence seems to be of minor importance because active faults are not in close vicinity and no evidence for active syn-sedimentary faulting can be found.

We also consider that Lake Ohrid is more productive during warm periods and humid climate (Wagner et al., 2008a). Vegetation around the lake was dense and forest-dominated during the last interglacial period (Wagner et al., 2008a; Vogel et al., 2010a). Thus, we expect to find deposits of hemipelagic mud and/or silt turbidites with a high content of organic matter and

calcite resulting in medium to low amplitudes representing deposition during interglacial periods (seismic facies IIIa). Thus, seismic facies IIIa represents a sedimentation that is mostly biogenic with a low terrestrial sediment input caused by a stabilization of the catchment area by forest dominated biomes. In contrast, the precipitation during cold (glacial) periods was increased and vegetation was less evolved leading to a higher level of erosion and input of clastic material (seismic facies IIIb) into Lake Ohrid (Wagner et al., 2008a; Vogel et al., 2010a). A comparable setting was suggested for the Ioannina region to the southwest of Lake Ohrid (Fig. 1, Tzedakis 1994; Wagner et al., 2008c).

Tzedakis (1994) found that the density of pollen analyzed in a 160 m long sediment core is a good indicator for changes in vegetation. A high pollen concentration indicates a high vegetation density and vice versa. Furthermore, Tzedakis (1994) successfully linked the pollen density and hence the vegetation changes to MIS and subsequently was able to estimate ages for the individual zones within the pollen curve. For our model a peak in pollen density therefore indicates a warm (interglacial) period whereas a reduced number of pollen point to a cold (glacial) period (Fig. 11). For our data we further assumed that changes in vegetation are rather rapid which would lead to a high impedance contrast and consequently a high amplitude reflection (Allen and Huntley, 1999). Using his chronological scheme and applying the assumptions made for the origin of low and high amplitude reflectors we are able to put ages on several seismic reflectors up to a depth of about 0.6 s TWTT (Fig. 11). The proposed seismic chronological model shows that the basin infill of Lake Ohrid is much older than 430 kyrs. The reader should note that in absence of long cores in Lake Ohrid this interpretation is based on several assumptions that are debatable as we lack direct chronological control for our data set, consequently it should be considered as a preliminary age model. However, this model includes significant more information for age estimations in comparison to previous attempts (Albrecht and Wilke, 2008; Lindhorst et al., 2010).

The fact that our calculated sedimentation rate of 0.43 mm/yr is similar to that obtained for the Ioannina record of Tzedakis (1994) gives us confidence that the conditions during deposition are comparable. However, sedimentary history of each individual tectonic basin is dependent on a combination of climatic and tectonic processes and is therefore highly variable over time and space, sometimes even within certain parts of the same sedimentary basin as shown by a tectono-sedimentary model for extensional grabens by Gawthorpe and Leeder (2000). By picking a transect in the seismic cross section within the center of Lake

Ohrid we tried to avoid the influence of subsidence to decrease the factor that the deposition was tectonically induced. Furthermore the influence of compaction increases with depth and although no obvious erosional/non-depositional features are observed we cannot fully exclude them due to our limitation in resolution.

Accumulation rates and ages of the basin infill

The calculated average accumulation rate of 0.43 mm/yr for the last 450 kyrs within the 2 km transect is significantly higher than 0.28 mm/yr and 0.1 mm/yr proposed by previous studies (Lindhorst et al., 2010; Vogel et al., 2010b, respectively). The discrepancy between our suggested values and sedimentation rates by Wagner et al. (2008c) and Vogel et al. (2010b) obtained by dating of sediment cores can be explained by taking into account that sedimentation rates maybe highly variable in space and time (glacial versus interglacial times). As the studied sediment cores are from more lateral parts of the lake, we can assume that sedimentation rates are higher compared to the central part (see also Wagner et al. 2008b) In contrast, our value is an average rate for the time span of 430 kyrs comprising several glacial and interglacial cycles. Using our suggested average accumulation rates for extrapolation allows age determination of reflectors below MIS 12 at 245, 280, 320 and 380 m to ~570 kyr, ~650 kyr, ~745 kyr and ~890 kyr (reflectors a, b, c, d in Fig. 6), respectively (TWTT to depth conversion is based on 1700 m/s sound velocity of sediments). An age for the basement at the deepest site within Lake Ohrid with a sediment cover of approximately 0.95 s TWTT (~800 m,) reveals an age of ~1.9 Ma (Fig. 9). The calculated ages can only be regarded as a minimum age and involve great uncertainties due to the lack of lithological information older than 130 ka and assumptions that are made to evolve the seismic chronostratigraphic model presented here. Sediments at greater subsurface depths are most likely more compact than younger deposits. Additionally we cannot exclude phases of erosion and/or non-deposition resulting in hiatus that is not resolvable by means of multichannel seismic data. However, our age estimation is in good agreement with estimates summarized by Albrecht and Wilke (2008) and indicates that Lake Ohrid is younger than 3 million years.

Tectono-sedimentary evolution

In order to reconstruct the tectono-sedimentary evolution we interpret Unit A (acoustic basement) as the pre-rift stage and subsequently the oldest unit before basin opening. Unit B represents fluvial and/or alluvial fan deposits show the basin evolution after faults became active but displacement was not yet great enough that the hanging wall was a basin filled with

water (e.g. Gawthorpe and Leeder, 2000). However, Unit B in the central part, most likely represents the time after initial basin opening although we cannot be certain whether the Central Basin faults are the first master faults of the initial pull-apart or if there are further faults deeper in the basin that are hidden under multiple reflectors (Fig. 6). Unit C is assigned to deep lacustrine sediments indicating that the lake is in an underfilled stage and subsidence is greater than sedimentation (Prosser, 1993; Carroll and Bohacs, 1999). As Unit C takes up the major part of the syn-sedimentary filling and has been dated to be at least older than 800 kyrs we speculate that Lake Ohrid has never dried out since its existence as water filled body because subsidence, which in general decreases over time, seems to be always greater than sedimentation. If subsidence would have stopped in Lake Ohrid we would expect to find deposits of shallow lacustrine sediments which would fit in the tripartite sediment succession of a complete cycle of half-graben developments with initial opening (fluvial deposits), subsidence phase (deep lacustrine sediments), and finally decrease or stopped subsidence (shallow lacustrine sediments). The fact that the third part is missing in our seismic profiles indicates that Lake Ohrid is still active and the basin continues to widen. Seismic Unit B has been deposited in a marginal shallow water environment within respective extensional basin evolution. This is best observed on Figs 6 and 7.

The Gradiste Sub-basin is a great example of all stages of basin evolution such as pre-rift (Unit A), fluvial (Unit B) and the lacustrine phase (Unit D, Fig. 7). Furthermore, the Gradiste Sub-basin after formation was most likely cut off from main Lake Ohrid, which is an important fact with respect to the high biodiversity within the Lake where endemic species are present, sometimes restricted to specific locations within the basin (Albrecht and Wilke, 2008; Lindhorst et al., 2010).

Active tectonics and comparison with onshore data sets

The central part of Lake Ohrid shows no evidence for neotectonic activity but all other lake areas suggest that the basin is still widening (Figs. 4 and 8). Our data suggest that the most active regions are around the Lini fault, within the EMBFZ and the Magic Mountain faults. Half-grabens within the hanging wall of these faults have been developed, creating depocentres that are filled with redeposited material from the footwalls (Figs. 4, 8, and 9). These sites are presently the deepest areas within Lake Ohrid suggesting that subsidence is locally larger than sedimentation. Rotated strata together with several mass movements are indicators for ongoing uplift of the footwall. Slide deposits from the mass movements are

separated by undisturbed lacustrine layers highlighting phases of quiescence along the faults and hence repeated fault activity. This makes Lake Ohrid to a favorable site to study paleoseismicity along individual faults.

The eastern margin of Lake Ohrid is heavily segmented and tectonically very active (Figs. 6, 8-10). Displacement occurs along several smaller fault segments observable in the seismic profiles where we see smaller half-grabens along with tilted basement blocks within the margin (Figs. 5-8). This pattern continues landwards and can also be observed within the adjacent mountains (Figs 4, 9, and Reicherter et al., 2011 their Fig. 12).

The Gradiste Sub-basin is an area that was influenced by recent extension. The basin is bounded by two major faults clearly offsetting syn-tectonic strata by several meters (Fig. 8). Faults dipping to the W and E are present within the sub-basin. Unfortunately a direct tracing of reflectors is not possible (Fig. 7); hence we cannot denote when subsidence started. Relatively thick sediments of Unit A can be found here overlying the acoustic basement implying that the basin was in a shallow water environment after initial opening: Most likely, the Gradiste Sub-basin was isolated from the main lake before the Lake Ohrid Basin got deep enough for accumulation of undisturbed deep lacustrine sediments.

Although the western margin has a larger sediment cover it still shows evidence for recent tectonic activity as indicated by major morphological steps and slumps. The Western Major Boundary fault runs in a NNW-SSE direction offsetting the modern lake floor. It plausibly continues as a half-graben bounding fault on the Lini Peninsula (Fig. 10, Reicherter et al., 2011). However in the south it has been cut by NW-SE trending faults with one prominent example interpreted within our data set namely the Udenisht Fault. The area where these two major faults meet coincides with the upper slope area of the Udenisht Slide implying that the mass movement event was seismically induced. Evidence for an onshore continuation of the Udenisht Fault is illustrated in Fig. 10.

Tectonic development of the Lake Ohrid basin

Based on our new geophysical dataset we developed a model of the temporal and spatial evolution of Lake Ohrid Basin up to recent times. First evidences for the graben development within our data set are the East and West Central Basin faults in the deepest part of Lake Ohrid interpreted as the first master faults active during the initial opening of the basin as they are covered by the oldest sediments found in the basin (Figs. 4, 10, 11, and 13). Analogue

modeling results of Wu et al. 2009 (Fig. 12) would suggest that within the principal deformation zone a dextral strike slip fault is located between the Central Basin faults, if the basin was initiated as a transtensional pull-apart (Fig. 6). With progressive transtensional deformation the pull-apart basin should show a rhomboidal geometry bounded by two sets of master normal faults, which are the Lini, Kaneo, Pescani, and Piskupat Faults in Lake Ohrid, acting as sidewalls as illustrated in the block diagram of the early stage geometry in Fig. 12 (Wu et al. 2009). The internal structure resembles a symmetrical graben (Fig. 6) formed with master normal faults on either side of the pull-apart basin as suggested by Rahe et al. (1998). En-echelon sidewall faults such as the Memelisht, Progradec, and Tushemisht Faults as well as the Orovnik and Podmolje Faults formed in the north and south, respectively (Fig. 12). We cannot resolve the actual time when the initiation of the basin took place because related reflectors are hidden under multiple reflectors. However, after opening, the basin must have been deep enough and filled with water for quite some time because we find thick undisturbed lacustrine sediment successions in the central part of the basin (Fig. 6). The subsequent evolution of the basin gets more and more complex with long- and short-lived faults and various overprintings. The Central Basin Faults have not been recently active as they are covered by undisturbed sediments of Unit C (Figs. 4 and 12).

Our seismic data suggest that N-S trending faults further away from the center of the basin than Piskupat and Pescani Faults are preferentially younger than those in the center resulting in the fault development displayed in Fig. 12. At present, Lake Ohrid is still an active graben with numerous major normal faults within the basin (Figs. 4-8). For example, the East and West Major Boundary faults have been interpreted to be the most active faults delineated by great offsets with fault scarps outcropping at the lake floor together with mass wasting processes that are presumably related to fault movement (Figs. 6 and 10). Slide deposits are usually on the hanging wall of major normal faults indicating a destabilisation of the footwall (Reicherter et al., 2011). In addition, we found evidence for neotectonic activity along the Lini fault and within the northern area of Lake Ohrid mainly within the Struga Graben. The Lini fault offshore of Lini Peninsula is a major normal fault with a large offset next to a deep depression suggesting that recent or ongoing subsidence is faster than sedimentation (Figs. 5 and 11). In addition, we found numerous antithetic faults offsetting the youngest sediment successions adjacent to the Lini fault further indicating that it is one of the most active regions within Lake Ohrid Basin. A segment of this Lini fault offshore Lini Peninsula fits into the synoptic model of the initial pull-apart basin as it trends in NE-SW direction and is part of the

rhomboidal shape of the early stage geometry. Therefore, we assume that this structure is one of the oldest faults in Lake Ohrid (Fig. 5 and 12). In the Struga Graben we found several faults that offset the present lake floor testifying that it is a very active area within Lake Ohrid. Most of the faults in the north are normal faults except for the Gorenci fault trending NNE-SSW. The Gorenci fault is characterized by a narrow zone of transparency within an area of stratified sediments with no or only minor offsets suggesting a strike-slip movement along this fault. Because the Gorenci fault has recently been or is still active within the E-W extensional regime it must be a sinistral fault (Fig. 12), conjugate to the NW-SE trending active dextral strike-slip faults mapped by Reicherter et al. (2011). In terms of the spatial and temporal fault evolution within our data set we can state that those faults within the central part of the basin must be old because they are covered by thick successions of undisturbed lacustrine sediments lacking any hint of active faulting. However, along the active margins of Lake Ohrid a relative age interpretation is impossible because the relatively small sediment packages at the margins are affected by faulting and associated mass movements (Figs. 4-8).

Another puzzling area within the context of basin evolution is the region around Magic Mountain. The Eastern and Western flank of this prominent intrabasinal high show clear evidence for active faulting as drag folds adjacent to the mountain in combination with several sliding events deposited on the hanging wall of this structure. Notwithstanding it remains uncertain whether it is part of the initial pull-apart or just an intra-basinal horst structure that remained from subsequent extensional tectonics within the lake.

Geodynamic context of basin development

The two phases of basin development observed in our data set correspond to the Cenozoic deformation pattern as observed in the regional area surrounding Lake Ohrid. During NE-SW shortening prior to basin development a fold and thrust belt formed with dominantly NW-SE trending fold axes and fault strike (Reicherter et al., 2011). According to Stancovic (1960) the Cerava and Crni Drim Rivers are older than Lake Ohrid. Hence, it is likely that during this compressional phase a river valley formed where Lake Ohrid is today. We cannot find structural evidence for this phase in our multichannel seismic data, but we interpreted high amplitude discontinuous reflectors as fluvial deposits on top of the acoustic basement suggesting river transport within the basin before it was deep enough for lacustrine sedimentation (Fig. 6).

Subsequent to compression a transtensional phase occurred within the Late Miocene due to a decrease in horizontal shortening and uplift (Burchfiel et al., 2008; Reicherter et al., 2011). This tectonic phase is visible in our data and would explain the initial opening of the Lake Ohrid as a pull apart basin as described above (Fig. 12). A comparable geodynamic situation might be given for the Dinaric-Hellenic region located farther to the west where late orogenic strike-slip faults indicate escape tectonics within an overall compressional regime (Picha, 2002).

The third deformation phase affecting the Lake Ohrid area is caused by the roll-back of the Hellenic slab leading to an E-W directed extension and subsequently, the formation of N-S extending sedimentary basins which are progressively younger toward the west (Burchfiel et al., 2008; Hoffmann et al., 2010). Lake Ohrid is the youngest of these basins developing in the latest Miocene or Early Pliocene and is still active today (Aliaj et al., 2001; Burchfiel et al., 2008; Dumurdzanov et al., 2005). The existing topography of the basin, fault scarps within the adjacent mountains, and the presence of active N-S trending faults bounding Lake Ohrid along its eastern and western margin are in good agreement with the development within this geodynamic setting as illustrated in Figure 12. A paleostress analysis of major faults around Lake Ohrid (Reicherter et al., 2011) point to a basin development within these three deformation phases described here such as E-W trending thrust faults, NW-SE trending dextral strike slip faults, and N-S trending normal faults. These phases are in good agreement with the major deformational phases.

Conclusion

Lake Ohrid initially opened as a pull-apart basin in the Late Miocene time during a short transtensional phase. Seismic cross sections suggest the formation of a symmetrical graben that rapidly deepened to host a lake as indicated by deep-lacustrine sedimentation in the entire central basin. The pull-apart geometry has a typical rhomboidal shape with two sets of major normal faults on each side namely the Lini, Piskupat, Pescani, and Kaneo Faults. Since the Pliocene, Lake Ohrid was influenced by an E-W directed extension related to the roll-back of the Hellenic subducting slab that led to the formation of N-S trending sedimentary basin within the SBER. Lake Ohrid is most likely the youngest basin as extension initiated farther to the east and progressed westward over time. A widening and deepening of Lake Ohrid Basin was the consequence of this extension. The oldest faults in the deepest part of Lake

Ohrid, the Central Basin Faults, which we interpret as the first master faults bounding the initial pull-apart basin are covered by a thick succession of undisturbed strata. Moving away from the center of the lake new faults became active and formed small grabens that filled with sediments. The grabens filled with sediments until subsidence decreased and sedimentation became larger than the subsidence. At this point, the faults became covered with sediments Faults located closest to the present shoreline are active indicting that the opening of the basin is still ongoing. The fact that the graben hosts a deep lake further suggests that sedimentation, in general, is smaller than subsidence; hence Lake Ohrid is in an underfilled stage. The architecture of the sedimentary infill is a result of a complex interaction of climatic and tectonic induced processes. We observed a regular succession within the seismic stratigraphy starting with the acoustic basement (Unit A) representing the pre-rift stage, followed by fluvial deposits (Unit B) interpreted as the stage after fault initiation and formation of small grabens within the marginal regions of the respective basin, and finally deep lacustrine sediments (Unit C) which make up the major part of the sedimentary infill A flattening of the strata toward the lake floor indicates that subsidence that the influence of subsidence on the infill architecture is no longer larger than sedimentation. This succession is part of a tripartite depositional pattern observed in rift lakes and linked to the tectonic activity within the broader region.

Within the central basin we did not observe evidence for active faulting but identified a thick succession of undisturbed sediments that inhibit a regular pattern of alternating sequences of low and high amplitude reflectors. Assuming that this depositional pattern reflects a change in the vegetation of the surrounding area we successfully evolved a chrono-stratigraphic model for Lake Ohrid basin. By applying this new chrono-stratigraphic model we calculated a mean accumulation rate of 0.43 mm/yr for the last 430 kyrs. Extrapolation of this accumulation rate for deeper strata revealed a minimum age for Lake Ohrid of ~2 Myrs. The actual age remains uncertain as we cannot account for compaction and possible hiatuses within the sediment succession. However, we have shown that Lake Ohrid is an old and deep sedimentary basin and can be used as a valuable archive for paleoenvironmental reconstruction over a long time period. Interpretation of new acquired geophysical data led to a better understanding of the tectonic and sedimentary evolution of Lake Ohrid.

Acknowledgement

We would like to thank the Macedonian colleagues G. Kostoski, S. Trajanoski, Z. Spirkovski, and Z. Brdaroski for logistic support during field campaigns in 2004-2009. M. Grün and S. Koch completed the field team and greatly contributed to the success multibeam campaign in 2009. We are grateful to W. Weinrebe and N. Lindhorst for their technical support during the field campaign in 2009. Thanks to the workgroup of H. Villinger for providing a Streamer system to successfully conduct a multichannel seismic survey. S. Hall kindly improved the English. The 3D synoptic models were made by S. Arend, Integrated School of Ocean Sciences (ISOS) Exzellenzcluster "The Future Ocean" Christian-Albrechts-Universität zu Kiel. The project was funded by the Deutsche Forschungsgemeinschaft (Projects KR2222-7).

References

ALBRECHT, C. & WILKE, T. (2008) Ancient Lake Ohrid: Biodiversity and Evolution. *Hydrobiologia*, **615,** 103-140.

ALBRECHT, C., VOGEL, H., HAUFFE, T. & WILKE, T. (2010) Sediment Core Fossils in Ancient Lake Ohrid: Testing for Faunal Change since the Last Interglacial. *Biogeosciences*, **7,** 3435-3446.

ALIAJ, S., BALDASSARRE, G. & SHKUPI, D. (2001) Quaternary Subsidence Zones in Albania: Some Case Studies. *Bulletin of Engineering Geology and the Environment*, **59,** 313-318.

ALIAJ, S., ADAMS, J., HALCHUK, S., SULSTAROVA, E., PECI, V. & MUCO, B. (2004). *Probabilistic Seismic Hazard Maps for Albania*. *13th World Conference on Earthquake Engineering*, Vancouver, B.C., Canada.

ALIAJ, S. (2006) The Albanian Orogen: Convergence Zone between Eurasia and the Adria Microplate. *The Adria Microplate: GPS Geodesy, Tectonics and Hazards***,** 133-149.

ALLEN, J., BRANDT, U., BRAUER, A., HUBBERTEN, H., HUNTLEY, B., KELLER, J., KRAML, M., MACKENSEN, A., MINGRAM, J. & NEGENDANK, J. (1999) Rapid Environmental Changes in Southern Europe During the Last Glacial Period. *Nature*, **400,** 740-743.

ALLEN, J. & HUNTLEY, B. (2009) Last Interglacial Palaeovegetation, Palaeoenvironments and Chronology: A New Record from Lago Grande Di Monticchio, Southern Italy. *Quaternary Science Reviews*, **28,** 1521-1538.

AMBRASEYS, N. & JACKSON, J. (1990) Seismicity and Associated Strain of Central Greece between 1890 and 1988. *Geophysical Journal International*, **101,** 663-708.

BELMECHERI, S., NAMIOTKO, T., ROBERT, C., VON GRAFENSTEIN, U. & DANIELOPOL, D. (2009) Climate Controlled Ostracod Preservation in Lake Ohrid (Albania, Macedonia). *Palaeogeography, Palaeoclimatology, Palaeoecology*, **277,** 236-245.

BURCHFIEL, B., NAKOV, R., DUMURDZANOV, N., PAPANIKOLAOU, D., TZANKOV, T., SERAFIMOVSKI, T., KING, R., KOTZEV, V., TODOSOV, A. & NURCE, B. (2008) Evolution and Dynamics of the Cenozoic Tectonics of the South Balkan Extensional System. *Geosphere*, **4,** 918.

CARESS, D. & CHAYES, D. (2008) Mb-System: Open Source Software for the Processing and Display of Swath Mapping Sonar Data.

CARON, B., SULPIZIO, R., ZANCHETTA, G., SIANI, G. & SANTACROCE, R. (2010) The Late Holocene to Pleistocene Tephrostratigraphic Record of Lake Ohrid (Albania). *Comptes Rendus Geoscience*, **342,** 453-466.

CARROLL, A. & BOHACS, K. (1999) Stratigraphic Classification of Ancient Lakes; Balancing Tectonic and Climatic Controls. *Geology*, **27,** 99-102.

CHANNELL, J. & KOZUR, H. (1997) How Many Oceans? Meliata, Vardar and Pindos Oceans in Mesozoic Alpine Paleogeography. *Geology*, **25,** 183-186.

DUMURDZANOV, N., SERAFIMOVSKI, T. & BURCHFIEL, B. (2005) Cenozoic Tectonics of Macedonia and Its Relation to the South Balkan Extensional Regime. *Geosphere*, **1,** 1-22.

GAWTHORPE, R. & LEEDER, M. (2000) Tectono-Sedimentary Evolution of Active Extensional Basins. *Basin Research*, **12,** 195-218.

HOFFMANN, N., REICHERTER, K., FERNANDEZ-STEEGER, T. & GRUETZNER, C. (2010) Evolution of Ancient Lake Ohrid: A Tectonic Perspective. *Biogeosciences*, **7,** 3377-3386.

HOLTVOETH, J., VOGEL, H., WAGNER, B. & WOLFF, G. (2010) Lipid Biomarkers in Holocene and Glacial Sediments from Ancient Lake Ohrid (Macedonia, Albania). *Biogeosciences*, **7,** 3473-3489.

HUGHES, P., GIBBARD, P. & WOODWARD, J. (2006) Middle Pleistocene Glacier Behaviour in the Mediterranean: Sedimentological Evidence from the Pindus Mountains, Greece. *Journal of Geological Society*, **163,** 857-867.

LEEDER, M.R., HARRIS, T. & KIRKBY, M.J. (1998) Sediment Supply and Climate Change: Implications for Basin Stratigraphy. *Basin Research*, **10,** 7-18.

LENG, M., BANESCHI, I., ZANCHETTA, G., JEX, C., WAGNER, H. & VOGEL, H. (2010) Late Quaternary Palaeoenvironmental Reconstruction from Lakes Ohrid and Prespa (Macedonia/Albania Border) Using Stable Isotopes. *Biogeosciences*, **7,** 3109-2122.

LÉZINE, A., VON GRAFENSTEIN, U., ANDERSEN, N., BELMECHERI, S., BORDON, A., CARON, B., CAZET, J., ERLENKEUSER, H., FOUACHE, E. & GRENIER, C. (2010) Lake Ohrid, Albania, Provides an Exceptional Multi-Proxy Record of Environmental Changes During the Last Glacial-Interglacial Cycle. *Palaeogeography, Palaeoclimatology, Palaeoecology*, **287,** 116-127.

LINDHORST, K., VOGEL, H., KRASTEL, S., WAGNER, B., HILGERS, A., ZANDER, A., SCHWENK, T., WESSELS, M. & DAUT, G. (2010) Stratigraphic Analysis of Lake Level Fluctuations in Lake Ohrid: An Integration of High Resolution Hydro-Acoustic Data and Sediment Cores. *Biogeosciences*, **7,** 3531-3548.

LINDHORST, K., GRUEN, M., KRASTEL, S. & SCHWENK, T. (2012) Hydroacoustic Analysis of Mass Wasting Deposits in Lake Ohrid (Fyr Macedonia/Albania). *Submarine Mass Movements and Their Consequences***,** 245-253.

MATZINGER, A., JORDANOSKI, M., VELJANOSKA-SARAFILOSKA, E., STURM, M., MÜLLER, B. & WÜEST, A. (2006) Is Lake Prespa Jeopardizing the Ecosystem of Ancient Lake Ohrid? *Hydrobiologia*, **553,** 89-109.

MATZINGER, A., SCHMID, M., VELJANOSKA-SARAFILOSKA, E., PATCEVA, S., GUSESKA, D., WAGNER, B., MÜLLER, B., STURM, M. & WÜEST, A. (2007) Eutrophication of Ancient Lake Ohrid: Global Warming Amplifies Detrimental Effects of Increased Nutrient Inputs. *Limnology and Oceanography*, **52,** 338-353.

MUÇO, B., VACCARI, F., PANZA, G. & KUKA, N. (2002) Seismic Zonation in Albania Using a Deterministic Approach. *Tectonophysics*, **344,** 277-288.

PICHA, F. (2002) Late Orogenic Strike-Slip Faulting and Escape Tectonics in Frontal Dinarides-Hellenides, Croatia, Yugoslavia, Albania, and Greece. *AAPG Bulletin*, **86,** 1659-1671.

POPOVSKA, C. & BONACCI, O. (2007) Basic Data on the Hydrology of Lakes Ohrid and Prespa. *Hydrological Processes*, **21,** 658-664.

PROSSER, S. (1993) Rift-Related Linked Depositional Systems and Their Seismic Expression. *Geological Society London Special Publications*, **71,** 35-66.

RAHE, B., FERRILL, D.A. & MORRIS, A.P. (1998) Physical Analog Modeling of Pull-Apart Basin Evolution. *Tectonophysics*, **285,** 21-40.

REED, J., CVETKOSKA, A., LEVKOV, Z., VOGEL, H. & WAGNER, B. (2010) The Last Glacial-Interglacial Cycle in Lake Ohrid (Macedonia/Albania): Testing Diatom Response to Climate. *Biogeosciences*, **7,** 3083-3094.

REICHERTER, K., HOFFMANN, N., LINDHORST, K., KRASTEL, S., FERNÃ¡NDEZ-STEEGER, T., GRUTZNER, C. & WIATR, T. (2011) Active Basins and Neotectonics: Morphotectonics of the Lake Ohrid Basin (Fyrom and Albania). *Zeitschrift der Deutschen Gesellschaft für Geowissenschaften*, **162,** 217-234.

ROBERTSON, A. (2004) Development of Concepts Concerning the Genesis and Emplacement of Tethyan Ophiolites in the Eastern Mediterranean and Oman Regions. *Earth-Science Reviews*, **66,** 331-387.

STANKOVIC, S. (1960) The Balkan Lake Ohrid and Its Living World. W. Junk.

SUHADOLC, P., SANDRON, D., FITZKO, F. & COSTA, G. (2004) Seismic Ground Motion Estimates for the M6.1 Earthquake of July 26, 1963 at Skopje, Republic of Macedonia. *Acta Geodaetica et Geophysica Hungarica*, **39,** 319-326.

SULPIZIO, R., ZANCHETTA, G., D'ORAZIO, M., VOGEL, H. & WAGNER, B. (2010) Tephrostratigraphy and Tephrochronology of Lakes Ohrid and Prespa, Balkans. *Biogeosciences*, **7,** 3273-3288.

TZEDAKIS, P. (1994) Vegetation Change through Glacial-Interglacial Cycles: A Long Pollen Sequence Perspective. *Philosophical Transactions of the Royal Society of London. Series B: Biological Sciences,* **345,** 403-432.

VOGEL, H., WAGNER, B., ZANCHETTA, G., SULPIZIO, R. & ROSÉN, P. (2010a) A Paleoclimate Record with Tephrochronological Age Control for the Last Glacial-Interglacial Cylce from Lake Ohrid, Albania and Macedonia. *Journal of Paleolimnology*.

VOGEL, H., WESSELS, M., ALBRECHT, C., STICH, H. & WAGNER, B. (2010b) Spatial Variability of Recent Sedimentation in Lake Ohrid (Albania/Macedonia). *Biogeosciences,* **7,** 3333-3342.

WAGNER, B., LOTTER, A., NOWACZYK, N., REED, J., SCHWALB, A., SULPIZIO, R., VALSECCHI, V., WESSELS, M. & ZANCHETTA, G. (2008a) A 40,000-Year Record of Environmental Change from Ancient Lake Ohrid (Albania and Macedonia). *Journal of Paleolimnology,* **41,** 407-430.

WAGNER, B., REICHERTER, K., DAUT, G., WESSELS, M., MATZINGER, A., SCHWALB, A., SPIRKOVSKI, Z. & SANXHAKU, M. (2008b) The Potential of Lake Ohrid for Long-Term Palaeoenvironmental Reconstructions. *Palaeogeography, Palaeoclimatology, Palaeoecology*, **259,** 341-356.

WAGNER, B., SULPIZIO, R., ZANCHETTA, G., WULF, S., WESSELS, M., DAUT, G. & NOWACZYK, N. (2008c) The Last 40 Ka Tephrostratigraphic Record of Lake Ohrid, Albania and Macedonia: A Very Distal Archive for Ash Dispersal from Italian Volcanoes. *J. Volcanol. Geoth. Res.*, **177,** 71-80.

WATZIN, M.C., PUKA, V. & NAUMOSKI, T. (2002) Lake Ohrid and Its Watershed, State of the Environment Report. Lake Ohrid Conservation Project**.,** 134 pp.

WESSEL, P. & SMITH, W. (1991) Free Software Helps Map and Display Data. *Eos Trans. AGU*, **72,** 445–446.

WU, J.E., MCCLAY, K., WHITEHOUSE, P. & DOOLEY, T. (2009) 4d Analogue Modelling of Transtensional Pull-Apart Basins. *Marine and Petroleum Geology*, **26,** 1608-1623.

WULF, S., KRAML, M., BRAUER, A., KELLER, J. & NEGENDANK, J.F.W. (2004) Tephrochronology of the 100 Ka Lacustrine Sediment Record of Lago Grande Di Monticchio (Southern Italy). *Quaternary International*, **122,** 7-30.

Figures

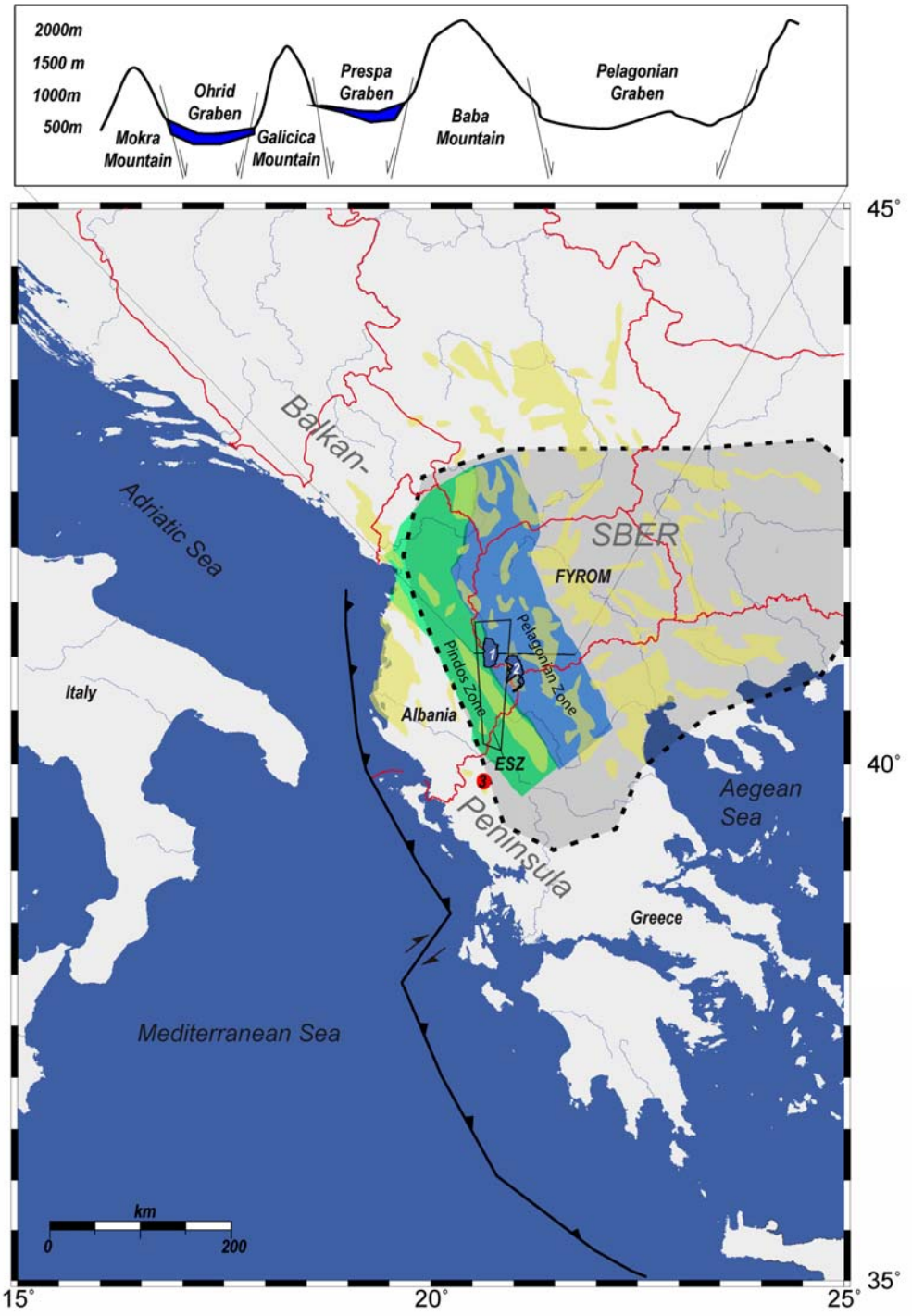

Fig. M3 1: Map of the Balkan Peninsula showing the location of Lake Ohrid (1) and its sister Lake Prespa (2). Geological units surrounding the lakes are illustrated (Pindos - greenish, Pelagonian – blueish adapted from Ghikas et al. 2010). ESZ: Earthquake Source Zone of the Korca-Ohrid area described by Aliaj et al. 2004. Grey area with dashed line marks the South Balkan Extensional Regime (SBER, Burchfiel et al. 2008). A cross section highlights the basin and range situation with Lake Ohrid being the westernmost and subsequently youngest graben. The Ioannina Basin (3) is marked. Black line with squares indicates the active subduction zone with a strike slip segment.

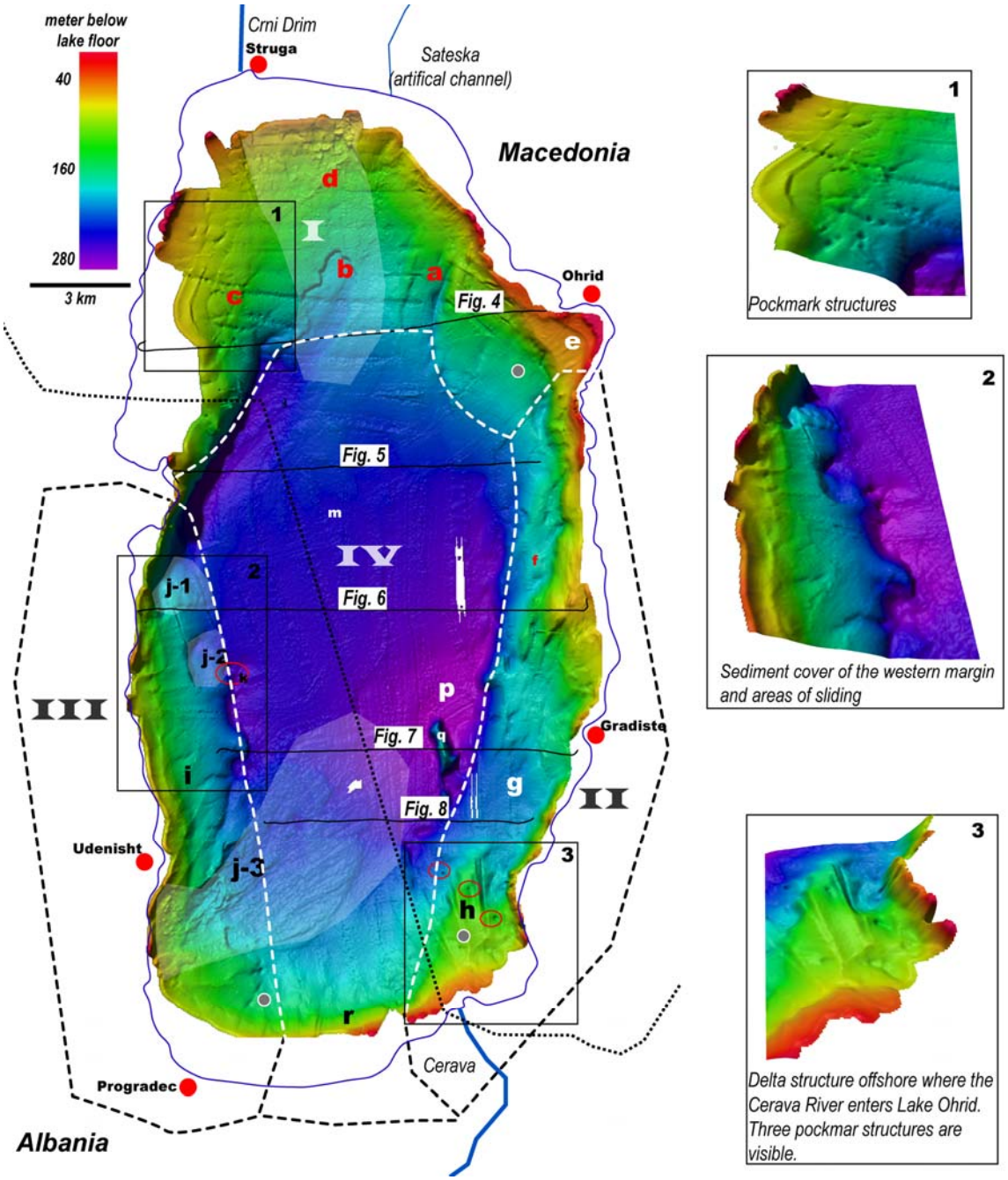

Fig. M3 2: Lake Floor morphology illustrating the most striking features within Lake Ohrid (blue line marks the shore line). The lake is divided in four main areas ***(I)*** *northern area with a) folds, b) graben with distinct morphological step, c) pockmark structures, d) rough topography, and e) terrace structures in Ohrid Bay,* ***(II)*** *Major Eastern Boundary Fault Zone with f) NE-SW trending lineations, g) Gradiste Sub-basin, and h) Cerava terrace structure.* ***(III)*** *Major Western Boundary Fault Zone with i) smooth topography zone, j)-1-2-3 slump areas, k) rounded pockmark-like shape, and l) NW-SE trending lineament.* ***(IV)*** *Central Basin with m) zone of smooth topography, o) exposure of Lini Fault, p) Magic Mountain, q) deepest sub-basin, and r) channel incisions. Grey points mark locations of sediment cores obtained in lake Ohrid.*

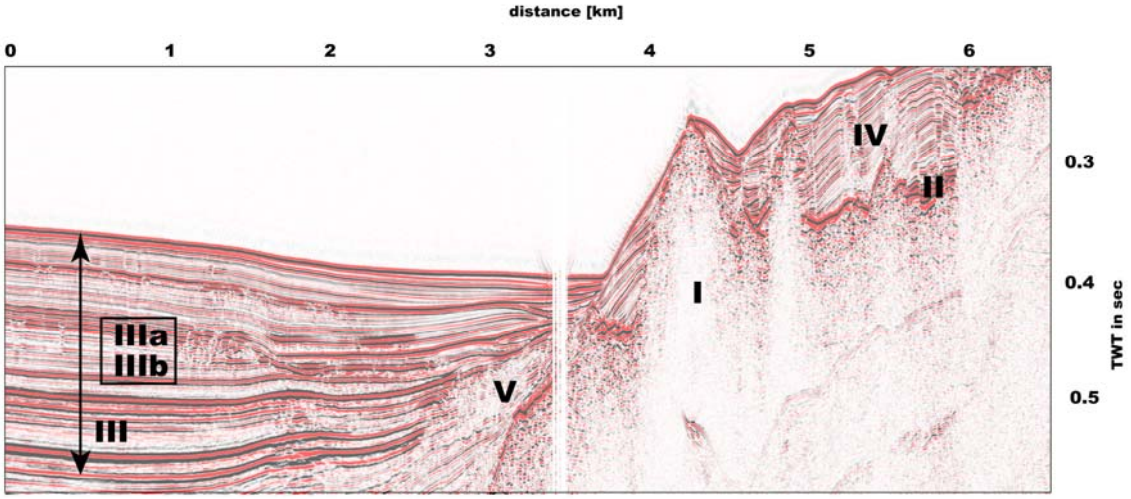

Fig. M3 3: Seismic facies defined in the multichannel seismic data in Lake Ohrid

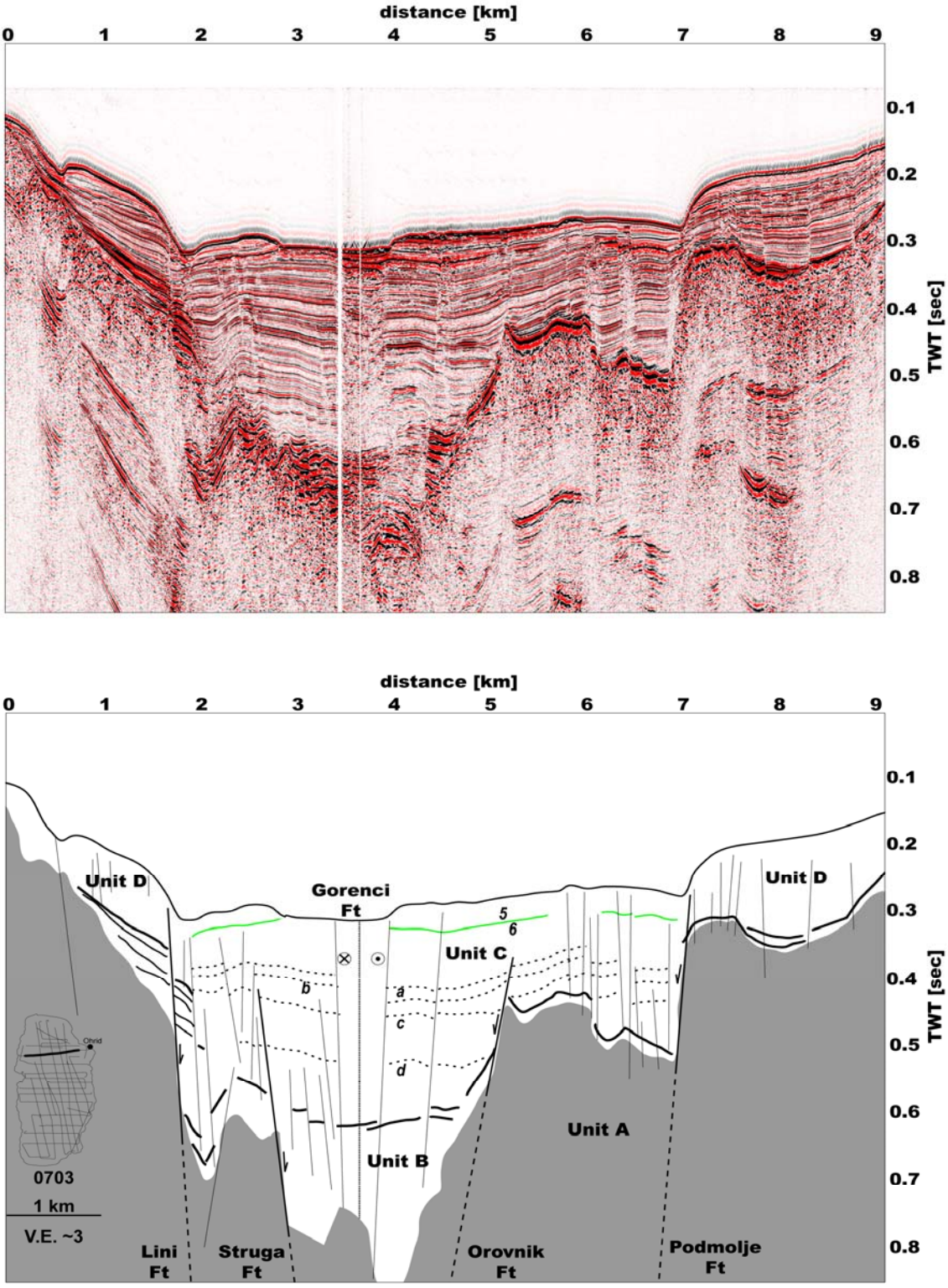

Fig. M3 4: Seismic cross section showing the horst and graben structure in the northern area of Lake Ohrid. Top: uninterpreted, bottom: line drawing and interpretation. Note the 500 m wide fault zone in the center of the profile that has been interpreted as active strike-slip fault most likely connected with a pull-apart basin that is currently opening.

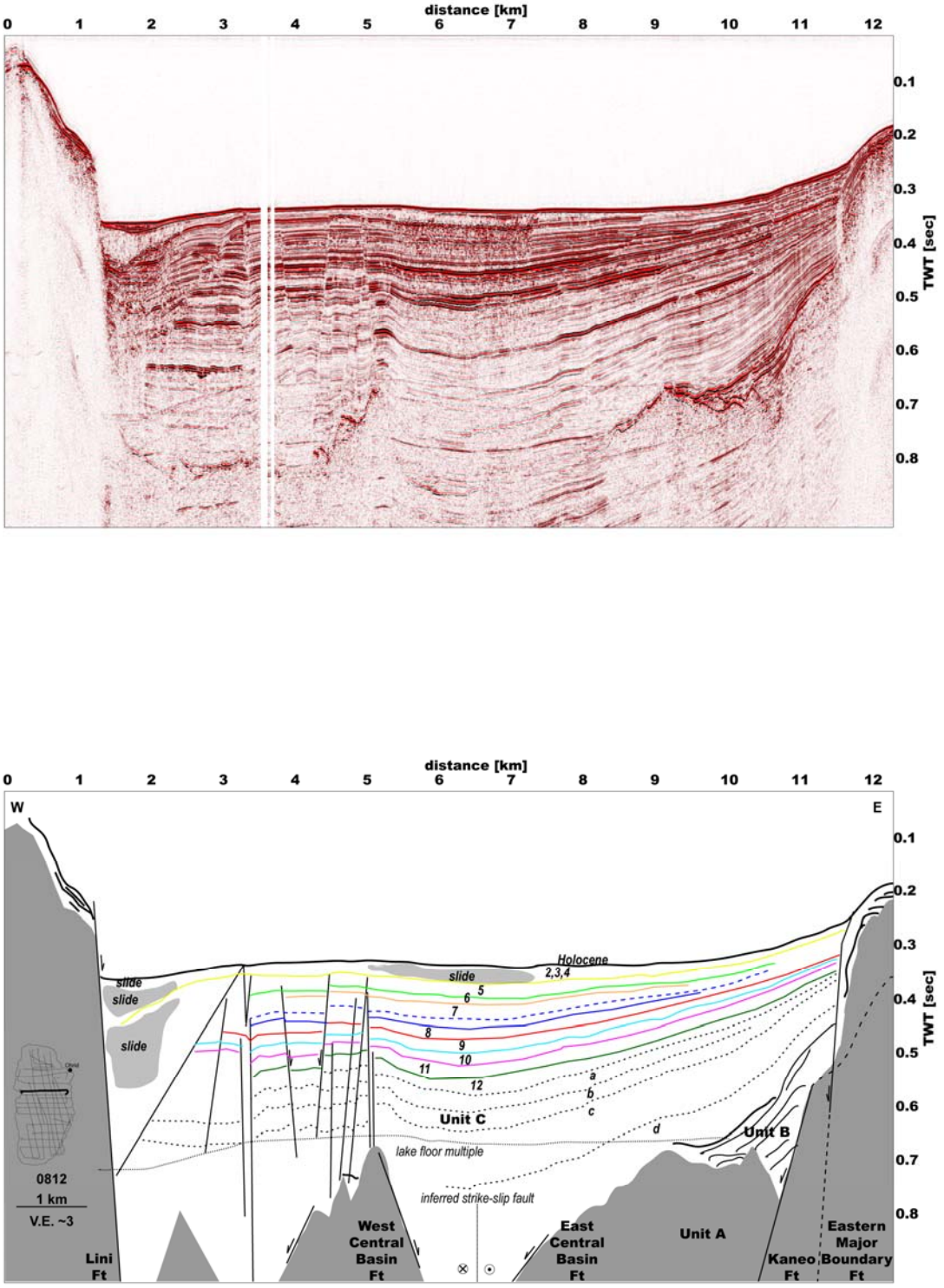

Fig. M3 5: Seismic cross section imaging the prominent Lini Fault and the associated half-graben. Top: uninterpreted, bottom: line drawing and interpretation.

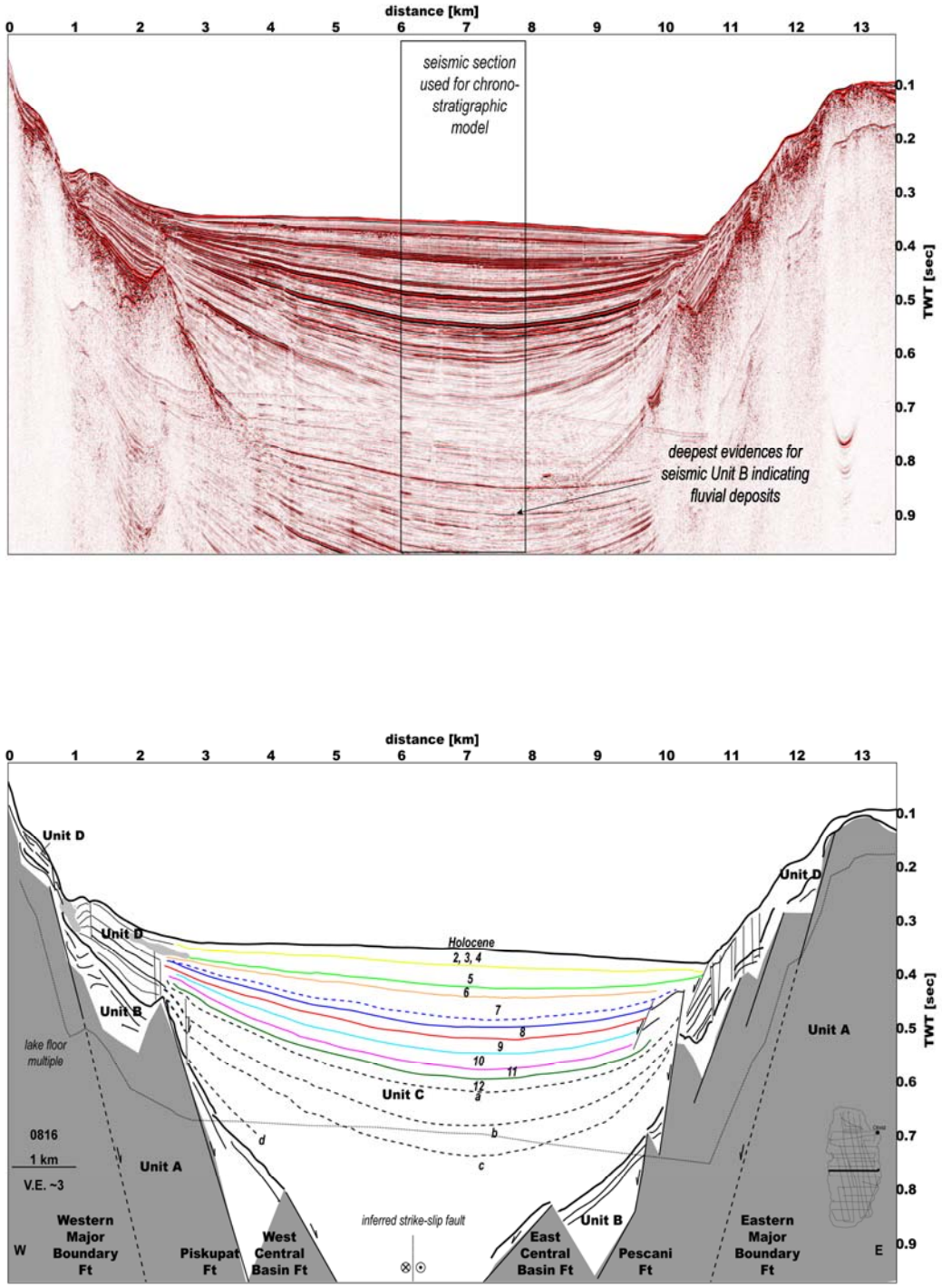

Fig. M3 6: Seismic cross section imaging the central part of Lake Ohrid characterized by thick sediment successions. Top: uninterpreted; bottom: line drawing and interpretation. The fault architecture points to symmetrical graben structure. A 2 km segment (black square) was used to develop seismic chrono-stratigraphical model which allowed us to interpret the basin in terms of glacial and interglacial cycles (see text for details).

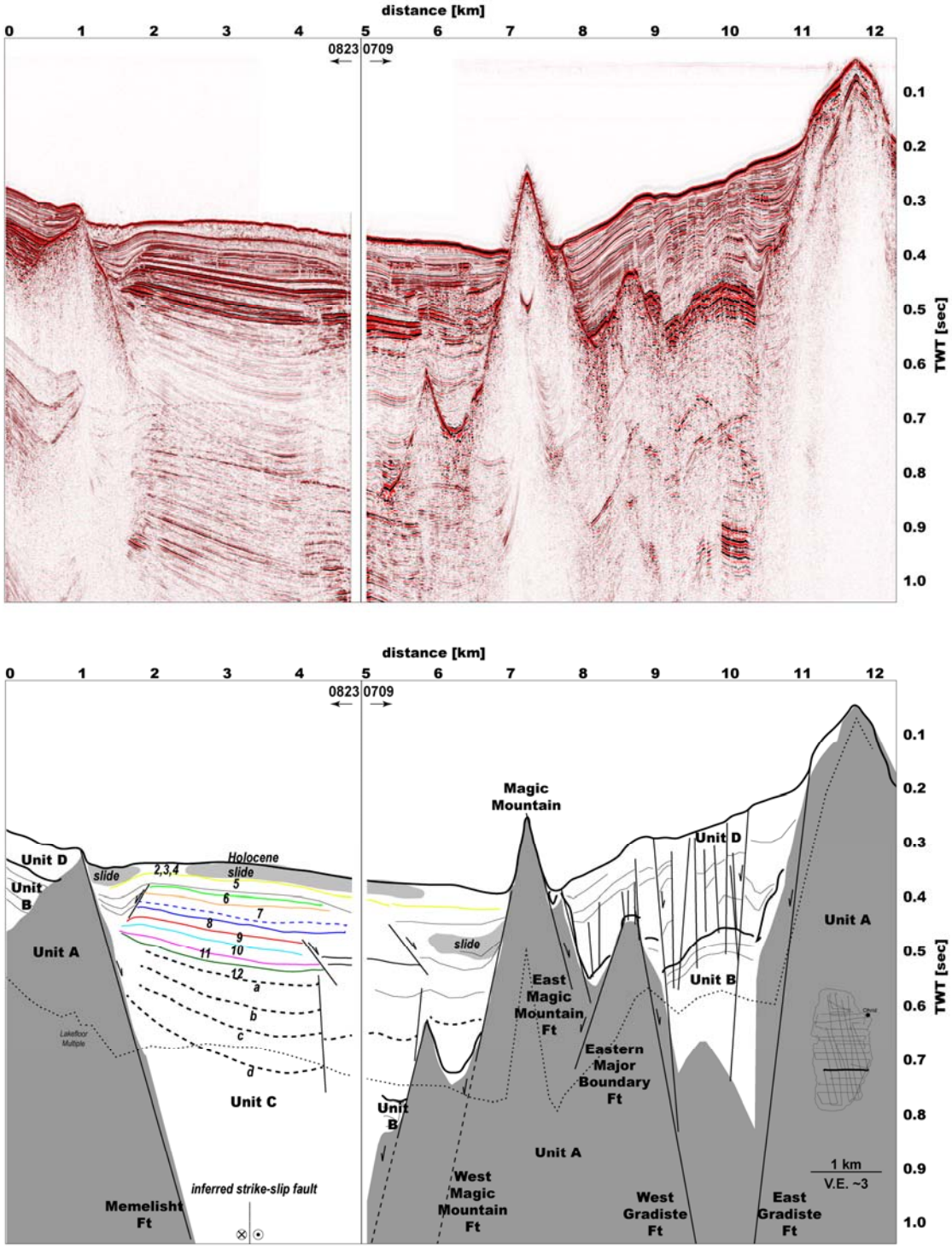

Fig. M3 7: Seismic cross section imaging the South central basin, Magic Mountain, and the active Gradiste Basin. Top: uninterpreted, bottom: line drawing and interpretation. The area is affected by extensive active faulting indicated by numerous mass wasting events especially adjacent to Magic Mountain but also by a roll over structure next to the Memelisht Normal Fault.

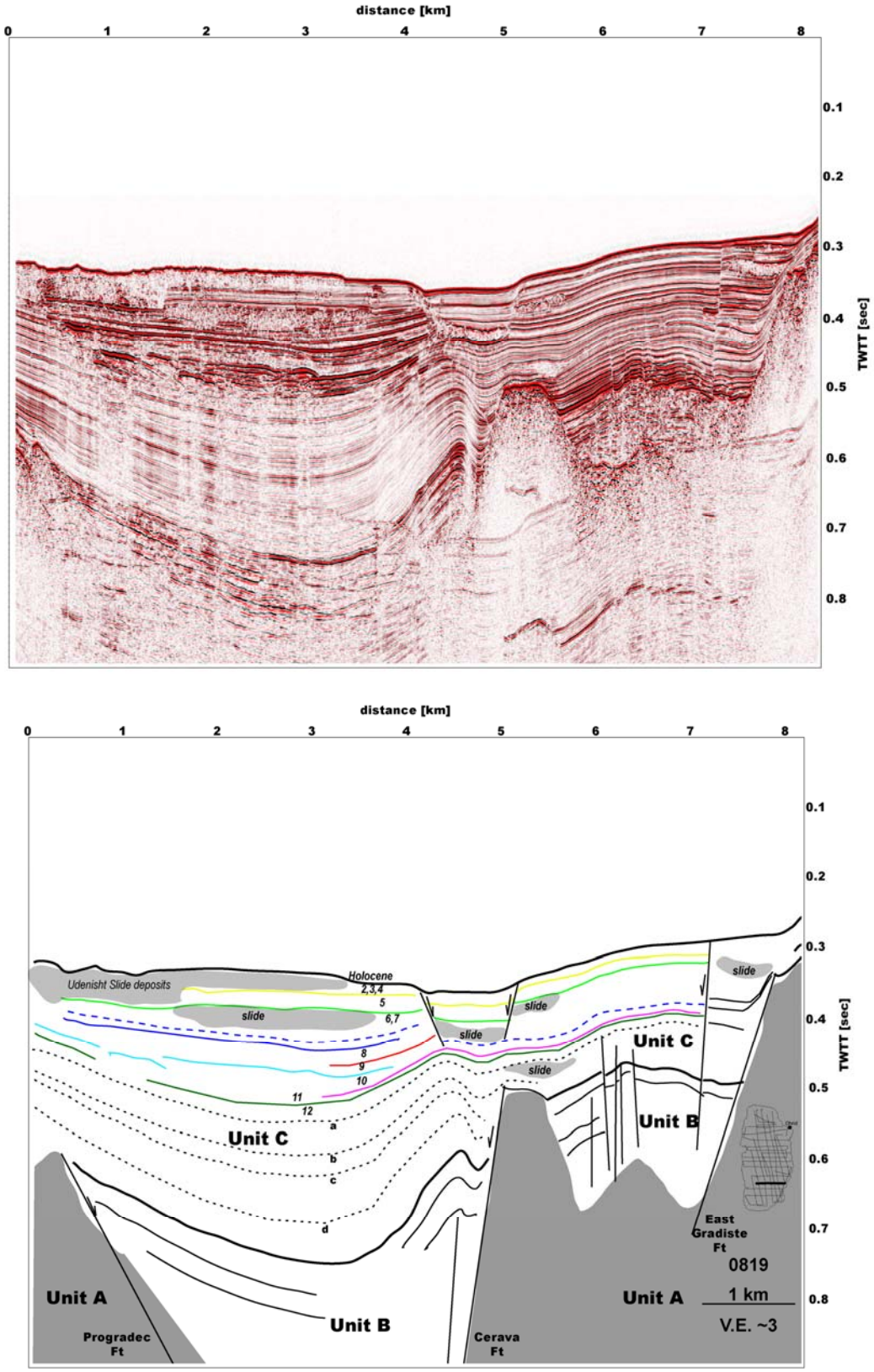

Fig. M3 8: Seismic cross section showing the complex basin structure within the southern area. Top: uninterpreted, bottom: line drawing and interpretation. (See text for further details).

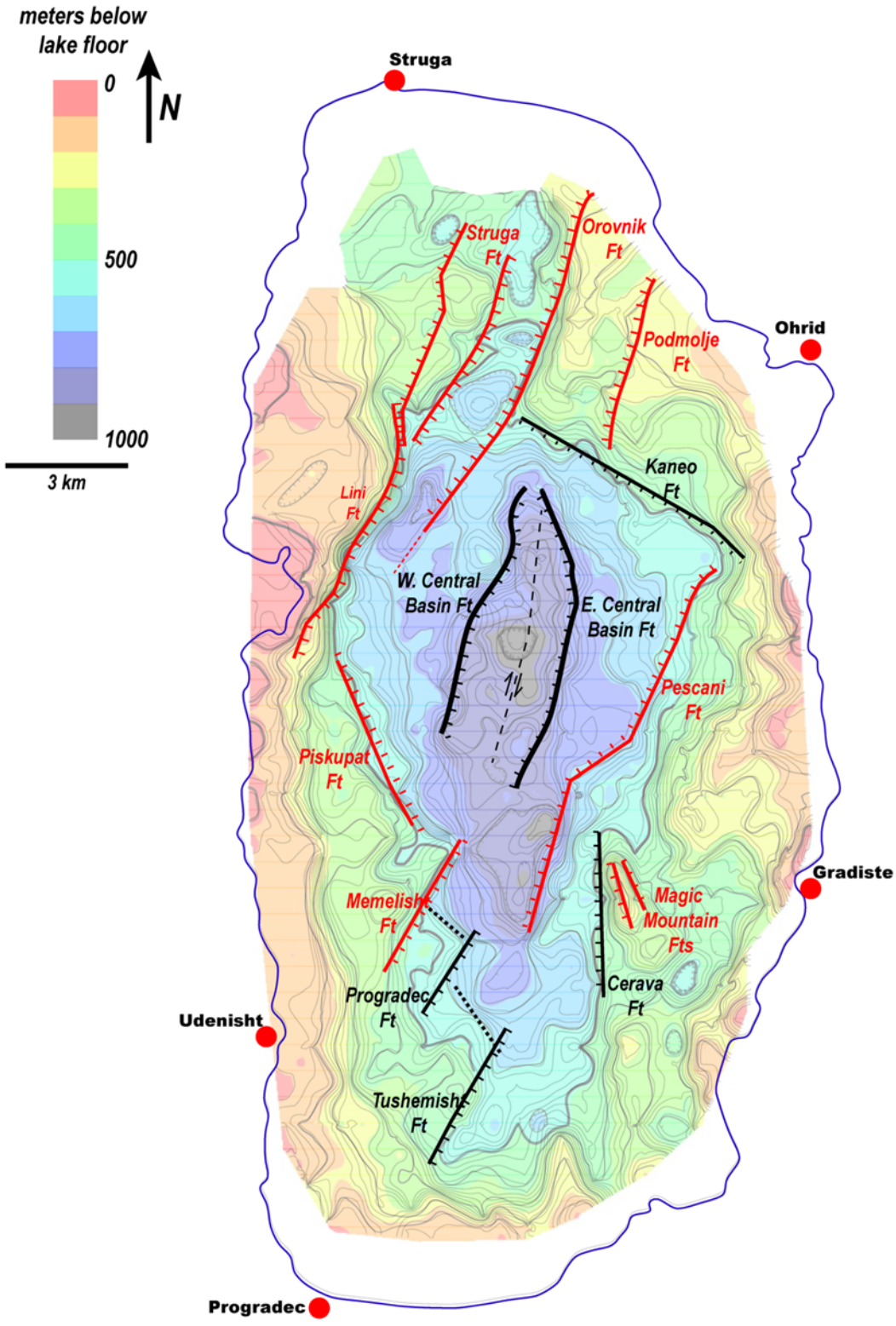

Fig. M3 9: Fault interpretation based on the acoustic basement as calculated from the picks within multichannel seismic lines. Black lines highlighting faults that are characterized by scarps forming the flank of the basement along with thick sediment cover of lacustrine deposits suggesting that those faults have been inactive for some time. Dashed line indicates an inferred dextral strike-slip fault related to the initial opening of the basin (see text for explanation). Blue line marks present shore.

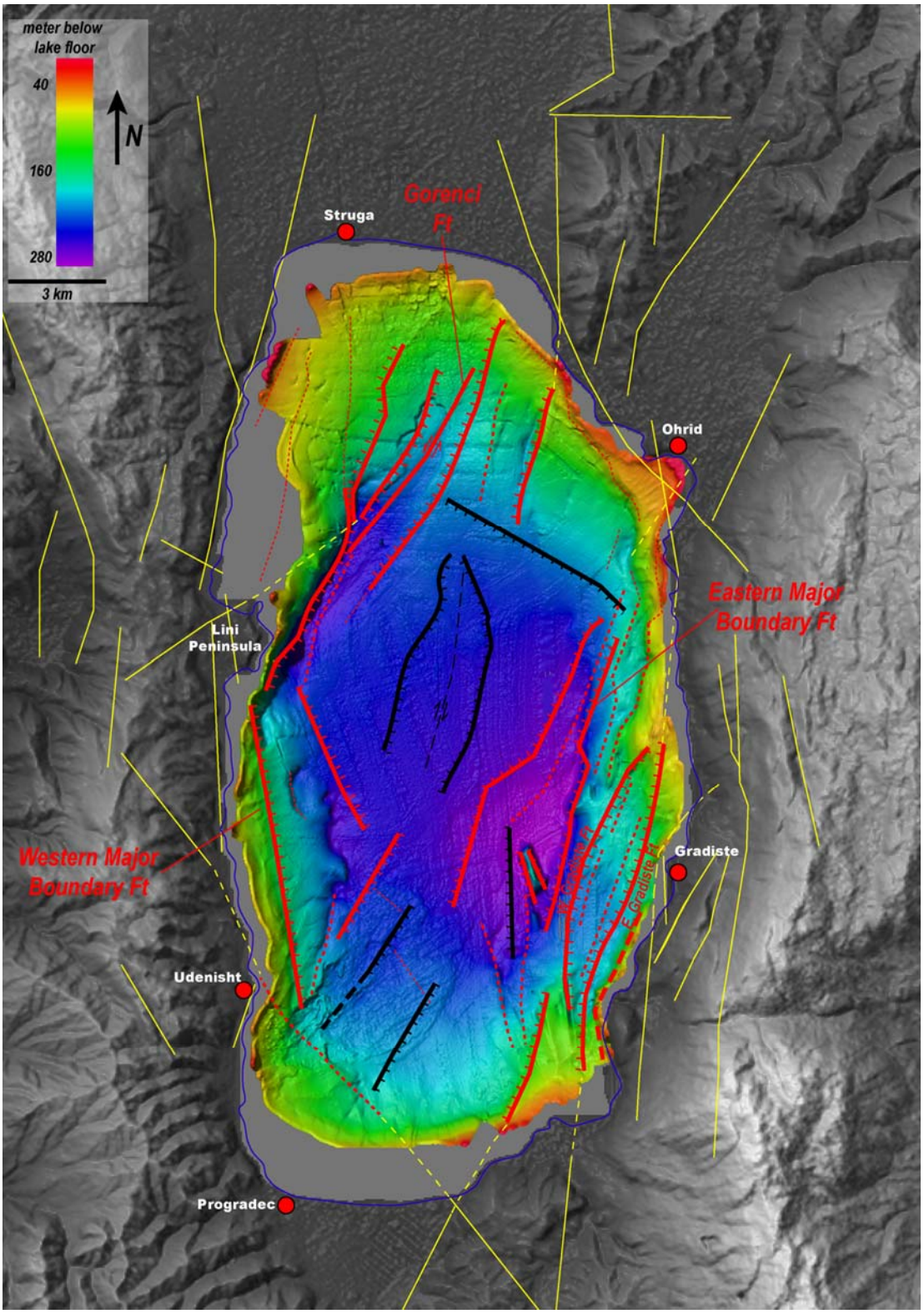

Fig. M3 10: Compilation of the bathymetric map and topography of the surrounding area. See also Fig. M3 9. Thick dashed red lines mark minor faults identified within the multichannel seismic data. Thin dashed red lines are inferred faults. Yellow lines mark faults mapped onshore (Hoffmann et al. 2010, Reicherter et al. 2010). Dashed yellow lines are inferred fault continuation of onshore and offshore data set.

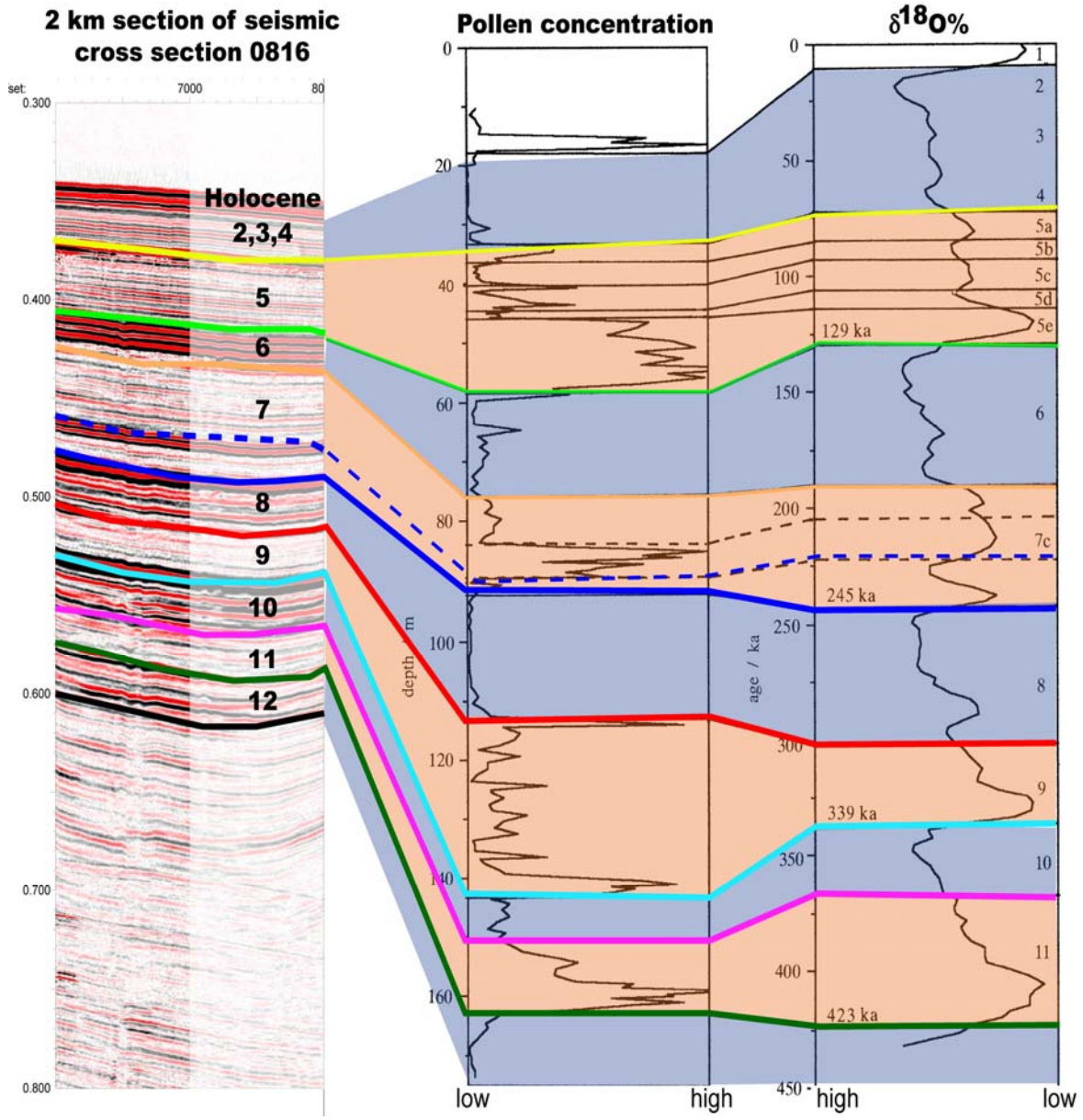

Fig. M3 11: Correlation of a 2 km transect of the seismic data central part within Lake Ohrid (see Fig. M3 6 for location) with pollen analysis and respective Marine Isotope stages (colored lines from 1 to12) adapting a model proposed by Tzedakis, (1994). Pollen concentration and $\delta^{18}O$ curves are extracted from a 160 m long sediment sequence of the Ioannina basin in northwest Greece (Tzedakis, 1994) Glacial stages (bluish) are characterized by low vegetation cover and a high precipitation with subsequently high sediment input of clastic material caused by enhanced erosion within the catchment area (high amplitude reflectors). In contrast, the interglacial (orange) are characterized by a dense vegetation cover leading to a stabilization of the soil within the catchment area and mostly biogenic sedimentation within the basin (low amplitude reflectors). See text for further details.

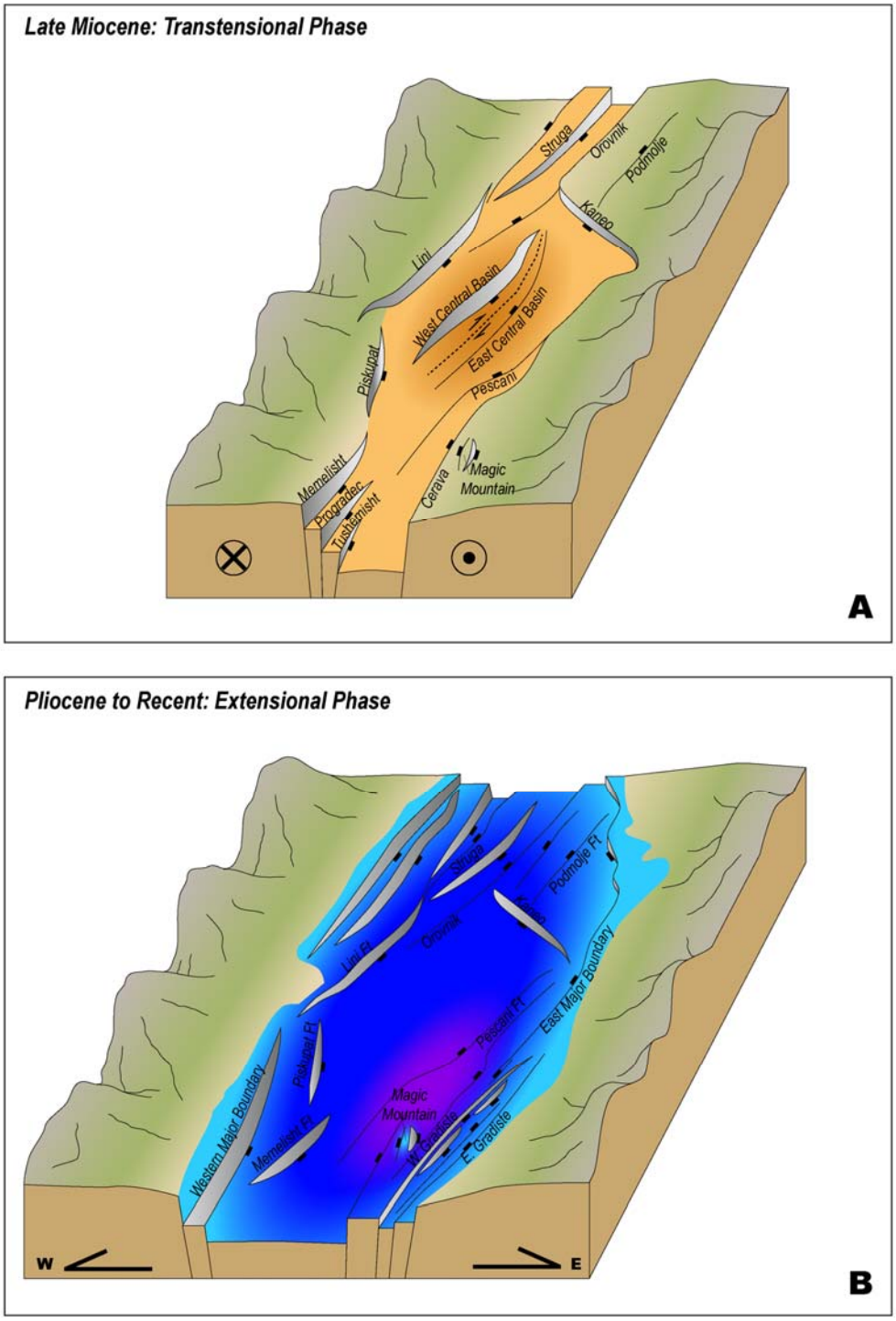

Fig. M3 12: Synoptic 3D models for the two major deformational phases of basin development: (A) Basin initiation as a pull-apart basin in a short transtensional phase during the Late Miocene and (B) Basin widening caused by E-W extension since Pliocene to recent.

6 Summary and Outlook

The main outcome of this work is an in depth insight in the morphology, surface structures, and the internal sedimentary structure of Lake Ohrid imaged by a combined seismo- and hydro-acoustic data set at different resolutions. The data set includes interpretations of 25 multichannel seismic lines, a dense grid of sediment echosounder profiles covering the entire lake imaging the uppermost 50 m of sediments, a detailed bathymetric map of the lake floor for water depths exceeding 50 m (Ohrid Bay is imaged even in shallower water depth, ~20 m), and a mosaic of sidescan sonar lines showing surface structures within the Ohrid Bay.

A major part of this work was the analysis of geophysical data in combination with sedimentological information, resulting in a better understanding of lake level fluctuations and their impact on biodiversity. Multichannel seismic data suggest that, in general, lake level progressively rose stepwise since the existence of Lake Ohrid. Offshore Sveti Naum, topset reflectors down to depths of 360 m below modern lake level indicate that lake surface of Lake Ohrid was significantly lower in periods prior to MIS 6. An analysis of sediment echosounder and bathymetric profiles in combination with core data within Ohrid Bay revealed two prominent terraces at 35 m and 60 m below present lake level. The lower terrace is most likely a relic of a fan delta that formed in a high energy shallow water environment close to a river mouth during MIS 6. In contrast, the upper terrace formed in a low energy regime, potentially under warm climate conditions with only minor rivers draining into Ohrid Bay during MIS 5. However, lake level lowstands had probably only a minor effect on the biodiversity since the changes in lake-surface, coastline, and habitat are small. On the other hand, the effect on speciation in shallow-lacustrine areas was presumably large because a drop in lake level of several tens of meters could have led to a disconnection of habitats of endemic species (e.g. along the eastern shore at Veli Dab).

A special focus of this thesis was the investigations of mass wasting events that are widespread within Lake Ohrid Basin. A detailed morphological map imaging the lake floor for water depths greater than 50 m shows two major areas affected by recent major sliding events: (1) The Struga slide in the north and (2) the Udenisht Slide Complex (USC) in the southwestern part of the lake. The latter one covers an area of 27 km², which is almost 10 % of the entire lake floor. The thickness of the slide deposits are up to 50 m resulting in a volume of ~0.11 km³, which is well within the range of a slides that are known to trigger

tsunamis. However, due to the fact that the Udenisht slide occurred in at least two phases in a retrogressive pattern it is unlikely that such a flow triggered a significant tsunami. In addition, the long run-out distance points to quick disintegration with intense sediment deformation, which also reduces the likelihood for tsunami generation. The missing sediment drape on top of the USC suggest a young age (<1,500 years). Ruptures along active faults crossing the USC area most likely acted as final trigger. Older slides imaged in subsurface depth up to 0.6 s TWTT suggest a long history of sliding in the southwestern part of the lake. Additionally, cluster of mass transport deposits can be found around Magic Mountain, Lini Fault, the Eastern and Western Major Boundary Faults, and some other major normal faults suggesting that they are seismically triggered. Slumps north of the USC show less disintegration compared to the USC and might have triggered tsunamis. Migrating fluids, resulting in over-pressured layers in combination with steep slope angles and ongoing seismicity, make future slope failures likely to occur.

A comprehensive analysis of the multichannel seismic data unraveled the tectonic evolution of Lake Ohrid Basin. The overall tectonic development took place in two main deformational phases: (1) transtensional and (2) extensional. Opening initiated most likely in Late Miocene time during a short transtensional phase caused by diminishing shortening and uplift of the surrounding area. A synoptic model demonstrates the early stage geometry of the basin after opening as a pull-apart basin. A rhomboidal shape is present in map view bounded by a set of two major normal faults (Lini and Kaneo - NE-SW; Piskupat and Pescani - NW-SE Faults). Seismic cross sections suggest the formation of a symmetrical graben during phase 1 where subsidence was significantly larger than sedimentation resulting in a formation of a lake indicated by deep lacustrine sedimentation in the deepest part of Lake Ohrid. Since the Pliocene, Lake Ohrid was influenced by an E-W directed extension related to the slab roll-back of the Hellenic subducting slab that led to the formation of N-S trending sedimentary basin within the South Balkan Extensional Regime (SBER). Lake Ohrid is the youngest basin within the SBER as extension started farther to the east and progressed westward over time. Seismic lines in an E-W direction show that Lake Ohrid widened and deepened as a consequence of this extension. The Central Basin Faults are the oldest faults in the deepest part of Lake Ohrid, which we interpret as the first master faults bounding the initial pull-apart basin. They are covered by thick succession of undisturbed strata, indicating that they are no longer active.

Towards the east and west, away from the center of the lake, new faults progressively became active and formed small grabens that were filled with sediments afterwards. These grabens show typical succession of fluvial deposits overlain by deep lacustrine sediments. The small sub-basins filled with sediments until subsidence decreased and sedimentation outpaced subsidence. At this point, sedimentation started to form drapes on those faults. Faults located closest to the present shoreline are active faults indicating that Lake Ohrid is still experiencing extension. The fact that the graben hosts a deep lake further suggests that sedimentation is smaller than subsidence; hence Lake Ohrid is in an underfilled stage.

The architecture of the sedimentary infill is a result of a complex interaction of climatic and tectonic induced processes. We observed a regular succession within the seismic stratigraphy starting with the acoustic basement representing the pre-rift stage, followed by fluvial deposits interpreted as the stage after fault initiation and formation of small grabens within the marginal regions of the respective basin, and deep lacustrine sediments which make up the major part of the sedimentary infill further indicating that subsidence is greater than sedimentation. This sediment succession is part of a tripartite depositional pattern observed in rift lakes and linked to the tectonic activity of the broader region. Reflectors flattening toward younger strata suggest decreasing subsidence rates over time. Deposition of shallow lacustrine sediments is not present in Lake Ohrid hence subsidence is still larger than sedimentation.

The limnological age of Lake Ohrid is highly debated and as geophysical data were not available so far one main goal of this thesis is to shed light on the temporal evolution of the sedimentation. In the central part of the basin a thick succession of undisturbed sediments was identified containing a regular pattern of alternating sequences of low and high amplitude reflectors. Assuming that this depositional pattern reflects a change in the vegetation of the surrounding area we successfully developed a chrono-stratigraphic model showing that sedimentation was influenced by several glacial and interglacial cycles back to MIS 12. By applying this new chrono-stratigraphic model we calculated a mean accumulation rate of 0.43 mm/yr of the past 430 kyrs. Extrapolation of this accumulation rate for deeper strata revealed a minimum limnological age for Lake Ohrid of ~2 Myrs. The actual age, however, remains uncertain as we cannot account for compaction and possible hiatuses within the sediment succession.

In addition, five drill sites proposed to ICDP in order to achieve scientific objectives of the SCOPSCO project were selected on the basis of the multichannel seismic data. The suggested

primary drill site (DEEP) is located in the central basin at water depth of 250 m in order to recover 700 m long continuous core providing substantial information for dating and to investigate the origin of the lake, the environmental history, tephra deposition, and the link between evolutionary changes with geological events. Four additional sites have been proposed to ICDP in order to unravel tectonic activity, hydrological regime, and lake level fluctuations of Lake Ohrid. Two sites (Lini and Gradiste) are located at active lake-bounding major normal faults, one at the western and the other located at the eastern side. Mass wasting bodies are found at both sites but probable trigger mechanisms seem to be different. At the eastern part (Gradiste), earthquakes are most likely triggers for the failures. For example, on the western side (Lini) neotectonic activity of the Lini Fault is evidenced by two mass wasting deposits of mainly undeformed sequences that are rotated antithetically. Finally, two sites (Struga and Cerava) were depicted to shed light on the hydrological history of Lake Ohrid as they are in the vicinity of clinform structures. Interestingly, the clinoform in the north (located at 0.25 s TWTT subsurface depth) is found close to the modern outflow of the lake (Crn Drim), suggesting major hydrological changes since the formation of the clinoform structure.

The findings of this study serve as a fundamental database for future studies at Lake Ohrid. The ICDP drilling campaign within the SCOPSCO project will profit from the findings presented here. Although this work led to a better understanding of the tectonic and sedimentary history of Lake Ohrid, questions still remain open. Those aspects include an exact chronological model for sediments within Lake Ohrid. Our chrono-stratigraphic model presented in this study is based on several assumptions and lacks a direct control on a long sediment record that is still missing for Lake Ohrid. Such a long sediment core will also allow a joint interpretation of the seismic and drilling data in order to refine the temporal and spatial resolution of the model for basin evolution.

Long sediment cores provide high resolution density-depth curves that are crucial information for interpretation of seismic reflectors. After correlation of cores with seismic data at the drill site it will be possible to track seismic reflectors within the basin and subsequently improve the sequence stratigraphy of Lake Ohrid. On the other hand, drilling at the Gradiste site that is disconnected from the main basin by major normal faults will allow to link sediment succession and their respective ages to deposits within the main part of the basin in order to shed light on the evolution of the Gradiste Sub-basin. This information is essential for a better

understanding of the evolution of speciation within parts of Lake Ohrid that were disconnected from the main lake after formation.

Specific tasks for the future are calculation of synthetic seismograms and the comparison with our seismic lines and drill data. Detailed stratigraphical information from the wells can be applied to seismic profiles which will improve the interpretation of seismic lines. For example, an age model calculated from sediment cores allows dating of slide and slump deposits identified within the multichannel seismic data. This leads to a better understanding and evaluation of trigger mechanisms proposed within this study. Dated slide deposits within the same stratigraphic level can be used to generate a paleoseismic catalogue and hazard map for Lake Ohrid contributing to studies carried out onshore. This study has shown that Lake Ohrid experienced significant lake level fluctuations since its existence. At this point it is still uncertain whether those changes are climatically or tectonically induced. An age control from the drill data in combination with onshore investigations will allow the reconstruction of a detailed lake level curve and shed light on the hydrological evolution of Lake Ohrid Basin.

Acknowledgement

Most importantly I would like to thank my supervisor Sebastian Krastel-Gudegast for encouraging me to do a PhD thesis in the first place which turned out to be the right decision. Beside all the scientific input and guidance in the last four years I am grateful for your faith in me that I could carry out the BLOSSOM field campaign mainly by myself with your support whenever things got complicated. I was able to do field work at the most beautiful lake in the world (subjective view).

I thank Kerstin Schrottke for being my second supervisor.

I would like to acknowledge all the colleagues contributing to this work through scientific discussions or by providing input to the manuscripts: Christian Berndt, David Buchs, Tebke Böschen, Gerhard Daut, Matthias Grün, Nadine Hoffmann, Klaus Reicherter, Tilmann Schwenk, Michael Stipp, Hendrik Vogel, Bernd Wagner, Martin Wessels.

I am very grateful to all the persons helping in the field. I would like to thank all the Macedonian colleagues from Ohrid for their support in the logistic. In particular, I would like to express my gratitude to Zoran Brdadovksi for not only being a good chief engineer but also a good cook and friend. Special thanks to Matthias Grün and Stephanie Koch who made the BLOSSOM experience unique and successful.

I warmly and sincerely thank my friend Sarah R. Hall, who helped to improve the manuscript by proof reading the English and for the fruitful discussions about geosciences we had throughout the past years. Thanks for encouraging me to stay in science with your never ending enthusiasm for Earth Sciences and field geology. Driving or walking through the country with you is always an enjoyable mini lecture in geosciences!

Special thanks goes to my colleagues Mathias Meyer and Andrea Anasetti, Felix Gross, Lili Fu and Julia Schwab who shared an office with me and made the time enjoyable not only by keeping my caffeine level high. Although now they moved offices I also thank all colleagues from the 2nd floor of building 4. Thanks to all the members of the geodynamic group for supportive critics and scientific input.

I would like to especially thank Ilse Stender for taking care of Greta and Clara which made the completion of the thesis possible. You really make a great job by being a nanny! But not by acting like one, but rather give them a second home where they get the warmth and love they deserve.

Many thanks to my friends and my family for your love and support and making the time besides work enjoyable.

I kindly thank my husband Norman for your love, patience and support. Thank you for your enthusiasm in constructing the multibeam holder that would have lasted another five years. And although only supporting me in the second part of the thesis a special thanks goes to Greta and Clara for not only being double trouble but also quadruple happiness!

References

Albrecht, C. and Wilke, T. (2008) Ancient Lake Ohrid: biodiversity and evolution. *Hydrobiologia*, **615,** 103-40, *doi:10.1007/s10750-008-9558-y*

Aliaj, S., Adams, J., Halchuk, S., Sulstarova, E., Peci, V. and Muco, B. (2004) Probabilistic seismic hazard maps for Albania. *13th World Conference on Earthquake Engineering*, Vancouver, B.C., Canada

Aliaj, S., Baldassarre, G. and Shkupi, D. (2001) Quaternary subsidence zones in Albania: some case studies. *Bulletin of Engineering Geology and the Environment*, **59,** 313-18,

Ambraseys, N. and Jackson, J. (1990) Seismicity and associated strain of central Greece between 1890 and 1988. *Geophysical Journal International*, **101,** 663-708,

Arsovsky, M. and Hadzievsky, D. (1970) Correlation between neotectonics and the seismicity of Macedonia. *Tectonophysics*, **9,** 129-42,

Belmecheri, S., Namiotko, T., Robert, C., von Grafenstein, U. and Danielopol, D. (2009) Climate controlled ostracod preservation in Lake Ohrid (Albania, Macedonia). *Palaeogeography, Palaeoclimatology, Palaeoecology*, **277,** 236-45,

Burchfiel, B., Nakov, R., Dumurdzanov, N., Papanikolaou, D., Tzankov, T., Serafimovski, T., King, R., Kotzev, V., Todosov, A. and Nurce, B. (2008) Evolution and dynamics of the Cenozoic tectonics of the South Balkan extensional system. *Geosphere*, **4,** 918,

Caron, B., Sulpizio, R., Zanchetta, G., Siani, G. and Santacroce, R. (2010) The Late Holocene to Pleistocene tephrostratigraphic record of Lake Ohrid (Albania). *Comptes Rendus Geoscience*, **342,** 453-66,

Carroll, A. and Bohacs, K. (1999) Stratigraphic classification of ancient lakes; balancing tectonic and climatic controls. *Geology*, **27,** 99-102,

Cohen, A. (2003) Paleolimnology: the history and evolution of lake systems. 500 pp.

Cvijic, J. (1911) Fundamentals of geography and geology of Macedonia and Old Serbia. *Book III, Serbian Academy of Sciences, Special Edition, Beograd (in Serbian).*

Denner, M. (2006) *Bathymetrie, Sedimentverteilung und Tektonik im Ohridsee in Albanien und Mazedonien*, Diploma Thesis at University of Leipzig.

Dilek, Y. (2006) Collision tectonics of the Mediterranean region: Causes and consequences. *GSA Special Papers*, **409,** 1-13,

Dumurdzanov, N., Serafimovski, T. and Burchfiel, B. (2004) Evolution of the Neogene-Pleistocene basins of Macedonia. *Geological Society of America Digital Map and Chart Series*, **1,** 1-20,

Dumurdzanov, N., Serafimovski, T. and Burchfiel, B. (2005) Cenozoic tectonics of Macedonia and its relation to the South Balkan extensional regime. *Geosphere*, **1,** 1-22,

Ghikas, C., Dilek, Y. and Rassios, A.E. (2010) Structure and tectonics of subophiolitic mélanges in the western Hellenides (Greece): implications for ophiolite emplacement tectonics. *International Geology Review*, **52,** 423-53,

Giaccio, B., Isaia, R., Sulpizio, R. and Zanchetta, G. (2008) Explosive volcanism in the central Mediterranean area during the late Quaternary-linking sources and distal archives. *Journal of volcanology and geothermal research*, **177,** v-vii,

Hoffmann, N., Reicherter, K., Fernandez-Steeger, T. and Gruetzner, C. (2010) Evolution of ancient Lake Ohrid: a tectonic perspective. *Biogeosciences*, **7,** 3377-86, *doi:10.5194/bg-7-3377-2010*

Holtvoeth, J., Vogel, H., Wagner, B. and Wolff, G. (2010) Lipid biomarkers in Holocene and glacial sediments from ancient Lake Ohrid (Macedonia, Albania). *Biogeosciences*, **7,** 3473-89, *doi:10.5194/bg-7-3473-2010*

Keller, J., Ryan, W., Ninkovich, D. and Altherr, R. (1978) Explosive volcanic activity in the Mediterranean over the past 200,000 yr as recorded in deep-sea sediments. *Bulletin of the Geological Society of America*, **89,** 591-604,

Leng, M., Baneschi, I., Zanchetta, G., Jex, C., Wagner, H. and Vogel, H. (2010) Late Quaternary palaeoenvironmental reconstruction from Lakes Ohrid and Prespa (Macedonia/Albania border) using stable isotopes. *Biogeosciences*, **7,** 3109-2122, *doi:10.5194/bg-7-3109-2010*

Lézine, A., Von Grafenstein, U., Andersen, N., Belmecheri, S., Bordon, A., Caron, B., Cazet, J., Erlenkeuser, H., Fouache, E. and Grenier, C. (2010) Lake Ohrid, Albania, provides an exceptional multi-proxy record of environmental changes during the last glacial-interglacial cycle. *Palaeogeography, Palaeoclimatology, Palaeoecology*, **287,** 116-27,

Lindhorst, K., Gruen, M., Krastel, S. and Schwenk, T. (2012) Hydroacoustic Analysis of Mass Wasting Deposits in Lake Ohrid (FYR Macedonia/Albania). *Submarine Mass Movements and Their Consequences***,** 245-53,

Lindhorst, K., Vogel, H., Krastel, S., Wagner, B., Hilgers, A., Zander, A., Schwenk, T., Wessels, M. and Daut, G. (2010) Stratigraphic analysis of lake level fluctuations in Lake Ohrid: an integration of high resolution hydro-acoustic data and sediment cores. *Biogeosciences*, **7,** 3531-48, *doi:10.5194/bgd-7-3651-2010*

Lister, G. and Davis, G. (1989) The origin of metamorphic core complexes and detachment faults formed during Tertiary continental extension in the northern Colorado River region, USA *Journal of Structural Geology*, **11,** 65-94,

Matter, M., Anselmetti, F., Jordanoska, B., Wagner, B., Wessels, M. and Wueest, A. (2010) Carbonate sedimentation and effects of eutrophication observed at the Kalista subaquatic springs in Lake Ohrid (Macedonia). *Biogeosciences*, **7,** 3755-67,

Matzinger, A., Jordanoski, M., Veljanoska-Sarafiloska, E., Sturm, M., Müller, B. and Wüest, A. (2006a) Is Lake Prespa Jeopardizing the Ecosystem of Ancient Lake Ohrid? *Hydrobiologia*, **553,** 89-109, *DOI 10.1007/s10750-005-6427-9*

Matzinger, A., Schmid, M., Veljanoska-Sarafiloska, E., Patceva, S., Guseska, D., Wagner, B., Müller, B., Sturm, M. and Wüest, A. (2007) Eutrophication of ancient Lake Ohrid: Global warming amplifies detrimental effects of increased nutrient inputs. *Limnology and Oceanography*, **52,** 338-53,

Matzinger, A., Spirkovski, Z., Patceva, S. and Wuest, A. (2006b) Sensitivity of ancient Lake Ohrid to local anthropogenic impacts and global warming. *Journal of Great Lakes Research*, **32,** 158-79,

Mountrakis, D., Tranos, M., Papazachos, C., Thomaidou, E., Karagianni, E. and Vamvakaris, D. (2006) Neotectonic and seismological data concerning major active

faults, and the stress regimes of Northern Greece. *Special Publication - Geological Society of London*, **260,** 649-70,

Muço, B., Vaccari, F., Panza, G. and Kuka, N. (2002) Seismic zonation in Albania using a deterministic approach. *Tectonophysics*, **344,** 277-88,

Nieuwland, D., Oudmayer, B. and Valbona, U. (2001) The tectonic development of Albania: explanation and prediction of structural styles. *Marine and Petroleum Geology*, **18,** 161-77,

Paterne, M., Guichard, F. and Labeyrie, J. (1988) Explosive activity of the South Italian volcanoes during the past 80,000 years as determined by marine tephrochronology. *Journal of Volcanology and Geothermal Research*, **34,** 153-72,

Popovska, C. and Bonacci, O. (2007) Basic data on the hydrology of Lakes Ohrid and Prespa. *Hydrological Processes*, **21,** 658-64,

Prosser, S. (1993) Rift-related linked depositional systems and their seismic expression. *Geological Society London Special Publications*, **71,** 35-66,

Reicherter, K., Hoffmann, N., Lindhorst, K., Krastel, S., Fernandez-Steeger, T., Grutzner, C. and Wiatr, T. (2011) Active basins and neotectonics: morphotectonics of the Lake Ohrid Basin (FYROM and Albania). *Zeitschrift der Deutschen Gesellschaft für Geowissenschaften*, **162,** 217-34,

Robertson (2012) Late Palaeozoic-Cenozoic tectonic development of Greece and Albania in the context of alternative reconstructions of Tethys in the Eastern Mediterranean region. *International Geology Review*, **54,** 373-454,

Robertson and Dixon, J. (1984) Introduction: aspects of the geological evolution of the Eastern Mediterranean. *Geological Society, London, Special Publications*, **17,** 1-74,

Robertson, Dixon, J., Brown, S., Collins, A., Morris, A., Pickett, E., Sharp, I. and Ustaomer, T. (1996) Alternative tectonic models for the Late Palaeozoic-Early Tertiary development of Tethys in the Eastern Mediterranean region. *Geological Society London Special Publications*, **105,** 239,

Robertson, A., Clift, P., Degnan, P. and Jones, G. (1991) Palaeogeographic and palaeotectonic evolution of the Eastern Mediterranean Neotethys. *Palaeogeography, Palaeoclimatology, Palaeoecology*, **87,** 289-343,

Schlische, R. and Olsen, P. (1990) Quantitative filling model for continental extensional basins with applications to early Mesozoic rifts of eastern North America. *The Journal of Geology*, **98,** 135-55,

Scholz, C. (1995) Deltas of the Lake Malawi Rift, East Africa: seismic expression and exploration implications. *AAPG Bulletin-American Association of Petroleum Geologists*, **79,** 1679-97,

Spirkovski, Z., Avramovski, O. and Kodzoman, A. (2001) Watershed management in the Lake Ohrid region of Albania and Macedonia. *Lakes & reservoirs: research and management*, **6,** 237-42,

Stankovic, S. (1960) The Balkan Lake Ohrid and Its Living Worldpp.

Suhadolc, P., Sandron, D., Fitzko, F. and Costa, G. (2004) Seismic ground motion estimates for the M6.1 earthquake of July 26, 1963 at Skopje, Republic of Macedonia. *Acta Geodaetica et Geophysica Hungarica*, **39,** 319-26,

Sulpizio, R., Zanchetta, G., D'Orazio, M., Vogel, H. and Wagner, B. (2010) Tephrostratigraphy and tephrochronology of lakes Ohrid and Prespa, Balkans. *Biogeosciences*, **7,** 3273-88, *10.5194/bg-7-3273-2010*

Sulpizio, R., Zanchetta, G., Paterne, M. and Siani, G. (2003) A review of tephrostratigraphy in central and southern Italy during the last 65 ka. *Il Quaternario*, **16,** 91-108,

Vogel, H., Wagner, B., Zanchetta, G., Sulpizio, R. and Rosén, P. (2010a) A paleoclimate record with tephrochronological age control for the last glacial-interglacial cylce from Lake Ohrid, Albania and Macedonia. *Journal of Paleolimnology*, *doi:10.1007/s10933-009-9404-x*

Vogel, H., Wessels, M., Albrecht, C., Stich, H. and Wagner, B. (2010b) Spatial variability of recent sedimentation in Lake Ohrid (Albania/Macedonia). *Biogeosciences*, **7,** 3333-42,

Vogel, H., Zanchetta, G., Sulpizio, R., Wagner, B. and Nowaczyk, N. (2010c) A tephrostratigraphic record for the last glacial–interglacial cycle from Lake Ohrid, Albania and Macedonia. *J. Quaternary Sci.*, **25,** 320-38,

Wagner, B., Lotter, A., Nowaczyk, N., Reed, J., Schwalb, A., Sulpizio, R., Valsecchi, V., Wessels, M. and Zanchetta, G. (2008a) A 40,000-year record of environmental change from ancient Lake Ohrid (Albania and Macedonia). *Journal of Paleolimnology*, **41,** 407-30,

Wagner, B., Reicherter, K., Daut, G., Wessels, M., Matzinger, A., Schwalb, A., Spirkovski, Z. and Sanxhaku, M. (2008b) The potential of Lake Ohrid for long-term palaeoenvironmental reconstructions. *Palaeogeography, Palaeoclimatology, Palaeoecology*, **259,** 341-56,

Wagner, B., Sulpizio, R., Zanchetta, G., Wulf, S., Wessels, M., Daut, G. and Nowaczyk, N. (2008c) The last 40 ka tephrostratigraphic record of Lake Ohrid, Albania and Macedonia: a very distal archive for ash dispersal from Italian volcanoes. *J. Volcanol. Geoth. Res.*, **177,** 71-80,

Wagner, B. and Wilke, T. (2010) Preface: Evolutionary and geological history of Balkan lakes Ohrid and Prespa (Eds B. Wagner, T. Wilke and V. Brovkin), **8**. Biogeosciences.

Watzin, M.C., Puka, V. and Naumoski, T. (2002) Lake Ohrid and its Watershed, State of the Environment Report. Lake Ohrid Conservation Project.**,** 134 pp,

Wulf, S., Kraml, M., Brauer, A., Keller, J. and Negendank, J.F.W. (2004) Tephrochronology of the 100 ka lacustrine sediment record of Lago Grande di Monticchio (southern Italy). *Quaternary International*, **122,** 7-30,

Appendix

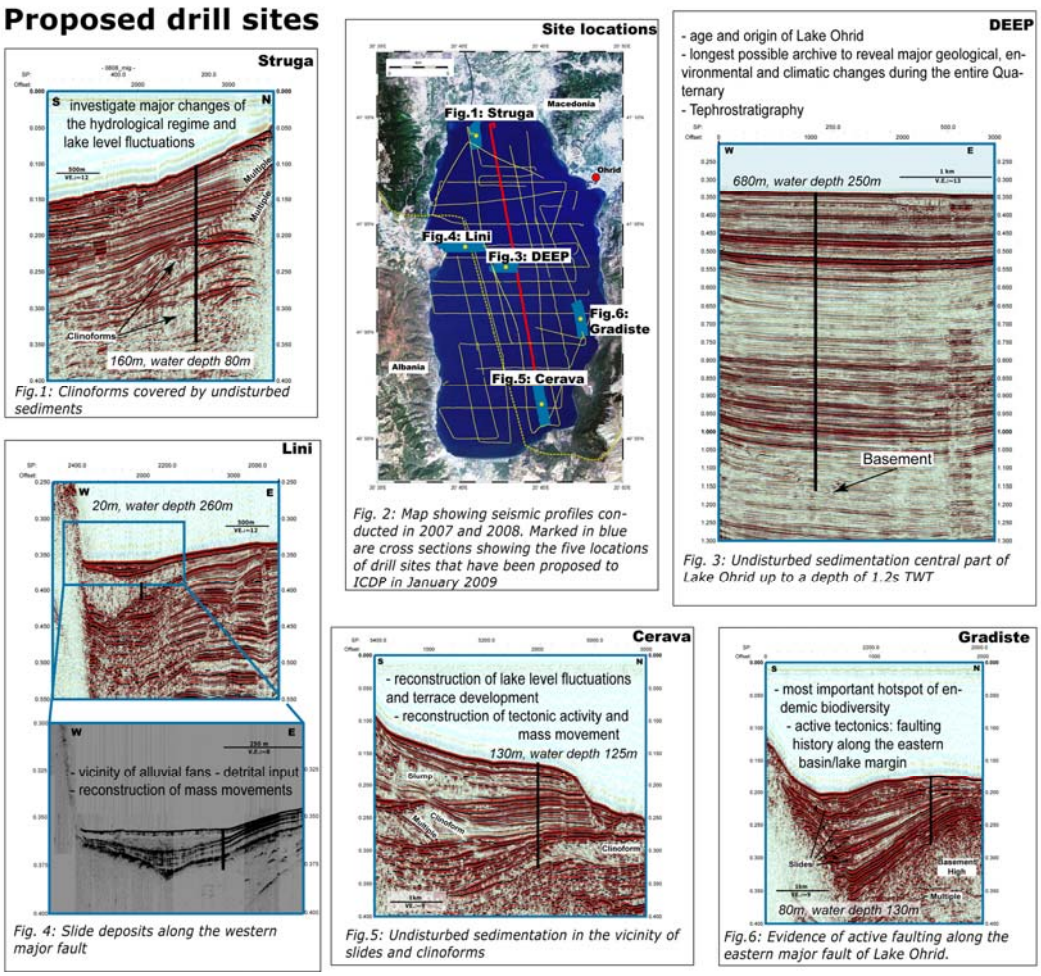

Fig. B 1: Seismic cross sections and the locations of proposed ICDP drill sites of the SCOPSCO project.

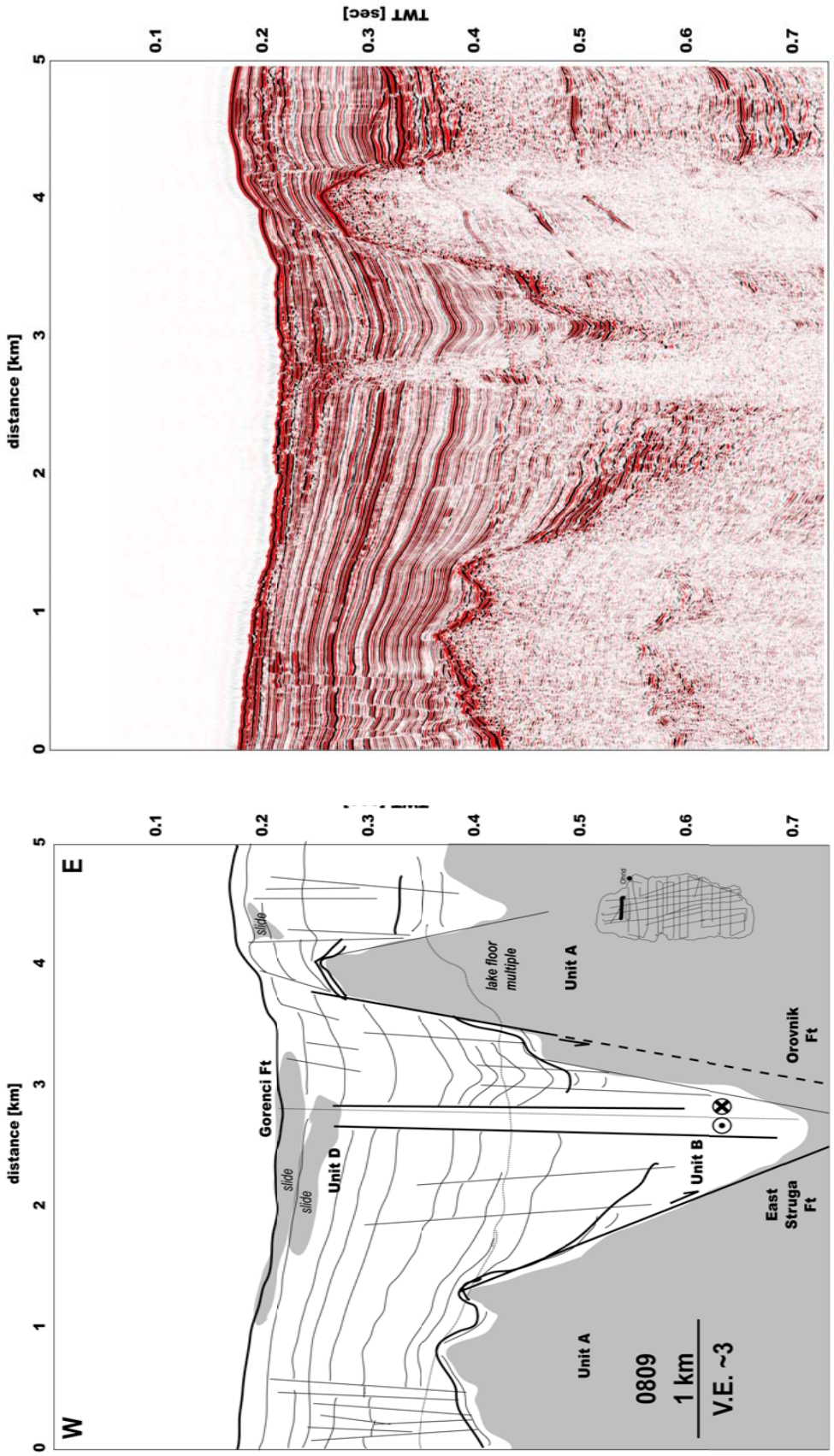

Fig. B 2: Seismic cross section showing sedimentary structures in the northern area. The active Gorenci strike-slip fault is imaged on the profile.

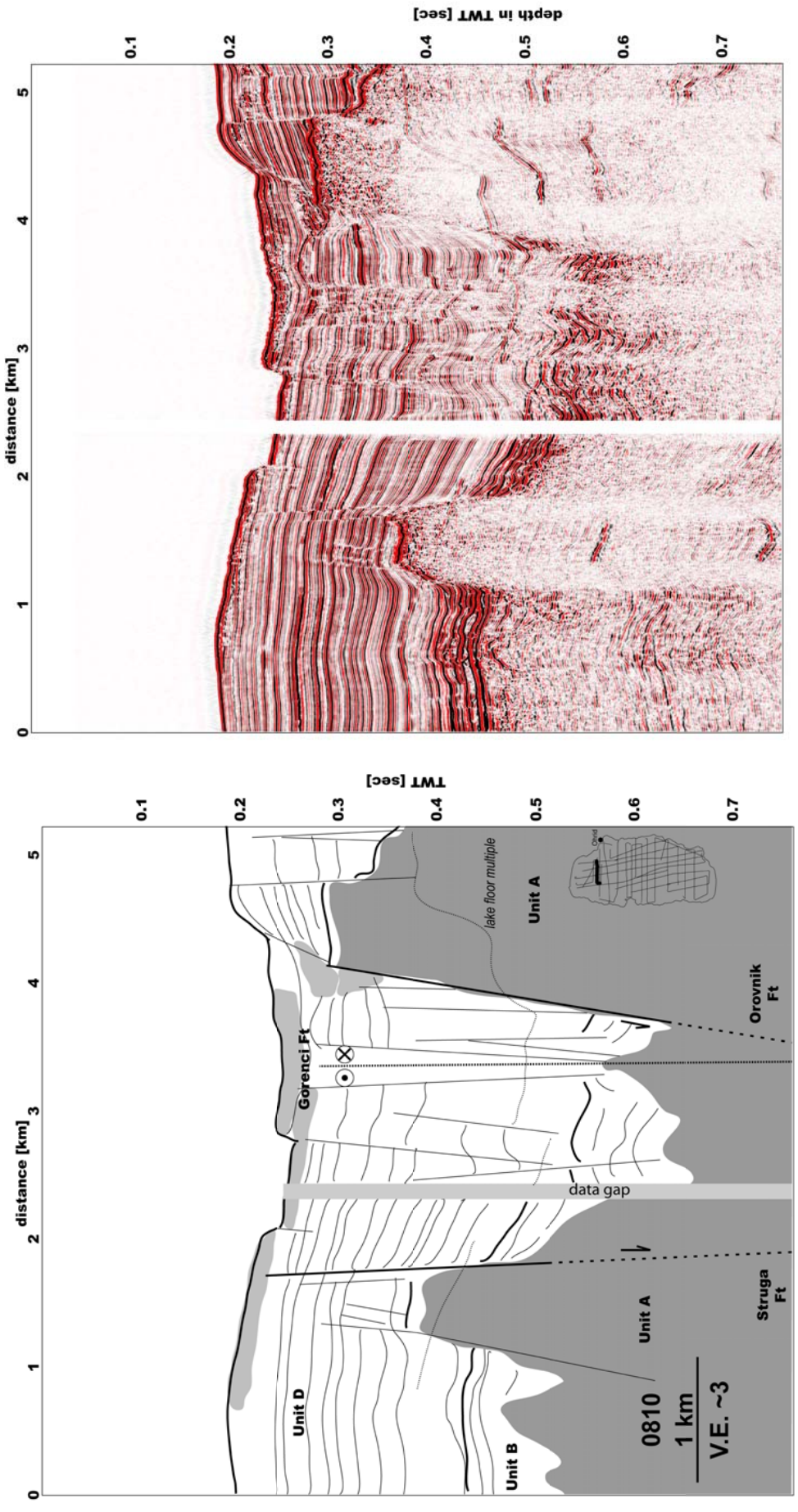

Fig. B 3: Seismic cross section showing sedimentary structures in the northern area. The active Gorenci strike-slip fault is imaged on the profile.

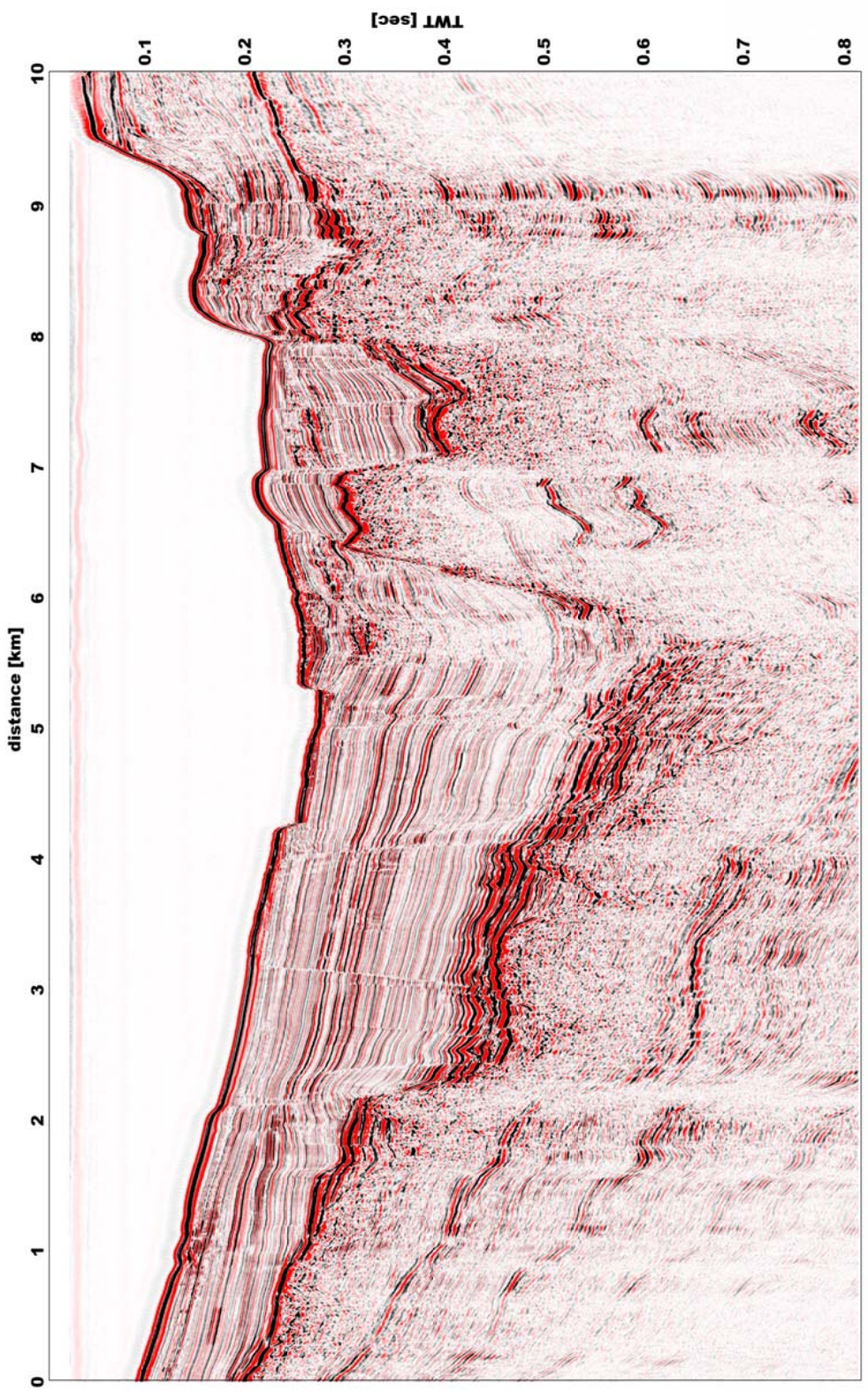
TWT [sec]
0.1
0.2
0.3
0.4
0.5
0.6
0.7
0.8
distance [km]
0
1
2
3
4
5
6
7
8
9
10

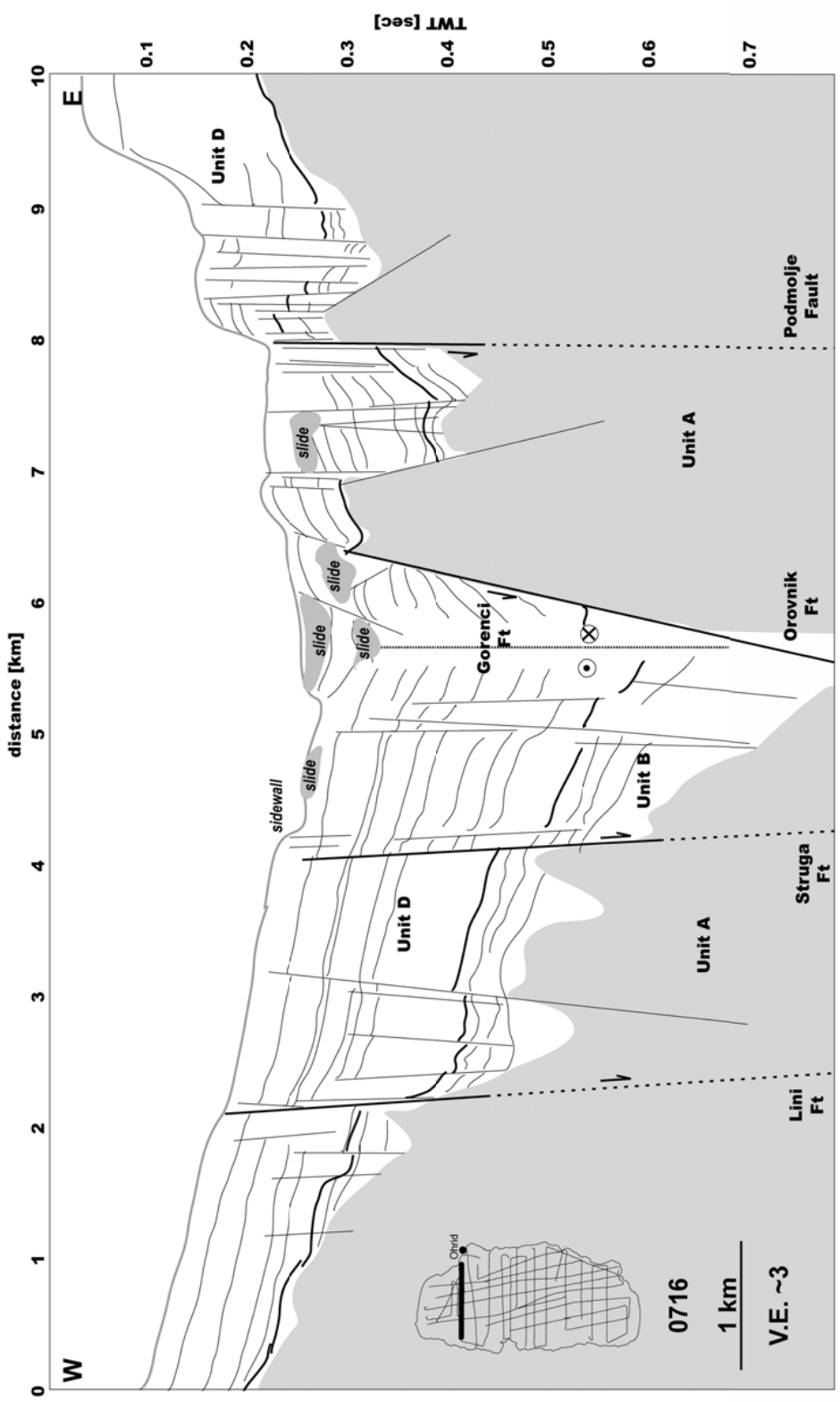

Fig. B 4: Seismic cross section showing sedimentary structures in the northern area. The active Gorenci strike-slip fault is imaged on the profile.

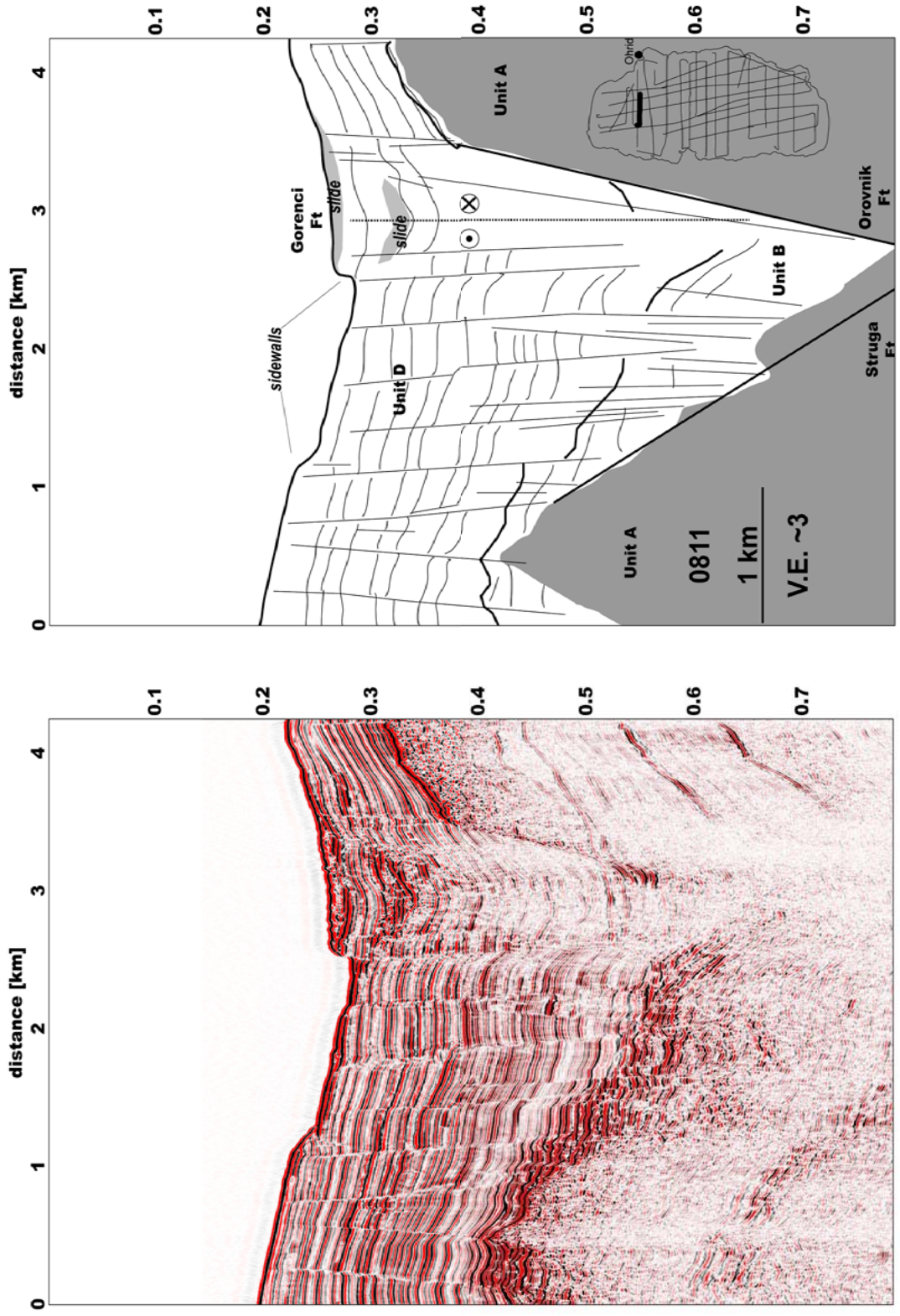

Fig. B 5: Seismic cross section showing sedimentary structures in the northern area. The active Gorenci strike-slip fault adjacent to the Struga graben illustrated by distinct sidewalls is imaged on the profile.

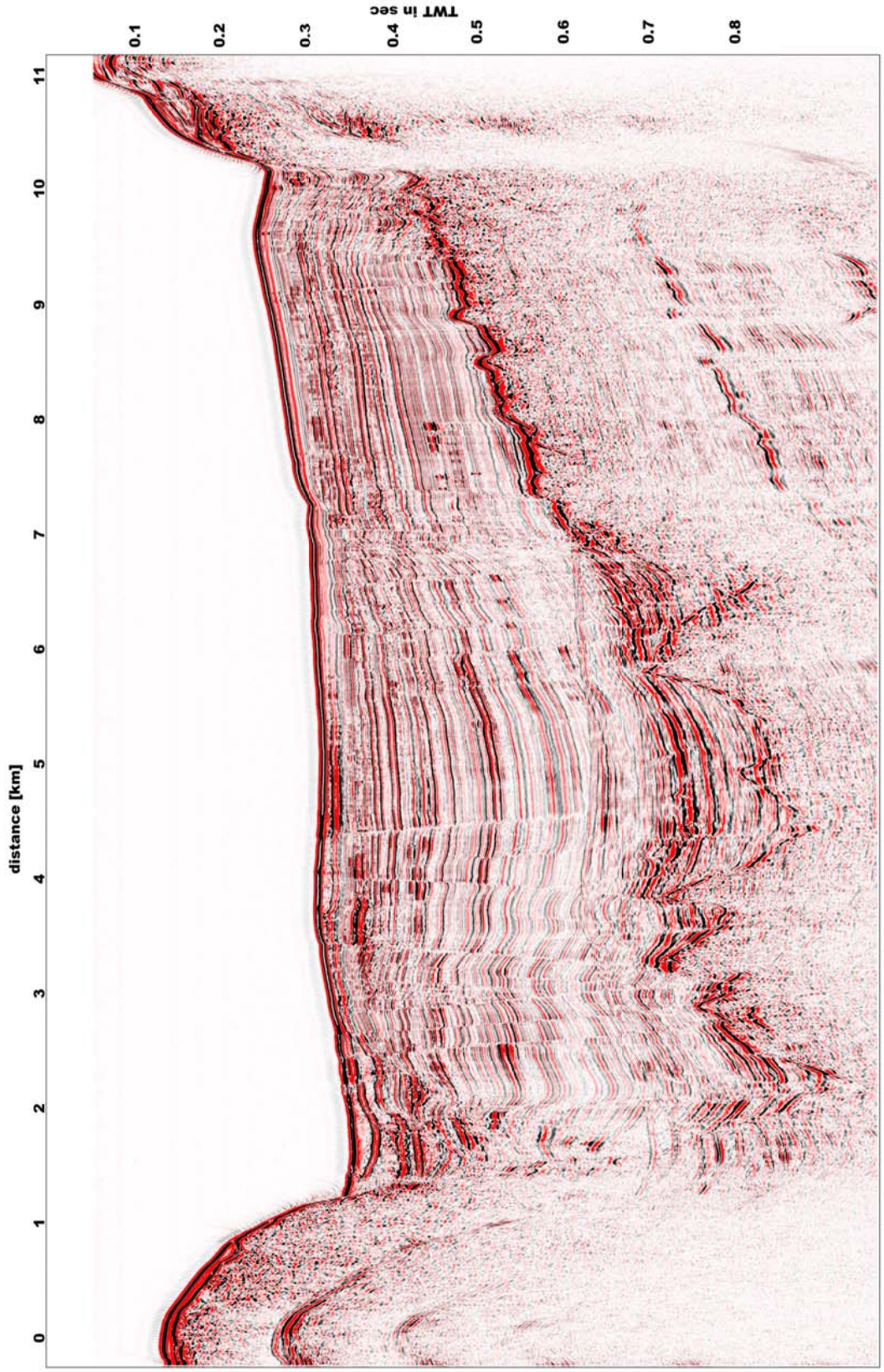
TWT in sec
0.1
0.2
0.3
0.4
0.5
0.6
0.7
0.8
distance [km]
0
1
2
3
4
5
6
7
8
9
10
11

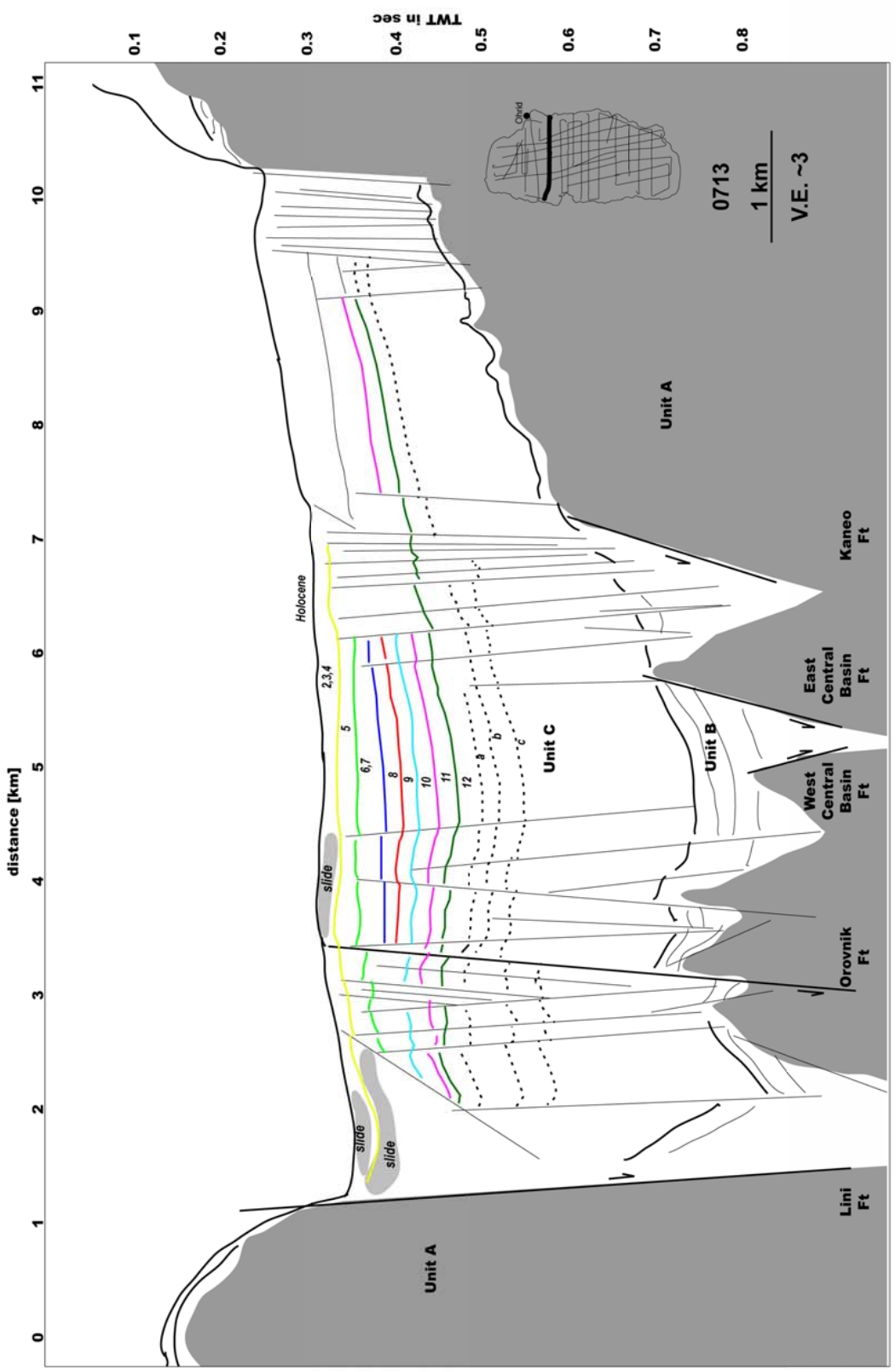

Fig. B 6: Seismic cross section imaging the half graben with Lini a major bounding fault. Colored lines and respective numbers from 1-12 indicate the chronological interpretation related to the Marine Isotope Stages.

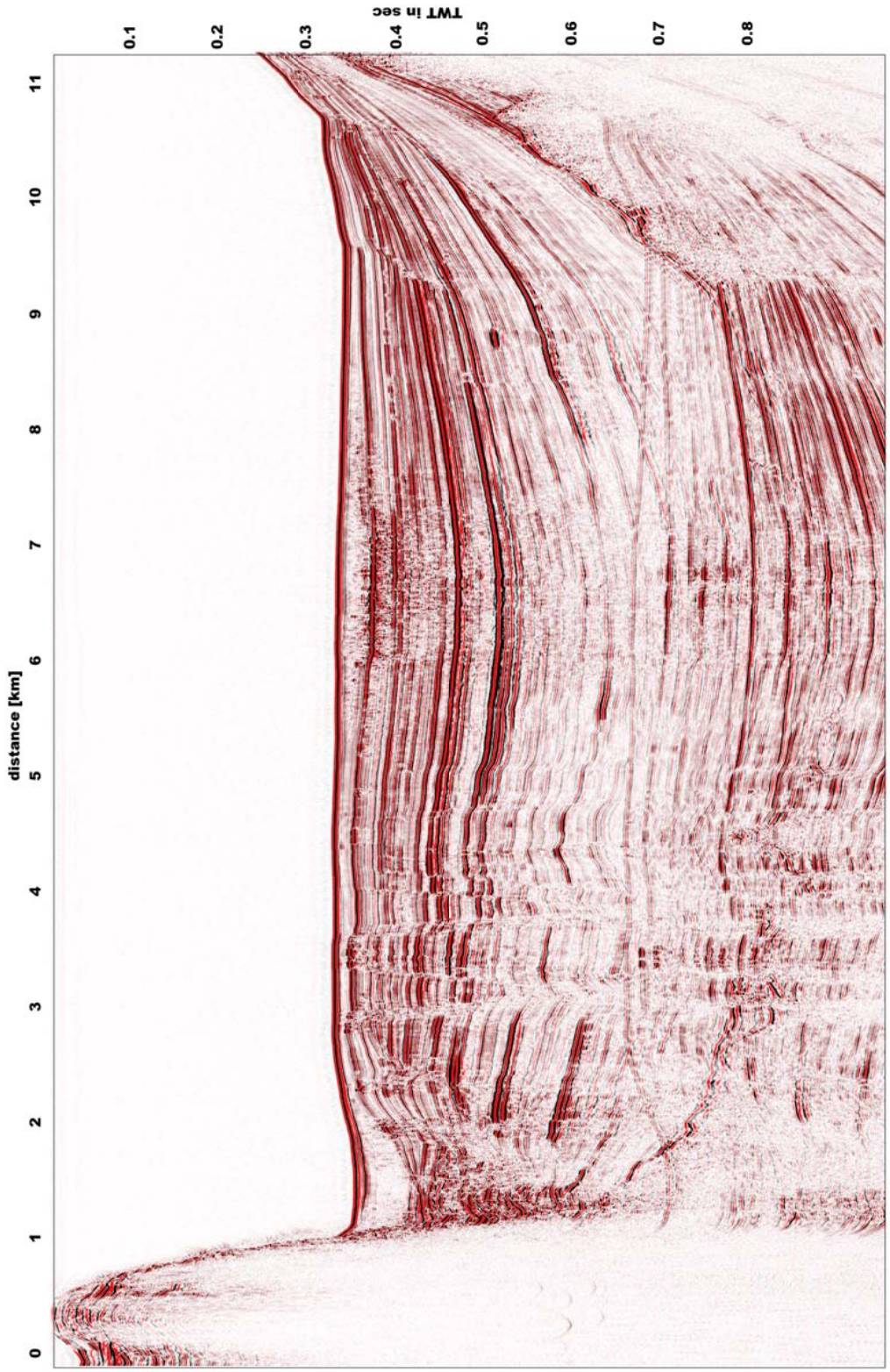
TWT in sec
0.1
0.2
0.3
0.4
0.5
0.6
0.7
0.8
distance [km]
0
1
2
3
4
5
6
7
8
9
10
11

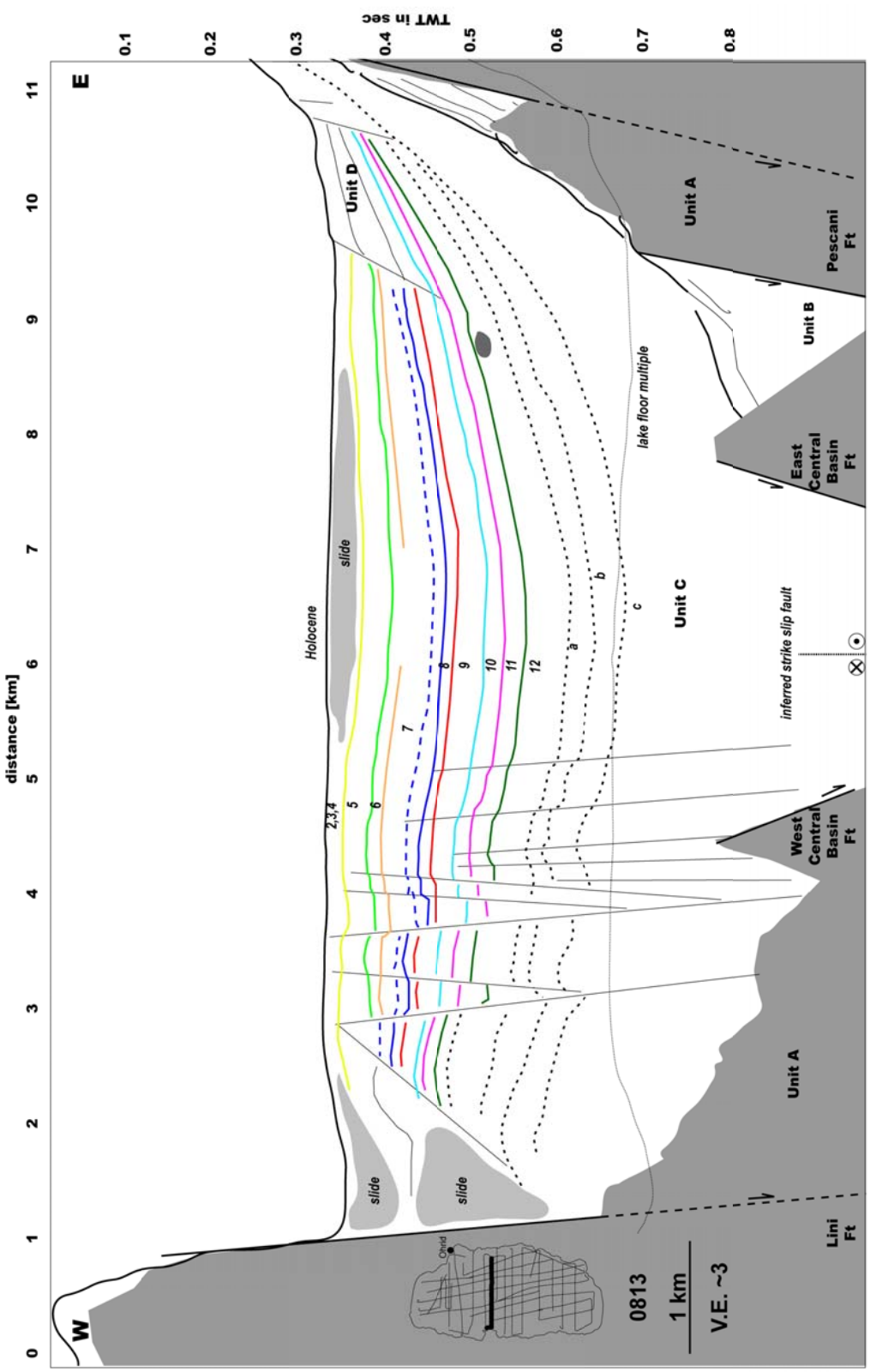

Fig. B 7: Seismic cross section imaging the half graben with Lini a major bounding fault. Colored lines and respective numbers from 1-12 indicate the chronological interpretation related to the Marine Isotope Stages. Dark grey area indicates bright spot. The inferred strike slip fault in between the Central Basin faults is marked that is most likely responsible for the initial basin opening.

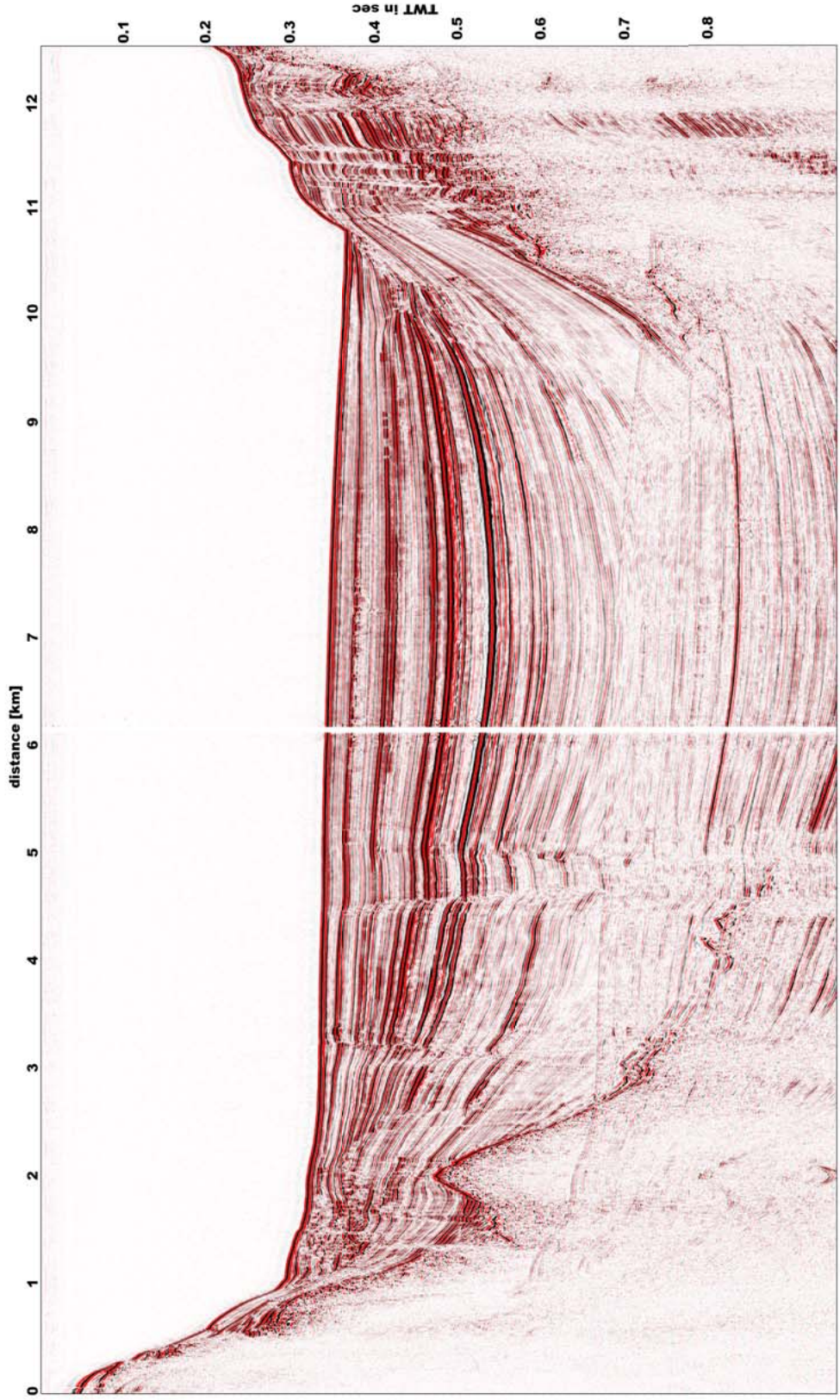
TWT in sec
0.1
0.2
0.3
0.4
0.5
0.6
0.7
0.8
distance [km]
0
1
2
3
4
5
6
7
8
9
10
11
12

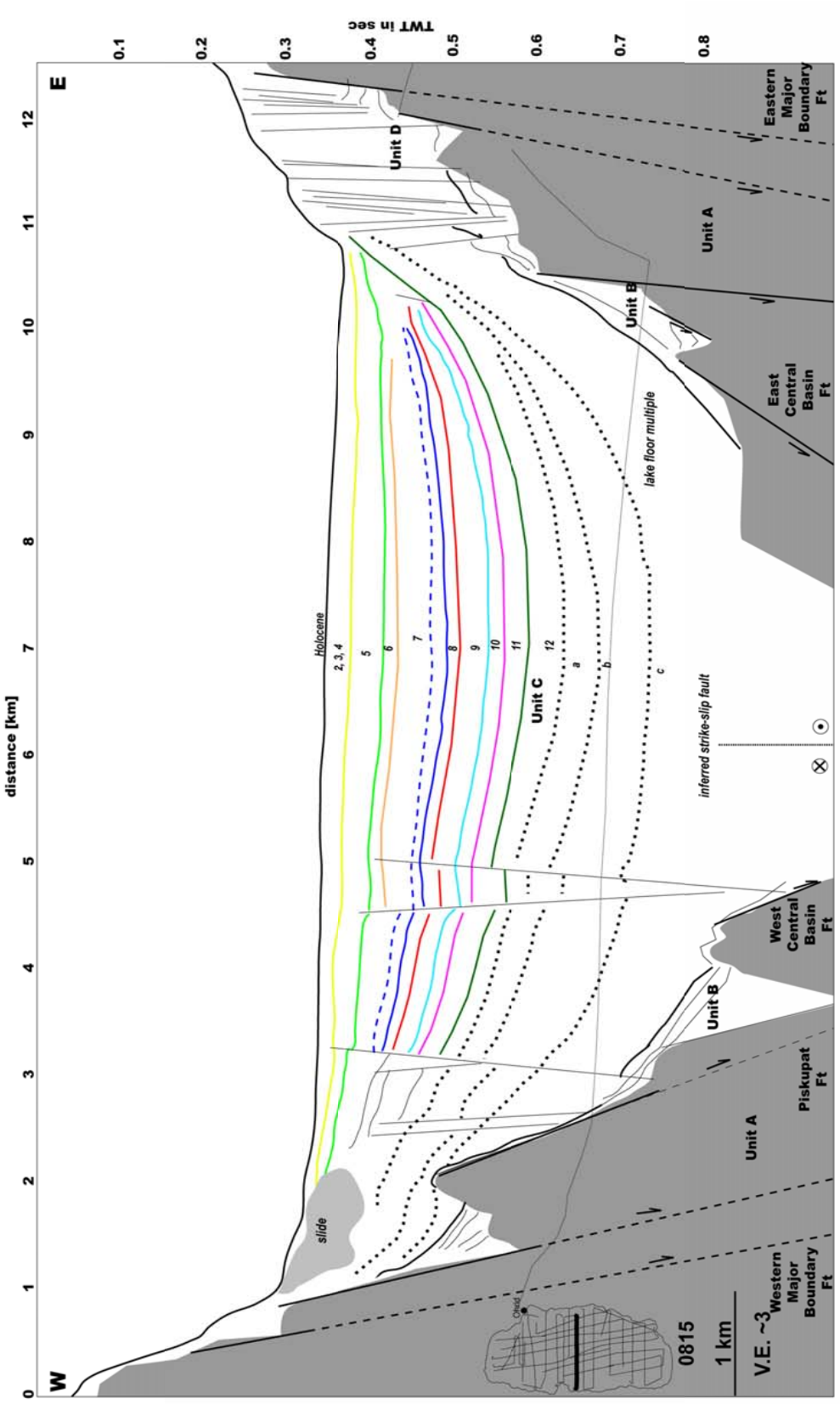

Fig. B 8: Seismic cross section imaging the central part of Lake Ohrid. Colored lines and respective numbers from 1-12 indicate the chronological interpretation related to the Marine Isotope Stages. Dark grey area indicates bright spot. The inferred strike slip fault in between the Central Basin faults is marked that is most likely responsible for the initial basin opening.

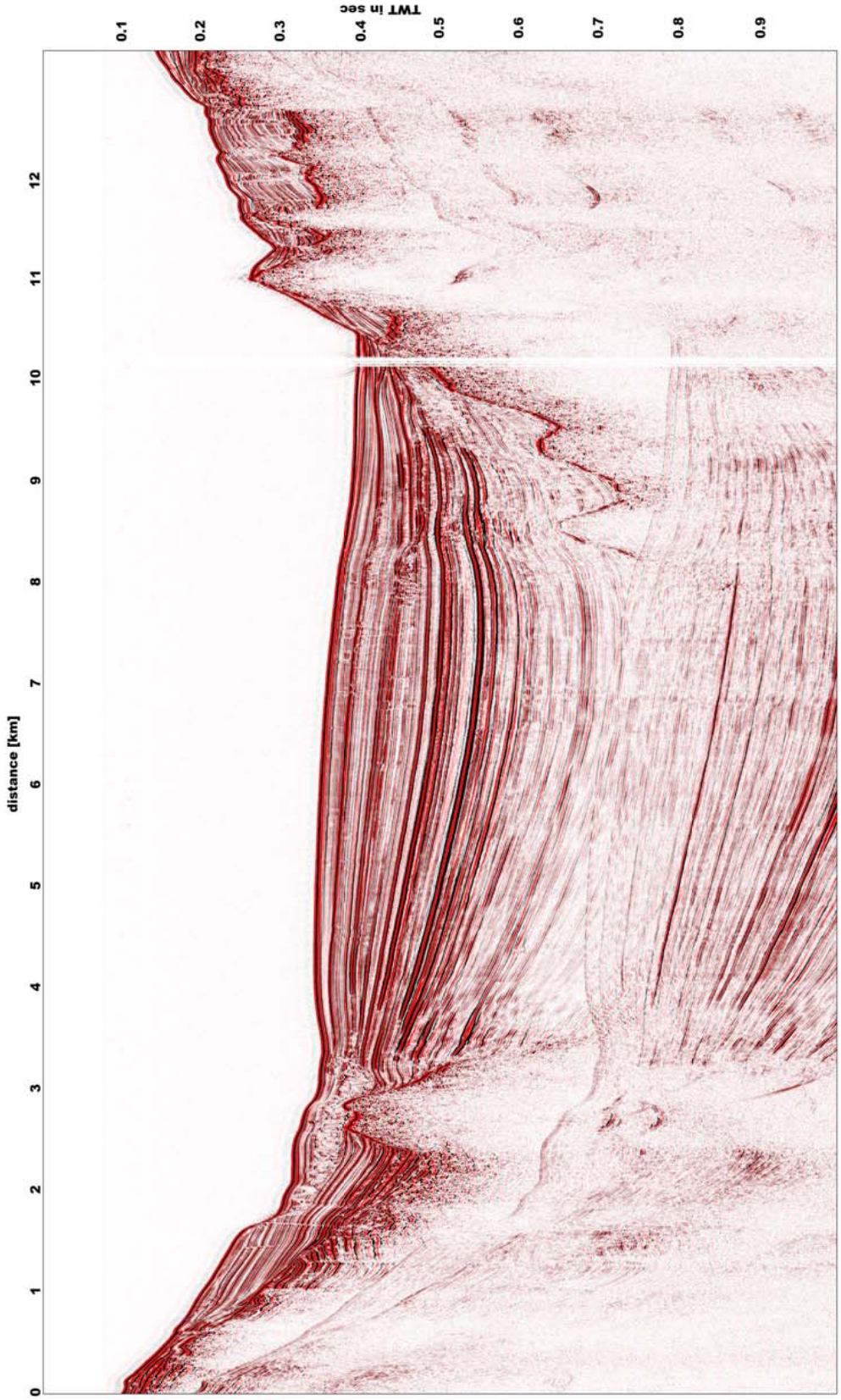
TWT in sec
0.1
0.2
0.3
0.4
0.5
0.6
0.7
0.8
0.9
distance [km]
0
1
2
3
4
5
6
7
8
9
10
11
12

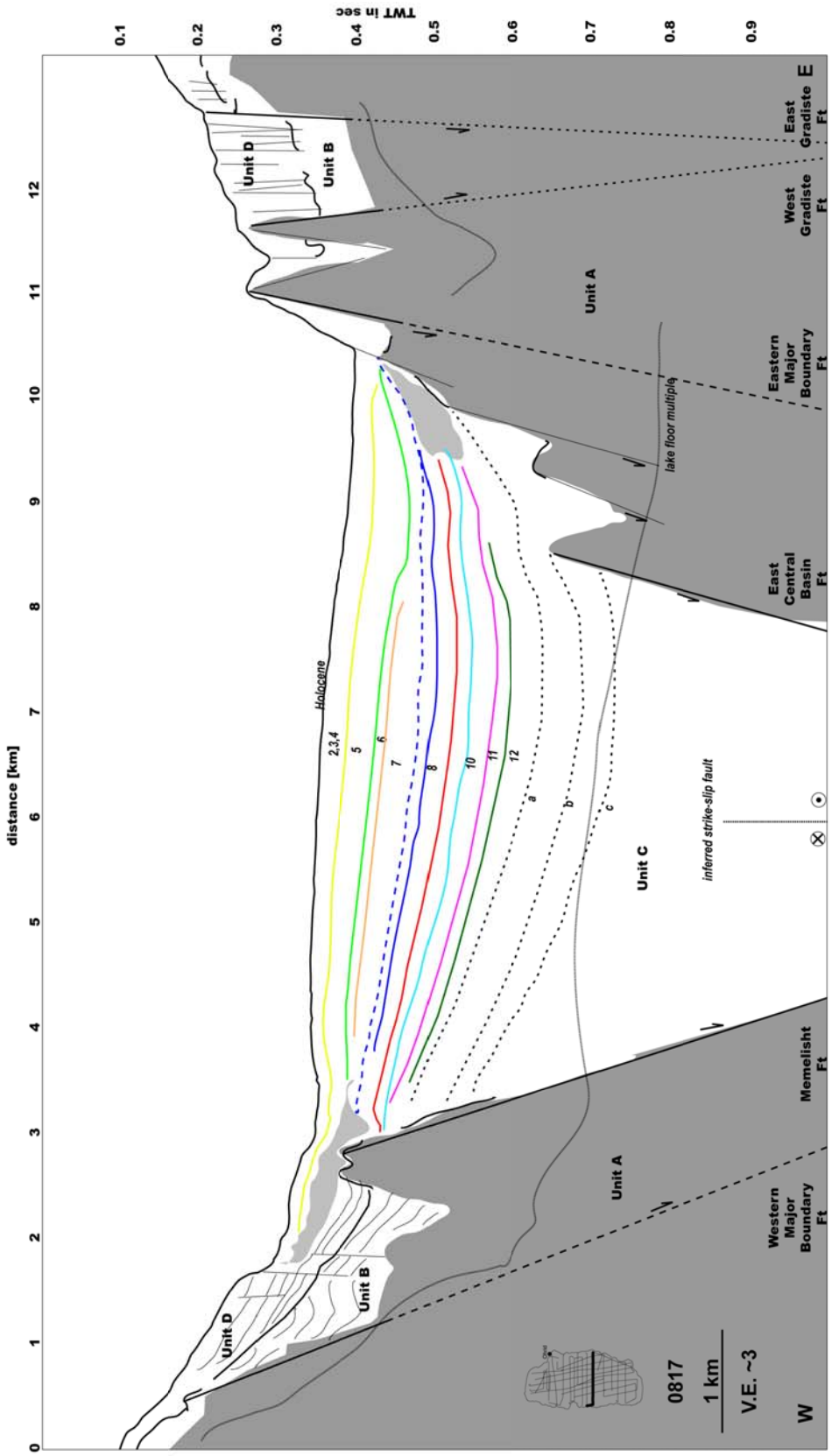

Fig. B 9: Seismic cross section imaging the central part of Lake Ohrid. Colored lines and respective numbers from 1-12 indicate the chronological interpretation related to the Marine Isotope Stages. Dark grey area indicates bright spot. The inferred strike slip fault in between the Central Basin faults is marked that is most likely responsible for the initial basin opening.

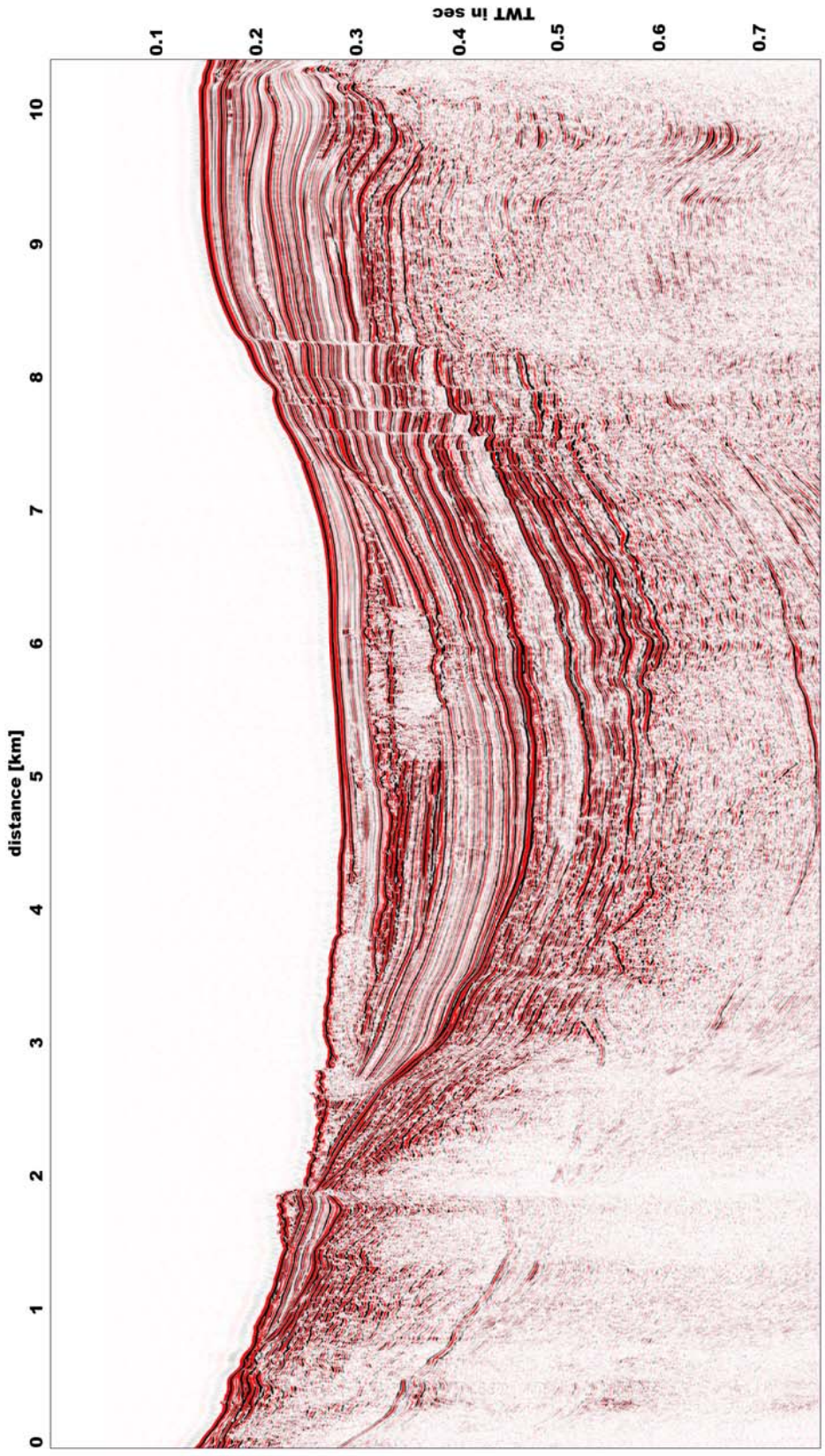
TWT in sec
0.1
0.2
0.3
0.4
0.5
0.6
0.7
distance [km]
0
1
2
3
4
5
6
7
8
9
10

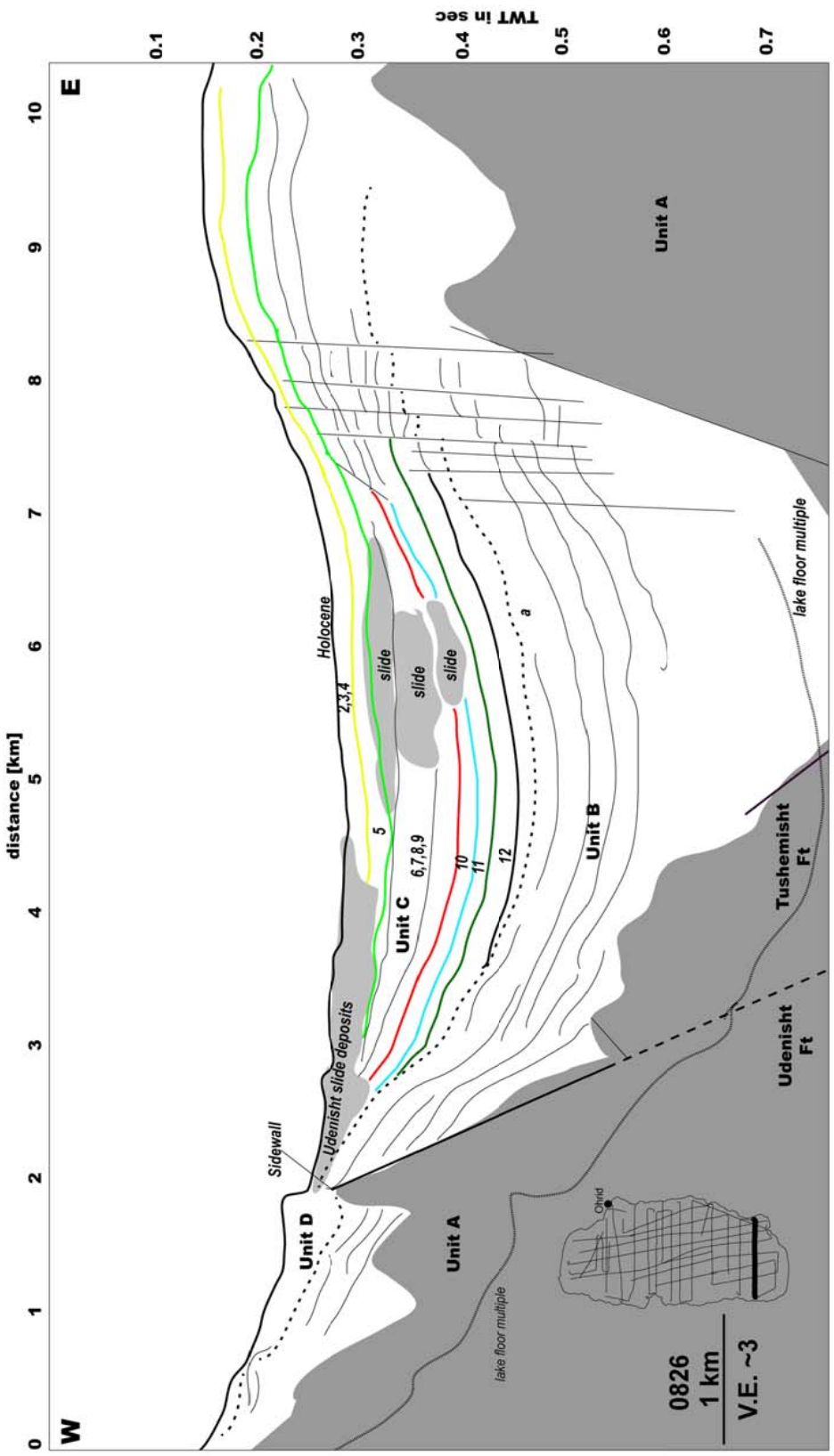

Fig. B 10: Seismic cross section imaging the southern area of Lake Ohrid. Colored lines and respective numbers from 1-12 indicate the chronological interpretation related to the Marine Isotope Stages. Slide deposits of the prominent Udenisht slide can be found in the western part of the profile

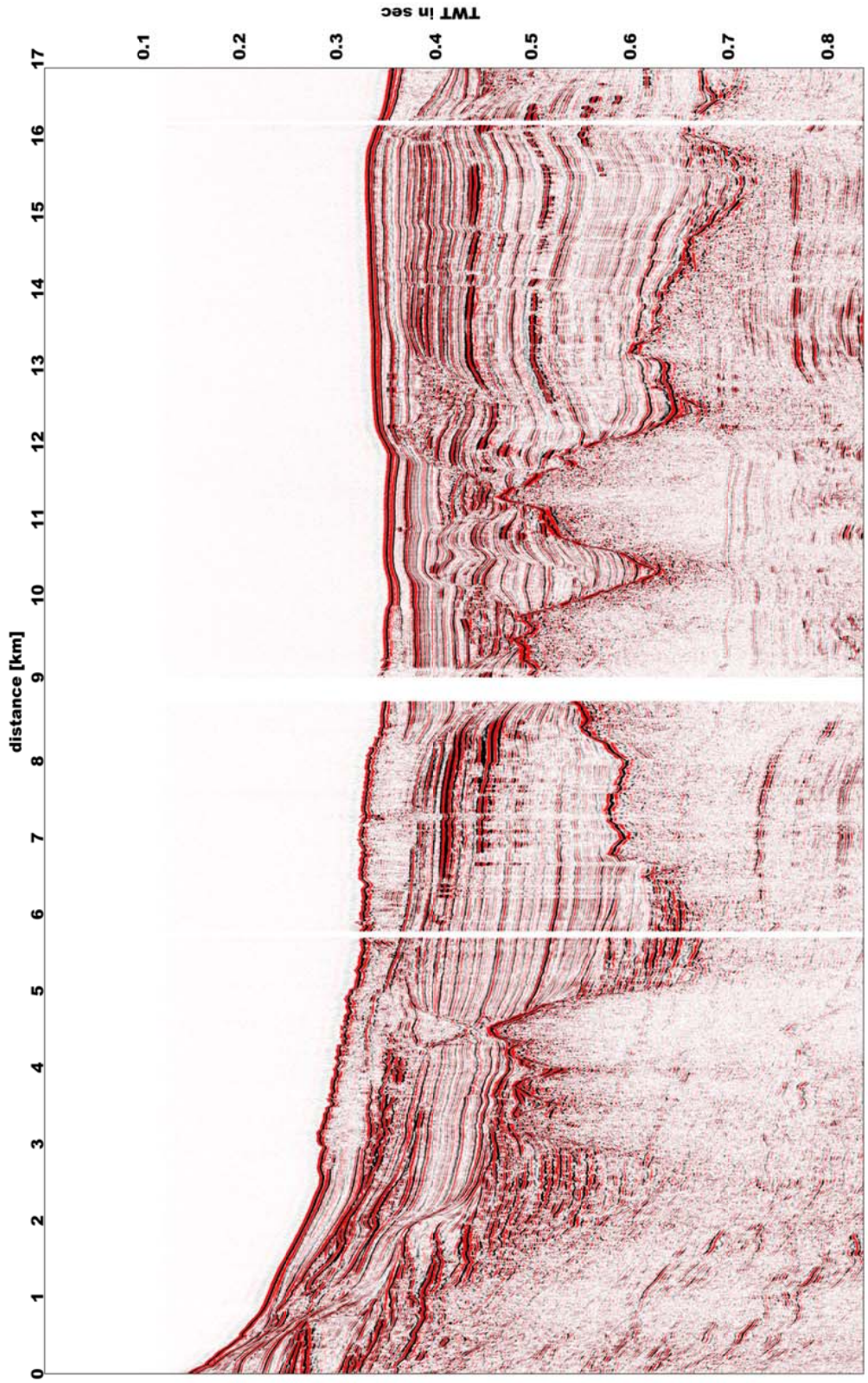
TWT in sec
0.1
0.2
0.3
0.4
0.5
0.6
0.7
0.8
distance [km]
0
1
2
3
4
5
6
7
8
9
10
11
12
13
14
15
16
17

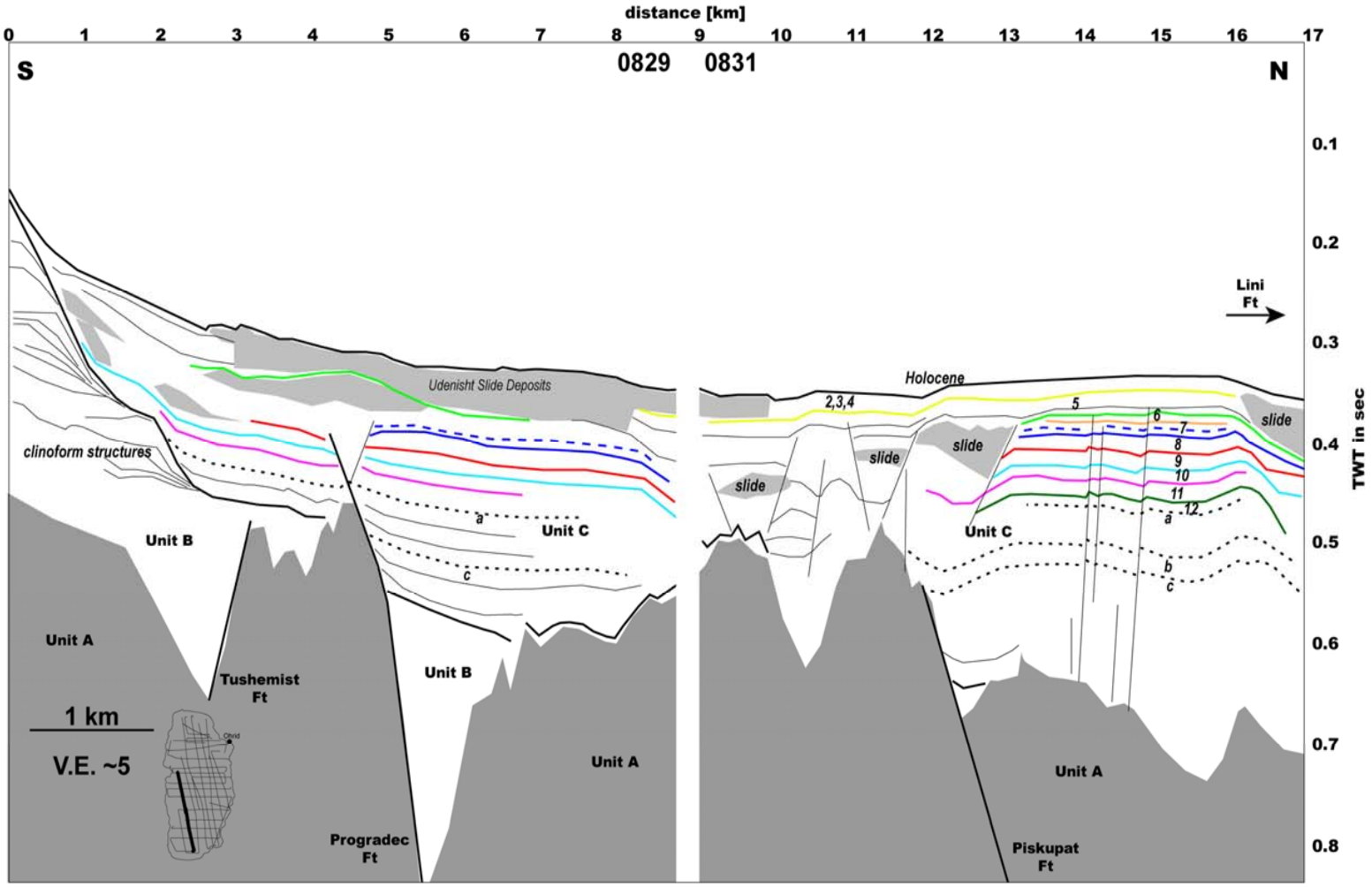

Fig. B 11: Seismic cross section imaging the internal sedimentary structure of the western margin. Colored lines and respective numbers from 1-12 indicate the chronological interpretation related to the Marine Isotope Stages. Slide deposits of the prominent Udenisht slide can be found in the southern part of the profile.

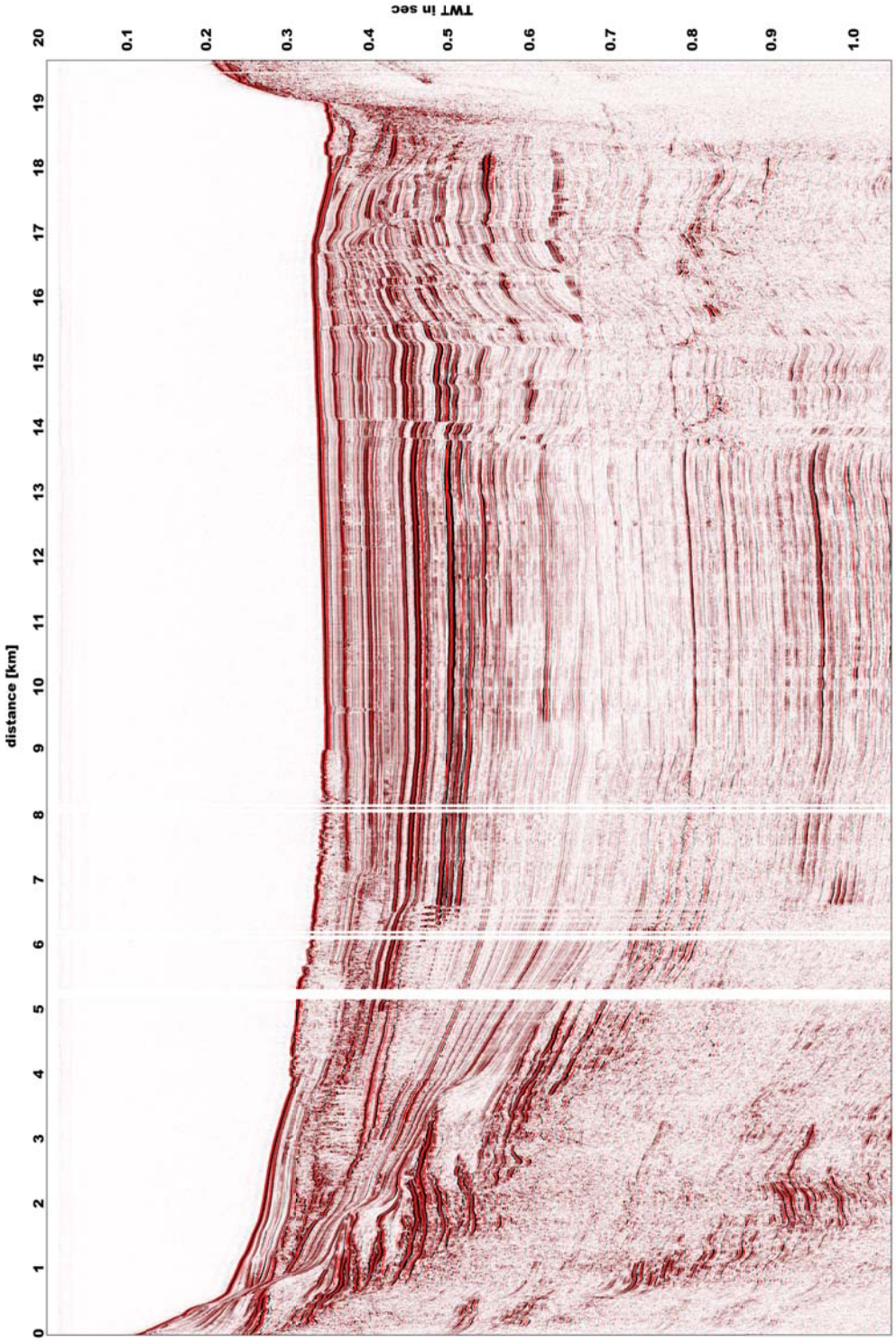
TWT in sec
0.1
0.2
0.3
0.4
0.5
0.6
0.7
0.8
0.9
1.0
distance [km]
0
1
2
3
4
5
6
7
8
9
10
11
12
13
14
15
16
17
18
19
20

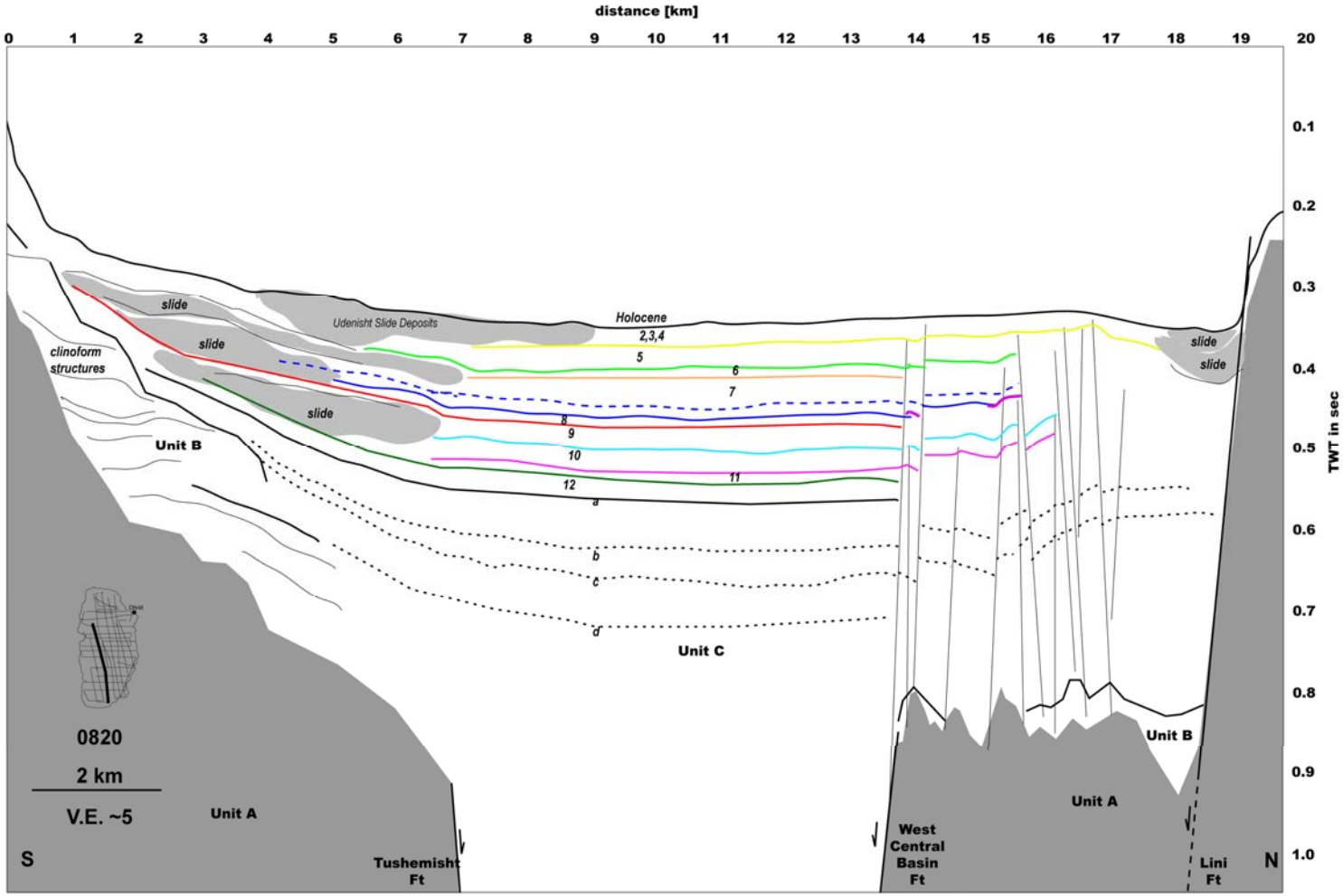

Fig. B 12: Seismic cross section imaging the internal sedimentary structure starting in the south toward the Lini fault. Several slide deposits can be found in the southern area. Colored lines and respective numbers from 1-12 indicate the chronological interpretation related to the Marine Isotope Stages. Toward the north an increase in faulting can be observed.

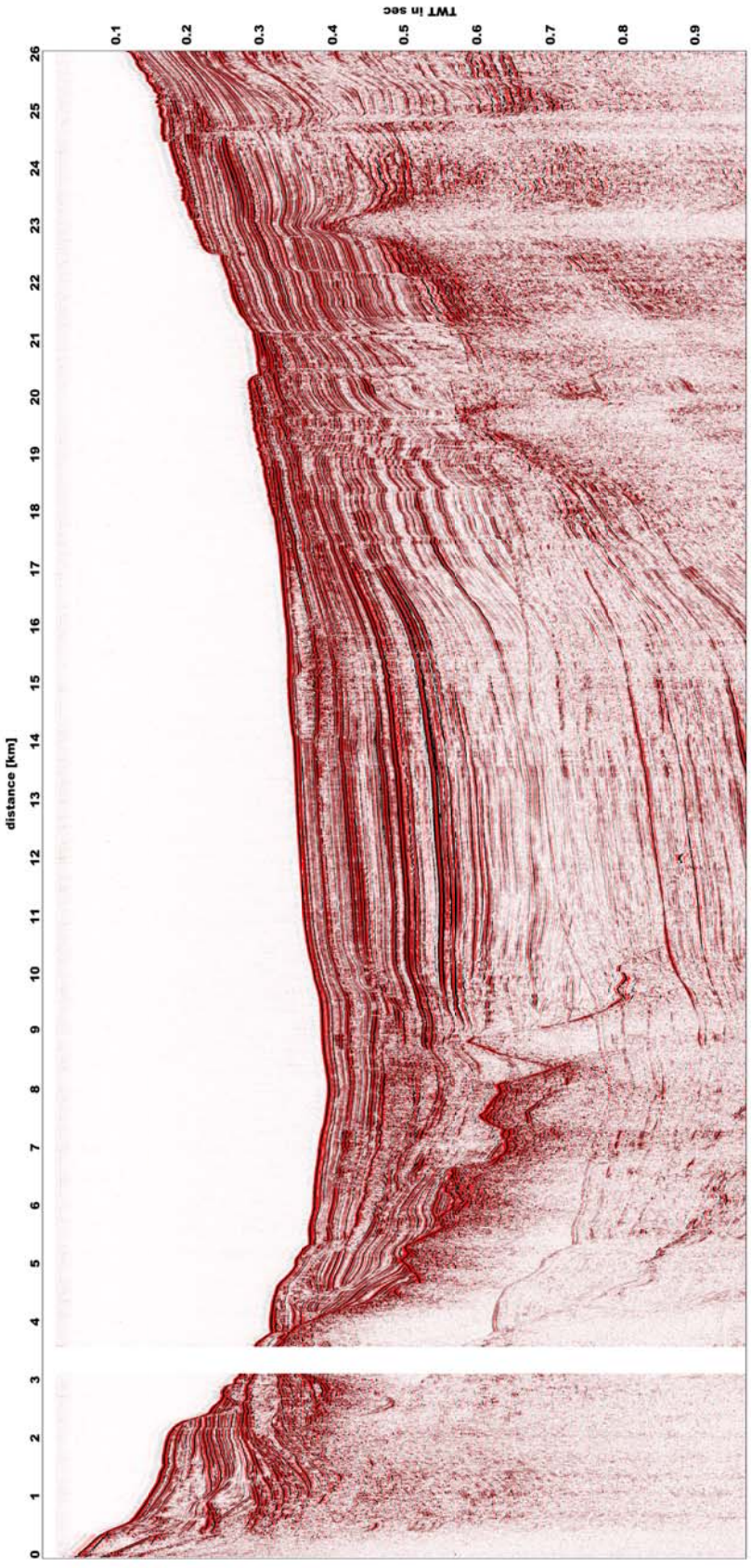
TWT in sec
0.1
0.2
0.3
0.4
0.5
0.6
0.7
0.8
0.9
distance [km]
0
1
2
3
4
5
6
7
8
9
10
11
12
13
14
15
16
17
18
19
20
21
22
23
24
25
26

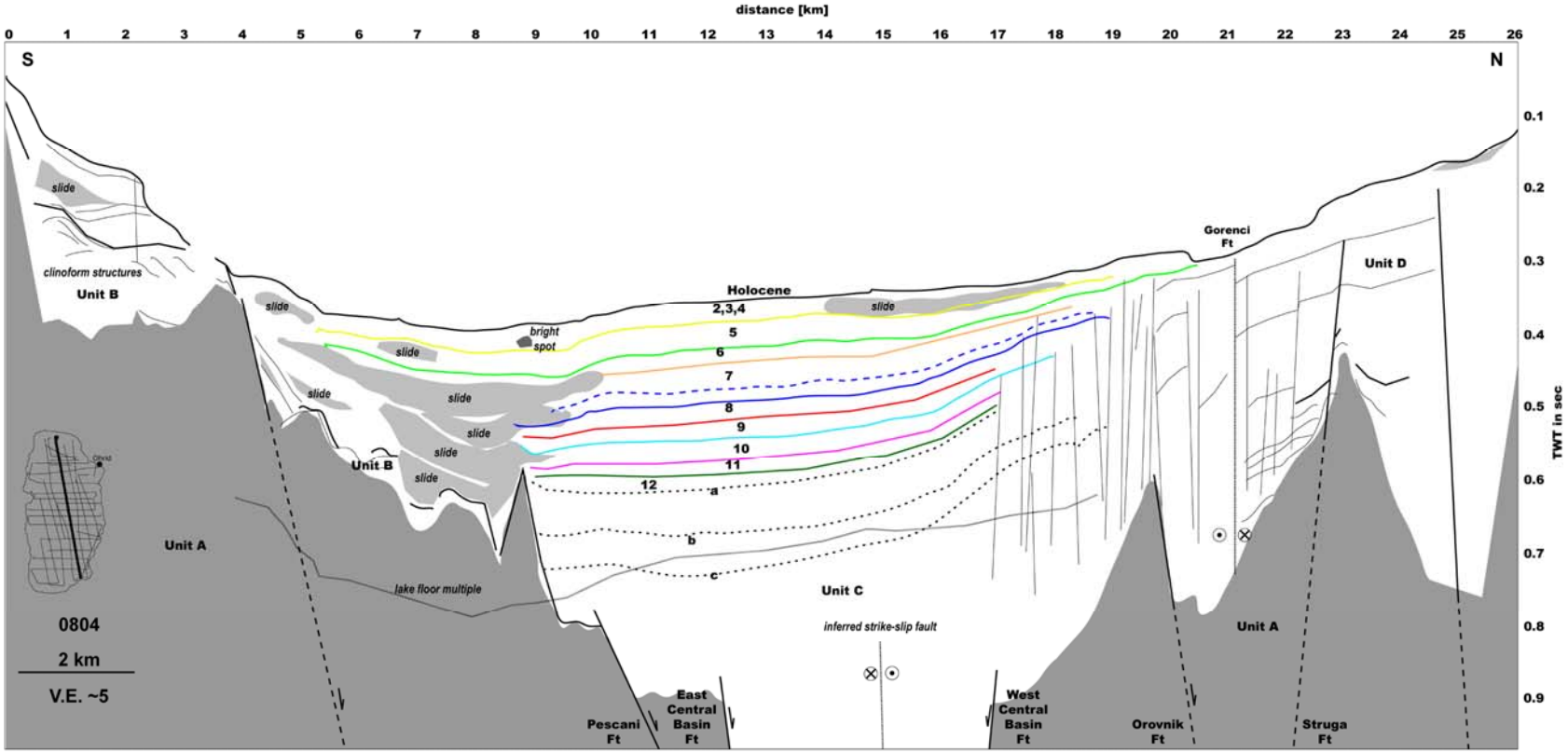

Fig. B 13: Seismic cross section crossing Lake Ohrid from south to north imaging the overall sedimentary structure of the basin. Several slide deposits can be found in the south. The central basin is characterized by thick undisturbed sediments. Colored lines and respective numbers from 1-12 indicate the chronological interpretation related to the Marine Isotope Stages. The inferred strike slip fault in between the Central Basin faults is marked that is most likely responsible for the initial basin opening. In the northern area the active Gorenci fault is detectable on the profile. Extensive faulting evidenced can be observed by numerous normal faults offsetting the syn-tectonic infill.

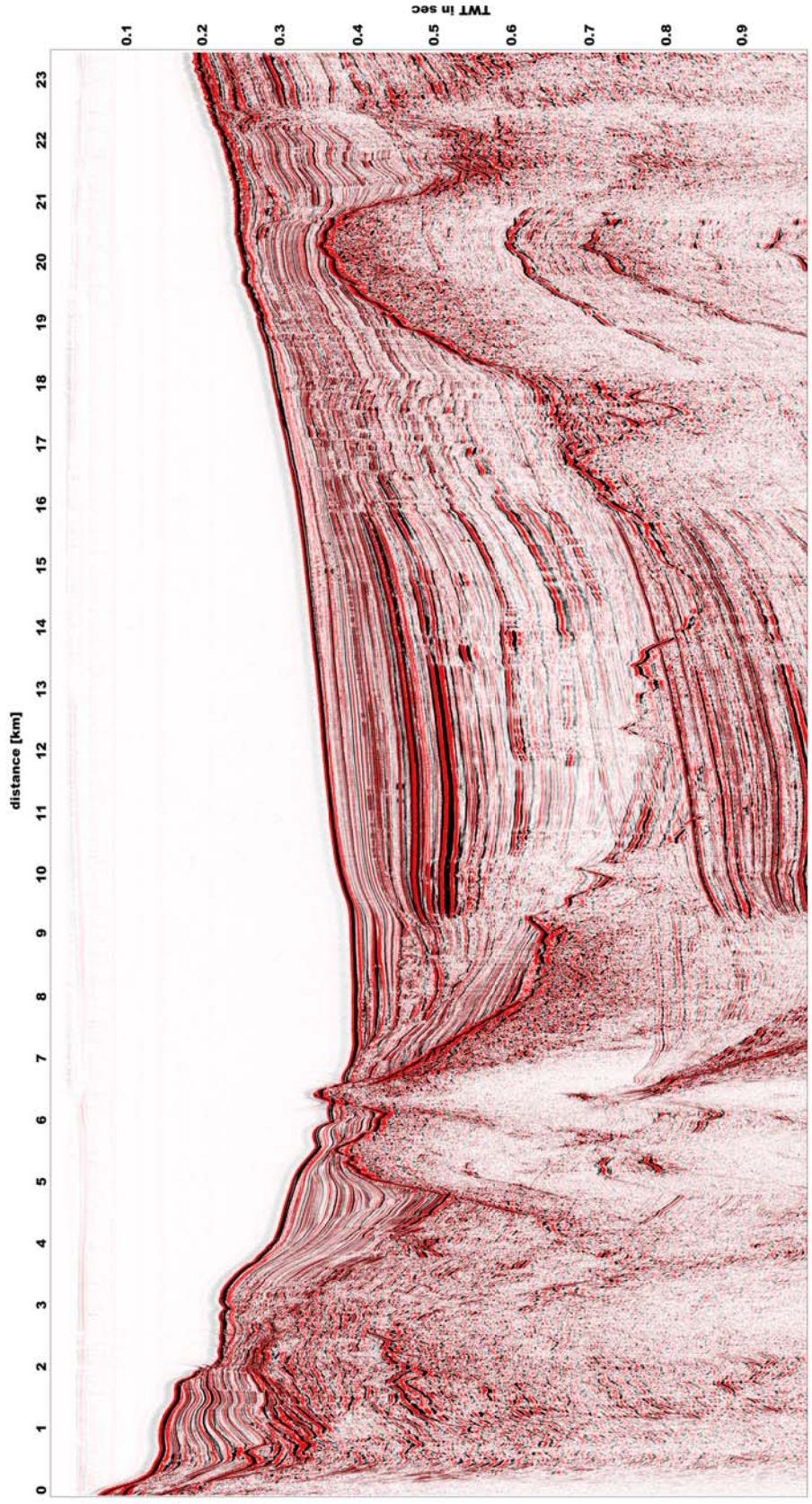
TWT in sec
0.1
0.2
0.3
0.4
0.5
0.6
0.7
0.8
0.9
distance [km]
0
1
2
3
4
5
6
7
8
9
10
11
12
13
14
15
16
17
18
19
20
21
22
23

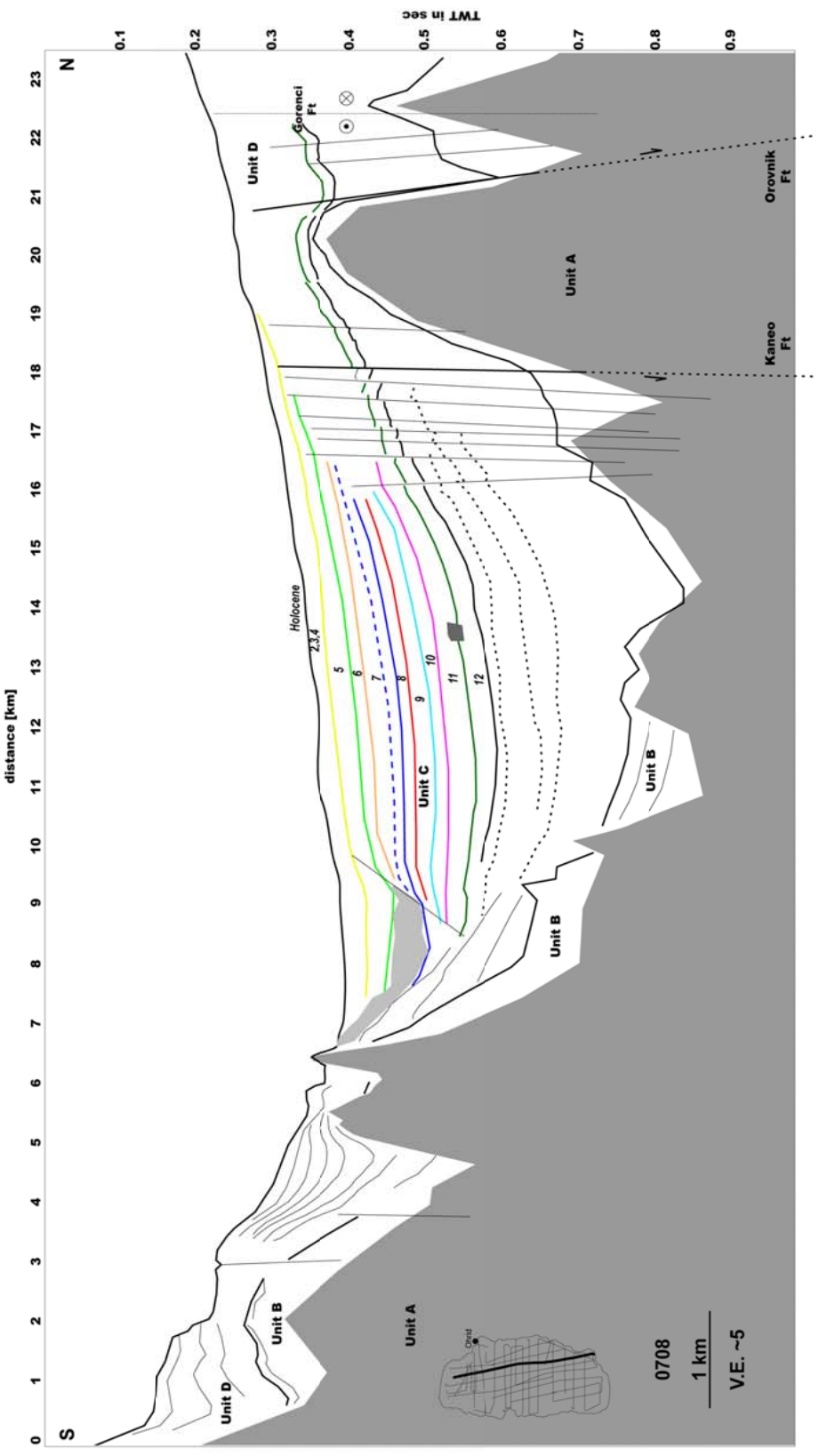

Fig. B 14: Seismic cross section crossing Lake Ohrid from south to north imaging the overall sedimentary structure of the basin. Colored lines and respective numbers from 1-12 indicate the chronological interpretation related to the Marine Isotope Stages. The active Gorenci fault is present in the north.

CURRICULUM VITAE

KATJA LINDHORST (GEB. ZIMMERMANN)

Date of birth	04 February 1981
Place of birth	Halberstadt
Permanent address	Bornsteinerstr. 11c, 24214 Bornstein
Email address	klindhorst@geomar.de

Education

1987-1991	Grundschule Anne-Frank Halberstadt
1991-1999 June 1999	Gymnasium Käthe-Kollwitz Halberstadt *Abitur*
1999-2002	Study of Computer Sciences at Bremen University
2002-2005 Sept. 2005	Study of Geosciences at University Bremen *Bachelor of Geosciences*
2005-2008 Jan. – June 2007 May 2008:	Study of Marine Geosciences at University of Bremen Semester abroad at University of California Santa Cruz (UCSC) *M. Sc. Marine Geosciences*
Since June 2008	Doctorate study within the working group 'Submarine Hazards at Continental Margins'; Cluster of Excellence: The Future Ocean at the Leibniz Institute of Marine Sciences at Kiel University (IFM-Geomar), Kiel, Germany (Since Jan. 2012: Helmoltz Centre for Ocean Research Kiel, Germany)